MASSEY UNIVERSITY
TE KUNENGA KI PŪREHUROA
UNIVERSITY OF NEW ZEALAND

# Heat-induced interactions between hemp and milk proteins and their impact on emulsification

A thesis presented in partial fulfilment of

the requirements for the degree of

**DOCTOR OF PHILOSOPHY**

**IN**

**FOOD TECHNOLOGY**

At Riddet Institute, Massey University, Palmerston North,

New Zealand

**Sihan Ma**

**2025**

Riddet Institute
Kōkiri - Te Hā o te Kai

## ABSTRACT

Hemp protein (HP) is a sustainable plant-based protein known for its high digestibility and favourable essential amino acid composition. However, like many plant proteins, HP suffers from low solubility, poor functional properties, and a high degree of aggregation in commercial powders, which limits its application in food systems. In response to the increasing demand for functional and sustainable food proteins, hybrid systems combining plant and milk proteins have emerged as promising solutions to overcome these challenges.

This project focused on the development of functional hybrid protein ingredients by combining hemp protein (HP) with milk protein, particularly whey protein isolate (WPI), through a strategy involving heat-induced aggregation and microparticulation. The overall objective was to understand the mechanisms of heat-induced interactions between HP and milk proteins, develop hybrid microparticles, and evaluate their emulsifying performance in both conventional oil-in-water emulsions and high internal phase emulsion (HIPEs) systems.

Initially, dispersion of commercial HP was subjected to microfluidisation to improve dispersibility and reduce particle size. Heat treatment of microfluidised HP in the presence of β-lactoglobulin (β-lg) or whey protein isolate (WPI) resulted in the formation of irreversible disulphide-linked hybrid aggregates. Notably, WPI was found to suppress heat-induced aggregation of HP, highlighting its stabilising role during thermal processing. Comparative studies with sodium caseinate (NaCN) also suppressed heat-induced aggregation but showed that casein–HP interactions were reversible, likely driven by

chaperone-like action, suggesting distinct binding mechanisms depending on the milk protein used.

The influence of pH on heat-induced HP/WPI aggregation revealed that pH 8 promoted the formation of small, covalently stabilised aggregates, making it the optimal condition for hybrid microparticle formation. Well-dispersed HP/WPI microparticles were then developed via microparticulation, combining heat-induced aggregation at pH 8 and high-pressure homogenisation. Emulsions stabilised by microparticulated HP/WPI (≥1.5%, w/w) exhibited comparable emulsifying ability to WPI-dominated emulsions and significantly improved thermal stability.

These hybrid microparticles were further tested in HIPEs systems, where they successfully stabilised emulsions. Compared to HIPEs stabilised by HP or WPI alone, those stabilised by microparticulated HP/WPI exhibited higher viscosity, greater storage modulus ($G'$), and enhanced resistance to deformation, suggesting the formation of stronger internal droplet networks driven by protein–protein and droplet–droplet interactions. Importantly, the HIPEs stabilised by these hybrid microparticles also showed excellent heat stability, maintaining their structure, rheology, and appearance after heating.

Overall, this project provided a new understanding of the heat-induced interactions between hemp and milk proteins and demonstrated a feasible approach for improving the functionality of hemp protein by forming hybrid protein systems with whey protein. Such findings will contribute to the development of novel functional food protein ingredients, enabling broader utilisation of plant proteins in emulsified and thermally processed food applications.

# ACKNOWLEDGEMENT

First and foremost, I would like to express my deepest gratitude to my chief supervisor Assoc. Prof. Alejandra Acevedo-Fani for her unwavering support throughout my PhD journey. I am extremely grateful that she accepted me as her student and guided me with dedication and care. Her mentorship has been instrumental in shaping my skills in hypothesis generation, critical thinking, experimental design, academic writing and presentation. She also helped me build up my capability to independently address research challenges. I sincerely appreciate her encouragement, patience and inspiration.

I would also like to thank my co-supervisors, Dist. Prof. Harjinder Singh and Prof. Aiqian Ye, for their continuous support and invaluable guidance. Their scientific insight, deep knowledge, constructive feedback and thoughtful discussions helped me navigate the complexities of my research. I am grateful to all my supervisors for creating a supportive and stimulating research environment.

I would like to thank the Riddet Institute, Massey University, for funding this PhD project and providing an excellent platform for my academic growth. I am also thankful to the research fellows and staff at the Riddet Institute, the School of Food and Advanced Technology, AgResearch and Manawatu Microscopy and Imaging Centre (MMIC). In particular, I would like to thank Prof. Mark Waterland, Dr Thomas Do, Dr Xinya Wang, Dr Debashree Roy, Dr Lirong Cheng and Dr Siqi Li for their valuable advice. I am deeply appreciative of the technical support provided by Ms Maggie Zou, Mr Jian Cui, Dr Peter Zhu, Ms Estelle Qian, Mr Steve Glasgow, Ms Michelle Tamehana, Mr. Chris Hall, Ms Jacinda Aplin (AgResearch), Ms Linda McVann (AgResearch), Mr Robert Wieliczko (AgResearch), Dr Matthew Savoian (MMIC) and Dr Yanyu (MMIC). I also wish to thank Ms Michelle Heayns, Ms Terri Palmer, Ms Rebecca Olsson, Ms Meg Wedlock, Ms Alex

Wood, Mr John Henley-King, Mr Tim O'Dea, and Mr Peter Jeffery for their administrative and IT support.

My thanks also go to Dr David Reid and Dr Yichao Liang at Fonterra for supplying the milk protein powder used in this study. To my fellow students and friends, Dr Xin Wang, Dr Chih-chieh Chuang, Dr Nan Luo, Dr Zheng Pan, Dr Mengxiao Yang, Dr Aylin Şen, Mr Jinxin Zhang, Ms Hao Cui, Mr Manfred Goh, Ms Di Lu, Ms Yusi Qin, thank you for your friendship and for the many joyful and insightful discussions we shared.

Finally, I am forever grateful to my beloved parents, Ms Runya Zhu and Mr Yongsheng Ma, for their unconditional love and unwavering support. Your encouragement gave me the strength to pursue my dreams with confidence. I owe a special thank you to my wife, Dan Wu, who has stood by me through every success and setback, sharing both the joys and the challenges of this journey. Your strength and optimism have been my anchor. To my two little sons, Liam Shuheng (书珩) Ma and Leo Shuyu (书瑜) Ma, who came into this world during my PhD, your smiles give me courage and purpose. Your presence fills my life and makes everything worthwhile. *This thesis is dedicated to you, with love.*

# Table of Contents

## List of Tables

## List of Figures

## List of Abbreviations

| | |
|---|---|
| α-la | α-lactalbumin |
| β-lg | β-lactoglobulin |
| AS | Acidic subunit |
| BS | Basic subunit |
| BSA | Bovine serum albumin |
| CLSM | Confocal Laser Scanning Microscopy |
| DIS | Dispersion |
| DLS | Dynamic laser scattering |
| DTT | Dithiothreitol |
| $G'$ | Storage modulus |
| $G''$ | Loss modulus |
| HIPEs | High internal phase emulsions |
| HP | Hemp protein |
| HPPs | Hemp protein particles |
| HP-AS | Hemp 11S globulin acidic subunit |
| HP-BS | Hemp 11S globulin basic subunit |
| NaCN | Sodium caseinate |
| pI | Isoelectric point |
| SDS-PAGE | Sodium dodecyl sulfate polyacrylamide gel electrophoresis |
| SH | Sulphydryl |
| SUP | Supernatant |
| TEM | Transmission electron microscopy |
| WPI | Whey protein isolate |

## List of Publications

Ma, S., Acevedo-Fani, A., Ye, A., & Singh, H. (2024). Heat-induced interactions of hemp protein particles formed by microfluidisation with β-lactoglobulin. *LWT*, *203*. https://doi.org/10.1016/j.lwt.2024.116370

Ma, S., Ye, A., Singh, H., & Acevedo-Fani, A. (2024). Heat-induced interactions between microfluidised hemp protein particles and caseins or whey proteins. *Food Chemistry*, 141290. https://doi.org/https://doi.org/10.1016/j.foodchem.2024.141290

Ma, S., Ye, A., Singh, H., & Acevedo-Fani, A. (2025). Emulsifying properties of hemp and whey protein complexes achieved by microparticulation. *Food Hydrocolloids*, 111833. https://doi.org/https://doi.org/10.1016/j.foodhyd.2025.111833

Ma, S., Ye, A., Singh, H., & Acevedo-Fani, A. High internal phase emulsion stabilised by hemp/whey protein particles: rheology properties and heat stability. *(in preparation for submission)*

# Chapter 1: Introduction

Chapter 1: Introduction

Proteins are essential macronutrients that support human metabolism by supplying energy and vital amino acids. In food systems, beyond their nutritional roles, proteins also contribute significantly to the structure, texture, and quality of food products due to their diverse physicochemical and functional properties. Their amphiphilic nature and chemical reactivity enable proteins to interact with each other and other food components such as fats, polysaccharides, and minerals (Ismail et al., 2020; Loveday, 2020; Sim et al., 2021).

In the last few years, the consumption of protein has grown because of the increasing population. The global human population is estimated at approximately 8.2 billion in 2024 and, according to the United Nations World Population Prospects 2024, the world population is projected to reach about 9.7 billion by 2050, with a peak near 10.3 billion in the 2084 (Ritchie & Rodés-Guirao, 2024; United Nations, 2024) . However, increasing the production of animal-derived proteins, including milk proteins, is associated with higher land use, greenhouse gas emissions, and other environmental pressures. These challenges have raised concerns about climate change, land degradation, and global food security. As a result, the food industry has been actively exploring plant proteins as alternatives to animal proteins (Akharume et al., 2021; Ismail et al., 2020; Schmitt et al., 2019).

Nevertheless, fully replacing animal proteins with plant proteins remains challenging due to several limitations. From a functional standpoint, the ability of proteins to act as emulsifiers, foaming agents, and gelling agents depends heavily on their solubility. Unfortunately, many plant proteins exhibit poor water solubility, restricting their use in aqueous food systems (Day, 2013; Kim et al., 2024; Sim et al., 2021). As such, plant

proteins often cannot fully replicate the functional performance of milk proteins in complex food formulations (Loveday, 2020).

Hemp protein (HP) has gained interest in the scientific community due to its complete essential amino acid profile, including high levels of arginine and sulphur-containing amino acids (e.g., cysteine) (Callaway, 2004). It also exhibits high digestibility (~90%), surpassing that of soy protein (~70%) (Wang et al., 2008). However, like many other plant proteins, HP has limited functional properties, including low water solubility/dispersibility and weak emulsifying capacities (Tang et al., 2006). Moreover, it displays poor gelling characteristics, with reports indicating that as much as 22% protein is needed to form a heat-induced gel (Malomo et al., 2014).

To overcome these functional limitations, various strategies have been proposed. These include refining the processing of plant proteins to minimise protein aggregation, via enzymatic hydrolysis (Malomo & Aluko, 2015b), pH-cycling (R. Wang et al., 2019), high-pressure homogenisation (Gong et al., 2019), utilising their low-solubility features in Pickering emulsions (Pickering emulsion) (Sarkar & Dickinson, 2020) and using the combination of plant and milk proteins to boost functional properties of plant protein (Guyomarc'h et al., 2021). In food colloidal systems, the partial replacement of milk proteins with plant proteins could be a strategy to improve techno-functionality, balance the nutritional composition of foods and contribute to more sustainable food production. Recent studies reported that plant-milk protein combinations may improve the technological functionality of plant proteins and achieve functional synergy (Alves & Tavares, 2019; Hinderink, Boire, et al., 2021; Lima Nascimento et al., 2023; McCann et al., 2018; Rout et al., 2024).

For instance, the addition of sodium caseinate (NaCN) has been shown to improve the thermal stability of hemp globulin dispersions (Chuang et al., 2019). The soy-milk protein and soy-whey protein mixtures achieved higher $G'$ in acid-induced and thermal-induced gels, respectively (Roesch & Corredig, 2005; Roesch et al., 2004). Pea protein can act as the space-filler in the casein micelle gel network to produce firmer acid-induced gels (Beghdadi et al., 2022). Emulsions stabilised by the pea-sodium caseinate blends showed better stability against aggregation than those using a single protein (Yerramilli et al., 2017).

Despite these studies, the mechanisms behind plant-milk protein interactions remain insufficiently understood, especially in the context of hemp–milk protein systems. To date, only Chuang et al. (2019) and X. Zhou et al. (2022) have reported that the interaction between hemp protein and sodium caseinate generates colloidally stable hybrid protein particles. This thesis aims to conduct more systematic research focusing on studying the heat-induced protein-protein interactions between hemp and milk proteins (mainly whey protein), and the technological functional properties, particularly emulsification, of the resulting hybrid protein system.

## Objectives

The main objective of this project is to investigate the heat-induced interactions between hemp protein (HP) particles and molecular milk proteins (whey protein isolate and sodium caseinate), in order to develop hybrid microparticulated protein systems and understanding how these hybrid systems function as stabilisers in both conventional oil-in-water (O/W) emulsions and high internal phase emulsions (HIPEs), with a focus on their emulsifying ability, rheological behaviour, and thermal stability.

The specific objectives of this research project are:

1. To investigate the effect of microfluidisation on the dispersibility of hemp protein (HP) and the heat-induced interactions of HP particles with β-lactoglobulin (β-lg) (Chapter 4).
2. To explore the heat-induced interactions between the microfluidised HP particles and commercially available whey protein isolate (WPI) and sodium caseinate (NaCN), and their impact on the heat stability of the resulting hybrid colloidal systems (Chapter 5).
3. To study the effect of pH on heat-induced aggregation of microfluidised HP and WPI, with the aim of optimising the processing conditions for microparticulation (Chapter 6).
4. To develop HP/WPI microparticles and evaluate their emulsifying performance and thermal stability in conventional oil-in-water emulsions (Chapter 7).
5. To investigate the rheological properties and heat stability of high internal phase emulsions (HIPEs) stabilised by HP/WPI microparticles (Chapter 8).

The literature review was presented in **Chapter 2,** and the specific objectives were studied in **Chapters 4 to 7**:

In **Chapter 4**, HP particles were processed via microfluidisation to improve their dispersibility and subsequently combined with β-lg, a major whey protein, to investigate heat-induced protein-protein interactions. The aim was to explore whether β-lg could be associated with HP particles during thermal treatment and potentially modulate their

aggregation behaviour. This chapter provided insights into the driving forces governing HP and β-lg interactions and their complexation.

Building on these findings, **Chapter 5** expanded the investigation by incorporating two commercially relevant milk proteins, whey protein isolate (WPI) and sodium caseinate (NaCN), to further explore heat-induced interactions with HP particles. These proteins represent the major fractions of milk protein systems, with distinct structural and functional properties: WPI contains globular proteins prone to aggregation, while caseins are flexible, heat-stable proteins. This chapter aimed to clarify the mechanisms by which milk proteins impact HP aggregation. WPI was found to form stable complexes with HP (via disulphide binding), while the interactions between HP and NaCN (via chaperone-like effect) were primarily reversible. This chapter extends earlier work by evaluating the interactions of HP particles with a broader range of milk proteins, providing deeper insight into designing hybrid microparticles.

Therefore, WPI was selected as the preferred material for hybrid protein microparticulation in subsequent studies, as it was shown to form stable, covalent complexes with HP particles. In **Chapter 6**, the focus shifted towards investigating the influence of pH on the heat-induced aggregation behaviour of HP and WPI mixtures. The objective of this study was to understand how pH conditions (ranging from pH 3 to 8) affect the particle size, microstructure, and composition of HP/WPI aggregates upon heating. This was an essential step to optimal pH conditions for producing hybrid microparticles. This chapter was a transition chapter and served as a foundation for the subsequent work on producing microparticulated hybrid protein. Heating HP/WPI mixtures at pH 8 was identified as the most favourable condition for generating hybrid protein aggregates.

Based on these findings, the study in **Chapter 7** applied the above-mentioned microparticulation method, combining thermal denaturation and high-pressure homogenisation, to create HP/WPI microparticles. The objective of this study was to evaluate how HP/WPI microparticles perform as emulsifiers, particularly at different protein concentrations. The emulsifying ability, morphology and interfacial composition of the emulsions containing 10% oil and 0.25–1.8% microparticulated HP/WPI were characterised and compared with those stabilised by a non-microparticulated HP/WPI. This allowed direct assessment of the impact of microparticulation on emulsifying performance. This study demonstrated that microparticulation of HP/WPI not only improved the dispersibility of HP, but also resulted in emulsions with good emulsifying properties and markedly improved heat stability.

Based on the previous outcomes, **Chapter 8** investigated the ability of microparticulated HP/WPI to stabilise the high internal phase emulsions (HIPEs) with 75% oil content and compared them to those stabilised by non-microparticulated HP/WPI blends or by the individual proteins. The microstructure, rheological behaviour, including linear and non-linear viscoelasticity, and thermal stability of those emulsions were analysed. The results suggest that the microparticulated HP/WPI can serve as an emulsifier for HIPEs, leading to a strengthened internal emulsion network and improved thermal stability.

Together, these chapters provide a systematic investigation into the mechanisms governing heat-induced interactions between hemp and milk proteins. The findings advance fundamental understanding of hybrid protein complexation, microparticulation, and emulsion stabilisation, highlighting the potential of plant-milk protein combinations can be utilised as effective emulsifiers with improved heat stability. This project contributes valuable insights into protein hybridisation, supporting the development of sustainable, functional protein ingredients in food colloidal systems.

# Chapter 2: Literature review

## 2.1 Plant proteins

### 2.1.1 Plant storage proteins

Plant protein refers to the protein from land plant origin, residing in the seeds and grains (Day, 2013). The most common sources of plant protein are listed in **Table 2-1**.

**Table 2-1: Major source of food plant protein**

| Origin | Cereals | Edible seeds | Pseudocereals | Legumes | Tubers | Oilseeds |
|---|---|---|---|---|---|---|
| | Wheat | Quinoa | Amaranth | Pea | Potato | Peanut |
| | Corn | Buckwheat | Chia | Soybeans | | Sunflower |
| **Proteins** | Barley | | | Faba beans | | Hemp seed |
| | Oats | | | Lupins | | Cottonseed |
| | Rice | | | Lentils | | Rapeseed |

Adapted from Loveday (2019).

Plant proteins mainly consist of numerous globular proteins that are covalently linked. Hydrophobic interactions are considered the main driving force for plant protein folding to reduce the contact area between water and non-polar groups. Besides, disulphide bonds, hydrogen bonding, electrostatic forces and van der Waals forces are also involved; therefore, globular proteins are folded in a compactly packed shape (Grossmann & Weiss, 2021; McClements & Grossmann, 2021). The functionality of plant proteins is decided by the degree of disintegration, denaturation and aggregation of these proteins during extraction, purification and utilisation.

According to their solubility in different solvents, plant proteins can be further classified into four protein fractions; albumins (water-soluble), globulins (soluble in dilute salt solutions), prolamins (soluble in water/ethanol solutions) and glutelins (soluble in

dilute acid/alkaline solutions) (Grossmann & Weiss, 2021; Osborne, 1924; Sim et al., 2021). Globulins and albumins are mostly contained in pulse crops, while prolamins and glutelins are in cereals such as wheat and maize (Grossmann & Weiss, 2021; Sim et al., 2021). Although solvent extraction methods are commonly used to classify plant proteins, there could be a certain overlap among the four protein fractions (Day, 2013). The major protein types of the common sources of plant protein are listed in **Table 2-2**.

**Table 2-2: Major protein types of common plant sources**

| Plant Source | 7S Globulin (Vicilin-type) | 11S Globulin (Legumin-type) | 2S Albumin | Prolamin | Glutelin |
|---|---|---|---|---|---|
| **Soybean** | β-Conglycinin | Glycinin | | | |
| **Pea** | Vicilin | Legumin | | | |
| **Lentil** | Vicilin | Legumin | | | |
| **Faba bean** | Vicilin | Legumin | | | |
| **Chickpea** | Vicilin | Legumin | | | |
| **Hempseed** | | Edestin | Albumin | | |
| **Sunflower seed** | | Helianthinin | Albumin | | |
| **Pumpkin seed** | | Cucurbitin | | | |
| **Rice** | | | Albumin | | Glutelin (main storage protein) |
| **Wheat** | | | | Gliadin | Glutenin |
| **Maize (Corn)** | | | | Zein | |
| **Barley** | | | | Hordein | |
| **Sorghum** | | | | Kafirin | |

Adapted from Shewry and Casey (1999); Sim et al. (2021); Tamayo Tenorio et al. (2018).

Another classification method based on the proteins' sedimentation coefficients in water at 20 °C ($S_{20,w}$) was used to fractionate legume proteins. They can be characterised as 7S globulins, 11S globulins and 2S albumins, in which the $S_{20,w}$ values for globulins are about 7 (vicilin-type), 11 (legumin-type) and 2 (albumins) (Shewry & Casey, 1999; Shewry et al., 1995).

The secondary conformation of globulins is similar; they contain a small fraction of α-helical and a high fraction of β-sheet (Marcone et al., 1998a, 1998b). In general, the 7S globulins are trimeric, made up of three subunits of 50-70 kDa, and 11S globulins are hexameric, consisting of six subunits of 60-80 kDa. The subunits are held together by non-covalent interactions, and each subunit of 11S globulins consists of a basic polypeptide and an acidic polypeptide linked by a disulphide bond (Shewry & Casey, 1999).

Solubility is an important functionality of food ingredients, serving as a prerequisite for other functional properties. Multiple factors influence the solubility of globular proteins, which involve the molecular weight, molecular flexibility, disintegration and association of subunits and the surface hydrophobic, basic and acidic subunits (Molina et al., 2004). Since globulins dominate the major seed storage protein, and they are similar in structure and molecular weights, some properties of legume and seed proteins are similar (Day, 2013), e.g., the denaturing temperatures of soy, pea and hemp proteins are significantly higher than whey proteins. However, the various globulin content in different types of plant protein (e.g. ~ 90% of globulins in total soy protein versus ~ 50-60% and 60-80% of globulins in pea and hemp protein, respectively) (Day, 2013; Wang & Xiong, 2019) and different 11S/7S globulin ratio might lead to different protein funcrtionalities. Generally, albumins are more soluble at neutral or acidic pH than globulins because albumins have a lower molecular weight (10-18 kDa), which could lead to a more flexible structure and higher hydrophilicity. In the globulin category, 7S globulins are usually more water-soluble than 11S globulins (Sim et al., 2021).

It is relatively challenging to separate the protein from raw plant materials compared with milk protein (Day, 2013). In general, plant protein flour is produced by mechanically dehulling and milling. The solvent (usually hexane) extraction is used to separate protein from fat and carbohydrate. For plant protein isolates, extraction and

fractionation processing (alkaline extraction and isoelectric precipitation) usually follow the production of defatted materials (Sim et al., 2021). Commercial plant protein ingredients contain various protein fractions (e.g. globulin and albumin). The harsh processing conditions may cause extensive protein denaturation and aggregation, and lead to low solubility and functionality. For instance, about 75% of pea protein isolates are insoluble (Hinderink, Schröder, et al., 2021). The denaturation and aggregation state would affect the functionality of plant proteins, which causes challenges when using them in food systems.

### 2.1.2 Hemp seed protein

Industrial hemp (*Cannabis sativa* L.) seeds have over 30% (w/w) fat, 25% protein (w/w) and dietary fiber, vitamins and minerals (Callaway, 2004; Dapčević-Hadnađev et al., 2019). Hemp seed proteins are comprised of about 25-37% albumin and 67-80% globulin and have no protease inhibitors. The absence of protease inhibitors in hemp seed proteins could improve protein digestibility (Aluko, 2017). In fact, it has been described that the protein digestibility from hemp seeds (~ 90%) is higher than that of soy protein isolate (around 71%) (Wang et al., 2008).

#### 2.1.2.1 Globulin

The globulin, so-called edestin, is the main storage protein in hemp seed, comprised mainly of 11S legumin-type and 7S vicilin-type globulin protein (Aluko, 2017). The 11S globulin predominates in hemp globulins, which represent about 93% of globulins and 65% of total proteins. However, the 7S globulin only represents about 7% of globulins and 5% of total proteins (Potin & Saurel, 2020). The 11S and 7S proteins could be separated by pH

precipitation, in which pH 6.4 could precipitate 11S protein and pH 4.6 could precipitate 7S protein (Wang et al., 2008).

The 11S globular edestin is a homohexamer (about 300 kDa) that is composed of six subunits (about 52 kDa) linked by non-covalent interaction, preferentially hydrophobic bonds (Aluko, 2017; Dapčević-Hadnađev et al., 2020; Patel et al., 1994; Wang et al., 2008). Each 11S edestin subunit is comprised of a basic subunit (2 bands around 18 and 20 kDa) and an acidic subunit (around 34 kDa), which is relatively homogenous (Potin & Saurel, 2020; Q. Wang, Y. Jin, et al., 2018). There are five cysteine residues found in each edestin subunit. Two cysteine residues form a disulphide bond linking the basic subunit and acid subunit. Within the acidic subunit, there are two cysteine residues forming an intrachain disulphide bond. The other cysteine residue keeps as a free thiol group (Chuang et al., 2019; Docimo et al., 2014; Tang et al., 2006), which may have an impact on the solubility and aggregation behaviour of edestin during processing. For example, under thermal treatment, the free thiol group may participate in thiol–disulphide exchange reactions, leading to the formation of new intermolecular disulphide bonds. This can contribute to protein aggregation and reduced solubility, which are critical factors influencing the techno-functionality of hemp protein in food applications.

The native 7S globulin (vicilin-type protein) is typically a trimeric structure with molecular weight of approximately 150–190 kDa. Unlike the majority of 11S globulins, 7S globulin is generally glycosylated and cannot form disulphide bonds (Bárta et al., 2023; Cattaneo et al., 2021; Kesari et al., 2017; Lawrence, 1999; Sun et al., 2021).

#### 2.1.2.2 Albumin

The albumin fraction in hemp seed proteins constitutes around 20%, which is composed mainly of 7 polypeptides (6-35 kDa, mainly below 18 kDa). No interchain disulphide bond was found in the albumin, and the reducing agent didn't affect the structure (Potin & Saurel, 2020). The less disulphide-bonded proteins in albumin contribute greater flexibility and less compact structure compared with other globular proteins (Malomo & Aluko, 2015a). The flexible hydrophilic structure could prevent folding and keep the residues in the water environment, resulting in high solubility, which is around 57% at pH 3 and 84% at pH 8. The high degree of flexibility of albumin is also confirmed by the low intrinsic fluorescence value. However, albumin has a more ordered secondary structure and little tertiary conformation at pH 3, while the tertiary conformation increases at pH 7 and 9 (Aluko, 2017; Potin & Saurel, 2020). In addition, cystine-rich and methionine-rich 2S albumin (10 kDa) was found in hemp proteins, consisting of one small and one large subunit (3 kDa and 7 kDa) linked by 2 disulphide bonds. The large subunit contains 6 cysteine and 5 methionine residues, while the small subunit contains 2 cysteine and 3 methionine residues (Odani & Odani, 1998; Potin & Saurel, 2020; Wang & Xiong, 2019).

### 2.1.3 Functionality of hemp proteins

#### 2.1.3.1 Solubility

Solubility is an important functionality, as generally, proteins are required to be solubilised before use. The solubility of proteins depends on intrinsic factors (presence of polar and non-polar amino acids) and extrinsic factors, such as pH, ion strength and temperature. In general, when attractive forces (e.g. electrostatic, hydrogen, hydrophobic interactions) are smaller than repulsive forces, protein solubility is increased (Sathe, 2012).

Globulins are insoluble in water but soluble in salt (e.g. NaCl) solutions (Malomo & Aluko, 2015a). Hemp globulin has a U-shape pH solubility profile in water with low solubility at pH 4-7 and reaches the lowest solubility at ~ pH 5, which is closer to its isoelectric point (Potin & Saurel, 2020). The occurrence of globulin aggregates may contribute to low protein solubility. Hemp globulin is soluble in alkaline conditions, and the dissociation of globulin would happen. Therefore, its solubility is around 38% at pH 7 and increases to over 90% when the pH is above 8 (Tang et al., 2006). Compared with other plant proteins, such as soy protein, hemp protein is less soluble because of the high free sulfhydryl content. This feature leads to extensive disulphide bonding among proteins, followed by their aggregation at neutral or acidic pH (Potin & Saurel, 2020; Wang & Xiong, 2019). The water solubility of albumin is lowest at pH 3 and increases with an increase in pH. In general, albumin has a higher solubility than globulin because of its flexible structure and low level of hydrophobic and aromatic amino acids (Aluko, 2017; Potin & Saurel, 2020).

The extraction methods and conditions affect hemp protein solubility. Under alkali extraction followed by isoelectric precipitation (HPI), proteins partially unfold at high pH, exposing hydrophobic and polar side chains that promote protein–protein association. Upon adjustment to the isoelectric pH, electrostatic repulsion is minimized and the unfolded proteins aggregate yielding insoluble aggregates and low solubility at pH 7. In contrast, micellisation (salt extraction followed by dialysis/dilution) (HMI) solubilises globulins under mild ionic strength and then gradually removes salt, allowing proteins to retain a more native conformation, resulting in relatively high solubility. DSC and FTIR indicate greater denaturation and structural alteration for HPI than HMI (Dapčević-Hadnađev et al., 2019; Tang et al., 2006; Yin et al., 2008).

### 2.1.3.2 Thermostability

Thermostability against heat-induced denaturation plays a crucial role in the functionality of proteins for the food industry. A single endothermic peak in the thermogram, which is attributed to edestin, shows the denaturation temperature of hemp protein is 89–96 °C, and the onset temperature is about 81.8–86.7 °C (Hadnađev et al., 2018; Shen et al., 2020; Tang et al., 2006). Wang et al. (2008) reported that the heat-stability of pH-precipitated hemp protein isolates is dominated by 11S edestin, as there is no thermal transition of 7S edestin, while 11S edestin has a similar denaturation temperature as HPI (at 91.9 °C). The tertiary structure of hemp protein is affected by both hydrophobic interaction and disulphide bridge (Tang et al., 2006). Raikos et al. (2015) suggested that heating above 80°C causes denaturation of around 60-80% of the native hemp protein, forming insoluble aggregates via covalent interactions. Similarly, Yin et al. (2008) reported that a significantly lower protein solubility was observed after heating hemp protein at 95°C for 10 min. The studies of improving the heat stability of hemp protein were limited; thus, further research is required to explore this area.

### 2.1.3.3 Gelation

Diverse microstructures of protein gels can be created by controlling the interactions of protein molecular chains. Strong gelation may occur if there is a balance of the interactions of protein-protein and protein-solvent, while if there is a high extent of protein-protein interactions or the interaction time from denaturation to aggregation is short, the coagulum may be formed instead of gel (Arntfield & Maskus, 2011). Many methods have been used to induce protein gelation, including heating, salt addition, pH changing and enzymatic cross-linking. However, to date, only heat-induced gelation of hemp protein has been reported.

The gel induced by heating is the most common method in plant protein gels. The process of heat-induced plant globulin gels is similar to that of milk globulins. In general, there are 3 steps: denaturation (unfolding and exploring active sites), aggregation (forming small self-aggregates through covalent and noncovalent interactions) and gelation (formation of a three-dimensional network) (Zheng et al., 2022). However, there is still a challenge to conduct a detailed comparison of the properties of different protein gels (e.g. strength, stiffness, critical gel concentration) because of the various conditions (e.g. pH, protein concentration, salt level), low solubility and high denaturation and aggregation in plant protein materials (Nicolai & Chassenieux, 2019).

There is limited literature reporting the gelation properties of hemp protein dispersions. This may be due to the poor gel-forming ability of hemp protein ingredients since the high level of protein aggregation of hemp protein material induced by preheat treatment and isoelectric precipitation, which limits the flexibility for the formation of the gel network (Malomo et al., 2014). A minimum concentration of 22% isoelectric-precipitated hemp protein isolate is required to form heat-induced gels (Malomo et al., 2014). In addition, the heat-induced gel structures of hemp protein isolate obtained by the isoelectric (HPI) method and micellisation (HMI) method were different due to the molecular difference described above. HPI gels, formed from pre-aggregated and partially denatured proteins, displayed granular and low-porosity networks. However, HMI gels, formed from more native-like, soluble proteins, formed filamentous networks which were more open and elastic with larger pores. Up to 300 mM NaCl addition hardly affects the microstructure of HPI gel, while increasing the pore size of HMI gel (Dapčević-Hadnađev et al., 2018; Malomo et al., 2014).

### 2.1.3.4 Emulsification

The emulsifying activity of hemp protein isolate was similar to the protein solubility as a function of pH from 3 to 8, where the lowest value was observed at its isoelectric point, suggesting the correlation between protein solubility and emulsifying activity (Tang et al., 2006). Generally, the emulsification property of hemp protein is relatively poor when compared with other proteins, such as canola protein (Teh et al., 2014). In addition, hemp protein exhibited lower emulsifying activity and stability when compared with soy protein, which is considered a plant protein standard (Tang et al., 2006). It is possibly because hemp protein has a higher tendency to form disulphide bonds, leading to aggregation at neutral and acidic pH.

Limited studies have been conducted to improve the emulsifying properties of hemp protein. The micellisation extraction method (dialysis salt-solubilised protein) could keep the protein in the native state and prevent aggregation, resulting in relatively high protein solubility (Dapčević-Hadnađev et al., 2019; Tang et al., 2006; Yin et al., 2008). However, it showed a high level of creaming and coalescence compared with emulsions stabilised with isoelectric precipitated proteins. The limited exposure of hydrophobic groups may reduce the protein's ability to interact effectively with the oil phase, which can compromise the emulsion stability (Dapčević-Hadnađev et al., 2019; Malomo & Aluko, 2015b). Moreover, the hydrolysis of hemp protein did not improve emulsification activity, possibly because the hydrolysate aggregates may inhibit the formation of the viscoelastic membrane around oil droplets in an emulsion system (Yin et al., 2008).

Overall, the functionality of hemp proteins is limited by their poor solubility and heat sensitivity, which in turn compromise their gelling and emulsifying properties. Therefore, it is necessary to explore the possible solutions to improve the functionality of

hemp protein, especially commercial hemp protein powder, and to promote its application in the food industry.

## 2.2 Milk proteins

Bovine milk consists of water, fat, lactose, proteins and minerals. About 1-2% of total milk proteins and phospholipids stabilise the fat (98% triglycerides) as an emulsion (Dewettinck et al., 2008). Lactose and some minerals are dissolved in water, while the rest of the minerals and most milk proteins are suspended in water as a colloidal suspension. Milk usually contains 3.5% proteins, which greatly influence the functional properties and nutritional value of food products. Milk protein can be classified into two categories: caseins (about 80%) and whey proteins (about 20%) (Boland & Singh, 2019).

### 2.2.1 Whey protein

Whey proteins make up 20% of total milk proteins, principally consisting of β-lactoglobulin (β-lg), α-lactalbumin (α-la), bovine serum albumin (BSA), immunoglobulins (Igs) and lactoferrin (Singh, 2009). Whey proteins recovered from cheese processing are referred to as ‘sweet whey’, while those recovered from acid are called ‘acid whey’. Sweet whey has caseinomacropeptides that are absent in acid whey (Boland, 2011). Whey proteins are a group of acid-soluble proteins with a relatively more ordered globular structure compared with caseins. However, whey proteins are heat-sensitive and can denature above 60°C (Brodkorb et al., 2016; Kilara & Vaghela, 2018). **Table 2-3** shows their general characteristics.

**Table 2-3: General characteristics of whey proteins.**

| Milk protein fractions | Protein% in fraction | Isoelectric point | Molecular weight (kDa) | Denaturation temperature | Number of disulphide bonds |
|---|---|---|---|---|---|
| **β-lactoglobulin** | 51 | 5.2 | 18.4-36.9 | 74-76°C | 2 |
| **α-lactalbumin** | 19 | 4.1 | 14.2 | 66-67°C | 4 |
| **Bovine serum albumin** | 6 | 4.8 | 69 | 62°C | 17 |
| **Immunoglobulins** | 12 | 5.5-8.3 | range | range | 21 |
| **Lactoferrin** | 1-2 | 8-9 | 78 | 70 and 90°C | 17 |

Adapted from Kilara and Vaghela (2018); Kim et al. (2020); McClements and Grossmann (2021).

β-Lactoglobulin (β-lg) comprises 10% of milk proteins and 50% of whey proteins. The molecular weight of β-lg is ~ 18.4 kDa, and its hydrodynamic radius is ~ 2 nm. There are two genetic variants of β-lg in which the aspartic acid in 'variant A' is substituted by glycine in 'variant B'. It contains 2 intramolecular disulphide bonds and 1 free sulfhydryl group. β-lg exists as a monomer when pH is higher than 8 or lower than 3, but it exists as a dimer (36.6 kDa) linked by non-covalent interaction under neutral pH and room temperature (Kilara & Vaghela, 2018). Changes in pH from 4 to 7.8 induce reversible conformational changes of β-Lg. When the pH is above 9, irreversible conformational changes occur because of the exposure of buried sulfhydryl and COOH groups under strongly alkaline conditions (Cheison & Kulozik, 2017). However, the unfolding of β-lg at low pH (2 to 3) is reversible due to the low thiol-disulphide interchange under acidic conditions (de la Fuente et al., 2002). β-lg is also relatively stable at low pH and resistant to pepsin proteolysis during digestion (Boland & Singh, 2019; Pelegrine & Gasparetto, 2005).

α-Lactalbumin (α-la) is the second most abundant whey protein. It is a compactly folded globular protein with a spherical shape, containing 4 disulphide bonds, binding a

calcium ion and no free thiol group and phosphate group. (Edwards & Jameson, 2020). High pressure can induce the unfolding of pure α-la to a reversible molten globule state at 200MPa due to the lack of free thiol groups and irreversibly lose native structure above 400MPa (Edwards & Jameson, 2020; Patel & Huppertz, 2014).

***Heat-induced denaturation of whey proteins***

The three-dimensional structure of whey proteins changes with elevated temperature and the whey proteins undergo unfolding, denaturation, and aggregation steps to form an open conformation structure (Brodkorb et al., 2016). The globular structure of native whey proteins is held by hydrogen bonding, van der Waals forces, electrostatic interactions and hydrophobic interactions. The thermal treatment can induce the rupture of these forces and result in the unfolds of proteins into random configurations. The unfolding causes the buried reactive chain groups, like hydrophobic side chains and free sulfhydryl groups exposed and is usually reversible, but they tend to interact with other proteins. Through the sulphydryl-disulphide interchange and hydrophobic interaction, the unfolded whey proteins would associate with each other and finally create large aggregates in the form of gel and precipitates (Singh & Havea, 2003).

β-lg can unfold under 78°C and starts aggregation at 78°C mainly through disulphide bonding and to some extent through hydrophobic interactions (Sava et al., 2005). The aggregation of β-lg is sensitive to pH since the accessibility and reactivity of thiol groups are dependent on pH. When pH is between 7 and 8.5, the thiol group has higher reactivity and is more available for reactions, while when pH is below 7, the protein needs to be heated to unfold and expose the thiol group. The rate of native β-lg turning to aggregates increases with the increase in pH from (pH 6.4-8), while the disulphide bond

interaction is not likely to occur at acidic pH (2-3) since the thiol groups are stable at low pH (de la Fuente et al., 2002).

Although α-la has a lower denaturation temperature than β-lg, α-la is heat stable in the absence of other proteins and can remain soluble at 100°C under favourable pH and calcium concentration conditions. This is because α-la lacks free thiol groups and can refold after heating (Kilara & Vaghela, 2018). Usually, proteins are more heat-sensitive in the presence of calcium since the calcium ionic intermolecular binding can cause aggregation during heating. However, calcium can form intramolecular ionic binding in α-la and promote the resistance to thermal unfolding (Kilara & Vaghela, 2018). In the presence of β-lg or BSA, heat-induced aggregates such as α-la-β-lg, α-la-BSA or α-la-α-la oligomers can be formed due to the participation of the free thiol groups from β-lg or BSA (Edwards & Jameson, 2020).

In heated milk, β-lg can associate with κ-casein on the surface of casein micelles through disulphide bonds. The extent of the association is dependent on the pH and heating conditions. About 30% of denatured whey proteins can associate with casein micelles, while an increasing amount of whey proteins bind with casein micelles at lower pH (Kethireddipalli et al., 2011). When heated at 75-90°C for 80 min, all β-lg can associate with casein micelles, while 130°C for 100s can only allow half of the β-lg to associate with casein micelles, although it denatures all β-lg (Corredig & Dalgleish, 1996; Oldfield, Singh, et al., 2005).

### 2.2.2 Caseins

Caseins are a mixture of phosphoproteins (Kim et al., 2020) and can be fractionated into four proteins, which are $\alpha_{s1}$-, $\alpha_{s2}$-, β- and κ-casein, with a weight ratio is about 38: 10:

36: 12 (Wusigale et al., 2020). Their molecular weights are about 19 -25 kDa, and isoelectric points are between 4.1 to 5.3 (Augustin et al., 2011; Boland & Singh, 2019; Dewettinck et al., 2008; Wusigale et al., 2020). All types of caseins have phosphate groups esterified to the serine residues (Singh, 2009). The phosphorylation enables the caseins to bind with ions (Dalgleish, 2011). Generally, caseins lack secondary and tertiary structures and are considered very hydrophobic proteins. **Table 2-4** shows their general characteristics.

**Table 2-4: General characteristics of caseins.**

| Milk protein fractions | Isoelectric point | Molecular weight (kDa) | Total number of amino acids | Number of phosphoserine residues | Non-polar residues (%) |
|---|---|---|---|---|---|
| **$\alpha_{S1}$-casein** | 4.4-4.8 | 23.6 | 199 | 8 | 36 |
| **$\alpha_{S2}$-casein** | 4.9 | 25.2 | 207 | 11 | 40 |
| **β-casein** | 4.8-5.0 | 24.0 | 209 | 5 | 33 |
| **κ-casein** | 3.5 | 19.1 | 169 | 1 | 33 |

Adapted from Huppertz et al. (2018); Kim et al. (2020); Wusigale et al. (2020).

The protein $\alpha_{S1}$-casein is moderately hydrophobic and contains 25 positively charged and 40 negatively charged amino acid residues. There are 13-15% α-helix, 34-46% β-sheet and 29-35% turn structures in $\alpha_{S1}$-casein. It has strong self-association and precipitates at pH 4 to 5 or in the presence of calcium at neutral pH (Huppertz et al., 2018; Malin et al., 2005). Similarly, $\alpha_{S2}$-casein has self-association behaviour but can precipitate at lower calcium concentrations than $\alpha_{S1}$-casein. The protein $\alpha_{S2}$-casein contains two Cys residues that can form intramolecular or intermolecular disulphide bonds with other $\alpha_{S2}$-caseins. Native $\alpha_{S2}$-casein appears mainly as a dimer (Huppertz et al., 2018). Different studies showed a variable estimate of the secondary structure of $\alpha_{S2}$-caseins. For instance, Farrell et al. (2009) reported 46% α-helix, 9% β-sheet and 12% turns, while Hoagland et al. (2001) reported 24%–32% α-helix, 27%–37% β-sheet and 24%–31% turns in $\alpha_{S2}$-casein.

β-Casein, another major type of casein in milk, is an amphipathic protein because the C-terminal contains a significant number of highly hydrophobic and weakly charged non-polar residues, while the N-terminal contains a considerable amount of charged molecules with low hydrophobicity. Under 5°C, most β-caseins present as monomers, while β-casein self-associates with the increase in temperature (Huppertz et al., 2018).

κ-Casein is the smallest casein in the milk casein family, containing a few phosphate groups compared with the other types of caseins. This results in fewer interactions with ions and low calcium sensitivity. However, κ-casein plays an important role in protecting the stability of casein micelles. Although half of κ-casein in milk is not glycosylated, κ-casein is the only type of casein that has the chance to be glycosylated (McSweeney & Fox, 2003). Similar to $\alpha_{S2}$-casein, κ-casein also contains two Cys residues that can form monomeric κ-casein (less than 10% of the total κ-casein) by intramolecular disulphide bonding and multimeric κ-casein (oligomers with more than 8 κ-casein monomers) by intermolecular disulphide bonding. The protein κ-casein is sensitive to heat treatment (above 90°C) compared with other individual caseins (Farrell et al., 2006; Huppertz et al., 2018).

The structure of caseins is flexible and open and this contributes to their thermal stability. Both $\alpha_{S1}$- and $\alpha_{S2}$-caseins are unfolded proteins with coil-like conformation. However, β- and κ-caseins have compact structures and present as molten globule-like proteins with a high degree of hydration and side-chain flexibility (McSweeney & Fox, 2003).

All caseins have a tendency to self-associate when individually dispersed in aqueous media and the environment, such as ionic strength, pH and temperature, strongly affects the extent of association. However, caseins also have a tendency to associate with

each other when jointly dispersed in the same aqueous media. β-casein is associated with $\alpha_{S1}$-casein with a smaller particle size than β-casein self-association (Farrell et al., 2006; Huppertz et al., 2018). It has been observed that the interaction of $\alpha_{S1}$- and κ-casein are stronger than the interaction of $\alpha_{S1}$- and β-casein (Huppertz et al., 2018).

### 2.2.3 Milk protein ingredients

In this study, the milk protein source was predominantly whey protein isolate (WPI), with some work using sodium caseinate (NaCas). Individual casein molecules can be separated by rennet and acid precipitation casein (by adding NaOH to achieve pH 4.6). The casein curds are then washed with water to remove whey proteins, lactose and minerals. The dewatering process would be carried out to dry the washed curds, followed by mixing with NaOH or $Ca(OH)_2$ to increase the pH to 6.7 – 7 to solubilise the caseins. The solution is then spray dried to obtain sodium caseinate or calcium caseinate (Singh, 2009). Sodium caseinate has good emulsification and foaming capability since the major caseins ($\alpha_{s1}$ and β) are amphiphilic, flexible and can provide strong electrostatic and steric repulsion. Sodium caseinate also has high heat stability and does not denature and aggregate under thermal treatment because it is relatively unstructured and there are no cysteine residues in $\alpha_{S1}$- and β-casein (Huppertz et al., 2018).

In WPI, whey proteins are mainly kept in their native state and have great solubility, acid stability, emulsification and foaming capability. However, the denaturation of whey proteins at high temperatures would result in protein aggregation with different morphologies, which are spherical particles, flexible strands, semi-flexible fibrils and fractal clusters (Nicolai & Durand, 2013). The protein was unfolded by heating to expose the hydrophobic groups and free thiol groups, followed by protein molecule aggregation

via covalent and non-covalent interactions, which may lead to a 3-dimensional network if the protein concentration is higher than the critical concentration (Mahmoudi et al., 2007; Pelegrine & Gasparetto, 2005). The network arrangements could be controlled by manipulating environmental conditions like temperature, ionic strength and pH to result in filamentous and particulate gels (Chen et al., 2006; Lefevre & Subirade, 2000).

pH plays an important role in WPI aggregation. When the pH is close to the pI of protein and ionic strength is low, or the pH is away from the pI of protein and ionic strength is high, the electrostatic repulsion is reduced and the protein molecules tend to form large spherical aggregates, which lead to the formation of particulate gels (Morris, 2009). β-lg at pH 5 still presents as a dimer form, and heating at 80°C results in a particulate gel with large β-lg aggregates (Lefevre & Subirade, 2000). However, when pH is far from the pI of the protein and ionic strength is low, the electrostatic repulsion is enhanced, and the protein tends to form filamentous gels with flexible linear strands (Lucey, 2017). Heating β-lg at pH > 6 or < 4 dissociates the native dimers below 75°C and then aggregates with each other when the temperature is above 80°C. The presence of electrostatic repulsion restricts the formation of large protein aggregates and makes the unfolded protein align in a linear strand. The morphology of protein aggregates has a great impact on the functional properties. Compared with particulate gels, which are relatively weak, coarse and brittle, the filamentous gels generally have better gel properties in terms of elasticity, strength and water holding capacity since the parallel alignment of polypeptide chains in filamentous gels favors more and stronger intermolecular interactions (Lefevre & Subirade, 2000; Lucey, 2020).

## 2.3 Protein interactions

### 2.3.1 Molecular forces in protein interactions

Proteins can be identified by their structures, including primary, secondary, tertiary and quaternary structures (Rehman et al., 2021). The microstructure of protein can be modified by molecular forces such as covalent disulphide linkages and non-covalent interactions (hydrogen, hydrophobic and electrostatic forces, van der Waals forces and steric repulsive forces). These forces can induce protein-protein interactions and change their functional properties like solubility, emulsifying ability and gelling ability (Alrosan et al., 2021).

The molecular forces are involved within a single protein molecule and the interactions with other proteins. The most common interactions are disulphide bonds, electrostatic interactions, hydrogen bonding, hydrophobic forces and van der Waals forces, which are shown in **Fig. 2.1**.

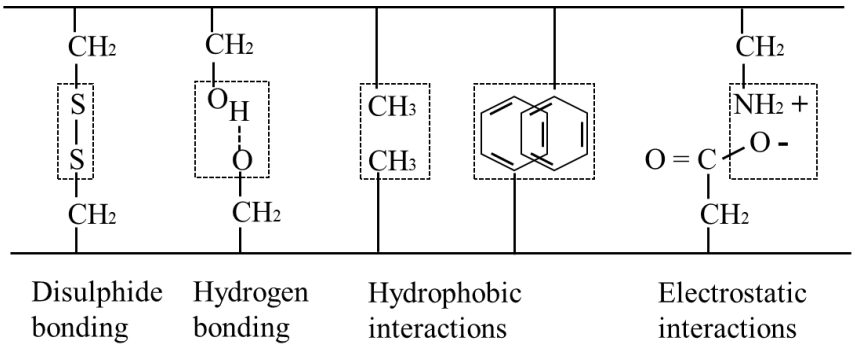


**Fig. 2.1.** Common protein-protein interactions

### 2.3.1.1 Covalent interactions

The peptide bond is covalent in the primary structure, while it will not be broken during denaturation unless it undergoes strong alkali, acid and enzyme treatment. The disulphide bond is the most common covalent bond affected by denaturation and changes the tertiary structure. A disulphide bond is formed between the thiol groups of cysteine, and the heat of formation of the bond is about 50 kcal/mol (Howell, 1992). Heating and high pH in the presence of oxidising agents can induce the formation of the disulphide linkage. The buried thiol groups or disulphide bonds in native proteins are exposed under heating and become chemically reactive. The reactivity of free sulphydryl is related to its pKa. The pKa of free Cys is about 8.3 and above this pH, the more reactive deprotonated thiolate groups ($S^-$) will be more than the non-reactive thiol group (SH), which can lead to a higher chance to create disulphide bonds between cysteine through sulfhydryl oxidation (**Fig. 2.2A**) (de la Fuente et al., 2002). The thiol/disulphide exchange interaction can also happen subsequently. The oxidised thiolate group can interact with another disulphide bond to break the old bond and form a new disulphide bond (**Fig. 2.2B**). High pH can induce a higher reaction rate of thiol/disulphide exchange and sulfhydryl oxidation. On the other hand, the reversible unfolding of β-lg in 7 M urea between pH 2.5 to 3.5 was found, since the protonated thiol groups are less likely ot form thiol-disulphide interchange participates (Pace & Tanford, 1968). However, the disulphide bonds in milk proteins can be formed at neutral and lower pH under thermal treatment. The higher temperature may lead to more unfolding of proteins and more exposure of free thiol groups and disulphide bonds, which could result in a higher reaction rate of thiol/disulphide exchange (Visschers & de Jongh, 2005).

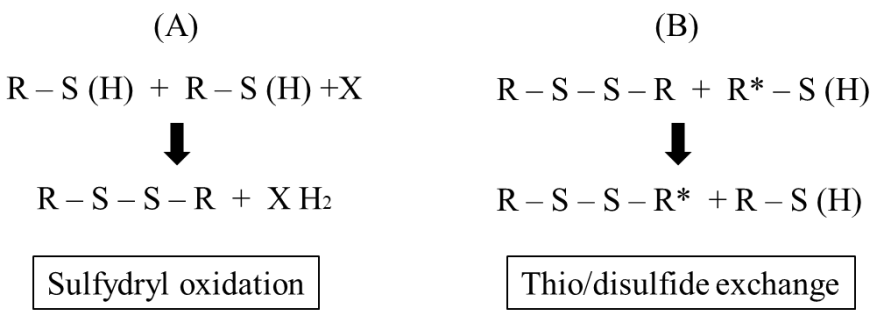


**Fig. 2.2.** Disulphide bond formation.

### 2.3.1.2 Non-covalent interactions

#### *2.3.1.2.1 Hydrogen bond*

The hydrogen bond is a type of short-range electrostatic bond between polar molecules with 1-6 kcal/mol energy. The electronegative atom (nitrogen, oxygen, sulfur or fluorine) and other partially negative groups (e.g. C=O) share a partially positive hydrogen atom (Howell, 1992). Hydrogen bonds play an important role in maintaining secondary and tertiary structures (Li-Chan & Lacroix, 2018). Hydrogen bonds can appear intermolecular or intramolecular to build the protein network. Moreover, they are weak at high temperatures and strong at cooling. This feature would impact protein folding and unfolding to expose hydrophobic groups, cysteine groups and disulphide bonds (Semenova & Dickinson, 2010). Hydrogen bonds are important interactions in the gel network to stiffen the protein network during cooling, and they usually work with other interactions.

#### *2.3.1.2.2 Hydrophobic interactions*

Hydrophobic interactions happen between non-polar groups with non-polar side chains or amino acids containing aromatic groups. The exposed non-polar groups would induce the disruption of the hydrogen bonding structure of surrounding water molecules

and change the entropy, which is thermodynamically unfavourable. Therefore, the water molecules would rearrange around non-polar groups and strongly interact with each other through hydrogen bonding. The absence of water molecules, in turn, leads to the attractive force between the non-polar groups, minimising the contact area between non-polar groups and water molecules. The entropy increases to reach a thermodynamically stable state (Wang et al., 2012). The hydrophobic interactions become strong with the increase in temperature up to around 60 °C, which largely affects the initial development of the protein network during gelation (Scheraga et al., 1962). Hydrophobic interactions play an important role in emulsion stabilisation and gel formation, which contribute to the adsorption of protein on the O/W interface and the development of the protein network, respectively.

#### *2.3.1.2.3 Electrostatic interactions*

The charged side chain of a protein contributes to the electric charges. Therefore, electrostatic interactions occur between the charged protein molecules. The electrostatic interactions can occur at large distances. The pI of the protein, salt concentration and pH environment affect the charge of the protein. When the pH is above or below pI, the protein is charged negatively or positively, respectively. Protein molecules are attractive when they have opposite charges and repulsive when they have like charges. Moreover, when the pH is close to pI, there is no surface charge on protein molecules, and protein precipitation occurs due to other driving forces such as hydrophobic interactions and hydrogen bonding (Howell, 1992). Besides, the protein structure would be affected by a strong electrostatic repulsive force if the pH is away from pI, which may promote protein unfolding and molecular flexibility (Lefevre & Subirade, 2000).

#### *2.3.1.2.4 Van der Waals interactions*

The transient charge induced by the shift of the electron density of molecules could result in the attractive interactions of nearby molecules. This weak attractive short-range force between polar or non-polar molecules is referred to as Van der Waals interactions, which exist among all types of molecules with similar magnitudes and have only a minor influence on the protein conformation in solution. However, when two molecules are very close, the overlapped electron clouds would induce a strong repulsive force to override the attractive force. When the biopolymer is as large as a colloidal particle, it might have a strong van der Waals attraction to promote the aggregation (Bryant & McClements, 1998; Howell, 1992).

### 2.3.2 Studies of plant protein–milk protein interactions

The studies on the aggregation or gelation of individual milk proteins or plant globular proteins, e.g. whey proteins, caseins, soy proteins and pea proteins, have contributed to our understanding of the mechanisms underlying protein-protein interactions and clarified the structure-function relationships (Chen et al., 2006; Clark et al., 2001; Forte et al., 2015; Maltais et al., 2009; Wang et al., 2012). However, the studies to explore the interactions in plant and milk protein combinations are still limited. The compilation of the studies concerning interactions in plant/ milk protein combinations is shown in **Table 2-5**.

**Table 2-5: Compilation of the studies of interactions in plant/milk protein combinations**

| Plant protein | Milk protein | System | Highlights | Reference |
|---|---|---|---|---|
| Pea proteins | β-Lg | Co-aggregates | New disulfide bonds and non-covalent interactions | Chihi et al. (2016) |
| Pea proteins | WPI | Co-precipitates | Disulphide bonds and electrostatic interactions | Kristensen, Christensen, et al. (2021b) |
| Pea legumin | β-Lg | Co-precipitates | Disulphide bonds, hydrophobic and electrostatic interactions | Kristensen, Christensen, et al. (2021a). |
| Pea proteins | WPI | Co-precipitates | Improved solubility and foaming capacity. | Kristensen, Denon, et al. (2021) |

| | | | | |
|---|---|---|---|---|
| Pea proteins | Casein micelle | Co-aggregates | Heating and high hydrostatic pressure induced soluble co-aggregates via disulfide bonding. | Serrano León et al. (2024) |
| Pea proteins | Casein micelle | Solution/ Gel | Absence of interaction increases the stiffness and firmness of the acid gel. | Beghdadi et al. (2022) |
| Pea proteins | Casein micelle | Gel | Gel properties depended on preheating route; blending ratios and preheating yield stronger, more homogeneous networks. | Xia et al. (2024) |
| Pea proteins | Casein micelle | Gel | Ratio and temperature control multi-scale structure (SAXS, USANS) and rheology; hybrid gels show elastic strengthening at specific casein: pea ratios. | da Silva et al. (2025) |
| Pea proteins | Casein micelle | Gel | pH-shifting increases solubility, surface charge, reduces particle size; enhanced compatibility with | Silva et al. (2025) |

| | | | | |
|---|---|---|---|---|
| | | | caseins leads to improved gel hardness and WHC; dependent on blend ratios. | |
| Pea legumin and vicilin | Casein micelle | Solution | Absence of interaction | Mession et al. (2017a) |
| Pea globulin | β-Lg | Gel | Enhance the gel network and create a compact structure. | Chihi et al. (2018) |
| Pea proteins | WPI | Gel | Up to half of the WPI could be replaced by any of the pea proteins without compromising gel strength. | Kornet, Shek, et al. (2021) |
| Pea globulin and albumin | WPI | Gel | Disulphide bonding in the pea albumin/WPI heat-set gelation formed the firmest gels with the least sensitivity to pH and ionic strength. | Kornet, Penris, et al. (2021) |

| | | | | |
|---|---|---|---|---|
| Pea legumin and vicilin | Casein micelle | Gel | No disulphide bonds between legumin and κ-casein; space-filling network in vicilin or pea protein-casein micelle acid gels. | Mession et al. (2017a) |
| Pea and soy proteins | Micellar casein | Gel | Soy and pea protein formed the gel independently of casein. | Silva, Cochereau, et al. (2019) |
| Pea and soy proteins | Micellar casein | Gel | Native GP influence gelation of casein by binding calcium, leading to an increase in critical temperature. | Silva et al. (2018) |
| Pea proteins | Sodium caseinate | Emulsion | The pea protein aggregate was disrupted and interacted with casein in the continuous phase due to high-pressure homogenisation. | Yerramilli et al. (2017) |
| Pea proteins | Sodium Caseinate or WPI | Emulsion | Synergistic effects of pea-caseinate or pea-WPI mixture. | Hinderink et al. (2019) |

| | | | | |
|---|---|---|---|---|
| Pea proteins | WPI | Emulsion | Transglutaminase crosslinking promotes β-LG adsorption, reduces interfacial viscoelasticity, and combination with maltodextrin improves droplet stability, preventing flocculation. | Kim et al. (2025) |
| Pea and soy proteins | Micellar casein | Emulsion | Heat-induced denaturation and aggregation of the globular protein; soy-casein emulsion had the highest heat stability. | Lin et al. (2017) |
| Pea and soy proteins | Micellar casein | Emulsion gel | Plant protein replaces the micellar casein and maintains the same stiffness. | Silva, Jacquette, et al. (2019) |
| Soy proteins | WPI | Gel | Soy/WPI complexes formed by disulfide bridges. | Roesch and Corredig (2005) |
| Soy proteins | WPI | Aggregates | Soluble aggregates after heating and size increased with increasing ionic strength. | Jose et al. (2016) |

| | | | | |
|---|---|---|---|---|
| 11S soy and sesame proteins | β-lg | Complexes | Disulphide bonds and hydrophobic interactions; Soluble soy/ β-lg complexes but insoluble sesame/ β-lg complexes. | Anuradha and Prakash (2009) |
| Soy proteins | Micellar casein | Gel | Absence of interaction | Beliciu and Moraru (2013) |
| Soy proteins | WPI | Gel | Soy protein acted primarily as particulate fillers, but the hydrophobic associations between soy and whey protein contribute to the elasticity. | McCann et al. (2018) |
| Soy proteins | WPI | Gel | The protein ratio is responsible for the predominance of the continuous network. | Comfort and Howell (2002) |
| Soy proteins | Micellar casein | Gel | Soy protein predominates the structure and rheological behaviour; casein may restrict the formation of a strong network. | Beliciu and Moraru (2011) |

| | | | | |
|---|---|---|---|---|
| Soy proteins | Casein micelles/ skim milk | Gel | Casein predominate in the gel network; the interaction with whey and soy can affect the gel strength. | Roesch and Corredig (2006) |
| Soy proteins | Skim milk | Gel | The network was predominated by caseins and soy protein improved gel strength. | Roesch et al. (2004) |
| Soy proteins | Sodium caseinate | Gel | Pre-heated soy aggregates improve the gel strength. | Martin et al. (2016) |
| Soy milk | Cow milk | Gel | Soy milk formed an acid gel, and casein worked as a filler, while the addition of rennet improved the soy-casein interactions. | Grygorczyk et al. (2013) |
| Rice proteins | Casein micelle | Co-aggregates | Tunable structure of co-assemblies via hydrophobic interactions by varying protein ratios. | T. Wang et al. (2019) |

| | | | | |
|---|---|---|---|---|
| Pea proteins | WPI | Co-precipitation | Co-precipitation was significantly affected by temperature, pH and protein ratio. | Kristensen et al. (2020) |
| Rice glutelin | Acid casein | Co-aggregates | Hydrogen bonds and van der Waals forces | He et al. (2020) |
| Zein | Sodium caseinate | Co-aggregates | Hydrophobic attraction and potentially electrostatic attraction. | Pan and Zhong (2016) |
| Zein | Sodium caseinate | Co-aggregates | Hydrophobic attraction and potentially hydrogen bonding. | Cuixia Sun et al. (2018) |
| Zein | Sodium caseinate | Co-aggregates | Hydrophobic interactions and encapsulation ability. | Wang and Zhang (2017) |
| Zein | WPI | Co-aggregates | Hydrophobic interactions and electrostatic attraction; core-shell structure complex with good physicochemical stability. | Wei et al. (2021) |

| | | | | |
|---|---|---|---|---|
| Rice proteins | Casein micelle | Co-aggregates | Improve the solubility of rice to above 90%; formation of rice protein/casein backbone in nanoparticles. | T. Wang et al. (2018) |
| Zein | WPI | Co-aggregates | Hydrophobic attraction and hydrogen bonding; core-shell structure; curcumin encapsulation. | Zhan et al. (2020) |
| Rice proteins | WPI | Complex | Hydrogen bond, hydrophobic force and electrostatic interactions. | R. Wang et al. (2019) |
| Napin | β-casein | Co-aggregates | Heat-reversible aggregation; temperature, salt, and chelating agents can control the aggregation. | Schwartz et al. (2015) |
| Rapeseed proteins | WPI | Gel | Formation of synergistic gels with increased moduli and decreased coarseness. | William Nicholas Ainis et al. (2019) |
| Napin | β-Lg | Assemblies | Charge anisotropy drives protein interactions; pH is related to potential phase separation. | W. N. Ainis et al. (2019) |

| | | | | |
|---|---|---|---|---|
| Soy proteins | Lactoferrin | Coacervates | Electrostatic interactions and hydrogen bonds; improved heat stability. | Zheng et al. (2020) |
| Pea proteins | WPC | Gel | Synergistic enhancement of elasticity and hardness. | Wong et al. (2013b) |
| Canola proteins | Whey proteins | Aggregates/Gel | Disulphide bonds; improved gelation capacity. | Momen et al. (2023) |
| Soy / Rice / Pea Proteins | MPC | O/W emulsion | Blending MPC with plant proteins improved solubility, emulsion stability, and viscosity control. | Khalesi et al. (2025) |

### 2.3.2.1 Interactions in co-aggregation

The protein-protein interactions are dependent on the intrinsic properties of the proteins (e.g. solubility, protein structure, molecular weight and presence of reactive groups) and processing conditions (e.g. heating temperature, pH and ionic strength) (Lin et al., 2017). The interaction and aggregation of proteins is commonly driven by external triggers, e.g. heat treatment and pH. Studying the behaviour of plant and milk proteins in aqueous dispersions is the basis for exploring the interaction mechanisms of network formation (gelation).

#### *2.3.2.1.1 Heat-induced interactions*

In a system with milk protein and plant proteins, the heat-induced interactions between whey protein and plant globulins via thiol-disulphide exchange reactions could be expected, since there are two disulphide bonds and one free thiol group in β-lg. Meanwhile, disulphide bonds and free thiol groups were reported in many plant globulins.

***Plant/whey protein aggregates***

The effect of heat treatment on the pea globulin-β-lg mixture has been studied by Chihi et al. (2016). They heated a soluble globulin and β-lg mixture at 85 °C for 60 min to produce globulin/β-lg aggregates. The surface hydrophobicity, sulphydryl content and SDS-PAGE results show that the protein-protein interactions were controlled by hydrophobic interactions and disulphide bonds due to the denaturation of globulin and β-lg and the exposure of hydrophobic groups and free thiol groups. The presence of β-lg controlled the particle size and formed globulin-β-lg aggregates with higher molecular weights and smaller diameters than the individual globulin aggregates. This indicates that

the interactions between plant and milk protein can be utilised as a method to create soluble blended protein material.

In the case of soy/milk protein combinations, disulphide bonds were formed between soy and whey proteins after heat treatment (90°C). The formation of soluble soy and whey protein aggregates was observed and can be inhibited by the addition of N-ethylmaleimide (NEM) (Roesch & Corredig, 2005).

The protein ratio and ionic strength are critical factors that can significantly influence the interactions. The higher whey: soy protein ratios would result in insoluble aggregates predominated by β-lg, soy β-conglycinin and basic subunits of soy glycinin. Anuradha and Prakash (2009) found that the increase of soy glycinin to β-lg ratio could raise the soluble protein content after co-heating. This suggested the impact of protein ratio on heat aggregation. Jose et al. (2016) reported soluble heat aggregation (95 °C for 60 min) of soy protein isolate and WPI blend (total 1% protein concentration, pH 7 and 0.1M ionic strength). The size of soluble aggregates increased with the reduction of soy protein proportion or an increase in the ionic strength to 0.3 M.

***Plant/casein aggregates***

When it comes to the other type of milk protein, casein, it could provide a chaperone-like effect, due to its unfolded, random and flexible conformation (Akbari et al., 2018). This function could assist in stabilising plant protein against precipitation rather than self-aggregation (Chuang et al., 2019).

However, studies have shown limited interactions between casein micelles and pea proteins under heat. Beghdadi et al. (2022) found that there was no size change when heating pea protein and casein micelles together at 85 °C for 60 min, indicating no

interaction between the two proteins. Mession et al. (2017a) reported a similar finding. They investigated the interactions between casein micelle and different pea protein fractions (11S legumin and 7S vicilin) through heat treatment (85 °C for 60 min). The legumin and vicilin showed self-aggregation through disulphide bonds and non-covalent interactions, respectively, while casein did not participate in the protein aggregates, and no disulphide bond was found between pea protein and casein. Interestingly, the individual pre-treatment of proteins can affect the protein-protein interactions. The heat-induced hydrophobic bonds were observed between individually preheated (85 °C for 60 min) pea protein and casein micelle mixture. This could be attributed to the increase in surface hydrophobicity of pea protein by preheating treatments (Beghdadi et al., 2022).

Similar to the finding in pea/casein co-aggregation work, there was no covalent interaction between soy protein and casein micelles after heat treatment (95 °C) since no new band was created in SDS-PAGE under non-reducing conditions. The 11S soy globulins aggregated themselves through disulphide bonds (Beliciu & Moraru, 2013).

When the protein combinations were presented on the oil/water interface, the globular protein (soy, pea and whey protein)-casein mixtures were used to stabilise the emulsion (10% protein and 10% oil) and underwent heat treatment (Liang et al., 2016). The heat treatment causes the denaturation and aggregation of the globular protein and reduces the heat stability of emulsions in terms of flocculation and viscosity change. The soy-casein emulsion had the highest heat stability while the whey-casein micelle had the lowest, which may be explained by the different globular protein-casein interactions discussed above.

#### *2.3.2.1.2 pH-induced interactions*

Changing the pH environment is an effective and economical method to modify the structure of proteins and promote protein-protein interactions. High alkaline pH can partially unfold globular proteins into a molten globule state (Jiang et al., 2010). The disordered tertiary structure of molten protein could promote the interactions between explored reactive groups that are retained after neutralisation (T. Wang et al., 2019). Meanwhile, the electrical charge on protein is greatly affected by pH conditions, which also leads to protein interactions (Sathe, 2012).

***Plant/whey protein aggregates***

Kristensen, Christensen, et al. (2021b) successfully created pea/WPI (20:80) co-precipitates by pH change (pH 11 to pH 4.6). They found that the covalent interactions significantly affect the protein co-precipitation since the high alkaline conditions can partially unfold the proteins and expose the free thiol group to facilitate the covalent interactions. The same phenomena are shown in legumin/β-lg co-precipitates, which are the main fractions of WPI and pea protein (Kristensen, Christensen, et al., 2021a). The pea/WPI co-precipitates improved the functionality of single pea protein, while they had low solubility and foaming capacity when compared with the simple pea and WPI blends (Kristensen, Denon, et al., 2021).

The zein/whey protein complex, prepared by adjusting pH from 12 to 7, exhibited excellent physicochemical stability. FTIR and dissociation tests indicated that the hydrophobic interactions and electrostatic attraction drove the complex formation. The author proposed a core-shell structure of the zein (core) /WPI (shell) complex with a spherical shape (Wei et al., 2021). Zhan et al. (2020) also observed a core-shell structure

of zein/WPI complex through transmission electron microscope images. The author used Fourier transform infrared analysis to determine that hydrophobic attraction and hydrogen bonding lead to the formation of complex. In addition, the bioactive component curcumin was successfully encapsulated in the complex and improve the solubility to aboce 0.65 mg/mL, indicating pH change is a feasible alcohol-free method for encapsulation.

***Plant/casein aggregates***

Casein micelles would be dissociated at an alkaline pH and resemble as smaller particles after neutralisation (Pan & Zhong, 2013). Controlling the dissociation and reassociation of caseins by pH change could be a method to create a hybrid protein complex without using an organic solvent. Zein and sodium casein were mixed at pH 11.5 and subsequently neutralised to pH 7.0, enabling the co-aggregation. It is proposed that soluble zein at alkaline pH could interact with dissociated casein. When the pH slowly decreased to 7, zein gradually lost its solubility, while the neighbouring casein could co-aggregate with zein via hydrophobic interactions and potentially electrostatic attraction. In addition, the segments from casein could provide steric hindrance and repulse electrostatic force to protect the complex from aggregation. The other studies also reported the zein/casein complex induced by pH-change with improved stability (Cuixia Sun et al., 2018) and have bioactive compounds encapsulation ability (Wang & Zhang, 2017; R. Wang et al., 2019).

Similarly, the rice protein (rice glutelin) and casein micelles were dissolved in an alkaline solution (pH 12), followed by neutralisation to create a protein complex via hydrophobic interactions. Using atomic force microscopy, cryo-transmission electron microscopy, and X-ray diffraction confirmed that the tunable structure from nanosheet to spherical particles could be achieved by varying casein: rice protein ratios from 9:1 to 7:3

(T. Wang et al., 2019). T. Wang et al. (2018) reported that the 1: 0.01 mass ratio of rice protein/casein could improve the solubility of rice protein to above 90%. They proposed that rice protein and casein interact under alkaline conditions and form a hybrid backbone which could retain the exposure of polar groups during acidification. These coexisting backbones packed together and formed nanoparticles.

#### 2.3.2.2 Interactions in gelation

When the protein-protein interactions occur at sufficiently high protein concentrations, gels can be formed with a three-dimensional network structure, which is stabilised by disulphide bonding and/or non-covalent interactions (Wu et al., 2021). The environmental factors, such as temperature, pH and ionic strength, would influence the exposure and interactions of the reactive groups of protein, thus affecting the microstructures and rheological properties. In addition, the mixing of two different types of proteins, e.g. plant/ milk protein combination, would also lead to interactions that differ from those observed in single-protein systems and can lead to diverse gel microstructures (Foegeding & Davis, 2011). Notably, the studies reported plant and milk protein interactions mainly using soluble fractions of plant protein.

##### *2.3.2.2.1 Heat-induced gel*

Heat-induced gel is built up by primary aggregates of denaturation of globular proteins linked by disulphide bonds and hydrophobic interactions. These aggregates extend to a network structure upon further heating. Most heat-induced gelation studies between plant and milk proteins used whey protein as the milk protein source. Kornet, Shek, et al. (2021) demonstrated that pea protein isolates could be considered as a substitution for whey

protein in heat-induced gel. Although the major driving forces of gelation were different between the two proteins, pea protein isolates under 15% protein concentration can form a gel with similar gel strength to WPI gel. When mixed WPI with pea protein isolates, half of the WPI can be replaced by pea protein isolates with no effect on gel strength, where the WPI dominated the gelation by forming a continuous network through hydrophobic interactions and disulphide bonding. Kornet, Penris, et al. (2021) further investigated the different pea fraction/WPI in heat-induced gels. The pea albumin/WPI mixture created the firmest gel compared with the pea globulin/WPI gel. This could be explained by the more disulphide bonds between albumin and whey proteins.

In terms of heat-induced soy/whey protein gelation, whey protein created the main network, and soy protein aggregates primarily worked as fillers, but the interaction with whey proteins can provide additional elastic properties. Generally, plant/whey protein can create a firm and homogeneous network with no phase separation (Hinderink, Boire, et al., 2021). Roesch and Corredig (2005) present the evidence of interaction between soy and whey proteins through disulphide bonds. The author also suggested that the protein ratio had a noticeable impact on the microstructure and rheological properties. McCann et al. (2018) also reported that whey protein is important in the network formation, and the ratio of soy to whey protein and their concentration are important to the gel properties and microstructures. Comfort and Howell (2002) reported the continuous phase formed by soy protein, which segregates whey proteins at 18% total protein concentration. When the soy protein to WPI ratio was about 85:15, the unstable gel was formed because the gel network is formed by soy protein, while the soy protein is not sufficient to fully segregate the whey proteins. The phase inversion was observed with the raising of the whey protein concentration. However, no apparent phase segregation was found in the heat-induced soy-WPI gel at 6% total protein concentration (Roesch & Corredig, 2005). This may be because

the large aggregates were removed before mixing proteins. In addition, at high soy protein proportions (100% and 90%), the gel could not able to be formed. When the soy proportion is 70%, the aggregates formed by WPI itself and soy-WPI proteins were observed, followed by the formation of the protein network. Ionic strength plays an important role in control protein-protein interactions and microstructure of gels. The increase in ionic strength in soy/ whey protein heat-induced gel results in coarseness of the gel structrure (Jose et al., 2016).

In contrast to the behaviour of soy/whey protein combination, heat-induced gels of soy proteins mixed with casein were structured by an independent gel network. The gel properties largely depended on the dominant protein and the minor protein presented as filler in the gel network. Beliciu and Moraru (2011) found a primarily soy protein network and the phase separation of casein micelles at 7.5% - 12.5% total protein concentration at 1: 1 protein mix ratio. In another study, no co-aggregation of soy and casein was observed (Silva, Cochereau, et al., 2019). As a result, the individual network of soy protein and caseins would lead to less rigidity of the heat-induced gel. They suggested that the addition of casein to plant protein may lead to a weaker and less homogeneous gel with large pores. Similarly, it is reported that the casein micelles negatively affected the gelation when total protein concentration was increased (Beliciu & Moraru, 2013).

Silva et al. (2018) compared the heat-induced gels made by different globular proteins (whey, pea and soy proteins) mixed with micellar casein. The critical temperatures of soy and pea protein were higher than those of whey protein. Pea and soy proteins exhibited higher critical gelation temperatures than whey, likely due to their ability to bind calcium from casein micelles, which restricted the formation of the casein network. In addition, soy protein showed greater calcium binding than pea protein. Meanwhile, the critical temperature decreases with the decrease in pH due to the reduced electrostatic

repulsion and more calcium release from casein micelles (Silva, Cochereau, et al., 2019). However, the gel stiffness increased in whey/casein gel since casein can interact with denatured whey protein to reinforce the gel network, while soy and pea protein formed the gel independently with casein.

#### *2.3.2.2.2 Acid-induced gel*

As a major type of cold-set gels, the acid-induced gels of blended protein were studied. Although heat-induced pea-casein micelle interactions were barely existing, the presence of pea protein can also impact the acid-induced gelling properties. The firmer and stiffer acid gel was formed by a heated pea-casein micelle mixture compared with heated whey-casein micelles. Not like heated whey-casein micelle, which acid gel was formed through covalent interactions, pea protein can first create an independent acid gel at a higher pH, followed by the other acid gel formed by casein micelle at a lower pH. The pea protein gel would be trapped in the casein micelle gel and work as a space-filler in the gel (Beghdadi et al., 2022). The different pea protein fractions would also affect the gel properties. Compared with the co-heated legumin-casein micelle acid gel, a higher $G'$ was obtained from co-heated vicilin-casein micelle gel, which is because of the more soluble vicilin aggregates and smaller particle size. Mession et al. (2017a) also observed that the space-filling network happened in pre-heated pea vicilin or total pea protein-casein micelle acid gels, while pre-heated pea legumin impaired the gelation, and no disulphide bonds were created between legumin and κ-casein.

It is suggested that the protein-protein interactions that occur in the preheated treatment are necessary before acidification to achieve better gel properties. The preheated pea globulins-β-lg co-aggregates can form a more elastic acid gel compared with those

from single pea globulin and the mixture of individually preheated pea globulin and β-lg. The single pea globulins or separately preheated protein created a soft gel with a more open structure and larger pores (Chihi et al., 2018; Guyomarc'h et al., 2021). The addition of whey protein can provide more disulphide bonds, which can enhance the gel network and create a compact structure (Chihi et al., 2018).

When it comes to the more complex system, soy protein/cow milk blends, the acid-induced gel had a higher $G'$ than that of a single skim milk powder gel when substituted milk protein with soy protein to soy: milk ratio at 3:7. The network was predominated by caseins and the presence of soy protein (2.7%) created a large pore size and increased the gelling pH due to the instability of soy proteins (Roesch et al., 2004). It is suggested that it is possible to use protein blends to make stronger gels. However, the protein mix ratio is important in controlling the rheological properties. In another study, the acid-induced gel of 0.18% soy proteins, 0.42% whey proteins, and 2.7% casein micelles mixture had similar elasticity to the mixture without soy proteins under this critical soy/whey protein ratio (Roesch & Corredig, 2006). It is reported that casein was responsible for the gel network, and the interaction of whey protein could enhance the gel strength, and the effect of interaction with soy protein could be suppressed under this concentration.

The combination of plant and milk proteins may control the gel structure. Individual milk gels have large pores and connected strands, while soy gels have packed soy protein aggregates. The soy/milk gel had a structure between the two individual gels. Grygorczyk et al. (2013) used soymilk and skim milk blends to create an acid-induced gel. At pH 6.5 - 5.6, only soy milk formed the gel and casein micelles worked as fillers with no interaction with soy protein. When adding both GDL and rennet into the milk blends, milk and soy milk both participated in a gel network with a lower $G'$ than the individual milk gel, indicating the different gel structure provided by protein blends.

In summary, plant and milk protein combinations with appropriate treatments seem to be an alternative approach to enhance the dispersibility and functionality of plant protein. Although the interactions behind the aggregation and gelation have been explored by some studies, the detailed mechanism in detail and tailoring of the aggregation behaviour of the mix protein system are still in need of further investigation.

### 2.3.3 Studies of hemp protein–milk protein interactions

There is very limited research on the interaction of hemp protein with milk proteins. Chuang et al. (2019) reported that sodium caseinate (0.2%) has a chaperone-like activity to inhibit the thermal-induced (90 °C) aggregation of hemp globulin (0.1%) under high ionic strength (0.5M), and a complex formed had good colloidal stability even at low ionic strength (0.17M). 2D SDS-PAGE confirmed that only κ-casein is complexed with hemp globulin through disulphide bonds. The change in surface hydrophobicity indicated that $\alpha_s$-casein and β-casein interacted with hemp globulin through non-covalent interactions. They suggested that individual hemp globulin was solubilised at high ionic strength and formed primary aggregates through disulphide bonds during heating. Due to the weak electrostatic repulsive force at high ionic strength, the following large aggregates were formed according to the diffusion-limited cluster aggregation (DLCA) regime, where the aggregation is only dependent on the diffusion of particles and no repulsive barrier in the system. However, the primary aggregates with steric hindrance were formed between the casein and hemp globulin through hydrophobic interactions and disulphide bonds. The further aggregates were smaller in size since the aggregation regime was changed to the reaction-limited cluster aggregation (RLCA) regime, which is a relatively slow aggregation with energy barriers.

In a subsequent study, Chuang et al. (2021) prepared a hemp globulin (1%)/sodium caseinate (0.5-2%) complex by pH cycling processing (from pH 7 to 12). The hemp globulin solubility was increased from around 25% to above 80%. Alkalisation converted the globular structure of hemp globulin into a molten, unfolded state. At this stage, disulphide bond dissociation and rearrangement happened to form new aggregates. The following pH neutralisation made the hemp globulin refold with lower solubility than its native state. When performing the pH cycling with hemp globulin/sodium caseinate mixture, the thiol-disulphide exchange occurred between the dissociated disulphide bonds from hemp globulin and κ-casein at high pH. At the neutralisation step, the hemp globulin was refolded and incorporated with sodium caseinate through hydrogen bonding. Some sodium caseinate exposed on the surface of aggregates provided steric hindrance and electrostatic repulsion to stabilise the aggregates. N-ethylmaleimide (NEM) pretreatment can block the free thiol groups of hemp globulin and lead to smaller aggregates after pH cycling, which suggests that disulphide bonds were important in the formation of the protein complex. The urea dissociation reagent or thermal treatment (60°C) did not dissociate the protein complex, which indicates that hydrogen bonding is essential in stabilising the aggregates. However, the disulphide bonds and hydrophobic interactions may not be critical to the protein complex since there was no dissociation after DTT and Triton X-100 treatment.

As discussed throughout this section, most research on milk/plant protein interactions has focused on soy and pea protein, which have demonstrated the potential for functionality improvement. However, most studies use only the soluble (non-precipitated) fractions of plant protein as study materials, which limits the applicability of the results to whole plant proteins. Research into the interaction mechanisms (including aggregation and gelation) of plant–milk protein mixtures is still in its early stages, especially given the wide

variety of plant protein sources available. To date, only the interactions between hemp protein and caseins have been reported, but there are no studies have investigated the interactions between hemp protein and whey proteins, highlighting a significant gap in current knowledge.

## 2.4 Microparticulated proteins

Understanding how proteins interact and how their structures link to functionality is essential for creating new food ingredients. Microparticulation is a technique to produce protein microparticles, typically combining thermal and mechanical treatments under specific pH conditions to achieve the desired particle size (usually 0.1-10.0 μm), surface-specific, internal properties and morphology (Beran et al., 2018). Microparticulated proteins are colloidal particles formed by mixtures of native proteins and protein aggregations (Shi et al., 2021). The thermal treatment induces the formation of insoluble protein aggregates through protein-protein interactions via mainly disulphide bonds and hydrophobic interactions, which were discussed in previous sections. Simultaneously or sequentially applying high shear could mechanically disrupt the growth of the aggregates, leading to different functionalities compared to their native forms (Dissanayake & Vasiljevic, 2009; Iordache & Jelen, 2003). In practical production, the drying process (usually spray-drying) is often applied after microparticulation, and it would not significantly affect the particle size, indicating good redispersibility of microparticulated protein (Toro-Sierra et al., 2013).

### 2.4.1 Microparticulated whey proteins

Whey proteins were the first processed by microparticulation and came out as the first patent in 1988 (Singer et al., 1988), followed by the commercial product launched, Simplesse®, by NutraSweet. Generally, microparticulated whey protein is produced by heat-induced aggregation at pH 4.0-5.5. Under these conditions, β-lg, α-la and BSA aggregate via covalent interactions and hydrophobic interactions. The shearing process disrupts the aggregates into particles with a size below 5 μm (Liu et al., 2011; R. Liu, Z. Tian, et al., 2018; Toro-Sierra et al., 2013).

To date, most studies of microparticulate protein have focused on whey proteins. Microparticulated whey protein has shown the advantage of enhancing the functionality (such as water holding capacity, gelation, rheological properties), as well as improved sensory properties (creaminess and lubrication) (Ipsen, 2017; K. Liu et al., 2016). These attributes enable broad applications, particularly as fat replacers in low-fat milk products like low-fat cheese (Sturaro et al., 2015), emulsions (Chung et al., 2014a) and yoghurt (Torres et al., 2011).

For example, in acid milk gels, the microparticulated whey protein has increased surface hydrophobicity, which may increase the gelation pH and hydrophobic interactions with casein (Morand et al., 2012). As a result, the incorporation of microparticulated whey protein could increase the porosity and reduce the firmness and storage modulus, which is due to the interaction between casein to create an open structure of the network (Silva & O'Mahony, 2018).

In low-fat yoghurt, removing fat would lead to a weaker gel network due to the increasing syneresis. The addition of microparticulated whey protein could work as an active filler to increase the elastic modulus and viscosity with a lower extent of syneresis

(Torres et al., 2018; Torres et al., 2016). The particle size of microparticles is a critical factor in the gelation. Small microparticles (below 1 μm) could improve the interaction with other proteins and lead to greater gel strength, whereas larger microparticles would inhibit the gelation and disrupt the coagulum, which leads to a weak gel network (Torres et al., 2016). Different from native whey protein, the microparticulated whey protein could prevent the formation of a dense protein network, since the dominant interactions are non-covalent interactions (G. Liu et al., 2016)

In emulsion, it has been proven that the emulsion stabilised with microparticulated whey protein has enhanced heat stability than that stabilised by standard whey protein concentrates, which is because fewer active sites in microparticulated whey proteins are available for heat-induced aggregation (Çakır-Fuller, 2015). Meanwhile, the reduced-calorie emulsions prepared with polysaccharides and microparticulated whey protein could achieve texture and appearance similar to standard emulsions (Chung et al., 2014b).

### 2.4.2 Microparticulated plant proteins

Compared to whey proteins, research on microparticulated plant proteins is still limited. As discussed in previous sections, plant proteins often exhibit poor solubility and limited functionalities. The microparticulation processing could be considered as a novel method to improve the functionality of plant protein, such as emulsifying properties (Shi et al., 2021). Due to the various aggregation behaviours of different plant proteins, the microparticulation methods for plant proteins are not limited only to the traditional heat-shearing processing, but some other techniques were also reported, such as pH-cycling, carbon dioxide-assisted spray nebulisation drying (CASND) and reduced-pressure

distillation. The compilation of the studies on microparticulated plant proteins is shown in **Table 2-6**.

**Table 2-6: Compilation of the studies in microparticulated plant proteins**

| Materials | Processing conditions | Highlights | Reference |
|---|---|---|---|
| **Canola proteins; Hemp proteins** | Carbon Dioxide Assisted Spray Nebulisation Drying (CASND) | Pilot-Scale production; improved solubility, emulsifying activity, emulsion stability and foaming capacity. | Beran et al. (2018) |
| **Soy protein hydrolysate/xanthan gum** | Heat treatment (10% solution, 90°C, 20 min) and homogenisation (8000 rpm, 6 min) | 8.7 μm average particle size; successfully replaced 50% fat in ice cream. | R. Liu, L. Wang, et al. (2018) |
| **Soy proteins/egg white proteins** | Heat treatment (15% solution, pH5.5, 95°C, 5, 10, 15min) and microfluidisation (50MPa, 2 passes) | Aggregated through disulphide bonds, spherical microparticles, better lubrication and heat stability. | T. Zhang et al. (2020) |

| | | | |
|---|---|---|---|
| **Zein proteins** | Reduced-pressure distillation (3% protein solution in 60% ethanol, pH 6.0, 20% w/w xanthan gum, 50°C, stirring 200 rpm) | 16 μm; fat substitution ratio for mayonnaise below 40% is acceptable. | Gu et al. (2016) |
| **Pea proteins** | Heat treatment (2.5% protein, 90°C, 60 min) and microfluidisation (7 or 130MPa, 3 passes) | < 150 nm, stabilised by disulphide bonds with higher surface hydrophobicity, reducing flocculation and creaming in emulsion. | Oliete et al. (2018) |
| **Mung bean proteins** | Heat treatment with homogenisation (5% protein solution, 83°C, 5–15 min, 17,000 rpm) and homogenisation (23,000–27,000 rpm, 5 to 20 min) and centrifugation (1000–4000 × g, 10 min) | 92% of 0.1–3.0 μm with 89% yield. | Sirikulchayanont et al. (2007) |

| | | | |
|---|---|---|---|
| **Zein proteins** | Colloidal milling (zein: water 1:3, 20,000 rpm) and microfluidisation (pH 3.86, 6.0, 8.0 and 10.0, first stage 50 MPa, second stage 125 MPa) | Small particles with open and porous structures obtained at pH 8.0. | Öztürk (2014) |
| **Wheat gluten proteins** | pH adjustment (pH 11 to pH 7.4) and $Na_2SO_3$ addition, and microfluidisation (50MPa) | SH-SS exchange; 1 – 2 μm; good flowability; lubrication effect similar to microparticulated whey protein. | Liu et al. (2025) |
| **Whey, potato and pea proteins** | Heat treatment with shearing (10°C above denature temperature,10 min, 100 – 1500 $s^{-1}$ shear rate) | Different interactions dominated in different protein aggregations. | Tanger, Quintana Ramos, et al. (2021) |
| **Pea and potato proteins** | Extrusion at 80°C and 130°C, and 800 rpm screw speed, pH 6.9 | Different microparticles influenced the milk dessert. | Tanger, Utz, et al. (2022) |

| | | | |
|---|---|---|---|
| **Pea proteins** | Extrusion 30-150°C and screw speed 200-1200 rpm | Hydrophobic interactions, almost the same creamy perception. | Tanger, Schmidt, et al. (2021) |
| **Soy proteins** | Heat treatment (95°C, 30 min, pH 5, 6 and 7) and microfluidisation (50 MPa) | pH 7: nano-scale microparticles; pH 5: micro-scale microparticles. | Lin et al. (2024) |
| **Soy proteins** | Heat treatment (93°C, 15 min, pH 3, 5, 7 and 9) and microfluidisation (110MPa for 1–3 passes). | pH 9: the smallest particle size (0.4 μm). | Monroy-Rodríguez et al. (2021) |

Tanger, Quintana Ramos, et al. (2021) compared aggregation behaviours of pea and potato proteins with whey protein during microparticulation. They found that whey protein microparticles were mainly aggregated through disulphide bonding, while potato protein microparticles were formed via hydrophobic interactions. Pea protein aggregates involved both mechanisms to a similar extent. The authors also confirmed that applying shear was critical for breaking down aggregates. Due to the structural and functional differences among various plant proteins, a universal aggregation model could not be established. In a later study, they examined the impact of these particles in a milk dessert system(Tanger, Utz, et al., 2022). Pea protein particles improved hardness and creaminess, while potato particles had a negative impact on the texture. This suggests that the impact of microparticles on food properties is highly protein-dependent. In another study, microparticles composed of soluble pea protein were formed through disulphide bonds. The microparticles were in the size of < 150 nm with improved surface hydrophobicity due to the rearrangement of particle structure. The emulsifying efficiency was improved, and it had a smaller droplet size and better stability, such as less flocculation (Oliete et al., 2018).

The appropriate pH could create plant microparticles with different sizes, morphology and rheological properties. Lin et al. (2024) explored the effect of pH (5 -7) on the soy protein microparticles. At pH 5, larger micro-scale aggregates were observed, while at pH 7, the particles were much smaller, at the nano-scale. The authors proposed that surface charge was screened at acid conditions, allowing hydrophobic and van der Waals forces to dominate, thereby promoting large aggregate formation. A separate study on zein protein found that alkaline treatment (pH 8) combined with microfluidisation produced particles with open, porous structures and improved water-holding capacity, hydrophobicity, and emulsion stability (Öztürk, 2014).

The methods, not limited to thermal-mechanical treatment, were used for microparticulation. Canola seed and hemp seed proteins were microparticulated by a novel Carbon Dioxide Assisted Spray Nebulisation Drying (CASND) technology in a pilot-scale (Beran et al., 2018). The results showed that the protein powders were about 600 nm average particle diameter with hollow spheres. Moreover, the foaming and emulsifying properties were improved by microparticulation. Liu et al. (2025) combine pH shifting, disulphide bond reductants and microfluidisation to produce wheat gluten protein microparticles. Disulphide–thiol exchange reactions were critical in particle formation, yielding 1–2 μm microparticles that exhibited good flowability. Meanwhile, it had a low friction coefficient, which obtained similar lubrication properties comparable to microparticulated whey protein.

In terms of microparticulation of hybrid systems, soy protein was mixed with xanthan gum (96:4 ratio) by heat-shearing treatment, generating 8.7 μm particles. The co-aggregation with xanthan gum helped system stabilisation. These particles could replace 50% of fat in ice cream without altering texture or appearance (R. Liu, L. Wang, et al., 2018). Zein/xanthan microparticles (about 16 μm) could replace the fat under 40% in mayonnaise without compromising the rheological, microstructure and sensory properties (Gu et al., 2016). To address soy protein's low free sulfhydryl content, egg white protein has been added as a donor, resulting in spherical particles (2–20 μm) with improved thermal stability and lubrication properties, suitable for high-protein beverages and semi-solid foods (T. Zhang et al., 2020).

Although most current applications of microparticulated proteins focus on fat replacement, their use should not be limited to this purpose. The application, such as gluten-free foods, high protein drinks and meat products, could be considered using microparticulated proteins to achieve specific protein functionality. Despite this potential,

current research remains focused on whey protein microparticles, while other proteins, such as plant proteins, which also have potential as microparticles, remain underexplored. The reduced solubility and large heat-induced aggregates during microparticulation processing cause the challenges of the utilisation of plant microparticles. Some studies removed the insoluble fraction or hydrolysed the plant protein to tackle these issues (R. Liu, L. Wang, et al., 2018; Oliete et al., 2018). The combination of plant and milk protein could be another feasible approach to restrict the extensive aggregation. However, little study to date has investigated the microparticulation of plant/milk hybrid proteins or their applications, presenting a significant research gap.

## 2.5 Emulsion

An emulsion is a dispersion system with two immiscible liquids, where one liquid is dispersed as spherical droplets (dispersed phase) in another surrounding liquid (continuous phase). The emulsion can be generally classified into three types. The oil-in-water (O/W) emulsion consists of oil dispersed in the continuous water phase. Conversely, the water dispersed in oil is a water-in-oil (W/O) emulsion. Above these two types, the O/W or W/O emulsions can act as dispersed phases in oil or water, creating oil-in-water-in-oil (O/W/O) or water-in-oil-in-water (W/O/W) emulsions (McClements, 2015). This study focuses specifically on O/W emulsions.

The process of forming an emulsion involves breaking up the oil phase into small droplets in the continuous phase, known as homogenisation, which applies high mechanical shearing energy, using a homogeniser, high-speed blender or microfluidiser. However, without stabilisers, pure oil and water tend to separate quickly because such mixtures are thermodynamically unstable. Therefore, to form kinetically stable emulsions for a period

of time, the emulsifier could be added to provide two most important functions: decreasing the interfacial tension between the oil and water interface and preventing droplet coalescence (Dickinson, 2015; McClements, 2007, 2015).

The emulsifiers are amphiphilic substances that can rapidly adsorb to the newly created interface of oil and water and act as a protective coating. The most commonly used emulsifiers in foods are small-molecule surfactants, biopolymers and some particulate materials (Dickinson, 2017). Various types of emulsifiers would largely affect the properties of their stabilised emulsions, such as stability, rheology, and microstructure. Proteins and polysaccharides are the two major polymers which are often used in food emulsification. In this study, we focused on the protein as an emulsifier. Amphiphilic proteins have both polar and nonpolar residues on the surface to produce desired water solubility and interfacial activity. The globular or flexible random coil structures of proteins would influence how they behave at interfaces. In addition, the stability of emulsions was determined by the electrical repulsion and steric hindrance provided by the protein layer formed at the interface (Dickinson, 2013; McClements & Jafari, 2018).

Milk proteins, including caseins and whey proteins, are considered effective emulsifiers, and their behaviour in emulsions has been extensively studied (Hu et al., 2003; Schröder et al., 2017). In contrast, plant proteins are not extensively used in food emulsions due to their relatively inferior emulsifying ability compared to animal proteins (Tang, 2017). Generally, a good protein emulsifier should meet three requirements: (1) fast adsorption, (2) good unfolding ability at the interface and (3) the ability to form a viscoelastic interfacial film (Damodaran, 2005). Most plant proteins do not meet these criteria because of their low solubility, tendency to aggregate, and rigid structures (Lima et al., 2023; Sarkar & Dickinson, 2020; X. Zhang et al., 2023). However, these same properties can be advantageous in a different approach. Researchers noticed that the low solubility of plant

proteins in both water and oil phase could be an adventage as particle emulsifiers in Prickering emulsions, offering an alternative strategy to conventional soluble emulsifiers.

### 2.5.1 Particle emulsifiers

Emulsions stabilised by particles are called Pickering emulsions since the first work by Pickering (1907). The particles could also adsorb on the interface and form a mechanical barrier to prevent the droplet from destabilisation (Dickinson, 2012). However, different from conventional molecular emulsifiers, whose adsorption is reversible, the particles require high energy for adsorption. Consequently, the adsorption is considered irreversible since the high desorption energy barrier (Tcholakova et al., 2008). Once anchored, the particles form a steric barrier to prevent Pickering emulsions from coalescence (Rayner et al., 2014). For instance, the microparticles that underwent microparticulation processing usually had higher surface hydrophobicity, encouraging stronger interactions at the interface and creating thicker, more stable films (Sun et al., 2015). In addition, microparticles can increase the viscosity of the continuous phase, slowing the movement of droplets and improving the stability against creaming (Sun et al., 2016).

Despite these advantages, the emulsifying performance is not always consistent, indicating the challenges of optimising particle emulsifiers. The opposite results of microparticles in the emulsifying stability were also reported (Dissanayake & Vasiljevic, 2009; Sun et al., 2016), since the absence of a standardised preparation method, which works for various types of proteins. It is worth noting that particle-stabilised emulsions tend to have large droplet sizes, because larger particles require more time and energy to reach and adsorb at the interface, which makes them have a high potential for gravitational creaming (Yang et al., 2017).

Therefore, it is important to carefully develop/modify the particle emulsifiers with a smaller particle size, better dispersibility and faster adsorption. For example, microparticulated whey protein had better emulsifying ability when prepared at low pH, since the size reduction was more significant at acidic pH compared to that at neutral pH (Dissanayake et al., 2012). Dissanayake and Vasiljevic (2009) suggested that partial heat treatment can expose hydrophobic groups, improving unfolding and adsorption at the interface. On the other hand, different from microparticulated whey protein, which prefers acidic modified conditions, microparticulated zein benefits more from alkaline treatment, which produces smaller particles and increases their loading on oil droplets, thereby enhancing emulsification performance (Öztürk, 2014).

Beyond whey proteins, plant proteins (such as legume and cereal proteins) are emerging as alternative proteins for particle-stabilised emulsions. Examples of plant protein particles stabilised Pickering O/W emulsions were listed in **Table 2-7**.

**Table 2-7: Examples of plant protein particles as emulsifiers for Pickering O/W emulsions**

| Protein types | Modification methods | Emulsion droplet size (μm) | Reference |
|---|---|---|---|
| **Zein** | Ultrasonication with stearic acid | 20-50 | Gao et al. (2014) |
| **Zein** | Ethanol precipitation | 100 | de Folter et al. (2012) |
| **Soy** | Soy suspension and ultrasonication | 0.5-1 | Gao et al. (2013) |
| **Soy** | SPI dispersion (pH 7), heat treatment (95 °C for 15 min) | 1 | Liu and Tang (2013); Liu and Tang (2014) |

| | | | |
|---|---|---|---|
| **Soy** | SPI dispersion (pH 7), heat treatment (100 °C for 30 min) | 25-80 | Liu and Tang (2016b) |
| **Soy** | SPI dispersion (pH 7), heat treatment (95 °C for 30 min) | 4-14 | Cui et al. (2014) |
| **Soy** | Add $Ca^{+2}$(5 mM), followed by GAD addition (50-200% equivalents) | 50 | (Liu et al., 2017) |
| **Soy** | Combination of pH (3 and 11) and high hydrostatic pressure (200 and 400 MPa for 10 min) | 24-61 | (Tan et al., 2021) |
| **Pea** | PPI dispersion subject to pH change (pH3) | 2-18 | (Liang & Tang, 2014) |
| **Pea** | PPI dispersion subject to pH change (pH3) | 8-22 | (Shao & Tang, 2016) |
| **Pea** | Heat treatment (95 °C for 1 h), blending (5 min), homogenisation (250/50 bar, two passes) | 25 | (S. Zhang et al., 2020) |
| **Wheat gliadin** | Dissolved in water/ethanol solvent; mixed with acetic acid; concentrated by rotary evaporator | 60 | (Hu et al., 2016) |
| **Sorghum kafirin** | Dissolve in acetic acid, followed by dialysis | 40-130 | (Xiao et al., 2016) |

| | | | |
|---|---|---|---|
| **Peanut** | Heat treatment (95 °C for 15 min), followed by NaCl addition (0–500 mM) | 30-60 | (Ning et al., 2020) |
| **Quinoa** | Addition of NaCl (0 – 500 mM), ultrasonication (100 W for 20 min) | 30 | (Qin et al., 2018) |
| **Hemp** | Anti-solvent precipitation (formic acid /water) | 0.3-0.5 | (Sun et al., 2023) |

Physico-chemical treatments (e.g., heat treatment, pH change and anti-solvent precipitation) are applied to optimise the particles' properties (Kim et al., 2020). Heat treatment for protein dispersions could be an efficient approach to preparing plant protein stabilisers. Soy proteins subjected to thermo-mechanical treatments to produce particles (Gao et al., 2013; Gao et al., 2014; Liu & Tang, 2013). The inter- and intar-particle disulphide bonds reinforced the internal structures of soy protein particles (Chen et al., 2014). It enhanced their interfacial activity and led to emulsions having better stability against coalescence and creaming by Pickering stabilisation and trapping the droplets in a gel-like particle network (Cui et al., 2014; Liu & Tang, 2016a; Liu & Tang, 2014).

Pea protein particles have been used to stabilise emulsions under acidic conditions (Shao & Tang, 2016). At low oil fraction, protein particles keep droplets well separated and stable, while at high oil fraction, the particles aggregate to form a network through droplet flocculation, resulting in gel-like structures. Zein particles, containing high hydrophobic groups, were processed by solvent precipitation and could stabilise emulsions (10-200 μm). However, these emulsions were sensitive to the environment, such as coalescence under acidic conditions and flocculation at high ionic strength (de Folter et al., 2012). Other plant

proteins, such as the gliadin from wheat (Hu et al., 2016) and Kafirin from sorghum (Xiao et al., 2016), have also been fabricated into particles by using the anti-solvent precipitation method and have shown potential as novel particle emulsifiers.

### 2.5.2 Emulsification of mixed plant and milk proteins

The combination of plant and milk proteins has attracted increasing attention recently, as it could reduce reliance on single-source animal proteins. An optimised mixed-protein system could take advantage of both proteins to enhance emulsion stability. However, limited studies have been conducted on the emulsifying properties of mixed proteins, especially those of complexed plant/milk proteins.

The synergistic effect between plant and milk proteins in terms of emulsion stabilisation has been reported by several studies. The intermolecular interactions through disulphide binding and hydrophobic interactions occur between mixed proteins, resulting in a thicker and denser interfacial layer to provide steric repulsion (Ho et al., 2018; Mao et al., 2013). For example, the synergistic effect of legume and whey protein, such as soy and whey protein, showed increased adsorption of both proteins on the interface, attributed to the interactions between the two proteins (X. Zhang et al., 2021). These blends formed interfacial films with greater elasticity and viscoelastic strength (Ho et al., 2018; Pizones Ruiz-Henestrosa et al., 2014).

In terms of bulk stability, other studies also reported that the mixed protein system exhibited positive results. The nanoemulsions prepared with sodium caseinate alone or pea protein alone were unstable due to depletion flocculation or excessive droplet and protein aggregation. However, the mixture of two proteins can stabilise emulsion against aggregation and creaming, since the aggregates of pea protein isolate may be disrupted by

high-pressure homogenisation and interact with sodium caseinate in a continuous phase to limit the depletion flocculation and pea protein aggregation (Yerramilli et al., 2017). In other studies, Ji et al. (2015) and Hinderink et al. (2019) suggested that the synergistic effect of the soy/sodium caseinate or pea/sodium caseinate mixture improves stability through steric hindrance.

However, not all interactions are cooperative. Some studies have also found competitive adsorption behaviour. For instance, in pea/whey protein or pea/sodium caseinates emulsions, the pea protein could displace sodium caseinate, while whey protein could displace pea protein at the interface (Hinderink et al., 2019). The compact structure and large aggregates of plant protein would lead to slow adsorption. The small molecular whey protein could adsorb faster and form a protein network through disulphide bonding to dominate the interface, which restricts the adsorption of the other proteins (Schröder et al., 2017; Tang, 2017; X. Zhang et al., 2021). In the case of caseins, the lack of a continuous interfacial network created by casein allows casein to dynamically switch between phases, further limiting stable mixed-protein layers (Hinderink et al., 2020).

To date, the adsorption behaviour of the mixture of different types of proteins is still not fully explored. Although the interactions between mixed proteins at the interface were observed, the competitive adsorption could inhibit the presence of plant proteins at the interface. One possible strategy to overcome this limitation is to pre-complex plant and milk proteins into hybrid microparticles, acting as Pickering emulsifiers to stabilise emulsions. For example, zein/casein particles (Feng & Lee, 2016) and hemp/casein particles (Chuang et al., 2020) have been used to stabilise the Pickering emulsions, resulting in higher protein packing and interfacial coverage. Nevertheless, very few studies have worked on the emulsifying potential of complexed plant/ milk protein particles, leaving a significant research gap.

### 2.5.3 High internal phase emulsion stabilised by protein particles

High internal phase emulsions (HIPEs) refer to an emulsion containing at least 74% oil fraction, resulting in semi-solid properties with unique structural and rheological characteristics (Dai et al., 2019; Wijaya et al., 2017). The move toward natural ingredients has driven interest in biopolymer particles, such as protein and starch, for HIPEs stabilisation (Linke & Drusch, 2017). HIPEs require fewer particle emulsifiers to stabilise closely packed droplets with enhanced storage stability and coalescence resistance, compared to those stabilised by traditional molecule surfactants (Xu et al., 2019). Consequently, the compact structures could result in viscoelastic, gel-like properties (Dai et al., 2019). The tuneable rheological properties of HIPEs (Kim & Mason, 2017) make these systems attractive for food applications like mayonnaise (X. Liu et al., 2018).

Because of the high oil content, HIPEs have the advantage in the encapsulation (Liu et al., 2019; Su et al., 2018). For example, HIPEs stabilised by whey protein had improved gel strength and β-carotene bioaccessibility (Liu et al., 2019). Those emulsions stabilised by whey protein microgels had better thermal stability, rheological behaviours (e.g. viscoelastic properties) (Zamani et al., 2018) and improved viability of probiotics (e.g. *Lactobacillus plantarum*) (Su et al., 2018).

One notable feature of HIPEs is their gel-like structure, which could be used to control their rheological properties. Gliadin particle-stabilised HIPEs exhibited a particle network and droplet network, which led to good stability above pH 4 (Hu et al., 2016). Wheat gluten-stabilised HIPEs mimicked mayonnaise with similar rheological properties, which is attributed to the homogeneous droplets and protein network. In addition, it exhibited better heat stability (X. Liu et al., 2018). For other plant proteins, peanut protein microgels stabilised emulsions with up to 87% oil, generating a homogeneous network

structure (Jiao et al., 2018). Soy β-conglycinin was used to form gel-like HIPEs at least 0.2%, with excellent heat stability (Xu et al., 2019). Higher protein concentrations led to greater elasticity, which shows the tunable texture behaviour. Quinoa protein, after high-pressure homogenisation, stabilised HIPEs with good storage stability. Both storage and heat treatment could improve the protein interactions to form a thicker interfacial layer and a stronger network in the continuous phase (R. Zhang et al., 2021).

In addition to single proteins, protein-based complexes have been reported. Among these, the protein-polysaccharide complexes are the most studied protein-based particles (Evans et al., 2013). Examples include soy glycinin/soy polysaccharide (Hao et al., 2020), zein/pectin (Zhou et al., 2018), gliadin/gum Arabic (L. Ma et al., 2020) and whey/low methoxyl pectin (Wijaya et al., 2017). However, as discussed previously, very limited studies have focused on the protein-protein complexes, especially plant–milk combinations, for HIPEs stabilisation. This represents a significant research gap. Given the growing interest in developing sustainable and functional emulsifiers, further exploration of hybrid protein-based particle systems is crucial.

## 2.6 Research gaps

Recent advances in food protein research have an increasing shift toward sustainable and functional protein systems, which has led to growing interest in the use of plant-based proteins as food ingredients. However, the large diversity of plant proteins in their protein composition, structures and functionalities continues to pose significant challenges in the development of new food products. Among these, hemp protein (HP) has emerged as a promising sustainable protein source due to its nutritional value and environmental benefits. Yet, similar to many other plant proteins, HP suffers from limited

techno-functionality, including low water solubility, weak emulsifying properties and heat instability, which restricts its full application in food products.

Improving the functionality of HP is therefore critical to enhancing its usability in food formulations. Previous studies have shown that plant-milk protein complexes can enhance dispersibility through molecular interactions, such as disulphide bonding and hydrophobic associations. However, most of the existing research has focused on conventional plant proteins, such as soy or pea. Hence, little is known about the interaction mechanisms between HP and milk proteins. Therefore, there is a greater scope for research to investigate hemp-milk protein interactions.

Heat stability is another critical functional attribute for proteins used in emulsified and processed food systems. However, HP alone is prone to denaturation and aggregation when exposed to heat, often resulting in sedimentation or phase separation, which must be addressed to enable its wider use. Microparticulation in combination with milk proteins, combining thermal treatment and mechanical shear, has been identified as an effective strategy to enhance heat stability and interfacial functionality by creating protein particles. Unlike traditional molecular emulsifiers, these protein particles can act as particle stabilisers, forming irreversible interfacial layers that resist coalescence and creaming, thereby improving emulsion stability. Despite these promising findings, research specifically addressing the formation and functionality of hybrid plant–milk protein microparticles, particularly those derived from hemp and milk proteins, remains scarce.

In summary, while hybrid protein systems offer a promising route for sustainable and functional food ingredients, several key knowledge gaps remain. First, the detailed mechanisms governing the interaction between HP and milk proteins are not well understood. Secondly, there is a lack of systematic investigation into the emulsifying

behaviour and thermal stability of HP/milk protein particles, especially in both conventional and high internal phase emulsions. Addressing these gaps will be essential for developing clean-label, sustainable, and high-performance emulsifiers for innovative food applications.

# Chapter 3: General materials and methods

## 3.1 Materials

Whey protein isolate (WPI) containing 92.0% protein, 0.9% fat, 1.6% ash and 5.2% moisture and sodium caseinate (NaCN) containing 92.3% protein, 0.6% fat, 4.0% ash and 4.8% moisture were purchased from Fonterra Co-operative Group Limited, Auckland, New Zealand. The hempseed protein (HP) concentrate powder was purchased from Davis Food Ingredients (Davis Trading Company Ltd., Palmerston North, New Zealand). The HP powder contained 59.8% protein, 2.4% fat, 10.7% ash, 6.8% moisture and 20.2% carbohydrate. All chemicals were purchased from Sigma-Aldrich Ltd. (St. Louis, MO, USA), and the reagents were made up in Milli-Q water (Milli-Q apparatus; Millipore Corp., Bedford, MA, USA).

## 3.2 Proximate analysis

The proximate composition of protein ingredients was analysed as follows: protein content was determined using the Kjeldahl method (AOAC 991.20, nitrogen factor 5.21; AOAC 2023a); fat, ash and moisture content were determined according to AOAC 922.06, AOAC 942.05 and AOAC 925.10 (AOAC 2023b,c,d, respectively); and carbohydrate content was calculated by subtracting the sum of the protein, ash and fat from the total solids.

## 3.3 Preparation of HP/WPI microparticle

A hemp protein (HP) dispersion was prepared by mixing HP powder in Milli-Q water at 2% (w/w) protein concentration. The mixture was stirred for 2 h at 20 °C. The pH was then adjusted to 11 with 1 M NaOH, followed by stirring for 2 h to increase protein

solubility. The dispersion was centrifuged at 3000 × g for 30 min to remove insoluble materials (e.g., fibres). The resulting supernatant was adjusted to pH 8 using 1 M HCl, and homogenised using a two-stage valve homogeniser (APV 1000, SPX, Silkeborg, Denmark) set at 300 bar (first stage) and 50 bar (second stage). The protein dispersion was passed twice through the homogeniser with no holding time between passes. The resulting dispersion was used in subsequent steps. Separately, a whey protein isolate (WPI) stock solution was prepared by dissolving WPI powder in Milli-Q water at 3% (w/w) and stirring for 2 h. The pH of the protein dispersion was adjusted to 8 using 1 M NaOH.

To prepare the HP/WPI microparticles, HP and WPI dispersions were mixed to achieve a final protein concentration of 1% HP and 1% WPI (w/w) in the mixture. The pH was re-adjusted to 8. Then, the protein mixture was subjected to a heat treatment of 95 °C for 30 min in a water bath. After the treatment was completed, the protein dispersion was rapidly cooled down to 20 °C in an ice bath. Finally, the pH of the protein dispersion was adjusted to 7 (using 1 M HCl), and passed twice through a two-stage valve homogeniser using the same pressure conditions described to produce HP dispersions.

### 3.4 Preparation of HP/WPI emulsions

To prepare emulsions stabilised by either microparticulated or non-microparticulated HP/WPI, two types of coarse emulsions were first prepared. For microparticulated emulsions, preformed HP/WPI microparticles were dispersed in water containing 10% (w/w) soybean oil to achieve final protein concentrations of 0.25%, 0.5%, 1.0%, 1.5%, or 1.8% (w/w). For non-microparticulated emulsions, a dispersion of HP particles / WPI mixture (at the same protein ratios used in microparticle preparation) was directly dispersed at corresponding total protein concentrations and oil concentration.

Coarse emulsions were prepared using a benchtop Ultra-Turrax mixer (IKA, Wilmington, NC, USA) for 30 s at room temperature. The resulting coarse emulsions were then passed 2 times through a two-stage homogeniser at 300 bar (first stage)/50 bar (second stage) to produce fine emulsions stabilised by either microparticulated or non-microparticulated HP/WPI. Sodium azide (0.02%, w/w) was added to inhibit microbial growth.

### 3.5 Preparation of high internal phase emulsions

High internal phase emulsions (HIPEs) were prepared by using four different emulsifying materials: microparticulated or non-microparticulated HP/WPI, HP dispersion, and WPI solution. Soybean oil and aqueous protein dispersion (2% protein) were mixed in containers at a volume ratio of 75:25. The HIPEs were then prepared using a benchtop Ultra-Turrax mixer (Wilmington, NC, USA) at 13500 rev $min^{-1}$ for 2 min at room temperature. Sodium azide (0.02%, w/w) was added to inhibit microbial growth.

### 3.6 Particle size analysis

The particle size of HP dispersions and their supernatant was measured using static light scattering on a Mastersizer 2000 (Hydro MU, Malvern, Worcestershire, UK). The refractive indices of hempseed protein and water were 1.45 and 1.33, respectively. The data were reported in volume-mean diameter ($d_{4,3}$) and Sauter-average diameter ($d_{3,2}$) and were calculated as the average of triplicate measurements.

### 3.7 Free sulphydryl content

Free sulphydryl (SH) contents of protein samples were measured using Ellman's reagent [5,5'-dithiobis (2-nitrobenzoic acid); DTNB] as described by Xu et al. (2022) with slight modifications. Protein samples (1 mg/mL) were mixed with Tris-glycine buffer (pH

8) containing 86 mM Tris, 90 mM glycine, 40 mM EDTA, and 8 M urea. Ellman's reagent (4 mg/mL) was also made in Tris-glycine buffer. A 1.5 mL sample was mixed with 20 μL Ellman's reagent, followed by 30 min incubation. The absorbance of the resulting 5-nitro-2-thiobenzoic acid (TNB) chromogen was measured by a spectrophotometer (Genesys 10-S; Thermo Fisher Scientific Inc., USA) at a wavelength of 412 nm. The Tris-glycine buffer with Ellman's reagent was used as a blank.

Free SH content was calculated using equation (Eq. 3.1):

$$SH\ (\mu mol/g) = (10^6 \times A \times D)/\ (1.36 \times 10^4 \times C) \qquad (Eq.3.1)$$

Where A is the absorbance value, C is the protein concentration, D is the dilution factor, $1.36 \times 10^4$ is the molar absorptivity of TNB, and $10^6$ is the conversion from molar basis to μmol/mL basis.

### 3.8 Surface hydrophobicity ($H_0$)

The surface hydrophobicity ($H_0$) of protein samples was measured using 8-aniline-1-naphthalene sulfonic acid (ANS) as a fluorescent probe (Chihi et al., 2016). The protein sample was diluted in 10 mM sodium phosphate buffer (pH 7) to obtain protein concentrations ranging from 0.0004 to 0.02%. Then, 20 μL ANS solution (8 mM) was added to a 4 mL protein sample and incubated for 15 min in the dark. The fluorescence intensity was measured using a spectrofluorometer (FP-6500, JASCO, Tokyo, Japan) with an excitation wavelength of 390 nm and an emission wavelength of 470 nm. The $H_0$ was calculated as the initial slope of fluorescence intensity versus protein concentration by linear regression.

### 3.9 Light microscopy

Aqueous dispersions of protein samples were mounted onto microscope slides and covered with glass coverslips. The samples were viewed under an Olympus BX53 light microscope (Olympus, Tokyo, Japan) equipped with an objective lens at 20× magnification. Images were captured and analysed using XIMEA CamTool 4.24 software (XIMEA GmbH, Münster, Germany).

### 3.10 Transmission electron microscopy

Sample preparation and negative staining for transmission electron microscopy (TEM) were performed as described by Vincekovic et al. (2014). An aliquot of 80 μL of protein solution was placed on a formvar/carbon-coated 200 mesh copper grid for 4 min. The excess sample was removed by filter paper. 80 μL of uranyl acetate (2%, w/w) was placed on the grid for another 4 min, and the excess staining solution was removed with filter paper. The stained sample was imaged at 6000x, 16500x and 20500x magnification by a transmission electron microscope (Philips CM10) (Eindhoven, the Netherlands) at 100 kV.

### 3.11 Confocal laser scanning microscopy

Confocal laser scanning microscopy (CLSM; Model Zeiss LSM900 with Airyscan 2, Carl Zeiss, Jena, Germany) was used to investigate the microstructure of emulsion using the staining protocols described by Gallier et al. (2012). Nile Red (1 mg/mL in acetone) and Fast Green FCF (1 mg/mL in Milli-Q water) were used to selectively stain neutral lipids and proteins, respectively. Each sample (100 μL) was mixed with Nile Red (2:100, v/v) and Fast Green FCF (6:100, v/v). The stained emulsion sample was placed on a concave microscope slide and covered by a coverslip (0.17 mm thick), avoiding an air bubble

between the sample and the coverslip. The freshly prepared sample slide was immediately examined by CLSM with a 63x oil immersion objective lens.

### 3.12 Sodium dodecyl sulphate polyacrylamide gel electrophoresis

The protein composition was studied by Tris-HCl sodium dodecyl sulphate polyacrylamide gel electrophoresis (SDS-PAGE) under reducing conditions as per the protocol described by Dave et al. (2019) and Manderson et al. (1998). The protein sample was mixed with non-reducing or reducing sample buffer to a final protein concentration of 1 mg/mL. Dithiothreitol was used as a reducing agent in the reducing sample buffer (200 mM), and the reducing samples were heated at 56 °C for 15 min. Samples (10 μL) were loaded onto Mini-Protean gels (Bio-Rad Laboratories, Richmond, CA, USA) and run at 150 V, followed by Coomassie brilliant blue staining and destaining (10% isopropanol and 10% glacial acetic acid in water, v/v). The destained gel was scanned using a Gel Doc XR (Bio-Rad Laboratories) molecular imager, and the densitometric analysis of protein composition was carried out with ImageLab software.

### 3.13 Total protein coverage on the emulsion droplet surface

The emulsions were centrifuged at 45,000 × *g* for 40 min at 20 °C. The subnatant layer and sediment layer were carefully collected. The cream layer was dispersed in deionised water and re-centrifuged at 45,000 × *g* for 40 min to obtain washed cream. The protein content in the subnatant and sediment was analysed separately using the Kjeldahl method.

Adsorbed protein (g) was calculated using equation (Eq. 3.2):

$$\text{Adsorbed protein (g)} = \text{Total protein (g) used in emulsion} - [\text{protein (g) in the subantant} + \text{protein (g) in the sediment}] \quad \text{(Eq.3.2)}$$

Total surface protein ($mg/m^2$) was calculated using equation (Eq. 3.3):

$$\text{Total surface protein } (mg/m^2) = \frac{[\text{Adsorbed protein (g)} \times d_{3,2}]}{[6 \times V \times \phi]} \times 10^{-2} \quad \text{(Eq.3.3)}$$

Where V (mL) is the volume of emulsions, and $\phi$ is the volume fraction of the oil in emulsions (Chang et al., 2016).

### 3.14 Protein composition on the emulsion droplet surface

The washed emulsion cream was spread and dried on a filter paper, then analysed using SDS-PAGE under reducing conditions as described in the previous section to determine the composition of the adsorbed protein at the surface of the emulsion. The resulting gels were scanned using a Gel Doc XR (Bio-Rad Laboratories) and analysed by ImageLab software for densitometric analysis. The percentage composition of each sample was expressed as the individual protein intensity as a fraction of the sum total.

### 3.15 Rheological properties

The rheological properties of the emulsions were measured using a rheometer (Discovery HR-20 rheometer, TA Instruments, USA) equipped with a 2° cone-and-plate geometry (diameter 40 mm). The temperature was maintained at 20 °C. Emulsion samples were loaded, and the cone was lowered into position. The excess sample was carefully removed using a spatula.

### 3.15.1 The shear viscosity experiment

The sample was first equilibrated for 1 min to allow the temperature to be stabilised. The shear viscosity of emulsions was characterised at the shear rate range of 0.1 – 300 $s^{-1}$. The apparent viscosity was recorded as a function of shear rate.

### 3.15.2 The small amplitude oscillation shear (SAOS) measurements

SAOS behaviour was characterised through the frequency sweeps (0.1 – 100 Hz, 0.5% strain). Storage modulus ($G'$) and loss modulus ($G''$) as a function of frequency were calculated by Trios software (TA Instruments).

### 3.15.3 The large amplitude oscillation shear (LAOS) measurements

The LAOS behaviour of HIPEs was examined through strain sweeps performed over a strain range of 0.1 – 1000% at a frequency of 1 Hz. The raw waveform data of stress and strain signals were collected directly by Trios software in transient mode and analysed by the MITlaos program (MITlaos v2.2 Beta) based on MATLAB R2020b (MathWorks, USA) (Ewoldt et al., 2007). The Lisssajous-Bowditch plots were constructed based on the instantaneous stress signal.

Using the LAOs moduli, the strain-stiffening index (S) was calculated according to Equations 1 – 3. A positive S value indicates intracycle strain stiffening, a S value equal to 0 represents a linear elastic/viscous response, and a negative S value indicates intracycle strain softening.

$$G'_M = \sum_{n\ odd} nG'_n \quad \text{(Eq.3.4)}$$

$$G'_L = \sum_{n\ odd} G'_n\,(-1)^{(n-1)/2} \quad \text{(Eq.3.5)}$$

$$S = \frac{G'_L - G'_M}{G'_L} \quad \text{(Eq.3.6)}$$

where $G'_M$ and $G'_L$ represent the tangent modulus and secant modulus at the minimum strain and the maximum strain. $G'_n$ and $G''_n$ are the elastic and viscous Fourier coefficients are calculated from the Fourier spectrum of the stress responses by the MITlaos program.

### 3.16 Heat stability of emulsions

A 10 mL sample of emulsion was transferred into a glass tube and heated in a water bath at different temperatures (60, 70, 80 and 90 °C) for 20 min, followed by rapid cooling in ice to 20 °C. The droplet size of the heated emulsions was analysed to investigate their heat stability.

### 3.17 Data analysis

Experiments were carried out in triplicate, and the results are reported as mean ± standard deviation. Statistical analysis was performed using SPSS software for Windows (version 29.0, SPSS Inc., Chicago, IL, USA). The data were analysed by independent t-tests between two groups, and one-way analysis of variance (ANOVA) for multiple comparisons, using Tukey's test with the level of significance set at $p < 0.05$.

MASSEY UNIVERSITY
TE KUNENGA KI PŪREHUROA
UNIVERSITY OF NEW ZEALAND

GRADUATE RESEARCH SCHOOL

# STATEMENT OF CONTRIBUTION
# DOCTORATE WITH PUBLICATIONS/MANUSCRIPTS

We, the student and the student's main supervisor, certify that all co-authors have consented to their work being included in the thesis and they have accepted the student's contribution as indicated below in the Statement of Originality.

| | |
|---|---|
| Student name: | Sihan Ma |
| Name and title of main supervisor: | Dr Alejandra Acevedo-Fani |
| In which chapter is the manuscript/published work? | Chapter 4 |

Describe the contribution that the student and members of the supervisory team have made to the manuscript/published work:[1]

Sihan Ma: Methodology, Investigation, Formal analysis, Data curation, Writing - original draft, Visualization.
Aiqian Ye: Methodology, Writing - review & editing, Supervision.
Harjinder Singh: Methodology, Writing - review & editing, Supervision, Funding acquisition.
Alejandra Acevedo-Fani: Conceptualisation, Supervision, Methodology, Validation, Resources, Writing - review & editing.

Please select one of the following three options:

- (●) **The manuscript/published work is published or in press**

  Please provide the full reference of the research output:

  Ma, S., Acevedo-Fani, A., Ye, A., & Singh, H. (2024). Heat-induced interactions of hemp protein particles formed by microfluidisation with β-lactoglobulin. LWT, 203. https://doi.org/10.1016/j.lwt.2024.116370

- ( ) **The manuscript is currently under review for publication**

  Please provide the name of the journal:

- ( ) **It is intended that the manuscript will be published, but it has not yet been submitted to a journal**

| | | | |
|---|---|---|---|
| Student's signature: | Sihan Ma — Digitally signed by Sihan Ma, DN: cn=Sihan Ma, c=NZ, email=s.ma@massey.ac.nz, Date: 2025.07.18 13:51:32 +12'00' | Main supervisor's signature: | Alejandra Acevedo Fani — Digitally signed by Alejandra Acevedo Fani, DN: cn=Alejandra Acevedo Fani, c=NZ, o=Massey University, ou=Riddet Institute, email=a.acevedo-fani@massey.ac.nz, Date: 2025.07.31 07:47:22 +12'00' |

*This form should be placed at the beginning of each relevant thesis chapter.*

[1] Refer to the Massey University Publishing and Authorship guidelines (OneMassey for staff, Stream for students) and/ or Contributor Roles Taxonomy (CRediT) guidelines for guidance.

# Chapter 4: Heat-induced interactions of hemp protein particles formed by microfluidisation with β-lactoglobulin

This chapter has been published in a peer-reviewed journal:

Ma, S., Acevedo-Fani, A., Ye, A., & Singh, H. (2024). Heat-induced interactions of hemp protein particles formed by microfluidisation with β-lactoglobulin. *LWT*, 203. https://doi.org/10.1016/j.lwt.2024.116370

## Abstract

This study explored the effect of microfluidisation on the dispersibility of hempseed protein (HP) and the interactions of microfluidised HP particles with β-lactoglobulin (β-lg) after heat treatment. Microfluidisation increased the dispersible protein fraction from 10% (non-microfluidised) to a maximum of 58% (200 MPa, 6 passes) in HP dispersions. Dispersible HP particles were within the micro-sized range ($d_{4,3} \leq 2\mu m$) after microfluidisation. Heat treatment (95°C, 10-60 min) of HP particles with β-lactoglobulin (β-lg) induced protein association by sulphydryl-disulphide exchange reactions; β-lg association with HP particles initiated within the first 20 min. Additionally, the particle size ($d_{4,3}$) values of co-heated HP particles with β-lg were significantly smaller than those found in HP particle dispersions heated alone, results that were in line with microscopy analysis. This suggests that β-lg could have restricted HP particle aggregation. In conclusion, combining microfluidisation and heat treatment could offer a venue to modify the physical properties of plant/milk protein mixtures.

## 4.1 Introduction

Consumers' demand for dairy alternatives is increasing rapidly and is largely driven by the ongoing changes in dietary patterns towards more sustainable diets. Although plant proteins have been proposed as new ingredients for dairy alternatives, it is very challenging to match the functionality and nutritional benefits of milk proteins. One of the approaches to balancing the nutritional composition and improving the techno-functionality of plant proteins is to combine plant proteins with milk proteins. In fact, recent studies suggest that in some instances, plant/milk protein interactions during processing may lead to functional synergies (Martin et al., 2016; Roesch et al., 2004). A previous study from our group indicated that the addition of sodium caseinate to hempseed protein (HP) globulins improved the thermal stability of HP globulins at a molecular level (Chuang et al., 2019).

HP is attracting attention as novel protein ingredient because of its high nutritional value and credible sustainability credentials (Q. Wang, J. Jiang, et al., 2018). Hempseed proteins have excellent digestibility (about 90%) (Callaway, 2004) and are considered of high quality due to their amino acid profiles (including high levels of arginine) being comparable with those of soybean and egg white, which are recognised as good protein sources (Tang et al., 2006). The hempseed proteins are comprised of 60–80% globulin (edestin) and 20–30% albumin (Kim & Lee, 2011). Edestin is a homohexamer (~300 kDa) that is composed of six subunits (~52 kDa) linked by non-covalent interactions. Each subunit is composed of a basic subunit (~18 or 20 kDa) and an acidic subunit (~34 kDa). Two cysteine residues form a disulphide bond linking the basic subunit and the acidic subunit. Another two cysteine residues form the intrachain disulphide bond in the acid subunit while one cysteine residue remains as a free thiol group (Potin & Saurel, 2020; Wang & Xiong, 2019).

The emulsification and gelation properties of HP are considered to be relatively poor (Shen et al., 2021), and the use of HP powder as a food ingredient has been limited due to its poor solubility in water. This could be due to the inherent insolubility of HP globulin at neutral pH and the adverse effects of extraction methods on protein structure. Heat treatment during oil extraction and following drying processing leads to complete or partial protein denaturation (Shi et al., 2021). Hempseed proteins undergo extensive aggregation upon thermal treatments above their denaturation temperature. The free thiol groups in HP are involved in protein thermal aggregation through thiol-disulphide exchange reactions and cause large aggregates (Aluko, 2017; Chuang et al., 2019; Dapčević-Hadnađev et al., 2020; Patel et al., 1994; Wang et al., 2008).

In general, several approaches have been applied to improve the solubility of HP. These include enzymatic hydrolysis to remove non-protein components and extract proteins (Malomo & Aluko, 2015b), pH cycling to change the tertiary structure of proteins (Jiang et al., 2009) and high-pressure processing to disrupt the quaternary and tertiary structure of proteins (Galazka et al., 2000). However, the functionality improvements using different pre-treatments depend on the intrinsic properties of individual proteins within each plant source. It has been previously reported that hempseed globulin (the major HP) becomes completely insoluble after pH cycling (Chuang et al., 2021).

Microfluidisation is a non-thermal process that can modify protein structure or aggregation state by applying ultra-high pressure, hydrodynamic cavitation and intense shearing at the same time. In the microfluidisation process, the fluid is divided into two or more microstreams and pumped into the interaction chamber where the collision of microstreams occurs. Before the collision, the dimension of micro-tubes decreases to provide a high shear rate and an intensive disruption effect. The collision creates high energy to disrupt the protein aggregates and creates smaller particles (Chen et al., 2012;

Mert, 2020). Upon microfluidisation of pea protein solution, for example, the solubility of pea protein was increased by 3.78-fold, along with a significant decrease in particle size (He et al., 2021).

β-Lactoglobulin (β-lg) was chosen in this study because it is the major protein in commercial whey protein products. It has a globular structure that is stabilised by hydrogen bonding, van der Waal forces, electrostatic interactions and hydrophobic interactions (Singh & Havea, 2003). Unfolding of β-lg occurs above 70 °C, and aggregation begins at 78 °C mainly through disulphide bonding and hydrophobic interactions (Sava et al., 2005). The unfolding of β-lg exposes the buried hydrophobic side chains and free sulphydryl groups that tend to interact with other protein molecules (Singh & Havea, 2003).

Heat-induced aggregation is one of the most important properties of food proteins, which will give food products with different structural and textural features (Chihi et al., 2016). The development of plant-whey protein aggregates may produce novel protein ingredients. Previous studies have shown that soy proteins could interact with whey proteins through disulphide bonds (Anuradha & Prakash, 2009; Roesch & Corredig, 2005). It has also been reported that β-lg can interact with pea globulin during heat treatment, leading to smaller aggregate sizes compared with single pea globulin aggregates (Chihi et al., 2016). However, there are no systematic studies on the heat-induced interactions between HP and β-lg, especially interactions at a molecule/particle level.

According to previous studies on plant-whey aggregates, we hypothesise that the heat treatment can induce interactions between HP and β-lg, which could lead to the formation of composite protein particulated materials. This study explored the effect of microfluidisation on the dispersibility of hempseed protein (HP) and the interactions of microfluidised HP particles with β-lactoglobulin (β-lg) after heat treatment.

## 4.2 Materials and methods

### 4.2.1 Materials

HP concentrate powder was purchased from Davis Food Ingredients (Davis Trading Company Ltd., Palmerston North, New Zealand). It contained 59.8% protein, 2.4% fat, 10.7% ash, 6.8% moisture and 20.2% carbohydrate. The protein content was determined using the Kjeldahl method (AOAC 991.20, Nitrogen conversion factor 5.21; AOAC, 2006). The fat, ash and moisture contents were analysed according to AOAC 922.06, AOAC 942.05 and AOAC 925.10, respectively (AOAC, 2006). The carbohydrate content was calculated by subtracting the sum of the protein, ash and fat from the total solids. β-Lactoglobulin from bovine milk ≥90% (PAGE) was purchased from Sigma-Aldrich Ltd. (St. Louis, MO, USA). Unless stated otherwise, all chemicals were purchased from Sigma-Aldrich Ltd., and the reagents were made up in Milli-Q water (Milli-Q apparatus; Millipore Corp., Bedford, MA, USA).

### 4.2.2 Preparation of HP particles

HP concentrate powder was dissolved at room temperature by stirring in Milli-Q water at 0.5, 1, 2 and 3 g/ 100g protein concentrations. The HP dispersions (pH 7) were passed through a microfluidiser (M-110P, Microfluidics, Newton, MA, USA) at 200 MPa with 2, 4 and 6 passes and then centrifuged at 500 × *g* for 15 min at 20 °C to remove the large particles (such as insoluble fibre). According to preliminary experiments, the microfluidisation pressure (200 MPa) chosen in this study aimed to get a minimal particle size. The resulting microfluidised HP supernatant was used for further work. Sodium azide (0.02 g/ 100g) was added to HP dispersions to inhibit microbial growth.

The protein content in the supernatant was determined by measuring total nitrogen content using the Kjeldahl method (AOAC 991.20, Nitrogen conversion factor 5.21;

AOAC, 2006) to calculate the percentage of dispersible protein by the following equation (Eq. 4.1):

$$Dispersible\ protein\ (\%) = \frac{PC\ microfluidised\ HP\ sup}{PC\ original\ HP} \times 100 \qquad \text{(Eq. 4.1)}$$

Where *PC Microfluifised HP sup* is the protein content (g/ 100g) of the supernantant fraction obtained after centrifugation of the microfluised HP dispersion, whereas *PC original HP* is the protein content (g/ 100g) of the HP dispersion prior to microfluidisation.

### 4.2.3 Heat treatment of protein solution

β-Lactoglobulin was dissolved in Milli-Q water with magnetic stirring for at least 2 h to prepare the β-lg (0.5 g/ 100g) stock solutions. The microfluidised HP supernatant and β-lg solution were mixed to achieve the different final protein concentrations. The pH of the protein mixture was adjusted to pH 7. The protein samples were heated at 95 °C for different holding times (10 to 60 min) in the water bath and were then cooled in ice to 20 °C immediately. 95 °C was chosen as heating temperature is because it was above the denature temperatures of both β-lg (74-76 °C) (Kim et al., 2020) and HP (92 °C) (Wang et al., 2008) To simplify sample nomenclature, the g/ 100g sign was omitted; as examples, 0.25 g/ 100g HP is referred to as 0.25HP, 0.25 g/ 100g β-lg is referred to as 0.25β-lg and the mixture of 0.25 g/ 100g HP and 0.25 g/ 100g β-lg is referred to as 0.25HP/0.25β-lg.

### 4.2.4 Particle size analysis

The particle size of HP dispersions and their supernatant was measured using static light scattering on a Mastersizer 2000 (Hydro MU, Malvern, Worcestershire, UK). The refractive indices of hempseed protein and water were 1.45 and 1.33, respectively. The data were reported in volume-mean diameter ($d_{4,3}$) and Sauter-average diameter ($d_{3,2}$) and were calculated as the average of triplicate measurements.

### 4.2.5 Transmission electron microscopy

Sample preparation and negative staining for transmission electron microscopy (TEM) were performed as described by Vincekovic et al. (2014). 80 μL of protein solution was placed on a formvar/carbon-coated 200 mesh copper grid for 4 min. The excess sample was removed by filter paper. About 80 μL of uranyl acetate (2 g/ 100g) was placed on the grid for another 4 min, and the excess staining solution was removed with filter paper. The stained sample was imaged by a Philips CM10 electron microscope at 100 kV (Eindhoven, the Netherlands).

### 4.2.6 Sodium dodecyl sulphate polyacrylamide gel electrophoresis

The protein composition was studied by Tris-HCl sodium dodecyl sulphate polyacrylamide gel electrophoresis (SDS-PAGE) under reducing conditions as per the protocol described by Dave et al. (2019) and Manderson et al. (1998). The protein sample was mixed with non-reducing or reducing sample buffer to a final protein concentration of 1 mg/mL. Dithiothreitol was used as a reducing agent in the reducing sample buffer (200 mM), and the reducing samples were heated at 56 °C for 15 min. Samples (10 μL) were loaded onto Mini-Protean gels (Bio-Rad Laboratories, Richmond, CA, USA) and run at 150 V, followed by Coomassie brilliant blue staining and destaining (10% isopropanol and 10% glacial acetic acid in water, v/v). The destained gel was scanned using a Gel Doc XR (Bio-Rad Laboratories) molecular imager, and the densitometric analysis of protein composition was carried out with ImageLab software.

### 4.2.7 Determination of the proportion of β-lg associated with HP particles

The heat-treated samples were centrifuged at 20,000 × *g* for 15 min to separate the supernatant (unassociated β-lg) and sediment (associated β-lg). The original protein mixture (untreated) and supernatants (heat-treated) were analysed using SDS-PAGE under reducing conditions. The resulting gels were scanned using a Gel Doc XR (Bio-Rad Laboratories) molecular imager and integrated using ImageLab software for densitometric analysis. The band intensity (%) of β-lg in the centrifugal supernatant was calculated as a percentage of that in the original protein mixture samples.

### 4.2.8 Statistical analysis

Experiments were carried out in triplicate, and the results are reported as mean ± standard deviation. Statistical analysis was performed using SPSS software for Windows (version 29.0, SPSS Inc., Chicago, IL, USA). The data were analysed by independent t-tests for between two groups, and one-way analysis of variance (ANOVA) for multiple comparisons, using Duncan's test with the level of significance set at $P < 0.05$.

## 4.3 Results and discussion

### 4.3.1 Effect of microfluidisation on HP dispersibility

HP powder was dispersed in water at different protein concentrations (0.5, 1, 2 and 3 g/ 100g) and then subjected to microfluidisation at 200 MPa with a number of passes. The original and the microfluidised HP dispersion were centrifuged at 500 × *g*. The supernatant represents the “dispersible” protein that does not sediment at room temperature (**Fig. 4.1**).

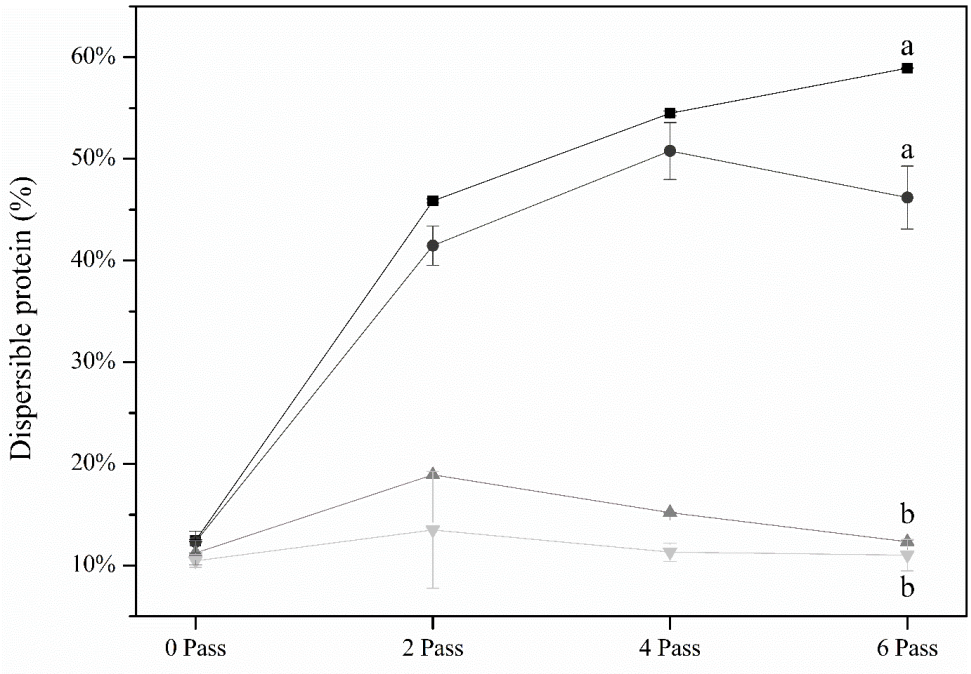


**Fig. 4.1.** Dispersible protein (%) of the supernatant of 0.5 (■), 1 (●), 2 (▲) and 3 g/100g (▼) M-HP, with up to 6 microfluidisation passes at 200 MPa; bars show standard deviation (n = 3). Different lowercase letters indicate that the different protein concentrations led to significant differences ($P < 0.05$) in dispersible protein.

In the original HP sample, approximately 10% of total protein was found in the supernatant at all concentrations tested (0.5 to 3 g/ 100g), indicating very low protein solubility/dispersibility of the HP powder. The low water solubility of hempseed proteins may arise from the extraction process and drying conditions used in the manufacture of commercial HP concentrate powder (e.g., alkaline-isoelectric precipitation, salt-dialysis extraction and spray drying), which may cause protein denaturation and aggregation (Cui et al., 2020). Moreover, HP globulin proteins in their native state have low water solubility at neutral pH, whereas HP albumins tend to be soluble in water at neutral pH (Aluko, 2017).

The protein content of the supernatant obtained from microfluidised HP increased after 2 passes (especially 0.5 and 1 g/100g), indicating that the breakdown of the large HP

aggregates into smaller aggregates/particles improved the protein dispersibility. Therefore, the smaller HP particles tended to remain in the supernatant. This is consistent with other studies, in which microfluidisation was shown to reduce particle size from 180 μm to 20 μm ($d_{4,3}$) and enhance protein solubility in pea protein from 22.6% to 85.3% (Moll et al., 2021) by dissociating large protein aggregates into small particles.

Interestingly, the protein content of supernatants from HP microfluidised at high concentrations (i.e., 2 and 3 g/100g) decreased from 4 passes onwards, indicating possible reaggregation of proteins. It has been suggested that intense shear and turbulence during microfluidisation could expose the buried hydrophobic groups, free thiol groups and disulphide bonds, leading to large aggregates and low solubility (Gong et al., 2019; Moll et al., 2021; Shen & Tang, 2012). Structural changes have been reported in peanut protein dispersion; microfluidisation induced an increase in β-sheet and random coil at the expense of α-helices and β-turns to create a loose and unfolded structure (Hu et al., 2011). Microfluidisation of soya protein was shown to increase surface hydrophobicity and disulphide bonds, enhancing protein-protein interactions (Shen & Tang, 2012).

Thus, it appears that during the microfluidisation process, large protein aggregates were broken down into small particles, but simultaneously soluble HP molecules may unfold, exposing hydrophobic residues or thiol groups. At some critical points in the microfluidisation process (i.e., the number of passes and pressures), protein molecules may interact with each other or with the protein particles generated during microfluidisation (Gong et al., 2019; Hu et al., 2011; Moll et al., 2021; Shen & Tang, 2012). This effect would be expected to be more pronounced at high protein concentrations, i.e., 2 and 3 g/100g HP, as higher protein concentrations would provide more active groups and the probability of interactions and protein reaggregation. The increase in the number of passes

also aggravated the reaggregation by providing more energy input and offering more chances for protein interactions.

Interestingly, in 1 g/100g HP with four microfluidisation passes, almost half of the HP was transferred into the supernatant and the dispersion was relatively stable under mild centrifugation conditions; hence the HP particles obtained by this processing condition were chosen as the material for further characterisation.

### 4.3.2 Particle size, microstructure and protein composition of HP particles

The 1 g/100g HP dispersion before microfluidisation had a bimodal size distribution characterised by a small peak at around 0.2 to 1 μm and a large peak from 3 to 100 μm (**Fig. 4.2A**). After microfluidisation, the disintegration of large HP aggregates was evidenced by a shift of the large-sized peak to the lower particle size range, ranging from <0.1 μm to 30 μm. The proportion of two peaks with small particles increased with microfluidisation passes, while the proportion of the other peak decreased gradually.

All supernatant fractions (**Fig. 4.2B**) had narrower size distributions compared with the original microfluidised dispersions (**Fig. 4.2A**). The size distributions of the supernatant obtained from different passes were similar to each other, with the main peak at about 0.2 μm and a shoulder at about 0.6 μm. The narrower size distributions and smaller particle size (0.4 μm, $d_{4,3}$) (**Fig. 4.2C**) indicated that the HP particles that remained in the supernatant were relatively monodisperse and uniform.

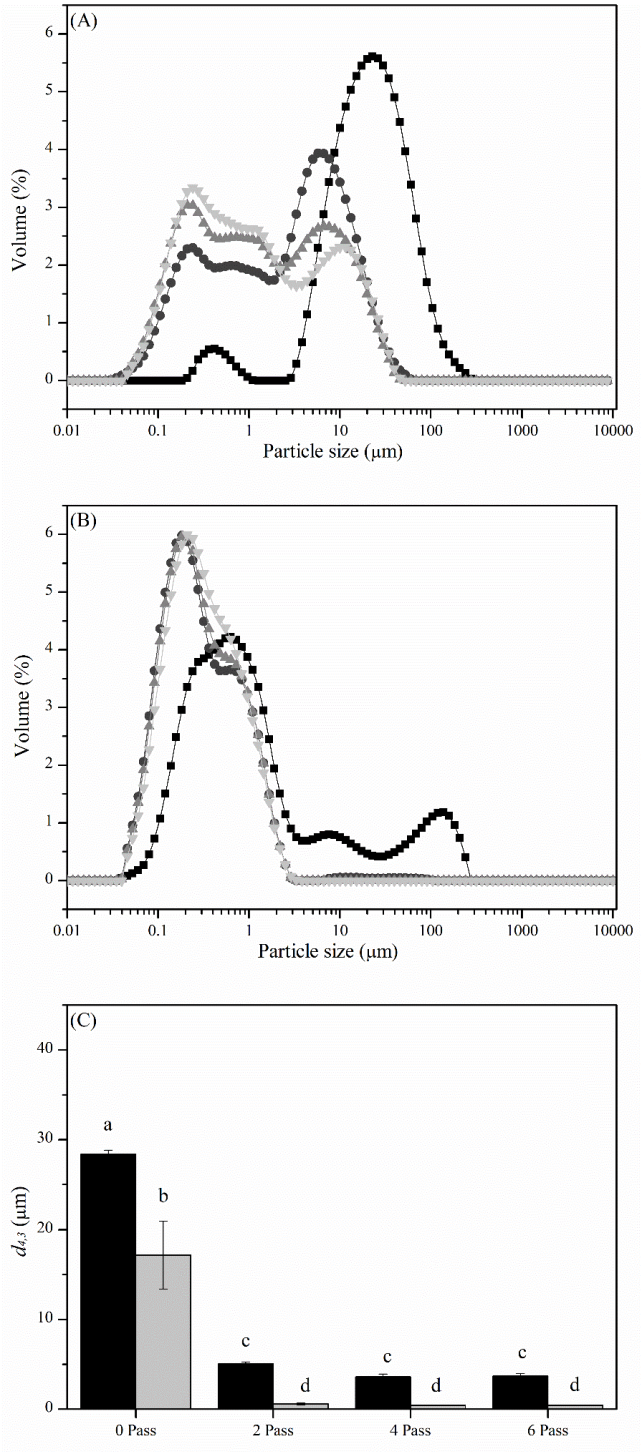


**Fig. 4.2.** Particle size distributions of (A) 1 g/100g HP dispersions and (B) corresponding supernatants and (C) their corresponding volume-weighted mean diameter ($d_{4,3}$, μm) after up to 6 microfluidisation passes (200 MPa): ■, no passes; ●, 2 passes; ▲, 4 passes; ▼, 6 passes. Different lowercase letters indicate that the results are significantly different ($P < 0.05$).

TEM examination showed the morphology of HP aggregates in 1 g/100g HP dispersions before and after microfluidisation. **Fig. 4.3A** shows the presence of large, polydisperse amorphous aggregates in the untreated HP dispersion. However, in the microfluidised HP dispersion (**Fig. 4.3B**), the HP particles/aggregates appeared to disintegrate and were much smaller than in the original HP aggregates. This observation is consistent with the particle size distribution results (**Fig. 4.2A**). Interestingly, the HP particles that remained in the supernatant (**Fig. 4.3C**) appeared to be uniform and spherical with diameters in the range of 0.1 to 0.2 μm, which corroborated the $d_{3,2}$ value (0.19 ± 0.01 μm).

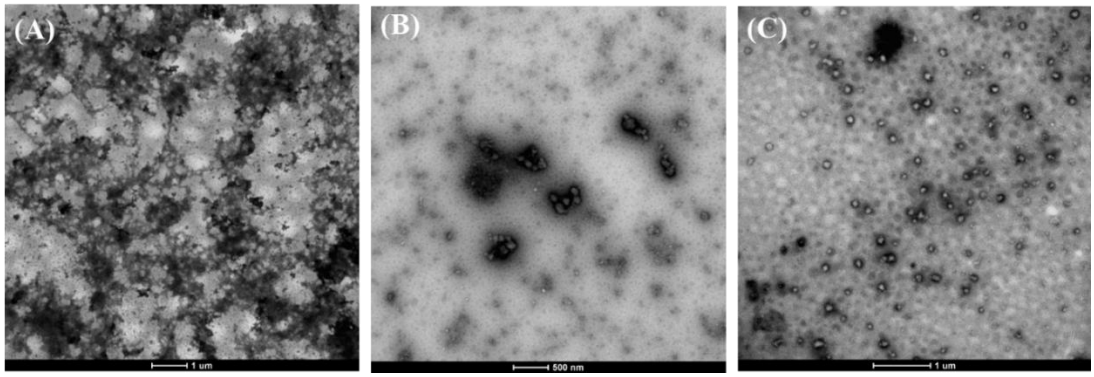


**Fig. 4.3.** Transmission electron micrographs of (A) 1 g/100g HP dispersion (Scale bar = 1 μm), (B) microfluidised (200 MPa, 4 passes) HP dispersion (Scale bar = 0.5 μm) and (C) its supernatant (Scale bar = 1 μm).

The protein composition of HP dispersions before and after microfluidisation and their supernatants were analysed using SDS-PAGE under reducing conditions (**Fig. 4.4A**). The loading protein concentration for the supernatant of non-microfluidised HP was 10 times higher than that for the other samples. The actual intensity of bands without dilution would be much lighter than as it appears in **Fig. 4.4A**. HP consists of water-soluble

albumins and salt-soluble globulins; some of these are marked as bands 1 to 7 in **Fig. 4.4A**. Globulins comprised approximately 7% 7S globulin of 48 kDa (band 1) and 93% 11S globulin consisting of an acid subunit of 34 kDa (band 2) and a basic subunit, shown as 2 bands of 20 kDa (band 3) and 18 kDa (band 4) (Potin & Saurel, 2020; Q. Wang, J. Jiang, et al., 2018). The albumin was composed mainly of 7 polypeptides of molecular mass below 35 kDa (some of which are indicated as bands 5–7) (Wang & Xiong, 2019).

The relative proportion of bands in each lane was estimated by the densitometric scanning of band intensity (**Fig. 4.4B**). Except for the supernatant obtained from non-microfluidised HP, the rest of the samples showed similar protein composition and relative proportions of four dominating bands; these were three heavy bands from 11S globulin subunits (bands 2–4) and one light band (band 7) from albumin. The other bands were either missing or had very low intensity. Compiling the band intensity data, the results showed that 11S globulin (including acid and basic subunits) was the major protein (80% of total protein) in untreated HP dispersion and microfluidised HP dispersion. This composition was consistent with other studies (Aluko, 2017; Tang et al., 2006). Due to the high solubility of hempseed albumin (Wang & Xiong, 2019), more albumin bands were observed in the untreated HP supernatant (above 55% of total protein).

The proportion of 11S globulin in the supernatant increased from 35% to about 80% after microfluidisation. This indicates that microfluidisation can effectively transfer about half of the "insoluble" globulin particles/aggregates into the supernatant. Moll et al. (2021) also reported the improvement of the colloidal properties of insoluble pea protein by microfluidisation. The solubility of the insoluble pea proteins increased from 23% to 86% at ≥125 MPa.

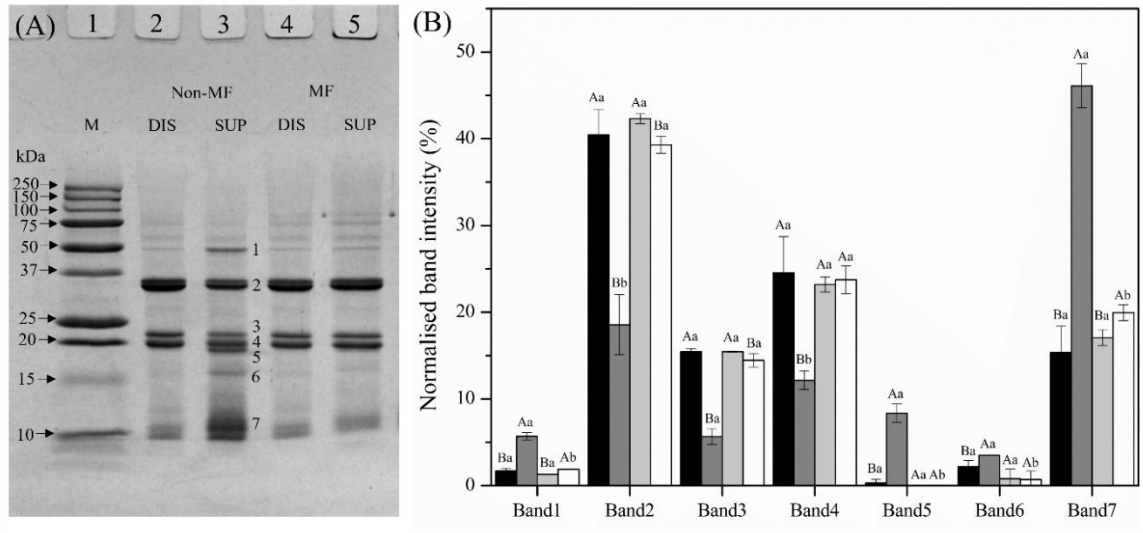


**Fig. 4.4.** Reducing SDS-PAGE (A) of non-microfluidised (Non-MF) and microfluidised (MF) HP dispersions (DIS) and their supernatants (SUP) (M, molecular mass marker) with (B) the normalised band intensity (%) analysis of a relative proportion of bands in each lane (■ and ■, non-microfluidised HP dispersion and supernatant, respectively; ■ and □, microfluidised HP dispersion and supernatant, respectively). In panel A, the protein bands labelled 1–7 are: 1, 7S globulin; 2–4, 11S globulin 34 kDa acid subunit (2) and 20 kDa (3) and 18 kDa (4) basic subunit; 5–7, albumin polypeptides. Statistical analysis was done by individual bands. Different uppercase letters mean the results between the Non-MF DIS and Non-MF SUP or between the MF DIS and MF SUP are significantly different ($P < 0.05$). Different lowercase letters mean the results between the Non-MF DIS and MF DIS or between the Non-MF SUP and MF SUP are significantly different ($P < 0.05$).

### 4.3.3 Effect of heat treatment on HP/β-lg interactions

The heat-induced interactions between HP and β-lg were determined. The particle size of unheated and heated protein mixtures was analysed and compared with individually heated HP supernatant (**Fig. 4.5**) to assess the extent of aggregation in these systems. The $d_{4,3}$ of 0.25HP/0.25β-lg mixture increased from 0.4 μm to 3.2 μm after heating, but the extent of increase was smaller than the individually heated 0.25HP, which reached 7.1 μm after heat treatment. This suggests that the presence of β-lg may have restricted the aggregation of HP particles during heating. In other plant protein and β-lg systems, Chihi et al. (2016) also reported the presence of β-lg in pea globulin formed globulin–β-lg aggregates and slowed the growth of aggregates during heat treatments.

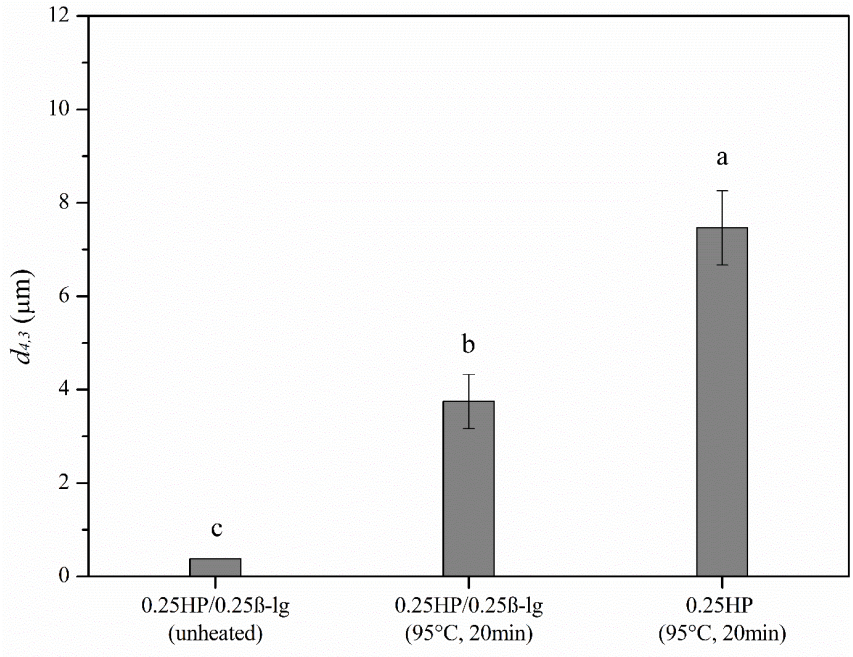


**Fig. 4.5.** Average particle size $d_{4,3}$ of unheated 0.25HP/0.25β-lg and of 0.25HP/0.25β-lg and 0.25HP after heat treatment at 95 °C for 20 min. Different lowercase letters indicate that the results are significantly different ($P < 0.05$).

TEM showed the presence of large HP aggregates in individually heated 0.25HP solution (**Fig. 4.6A**), suggesting HP particles are susceptible to aggregation by heat treatment. However, heated HP dispersion in the presence of β-lg showed relatively small particles with spherical shapes (**Fig. 4.6B**), confirming the particle size results (**Fig. 4.5**). A speculative hypothesis which could be confirmed by the following SDS-PAGE results is that the interactions between HP particles and β-lg may, to some extent, have prevented HP particles from aggregating. It is possible that during heating, the unfolded β-lg interacted with the surface of HP particles, and the association of β-lg with the HP particle surface could have restricted the self-aggregation of HP particles. Some other studies also reported that plant globulins can interact with whey proteins to form aggregates through disulphide bonds and hydrophobic interactions under heat treatment, such as pea globulin/β-lg (Chihi et al., 2016) and soy protein/whey protein (Roesch & Corredig, 2005). In HP and other milk protein mixtures, Chuang et al. (2019) also found that hempseed globulin could form large protein aggregates when heated alone and interacted with sodium caseinate under thermal treatment and formed smaller aggregates.

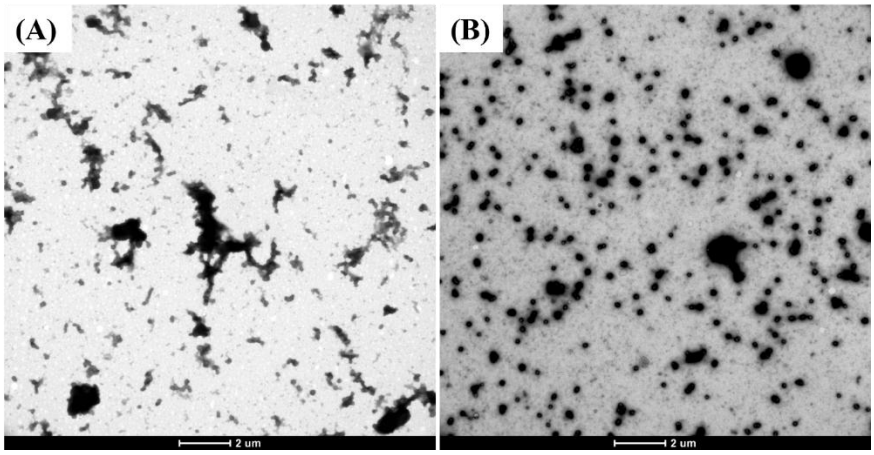


**Fig. 4.6.** Transmission electron micrographs of (A) 0.25HP and (B) 0.25HP/0.25β-lg after heating at 95 °C for 20 min.

To explore the interactions between HP and β-lg, the unheated and heated individual proteins (0.25HP or 0.25β-lg), or their mixtures (0.25HP/0.25β-lg) using SDS-PAGE (**Fig. 4.7A**). Unheated 0.25HP gave a major band at ~52 kDa (band A), which is the subunit of 11S globulin (**Fig. 4.7A**, lane 2). The hexamer of 11S globulin was probably disrupted under the non-reducing PAGE conditions (Hadnađev et al., 2018). Upon heat treatment, band A (heated 0.25HP) completely disappeared (**Fig. 4.7A**, lane 5), which suggests that 11S globulin aggregated via sulphydryl-disulphide exchange reactions leading to the formation of intermolecular disulphide bonds during the heat treatment.

This result is expected because hempseed globulin, similar to other plant globulin proteins, can be denatured by heating, forming soluble and/or insoluble aggregates (Wang & Xiong, 2019), and the denaturation temperature for hempseed globulin is 91.9 °C (Wang et al., 2008). Commercial HP contains aggregated protein particles, possibly due to denaturation/ aggregation during the protein powder manufacturing. Such aggregates were broken down to some extent during the microfluidisation process, but heat treatment may have modified the surface structure of HP particles, exposing the hydrophobic groups and thiol groups and so allowing further particle-particle interactions. Conversely, unheated 0.25β-lg showed only one band (band B) representing the monomer of β-lg (**Fig. 4.7A**, lane 3), but after heat treatment, two predominant bands could be observed: β-lg monomers (band B) and heat-induced dimers (band C) (**Fig. 4.7A**, lane 6). This is in agreement with previous studies that heat treatment above the denaturation temperature results in the formation of β-lg dimers and trimers that are linked via disulphide bonds (Schokker et al., 1999).

In the protein mixtures, unheated 0.25 HP/0.25β-lg showed two distinct bands corresponding to HP 11S globulin and β-lg (**Fig. 4.7A**, lane 4). But after heating, the band corresponding to 11S globulin disappeared, and the intensity of both β-lg monomers and

dimers (**Fig. 4.7A**, lane 7) was reduced compared with that when the β-lg solution was heated alone. This could be explained by the formation of disulphide bonds between HP particles and β-lg upon heating, which led to the formation of HP/β-lg aggregates with larger molecular weight protein aggregates that remained at the top of the stacking gel.

To further explore the protein-protein interactions, the unheated and heated protein mixtures (Total) and their supernatant (SUP) and sediment (SED) fractions were analysed using reducing SDS-PAGE (**Fig. 4.7B**). Under reducing conditions, the covalent interactions formed between two proteins during heating were further disrupted by breaking the disulphide bonds using a reducing reagent (dithiothreitol).

Under reducing conditions, the total fraction of unheated 0.25HP/0.25β-lg mixture had three HP globulin bands (**Fig. 4.7B**, lane 2) consisting of band D, 34 kDa (acid subunit), band E (20 kDa) and band F (18 kDa) (two basic subunits) (Potin & Saurel, 2020; Q. Wang, Y. Jin, et al., 2018). There was one band (band G) representing β-lg in the unheated protein mixture. After centrifugation of unheated 0.25HP/0.25β-lg mixture, all three HP bands were observed in the sediment (**Fig. 4.7B**, lanes 3 and 4), indicating that HP particles were completely sedimented at 20,000 × *g*. As expected, no virtually β-lg band was found in the sediment of either heated 0.25% β-lg (data not shown) or unheated 0.25HP/0.25β-lg mixture, suggesting that native β-lg and heat-treated 0.25β-lg aggregates remain soluble under these conditions.

Interestingly, although the total fraction of 0.25HP/0.25β-lg mixture showed all protein bands corresponding to HP and β-lg after heat treatment, the sediment and supernatant fractions were remarkably different from their unheated counterparts. In fact, the sediment fraction of the heated 0.25HP/0.25β-lg mixture showed a β-lg monomer band (**Fig. 4.7B**, lane 7), which was absent in the sediment of the unheated mixture (**Fig. 4.7B**, lane 4). This suggests that β-lg interacted with HP particles, possibly via sulphydryl-

disulphide exchange reactions during heating, becoming associated with the sedimentable fraction. However, it should be noticed that the β-lg monomer was also seen in the supernatant of the heated mixture, suggesting that only a proportion of β-lg interacted with the HP particles (**Fig. 4.5B**, lane 6).

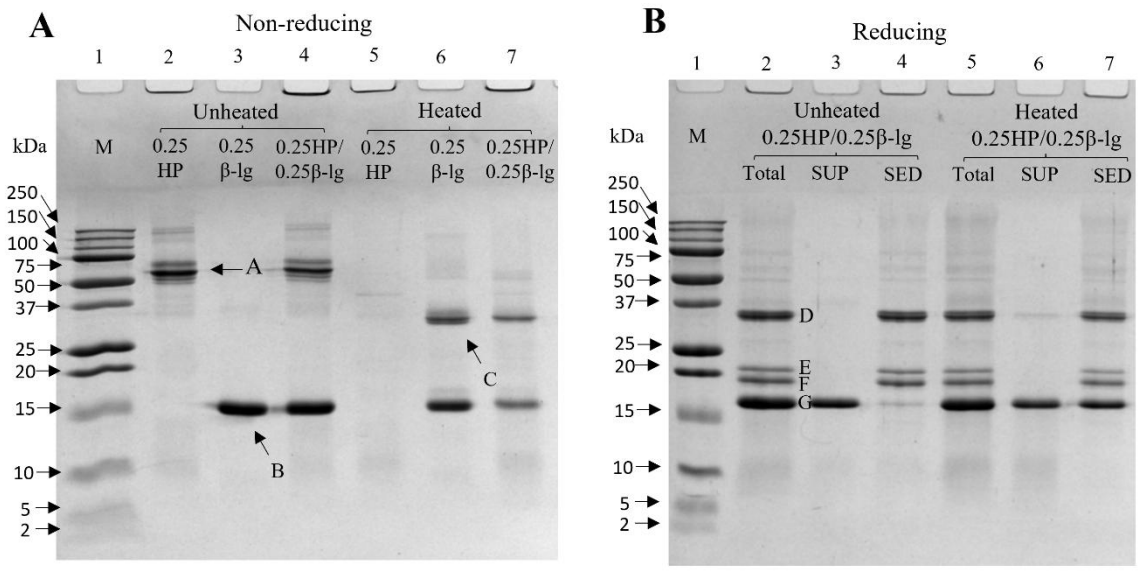


**Fig. 4.7.** Panel A: non-reducing SDS-PAGE of unheated (lanes 2–4) and heated (lanes 5–7; 95 °C, 20 min) dispersions of 0.25HP (lanes 2 and 5), 0.25β-lg (lanes 3 and 6) and 0.25HP/0.25β-lg (lanes 4 and 7). Lane 1, molecular mass marker. Panel B: reducing SDS-PAGE of unheated (lanes 2–4) and heated (lanes 5–7; 95 °C, 20 min) dispersions of 0.25HP/0.25β-lg (lanes 2 and 5; total) and the corresponding supernatants (lanes 3 and 6; SUP) and sediments (lanes 4 and 7; SED). Lane 1, molecular mass marker. Letters indicate: A, subunit of 11S globulin; B, β-lg monomers; C, β-lg dimers; D, HP globulin acid subunit; E, HP globulin basic subunit; F, HP globulin basic subunit; G, β-lg.

### 4.3.4 Effect of heating time at 95 °C on HP/β-lg interactions

To understand the effect of heating time on the interaction between HP and β-lg, the supernatants from heated HP/β-lg mixtures at different times were analysed using SDS-PAGE under reducing conditions (**Fig. 4.8A**). Only β-lg monomer was observed in the SDS-PAGE gel at all heating times, indicating that all HP particles were sedimented. The heated 0.25HP/0.25β-lg samples had lighter β-lg monomer bands (**Fig. 4.8A**, lanes 3–7) compared with the unheated sample (0 heating time; **Fig. 4.8A**, lane 2), which indicates that some of β-lg was associated with the HP particles while a proportion of β-lg did not interact with HP particles and thus remained in the supernatant.

The band intensity (%) was estimated by the densitometric scanning of these gels to monitor the loss of β-lg in the supernatant due to its association with HP particles (**Fig. 4.8B**). The intensity of β-lg monomer was significantly reduced from 100% (0 min) to 68% and 66% after 10 to 20 min of heat treatment, but then remained steady until 60 min. This suggests that the rapid protein-protein interactions took place in the first 10 to 20 min and tended to plateau on prolonged heating.

Interestingly, Anema and Li (2003a) reported similar association behaviour of β-lg with casein micelles in a heated milk system. Whey proteins were rapidly associated with casein micelles at high temperatures (90–100 °C) during the initial period of heating, but not all whey proteins were associated with the casein micelles. A proportion of denatured whey proteins remained in the milk serum as disulphide-bonded and hydrophobically associated aggregates. The proportions of denatured β-lg associated with the casein micelles varied from 50% to 80%, depending on the heating conditions, but not all β-lg was associated with casein micelles (Anema & Li, 2003a). A similar study reported that the extent of association of β-lg increased with an increase in heating time, and a maximum of

50% β-lg was associated with casein micelles (Oldfield, Taylor, et al., 2005; Oldfield et al., 1998).

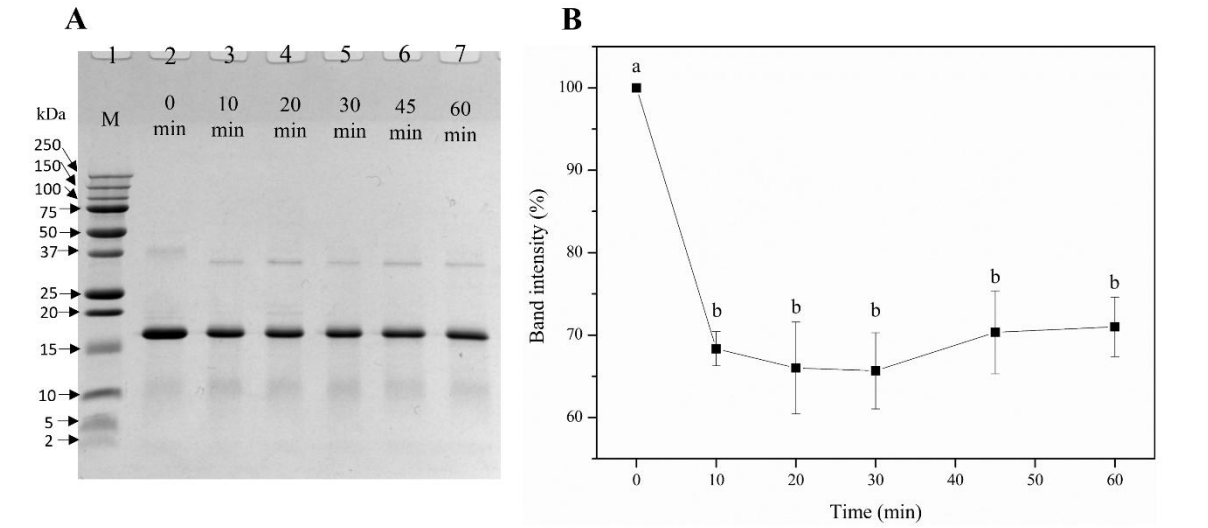


**Fig. 4.8.** Reducing SDS-PAGE (A) of the supernatant obtained from heating 0.25HP/0.25β-lg dispersions at 95 °C for (lanes 2–7, respectively) 0, 10, 20, 30, 45 and 60 min (lane 1, molecular mass marker) with changes in band intensity (%) of β-lg in the corresponding supernatants (B). Different lowercase letters indicate that the results are significantly different ($P < 0.05$).

To explore the role of disulphide bond formation in the association of β-lg with HP particles, the individually heated 0.25β-lg and heated protein mixture were analysed by non-reducing SDS-PAGE. When 0.25β-lg was heated alone, the band intensity of β-lg monomer (band A) decreased with an increase in heating time, while β-lg dimer (band B) increased with increasing heating time (**Fig. 4.9A**). Schokker et al. (1999) explained the formation of β-lg aggregates upon heating a pure solution of β-lg. At low protein concentrations and short heating times, the free sulphydryl group and hydrophobic side chains of β-lg would be exposed, but this unfolding of β-lg could be partly reversible. Upon

prolonging heating time, the reactive β-lg monomers aggregated and formed certain dimers, trimers and oligomers through sulphydryl oxidation, thiol/disulphide exchange and non-covalent interactions.

A similar trend was observed in the co-heated 0.25HP/0.25β-lg mixture, but the band intensity of the β-lg dimer was much lower (**Fig. 4.9B**). The band intensity of β-lg monomer in 0.25β-lg and the protein mixture both decreased with heating time (**Fig. 4.9C**). However, the decrease in band intensity from the protein mixture was faster during the first 10 and 20 min, compared with 0.25β-lg heated alone. This indicates that during the first 20 min, unfolded β-lg preferentially interacted with HP particles. It appears that once β-lg is unfolded, it tends to interact with HP particles or self-aggregate into dimers in the first 20 min. No percentage difference was seen at longer heating times (30–60 min), suggesting the amount of β-lg involved in these interactions was the same in 0.25β-lg or 0.25HP/0.25β-lg.

Regarding the changes in β-lg dimer (**Fig. 4.9D**), the band intensity of β-lg dimer in 0.25β-lg increased with the increase in heating time from 7% to 70% at 30 min and remained steady thereafter. Most interestingly, β-lg dimer in the heated protein mixture showed a relatively small increase in dimer formation. The percentage difference in dimer formation between the β-lg solution and the protein mixture increased to 45% in the first 30 min and stayed steady for the rest of the heating time. This suggests that there were fewer β-lg dimers remaining in the supernatant of the protein mixture after heating, possibly due to their association with HP particles.

One possible explanation is that once the β-lg monomer was denatured, it preferentially interacted with HP; therefore, there was less probability of β-lg forming dimers. Another possibility is that the β-lg dimers were rapidly formed before their interaction with the HP particles, since the denaturation temperature of β-lg (74–76 °C) is

lower than that of hempseed globulin (91.9 °C). In this scenario, β-lg dimers or higher polymers would be expected to associate with HP particles. These heat-induced molecule/particle interactions may be a similar case to that of heated milk containing whey proteins and casein micelle particles. The rate of whey protein denaturation was higher than the rate of whey-casein micelles association, and the β-lg aggregates were found to associate with casein micelles (Anema, 2007; Anema & Li, 2003a; Oldfield, Singh, et al., 2005).

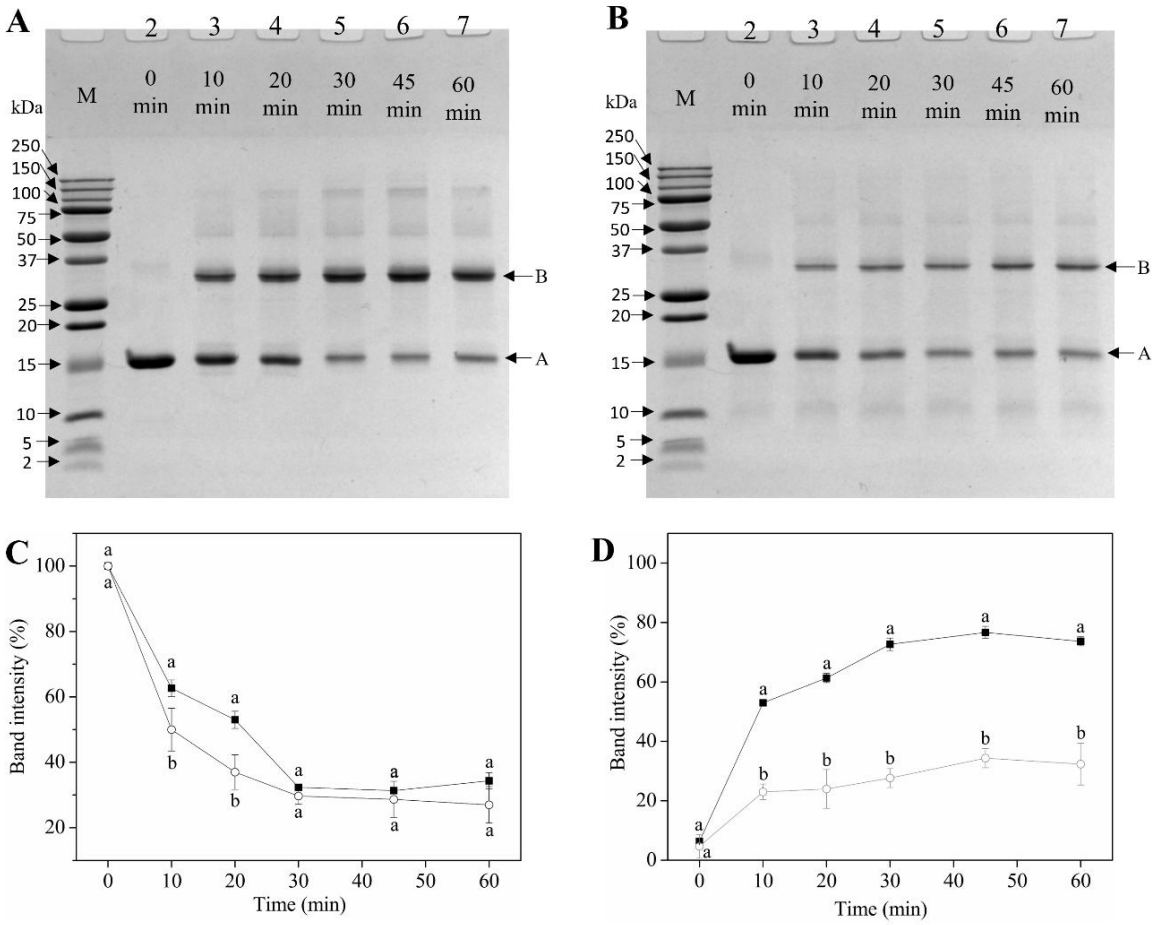


**Fig. 4.9.** Non-reducing SDS-PAGE of the supernatants obtained from heating (A) 0.25β-lg and (B) 0.25HP/0.25β-lg dispersions at 95 °C for (lanes 2–7, respectively) 0, 10, 20, 30, 45 and 60 min (lane 1, molecular mass marker; lettered arrows indicate: A, β-lg monomer; B, β-lg dimer) with changes in band intensity (%) of (C) β-lg monomer and of (D) β-lg dimer in the corresponding supernatants of the 0.25β-lg (■) and 0.25HP/0.25β-lg (○) dispersions. Statistical analysis was done by individual heating time. Different lowercase letters indicate that the results between 0.25β-lg and 0.25HP/0.25β-lg at different time points are significantly different ($P < 0.05$).

### 4.3.5 Effect of HP to β-lg ratio on heat-induced interactions

In a milk system, Dalgleish et al. (1997) showed that the association of β-lg with casein micelles was dependent on the β-lg: casein micelles ratio, as there were only a certain number of sites on the surface of casein micelles that could interact with β-lg. The interaction between β-lg and casein micelles was limited when the β-lg:κ-casein ratio was above 0.6. However, the β-lg bound more efficiently to the casein micelles at this saturating level (i.e., β-lg:κ-casein <0.6).

Similar to that reported for casein micelle and β-lg association, it was thought that there would be a limited number of sites at the HP particle surface with which β-lg could interact. To investigate this, the association of β-lg with HP at higher HP:β-lg ratios (0.25HP/0.1β-lg and 0.25HP/0.05β-lg) was analysed using SDS-PAGE under reducing conditions, and the change in the band intensity for β-lg (**Fig. 4.10A**, band A) was estimated by the densitometric scanning (**Fig. 4.10B**).

The intensity of the β-lg band decreased after heat treatment in each group (**Fig. 4.10A**), and the proportion of β-lg remaining in the supernatant decreased from about 70% at 0.25HP/0.25β-lg to about 20% at 0.25HP/0.05β-lg (**Fig. 4.10B**). Clearly, at higher HP:β-lg ratios, more reactive groups from the HP particles were available for interacting with β-lg. This percentage difference proved our hypothesis that the HP:β-lg ratio was an important factor affecting the extent of β-lg association.

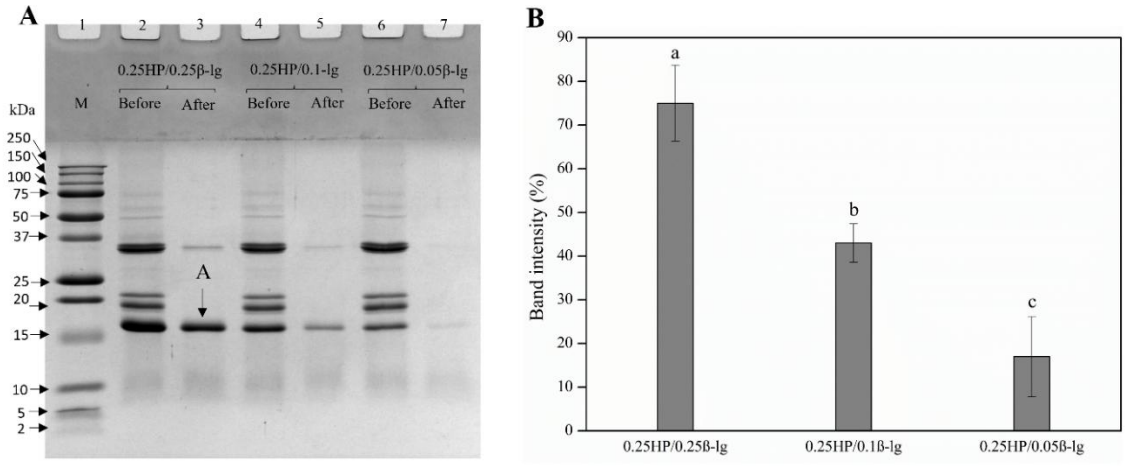


**Fig. 4.10.** Reducing SDS-PAGE (A) of dispersions of 0.25HP/0.25β-lg (lanes 2 and 3) 0.25HP/0.1β-lg (lanes 4 and 5) and 0.25HP/0.05β-lg (lanes 6 and 7) (lane 1, molecular mass marker) before heat treatment at 95 °C for 20 min (lanes 2, 4 and 6) and the corresponding supernatants after heat treatment (lanes 3, 5 and 7; β-lg band indicated by the letter A), with changes of band intensity (B; %) of β-lg in the supernatants. Different lowercase letters indicate that the results are significantly different ($P < 0.05$).

### 4.3.6 Hypothetical mechanism of heat-induced interactions between HP particles and β-lg

According to all the results above, a possible mechanism by which HP/β-lg hybrid particles are produced after heat treatment is proposed (**Fig. 4.11**). When HP is heated individually (**Fig. 4.11A**), the surface of HP particles may be modified to expose the free thiol groups to allow thiol-disulphide interchange to form larger aggregates. The hydrophobic interactions may also contribute to the aggregation process.

Heat treatment causes unfolding of β-lg, exposing free sulphydryl groups. The irreversible aggregates are formed by sulphydryl-disulphide interchange reactions and hydrophobic interactions (Brodkorb et al., 2016; Singh & Havea, 2003). When the HP particles and β-lg are heated together (**Fig. 4.11B**), the β-lg would first unfold at around

75 °C (Sava et al., 2005), and a proportion of the unfolded β-lg monomers may associate with HP particles. The free sulphydryl group of β-lg may be responsible for initiating this association via interaction with disulphide bonds present at the surface of HP particles.

Simultaneously, some β-lg monomers may self-aggregate into dimers or large aggregates. With increasing heat treatment to the denaturation temperature of HP (91.9 °C), more reactive groups, possibly thiols, of HP could be exposed on the surface of HP particles, allowing further association of β-lg with HP particle surfaces. Since the β-lg would occupy the reactive groups of HP particles, the aggregation of HP would be restricted, resulting in smaller aggregates compared with the individually heated HP particles.

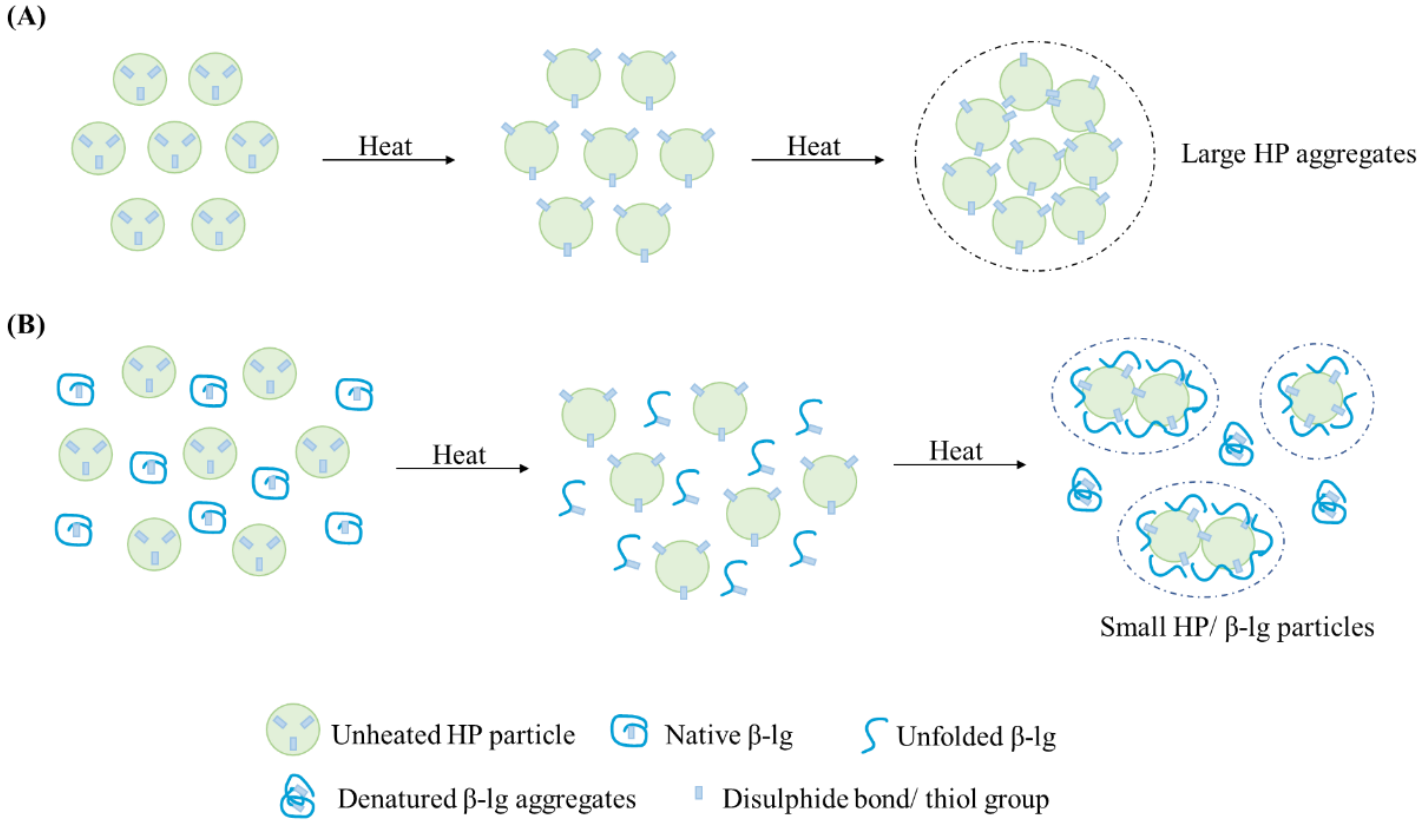


**Fig. 4.11**. Schematic representation of possible mechanisms by which large HP aggregates form in the absence of β-lg (A) and by which HP particles and β-lg interact (B) during heat treatment (95 °C, 20 min).

## 4.4. Conclusions

The HP aggregates were successfully disrupted by microfluidisation. Although hempseed globulin is insoluble in water, a large amount of the HP globulin was transferred into the supernatant phase after microfluidisation treatment. The HP particles and β-lg associate on heating above 90 °C because the exposed reactive thiol groups of β-lg can interact with disulphide bonds on the surface of HP particles. The association of β-lg could limit the HP self-aggregation and could avoid the undesired large aggregates that may lead to inferior functionalities. Thus, HP/β-lg hybrid particles with uniform spherical shapes could be formed via heat treatment.

This is an exploratory study to offer an approach for improving the dispersibility of plant proteins and developing novel hybrid protein particles as food materials. Moreover, it is also interesting to understand the potential utilisation of these new hybrid particles in food applications such as emulsion, gelation and fat replacement.

## INDUSTRIAL RELEVANCE

The plant protein industry is rapidly growing, driven by consumers' preferences to reduce their consumption of animal protein due to environmental, health, and/or ethical reasons. Unfortunately, plant proteins pose various technological challenges that limit rapid food innovation. Nowadays, scientific advances towards developing high-performance and eco-friendly protein ingredients are critically needed. One promising strategy is combining plant proteins with milk proteins to improve techno-functionality. However, to accomplish this outcome, fundamental knowledge of protein-protein interactions will contribute to advancing the generation of novel protein ingredients. This study particularly provides underlying insights that can be applied to develop microparticulated plant/milk protein ingredients for food applications.

MASSEY UNIVERSITY
TE KUNENGA KI PŪREHUROA
UNIVERSITY OF NEW ZEALAND

GRADUATE RESEARCH SCHOOL

# STATEMENT OF CONTRIBUTION
# DOCTORATE WITH PUBLICATIONS/MANUSCRIPTS

We, the student and the student's main supervisor, certify that all co-authors have consented to their work being included in the thesis and they have accepted the student's contribution as indicated below in the Statement of Originality.

| | |
|---|---|
| Student name: | Sihan Ma |
| Name and title of main supervisor: | Dr Alejandra Acevedo-Fani |
| In which chapter is the manuscript/published work? | Chapter 5 |

Describe the contribution that the student and members of the supervisory team have made to the manuscript/published work:[1]

Sihan Ma: Investigation, Methodology, Formal analysis, Data curation, Writing - original draft, Visualization.
Aiqian Ye: Methodology, Writing - review & editing, Supervision.
Harjinder Singh: Methodology, Writing - review & editing, Supervision, Funding acquisition.
Alejandra Acevedo-Fani: Conceptualisation, Supervision, Methodology, Validation, Resources, Writing - review & editing.

Please select one of the following three options:

- (●) **The manuscript/published work is published or in press**

  Please provide the full reference of the research output:

  Ma, S., Ye, A., Singh, H., & Acevedo-Fani, A. (2024). Heat-induced interactions between microfluidized hemp protein particles and caseins or whey proteins. Food Chemistry, 141290. https://doi.org/10.1016/j.foodchem.2024.141290

- ( ) **The manuscript is currently under review for publication**

  Please provide the name of the journal:

- ( ) **It is intended that the manuscript will be published, but it has not yet been submitted to a journal**

| | | | |
|---|---|---|---|
| Student's signature: | Sihan Ma — Digitally signed by Sihan Ma, DN: cn=Sihan Ma, c=NZ, email=s.ma@massey.ac.nz, Date: 2025.07.18 13:54:24 +12'00' | Main supervisor's signature: | Alejandra Acevedo Fani — Digitally signed by Alejandra Acevedo Fani, DN: cn=Alejandra Acevedo Fani, c=NZ, o=Massey University, ou=Riddet Institute, email=a.acevedo-fani@massey.ac.nz, Date: 2025.07.31 07:48:12 +12'00' |

*This form should be placed at the beginning of each relevant thesis chapter.*

[1] Refer to the Massey University Publishing and Authorship guidelines (OneMassey for staff, Stream for students) and/ or Contributor Roles Taxonomy (CRediT) guidelines for guidance.

# Chapter 5: Heat-induced interactions between microfluidised hemp protein particles and caseins or whey proteins

This chapter has been published in a peer-reviewed journal:

Ma, S., Ye, A., Singh, H., & Acevedo-Fani, A. (2024). Heat-induced interactions between microfluidised hemp protein particles and caseins or whey proteins. *Food Chemistry*, 141290. https://doi.org/10.1016/j.foodchem.2024.141290

## Abstract

The rising demand for sustainable proteins leads to increased interest in plant proteins like hemp protein (HP). However, commercial HP's poor functionality, including heat aggregation, limits its use. This study explored the heat-induced interactions of hemp protein particles (HPPs) with milk proteins, specifically whey proteins and caseins. Using various analysis techniques—static light scattering, TEM, SDS electrophoresis, surface hydrophobicity, and free sulfhydryl content—results showed that co-heating HPPs with whey protein isolate (WPI) or sodium caseinate (NaCN) at 95°C for 20 minutes reduced HPPs aggregation. HPPs/WPI particles had a $d_{4,3}$ of ~3.8μm, while HPPs/NaCN were ~1.9μm, compared to ~27.5μm for HPPs alone. SDS-PAGE indicated that whey proteins irreversibly bound to HPPs, through disulphide bonds, whereas casein bound reversibly, possibly involving the chaperone-like property of casein. This study proposes possible mechanisms by which HPPs interact with milk proteins and impact protein aggregation. This may provide opportunities for developing hybrid protein microparticles.

## 5.1 Introduction

In the last decade, the application of plant proteins in food products has increased considerably because of a need to balance and diversify overall protein resources and feed a growing world population within planetary boundaries (Akharume et al., 2021). However, the inferior functional properties of most plant proteins have limited their wider implementation as food ingredients (Day, 2013; Hadnađev et al., 2018). To overcome this challenge and meet the requirements of functionality, plant proteins can be combined with dairy proteins under specific conditions to create hybrid protein ingredients (Boland et al., 2013). For example, it has been reported that hemp globulin and sodium caseinate complexes exhibited good emulsification properties, forming stable oil-in-water emulsions (Chuang et al., 2020). Similarly, pea and whey protein mixtures exhibited improved gelling properties in terms of storage modulus and gel hardness compared with pea protein alone (Wong et al., 2013a).

Microparticulation of proteins is a technique that produces uniform spherical particles, with sizes often between 0.1 and 10.0 μm. The functional properties of microparticulated proteins depend on their morphology, size, surface and internal features of the particles (Beran et al., 2018). This technique was initially proposed to modify whey proteins to create protein ingredients with unique properties, including fat-mimetic ability, increased heat stability and protein fortification, without affecting the product quality (Ipsen, 2017). More recently, plant proteins, such as soy and zein, have been explored in this context and proposed as fat replacers for plant-based food products (Nourmohammadi et al., 2023). However, a gap that exists in the literature is the potential of hybrid microparticles produced by combinations of plant and milk proteins, which could extend milk protein applications while facilitating the use of plant proteins in food formulations.

Hempseeds are a good source of high-quality protein with low allergenicity (Callaway, 2004; Q. Wang, J. Jiang, et al., 2018). Hemp protein (HP) contains about 25% albumin and 67–75% globulin (Aluko, 2017). The 11S globulin (edestin) is a homohexamer containing six subunits (52 kDa) linked by non-covalent interactions. Each subunit has a basic subunit (around 18 and 20 kDa) and an acid subunit (around 34 kDa) connected covalently (Potin & Saurel, 2020; Q. Wang, Y. Jin, et al., 2018) and five cysteine residues are found in each subunit. Two cysteine residues form a disulphide bond linking the basic subunit and the acid subunit. Within the acid subunit, two cysteine residues form the intrachain disulphide bond. The other cysteine residue remains as a free thiol group, which makes HP prone to aggregation under specific conditions (Chuang et al., 2019; Docimo et al., 2014; Tang et al., 2006). HP forms large aggregates upon heating above its denaturation temperature (92 °C). This has been attributed to the relatively high free thiol content of edestin, which can undergo thiol-disulphide interchange reactions, resulting in aggregation (Tang et al., 2006). Thus, maintaining the thermal stability of HP during food processing remains a challenge.

Milk proteins contain about 20% whey proteins and 80% caseins (Goulding et al., 2020; Singh & Havea, 2003). Whey proteins contain two main fractions, β-lactoglobulin (β-Lg; 54%) and α-lactalbumin (α-La; 21%) (Hussain et al., 2012). Whey proteins in their native state are globular proteins with good solubility. However, they unfold and expose buried hydrophobic groups and sulphydryl groups upon heating above 75 °C. Through the sulphydryl-disulphide interchange and hydrophobic interactions, unfolded whey proteins link together forming aggregates (Anema, 2020; Dissanayake & Vasiljevic, 2009). In contrast, caseins (containing about 10% $\alpha_{S1}$-casein, 40% $\alpha_{S2}$-casein, 40% β-casein and 10% κ-casein) show excellent heat stability because of their flexible secondary and tertiary structures (Broyard & Gaucheron, 2015). Moreover, caseins can act as chaperones and

inhibit the aggregation of globular proteins under stressful environments, such as high temperatures (Yong & Foegeding, 2010). The hydrophobic amino acid side chains of caseins can interact with unfolded whey proteins and the negatively charged group can create repulsion to keep the folded chain flexible (Akbari et al., 2018; Koudelka et al., 2009). Most of this research has been carried out in milk protein systems where caseins (particularly β-casein) have been shown to inhibit heat-induced aggregation of whey proteins (Akbari et al., 2018; Guyomarc'h et al., 2009; Kehoe & Foegeding, 2011, 2014; Koudelka et al., 2009; Liyanaarachchi et al., 2015).

Previous studies reported that the combination of plant proteins with whey proteins may reduce the heat-induced aggregation of plant proteins (Ma, Acevedo-Fani, et al., 2024). For instance, co-heating soy 11S globulin with β-lg (Anuradha & Prakash, 2009) and pea globulin with β-lg (Chihi et al., 2016) led to the formation of smaller aggregates compared with individually heated soy and pea globulin. However, only one study has reported that the addition of sodium caseinate inhibits heat-induced aggregation of molecular HP globulin and increase protein solubility in a high-salt environment (Chuang et al., 2019). From these studies, it appears that both whey proteins and caseins can restrict the heat-induced aggregation of the above-mentioned plant proteins via different mechanisms.

However, the main limitation of the previous studies is that they described heat-induced interactions using relatively pure isolated protein fractions. Particularly, for HP/milk protein mixtures, there is no information on protein-protein interactions using commercial protein ingredients. The processing conditions used in the production of commercial protein ingredients, particularly plant proteins, often cause extensive denaturation and aggregation of proteins. As a result, the commercial HP ingredients have poor solubility in water. In this study, therefore HP dispersions were first microfluidised to generate hemp protein particles (HPPs) and then their heat-induced interactions with milk

proteins (whey protein isolate, WPI or sodium caseinate, NaCN) were studied. The aim of this study is to understand the possible mechanism of heat-induced interactions between hemp protein and two major milk protein fractions, whey protein and casein, in order to understand how these interactions influence aggregation behaviour and microstructure formation. The findings provide new insights that can inform the produce of new functional HP/milk protein microparticles for potential food applications.

## 5.2 Materials and methods

### 5.2.1 Materials

Whey protein isolate (WPI) containing 92.0% protein, 0.9% fat, 1.6 % ash and 5.2% moisture and sodium caseinate (NaCN) containing 92.3% protein, 0.6% fat, 4.0% ash and 4.8% moisture were purchased from Fonterra Co-operative Group Limited, Auckland, New Zealand. The hempseed protein (HP) concentrate powder was purchased from Davis Food Ingredients (Davis Trading Company Ltd., Palmerston North, New Zealand). All chemicals were purchased from Sigma-Aldrich Ltd. (St. Louis, MO, USA), and the reagents were made up in Milli-Q water (Milli-Q apparatus; Millipore Corp., Bedford, MA, USA).

### 5.2.2 Proximate analysis

The proximate composition of HP was analysed as follows: protein content was determined using the Kjeldahl method (AOAC 991.20, nitrogen factor 5.21); fat, ash and moisture content were determined according to AOAC 922.06, AOAC 942.05 and AOAC 925.10, respectively (AOAC, 2023); and carbohydrate content was calculated by subtracting the sum of the protein, ash and fat from the total solid. The HP powder contained 59.8% protein, 2.4% fat, 10.7% ash, 6.8% moisture and 20.2% carbohydrate.

### 5.2.3 Preparation of hemp protein particles

A dispersion of HP was prepared by mixing HP powder in Milli-Q water at 1% (w/w) protein concentration and stirring for 2 h at 20 °C. The pH was adjusted to 11, using 1 M NaOH, followed by 2 h stirring. The HP dispersion was centrifuged (3000 × *g*, 30 min) to remove insoluble material (such as insoluble fibre). The resulting supernatant (mostly containing HP) was collected and adjusted to pH 7 using 1 M HCl. The dispersion composed by the supernatant was processed by microfluidisation (M-110P, Microfluidics, Newton, MA, USA) at 200 MPa and 2 passes to produce HP particles (HPPs) that were used in the mixtures with milk proteins.

### 5.2.4 Preparation of HPPs/WPI and HPPs/NaCN mixtures

Stock solutions of WPI or NaCN were prepared by dissolving 1% (w/w) protein in Milli-Q water with magnetic stirring for 2 h. HPPs dispersion was mixed with WPI or NaCN to achieve a final protein concentration in the mixture at 0.25% HP and 0.25% WPI or NaCN. The pH of the protein mixtures was adjusted to pH 7 using 1 M NaOH, followed by heating at 95 °C for 20 min in the water bath. The heating condition was selected based on our previous study that suggested the most interactions between HP and β-lg happened in the first 20 min. After the heat treatment, the samples were cooled down in ice to 20 °C immediately. Sodium azide (0.02%, w/w) was added to inhibit microbial growth.

### 5.2.5 Particle size analysis

The particle size of unheated HPPs and heated HPPs/WPI and HPPs/NaCN mixtures was measured by static light scattering using a Mastersizer 2000 and a Hydro MU unit (Malvern Instruments, Worcestershire, UK). The refractive indices of hemp protein

and water were 1.45 and 1.33, respectively. The data was reported in volume-weighted mean diameter $d_{(4, 3)}$, calculated as the average of triplicate measurements.

### 5.2.6 Transmission electron microscopy

Sample preparation and negative staining for transmission electron microscopy (TEM) were performed as described by Vincekovic et al. (2014). An aliquot of 80 μL of protein solution was placed on a formvar/carbon-coated 200 mesh copper grid for 4 min. The excess sample was removed by filter paper. 80 μL of uranyl acetate (2%, w/w) was placed on the grid for another 4 min and the excess staining solution was removed with filter paper. The stained sample was imaged at 6000x, 16500x and 20500x magnification by a transmission electron microscope (Philips CM10) (Eindhoven, the Netherlands) at 100 kV.

### 5.2.7 Sodium dodecyl sulphate polyacrylamide gel electrophoresis

The protein composition was analysed using sodium dodecyl sulphate polyacrylamide gel electrophoresis (SDS-PAGE) with a Tris-glycine gel under non-reducing and reducing conditions as per the protocol described by Dave et al. (2019) and Manderson et al. (1998). The protein sample was mixed with non-reducing or reducing sample buffer to a final protein concentration of 1 mg/mL. Dithiothreitol was used as a reducing agent in the reducing sample buffer (200 mM) and the reducing samples were heated at 56 °C for 15 min. Ten microlitre samples were loaded onto Mini-Protean gels (Bio-Rad Laboratories, Richmond, CA, USA) and run at 150 V, followed by Coomassie brilliant blue staining and destaining (10% isopropanol and 10% glacial acetic acid in water, v/v). The destained gel was scanned by the molecular imager Gel Doc XR (Bio-Rad Laboratories, Richmond, CA, USA) and analysed by ImageLab software.

### 5.2.8 Free sulphydryl content

Free sulphydryl (SH) contents of unheated and heated HPPs, WPI, NaCN and their mixtures were measured using Ellman's reagent [5,5'-dithiobis (2-nitrobenzoic acid); DTNB] as described by Xu et al. (2022) with slight modifications. Protein samples (1 mg/mL) were mixed with Tris-glycine buffer (pH 8) containing 86 mM Tris, 90 mM glycine, 40 mM EDTA, and 8 M urea. Ellman's reagent (4 mg/mL) was also made in Tris-glycine buffer. A 1.5 mL sample was mixed with 20 μL Ellman's reagent followed by 30 min incubation. The absorbance of resulting 5-nitro-2-thiobenzoic acid (TNB) chromogen was measured by a spectrophotometer (Genesys 10-S; Thermo Fisher Scientific Inc., USA) at a wavelength of 412 nm. The Tris-glycine buffer with Ellman's reagent was used as blank.

Free SH content was calculated using equation (Eq. 5.1):

$$SH\ (\mu mol/g) = (10^6 \times A \times D)/ (1.36 \times 10^4 \times C) \quad \text{(Eq. 5.1)}$$

where A is the absorbance value, C is the protein concentration, D is the dilution factor, $1.36 \times 10^4$ is the molar absorptivity of TNB and $10^6$ is the conversion from molar basis to μmol/mL basis.

### 5.2.9 Surface hydrophobicity ($H_0$)

The surface hydrophobicity ($H_0$) of unheated and heated HPPs, WPI, NaCN and their mixtures was measured using 8-aniline-1-naphthalene sulfonic acid (ANS) as a fluorescent probe (Chihi et al., 2016). The protein sample was diluted in 10 mM sodium phosphate buffer (pH 7) to obtain protein concentrations ranging from 0.0004 to 0.02%. Then 20 μL ANS solution (8 mM) was added to a 4 mL protein sample and incubated for 15 min in the dark. The fluorescence intensity was measured using a spectrofluorometer (FP-6500, JASCO, Tokyo, Japan) with an excitation wavelength of 390 nm and an emission

wavelength of 470 nm. The $H_0$ was calculated as the initial slope of fluorescence intensity versus protein concentration by linear regression.

### 5.2.10 Heat stability of the HPPs/WPI and HPPs/NaCN mixtures

45 mL heated HPPs/WPI and HPPs/NaCN mixtures as described in **Section 5.2.4** were centrifuged (20,000 × *g*, 15 min) to collect true hybrid microparticles and remove the unbonded free protein. To test the heat stability of the HPPs/WPI and HPPs/NaCN particles and eliminate the impact of supernatant protein, the pellet was re-dispersed in Milli-Q water to reach the same volume as before centrifugation. These dispersions were reheated for a second cycle at 95 °C for 20 min using a water bath and the particle size was measured, as described in **Section 5.2.5**.

### 5.2.11 Data analysis

Experiments were carried out in triplicate, and the results are reported as mean ± standard deviation. Statistical analysis was performed using SPSS software for Windows (version 29.0, SPSS Inc., Chicago, IL, USA). The data were analysed by independent t-tests between two groups, and one-way analysis of variance (ANOVA) for multiple comparisons, using Tukey's test with the level of significance set at $p < 0.05$.

## 5.3 Results and discussion

### 5.3.1 Particle size distributions of HPPs/milk protein dispersions

The effect of heat treatment on the particle size of different protein mixtures was investigated and the particle size distributions and volume-weighted mean diameter ($d_{4,3}$) are shown in **Fig. 5.1**. As can be seen from the size distributions (**Fig. 5.1A**), the unheated HPPs dispersion had a bimodal particle size distribution characterised by two peaks at 0.1–

1 μm and 1– 10 μm indicating the heterogeneity of the HPPs even after microfluidisation. The $d_{4,3}$ value of HPPs was about 2.0 μm (**Fig. 5.1B**).

Heat treatment at 95 °C resulted in the formation of large-size HPPs aggregates as evidenced by a shift of the peaks to the right and a large population of particles located in the 1 to 100 μm particle size range (**Fig. 5.1A**), with a $d_{4,3}$ of 27.5 μm (**Fig. 5.1B**). In native HP, heat-induced aggregation was expected because of the large percentage of globulin in its composition (60–80%), which is a group of proteins sensitive to heat (Wang & Xiong, 2019). In particular, it has been reported that HP heated at temperatures ≥80 °C results in extensive aggregation (Raikos et al., 2015) due to the high content of cysteine residues (Wang & Xiong, 2019) and disulphide bond formation. In our study, although the manufacturing process for hemp protein powder and the microfluidisation process used for creating HPPs may have changed the protein structure, we hypothesise that the heat treatment was still able to modify the surface structure of HPPs and expose the free thiol groups and hydrophobic groups for further particle-particle interactions.

Interestingly, the heated HPP/WPI dispersion had a greater population of particles located between 0.1 to 10 μm (**Fig. 5.1A**) and the $d_{4,3}$ was much smaller (3.8 μm) (**Fig. 5.1B**) than the heated HPP. The relatively low degree of aggregation observed in heated mixtures compared with heated HPPs dispersions suggests that whey proteins could restrict aggregation of HPP (Ma, Acevedo-Fani, et al., 2024). In other plant protein/whey protein systems, similar phenomena have been observed (Anuradha & Prakash, 2009; Chihi et al., 2016).

On the contrary, heating of HPPs in the presence of NaCN resulted in a particle size distribution similar to that of unheated HPPs (**Fig. 5.1A**) with $d_{4,3}$ of 1.9 μm (**Fig. 5.1B**). This indicates that the caseins were also able to inhibit HPPs aggregation during heating. A similar effect has been seen in recent studies using soluble pea proteins and casein

micelles combinations, and HP globulin/NaCN mixtures (Beghdadi et al., 2022; Chuang et al., 2019). Chuang et al. (2019) reported the addition of 0.05% NaCN in 0.1% molecular HP globulins at a high salt concentration (0.5 M ionic strength) could form small intermediate aggregates and delay the formation of large aggregates. It has also been shown that NaCN restricts heat-induced aggregation of whey proteins (Morgan et al., 2005). For instance, mixing $\alpha_{S1}$-casein with whey protein (1: 1) reduced whey protein aggregation during thermal treatments and this is due to casein's chaperone effect (Bhattacharyya & Das, 1999). Liyanaarachchi et al. (2015) also reported that casein can govern the aggregation of whey protein and prevent the denaturation of whey protein during heat treatment, owing to its chaperone-like activity. Therefore, it is likely that NaCN could have restricted the aggregation of HPPs via a chaperone-like effect. This will be discussed in detail in **Section 5.3.3**.

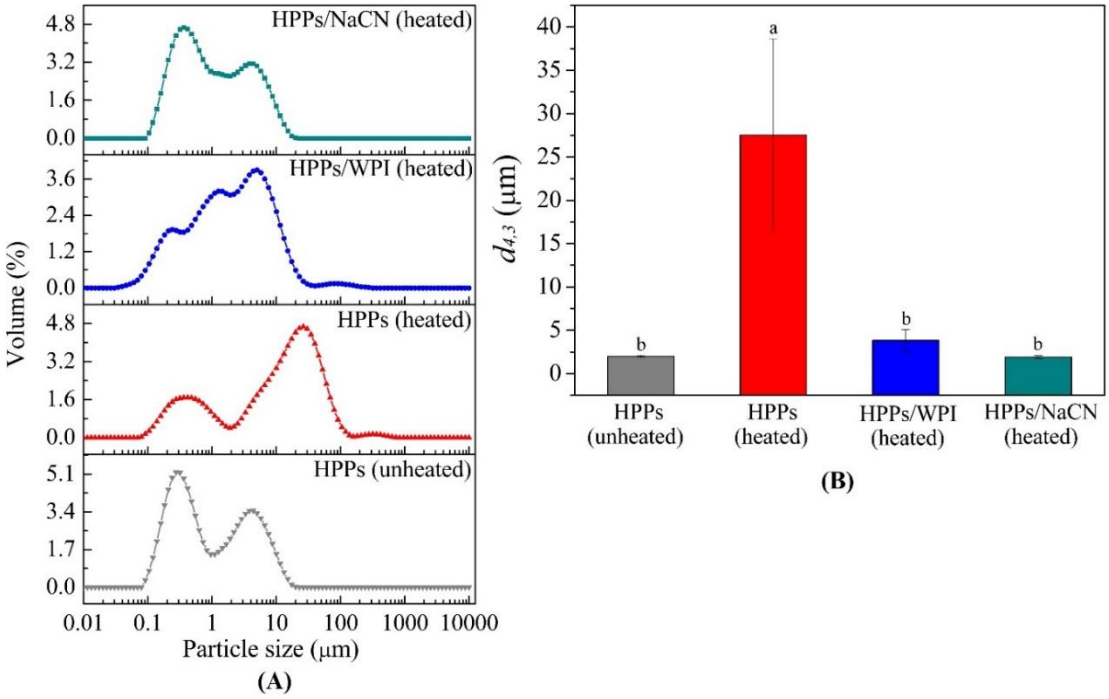


**Fig. 5.1.** Particle size distributions of (A) hemp protein particles (HPPs) (unheated and heated, 95 °C for 20 min), HPPs/whey protein isolate (WPI) (heated) and HPPs/sodium caseinate (NaCN) (heated) dispersions and (B) their corresponding volume-weighted mean diameter ($d_{4,3}$, μm). Different lowercase letters indicate significant differences ($p < 0.05$).

### 5.3.2 Morphology of HPPs and HPPs/milk protein dispersions

The morphology of HPPs, WPI, NaCN and their mixtures (HPPs/WPI and HP/NaCN) was analysed by transmission electron microscopy (TEM) (**Fig. 5.2**). TEM images of unheated HPPs showed the presence of large aggregates with an irregular shape that seems to be composed of smaller protein particles, as seen in **Fig. 5.2A**. Heat treatment led to the formation of even larger and amorphous HPPs aggregates (**Fig. 5.2B**), which is consistent with particle size analysis showing that heat treatment induced a considerable increase in the volume-weighted mean diameter ($d_{4,3}$ = 27.5 μm).

The heated WPI and NaCN on the other hand showed well-dispersed small particles (**Fig. 5.2C, D**). Co-heating HPPs and WPI resulted in spherical particles (**Fig. 5.2E**), which appear to be smaller than those observed in heated HPPs but much larger than the particles in the heated WPI, which could indicate that both proteins could have participated in the microparticles formation. On the contrary, there were two main types of aggregates/particles observed in the heated HPPs/NaCN mixture (**Fig. 5.2F**); large aggregates that resemble HPPs-rich particles and small aggregates that could be casein-rich particles. This observation will be discussed further in the following sections.

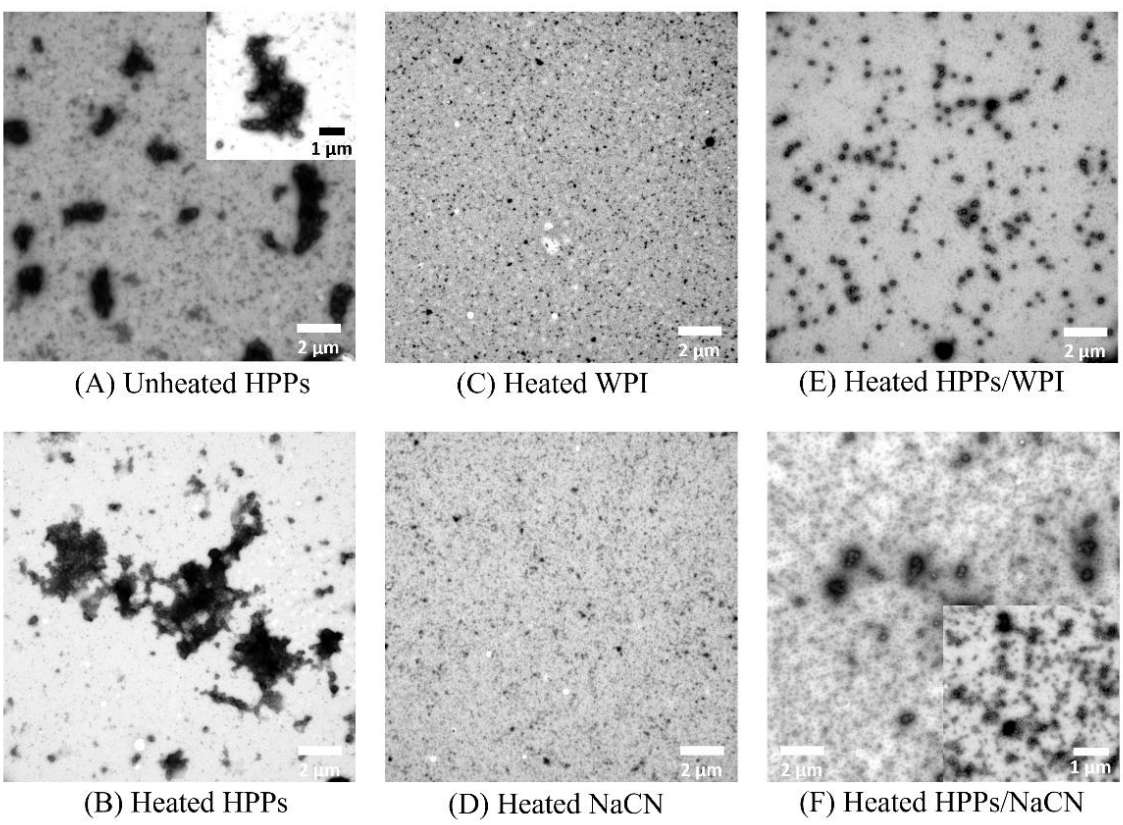


**Fig. 5.2.** Transmission electron microscopy of unheated/ heated hemp protein particles (HPPs) and heated whey protein isolate (WPI), sodium caseinate (NaCN) and their mixture with HPPs.

### 5.3.3 Protein composition of HPPs and HPPs/milk protein dispersions

To analyse the protein interactions in HPPs/WPI and HPPs/NaCN dispersions before and after the heat treatment, SDS-PAGE was conducted on the dispersions and their corresponding supernatant and sediment fractions obtained by centrifugation. **Fig. 5.3** shows the SDS-PAGE protein patterns obtained from HPPs/WPI dispersions before and after heating under non-reducing conditions (**Fig. 5.3A**) and reducing conditions (**Fig. 5.3B**).

Under non-reducing conditions (**Fig. 5.3A**), the composition of the unheated HPPs/WPI (lane 2) was characterised by the presence of a thick band at 52 kDa that corresponded to 11S globulins, a predominant protein in HP that is known to have six non-covalently linked subunits (Shen et al., 2021). Other predominant bands identified below 20 kDa were β-lg and α-La, the two main proteins in WPI (Singh, 2009) (**Fig. 5.3A**, lane 1). In the unheated mixture, proteins from HPPs and WPI could be separated upon centrifugation, observing that the whey proteins remained in the supernatant (**Fig. 5.3A**, lane 3), while HPPs migrated into the sediment. No clear bands were seen from HP in the gel, probably because the sediment was not fully solubilised in the non-reducing buffer (**Fig.5.3A**, lane 4). After heating, the total and supernatant fractions had a similar composition (**Fig. 5.3A**, lanes 5 and 6) mainly consisting of whey proteins (β-lg and α-La) and albumins from HP (~10 kDa). It is well studied that heat (above 70 °C) can promote the formation of β-lg dimers (Boland, 2011; Wijayanti et al., 2014). Hence, it was also possible to observe β-lg dimers (~35 kDa) that are formed within these temperature/time settings (Schokker et al., 1999).

Under reducing conditions (**Fig. 5.3B**), there were a significantly larger number of bands in total, supernatant and sediment before and after heating. Under reducing conditions, disulphide bonds are reduced due to the presence of β-mercaptoethanol, and

SDS breaks down the hydrophobic interactions. Therefore, all protein aggregates are separated into their individual monomeric protein forms. For instance, the total fraction of the unheated HPPs/WPI dispersion showed 5 main predominant bands (**Fig. 5.3B**, lane 2); three from HPPs and two from WPI. The band at 34 kDa corresponded to the acidic subunit of 11S globulin in HP (edestin), and two bands at 18 and 21 kDa were linked to their basic subunits. It is known that the disruption of disulphide bonds of edestin cause the separation of their elementary basic and acid units (Potin & Saurel, 2020; Q. Wang, Y. Jin, et al., 2018). In addition, β-lg and α-La bands (18 and 14 kDa, respectively) were also observed in the total fraction (**Fig. 5.3B**, lane 2). After centrifugation, the supernatant (**Fig. 5.3B**, lane 3) was mainly composed of whey proteins (β-lg and α-La), whereas the sediment fraction (**Fig. 5.3B**, lane 4) was rich in HP globulins.

When the HPPs/WPI mixture was heated, the intensity of both β-lg and α-La bands in the supernatant (**Fig. 5.3B**, lane 6) was considerably reduced compared with the total fraction (lane 5), suggesting possible interactions between HPPs and WPI. However, a proportion of β-lg and α-La also remained in supernatant (**Fig. 5.3B**, lane 6). In contrast, the sediment fraction (**Fig. 5.3B**, lane 7) from heated HPPs/WPI showed bands related to 11S globulin (acid and basic units) β-lg and a faint α-La band. This result suggests that heat-induced interactions preferentially occur between HPPs and β-lg and to a lesser degree between HPPs and α-La, as indicated by the great proportion of α-La remaining in the supernatant fraction.

Whey proteins are globular proteins in their native state, the sulphydryl groups are buried within the tertiary structure (Anema, 2020; Hoffmann & van Mil, 1997). Heat treatment ruptures the forces that hold the globular structure and exposes the sulphydryl groups, resulting in thiol oxidation and thiol/disulphide exchange to form disulphide bridges between different protein molecules and eventually resulting in large aggregates

(Anema, 2020; Singh & Havea, 2003). In the presence of HPPs, denatured whey proteins may either self-aggregate or interact with the disulphide bonds on the surface of the HPPs to generate HPPs/WPI hybrid particles. This interaction could also explain the smaller particle size in the mixture compared with heated HPPs. It is possible that the reactive groups on the surface of HPPs were occupied by denatured whey proteins, which led to fewer sites for HPPs to self-aggregate. In a milk system, Corredig and Dalgleish (1999) found that the amount of β-lg binding with the casein micelles during heat treatment of milk was limited by the available active sites on the micelles. In addition, the improved thermal stability of microparticulated whey proteins was revealed because there were little or no reactive sites available for aggregation after heating (Ryan et al., 2012; Shi et al., 2021). In this study, the binding of denatured whey protein on the surface of HPPs may have acted as a barrier limiting the growth of HPPs, but the location of whey proteins in the particles needs to be confirmed with further studies.

It is worth noting that although α-La interacted with HPPs, the proportion of interacted α-La was less than the proportion of interacted β-Lg. α-La is not able to form aggregates when heated alone since it lacks free thiol groups (Wijayanti et al., 2014). In heated milk, α-La firstly forms aggregates with β-Lg, then associates with casein micelles (Anema & Li, 2003b). A similar scenario may occur in heated HPPs/WPI mixtures, although this association behaviour may vary with heating conditions (such as heating rate, temperature and pH) (Anema, 2021).

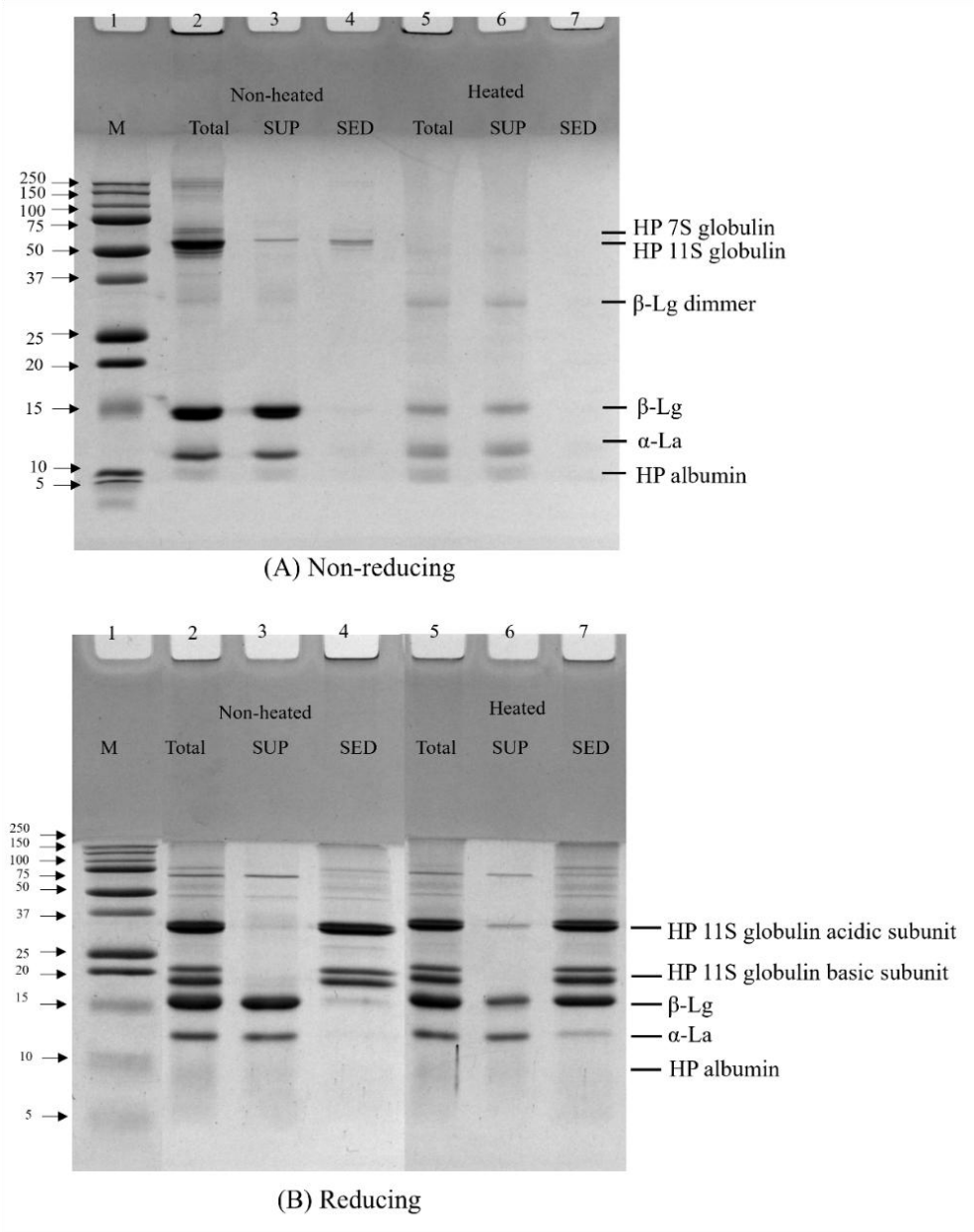


**Fig. 5.3.** SDS-PAGE under (A) non-reducing conditions and (B) reducing conditions of heated (95 °C for 20 min) and unheated hemp protein particles/whey protein isolate (HPPs/WPI) dispersion and their supernatant and sediment. Lanes are: 1, marker; 2, unheated HPPs/WPI dispersion; 3, supernatant from unheated HPPs/WPI dispersion; 4, sediment from unheated HPPs/WPI dispersion; 5, heated HPPs/WPI dispersion; 6, supernatant from heated HPPs/WPI dispersion; 7, sediment from heated HPPs/WPI dispersion.

**Fig. 5.4** shows the SDS-PAGE patterns obtained from HPPs/NaCN dispersions before and after heating and under non-reducing conditions (**Fig. 5.4A**) and reducing conditions (**Fig. 5.4B).** Under non-reducing conditions, $\alpha_{S1}$- and β-caseins were observed as the two most predominant protein bands in NaCN (**Fig. 5.4A**, lane 1), while $\alpha_{S2}$- and κ-caseins presented as two faint bands. Similar to WPI and HPPs mixtures, the unheated NaCN and HPPs could be separated upon centrifugation, with NaCN in the supernatant and HPPs in the sediment (**Fig. 5.4**, lanes 2 and 3). After the heat treatment, the casein bands remained in the supernatant (**Fig. 5.4A**, lane 6), while the HP bands could not be seen in the sediment under non-reducing conditions (**Fig. 5.4A**, lane 7). This indicates that HP particles formed aggregates with very large molecular weights that could not enter the stacking gel.

However, under the reducing conditions (**Fig. 5.4**), the HPPs bands were clearly visible in the sediment after heating, indicating inter-HPPs aggregation involved new disulphide linkages (**Fig. 5.4B**, lane 7). Interestingly, in contrast to whey proteins (**Fig. 5.3**), barely any casein proteins were detected in the sediment of the heated HPPs/NaCN mixture (**Fig. 5.4B**, lane 7), suggesting caseins did not form stable complexes with HPPs during heat treatment. Only a tiny amount of $\alpha_{s1}$-casein remained, which could be due to trace association with HP or incomplete removal of free caseins during the washing step prior to SDS-PAGE analysis. Overall, the absence of significant casein in the sediment indicates that most caseins did not form stable complexes with HP, in contrast to the stronger interactions observed for HP/WPI.

In contrast to HPPs/WPI complexation, the mechanism of restricting the aggregation of HPPs in the presence of NaCN could be attributed to the molecular chaperone-like properties of caseins (especially $\alpha_{S1}$- and β-caseins) that could prevent protein aggregation under unfavourable conditions (Kehoe & Foegeding, 2011; Yong &

Foegeding, 2010). Akbari et al. (2018) suggested that hydrophobic interactions are the driving force for casein self-assembling and the first interaction between caseins and their substrate proteins. The high number of proline residues in both $\alpha_{S1}$- and β-caseins gives them flexible, open and disordered structures that facilitate the binding with other target proteins (Treweek et al., 2011). The steric hindrance provided by caseins could prevent further protein aggregation (Chuang et al., 2019). Chuang et al. (2019) proposed the hydrophobic groups from $\alpha_{S1}$- and β-casein interacted with other HP globulin molecules through hydrophobic interaction. In terms of the caseins and HPPs interactions in this study, it is possible that heat treatment altered the surface structure of HPPs to expose more hydrophobic groups which could interact with caseins, hence preventing the aggregation of HPPs.

However, it is widely accepted that as temperature decreases, the magnitude of hydrophobic interactions would be decreased (Dias et al., 2010; McClements & Keogh, 1995; Scheraga et al., 1962). Sun et al. (2022) also highlighted that temperature effects the hydrophobic interactions, which in turn influences protein stability. It was found that in NaCN, caseins would aggregate through hydrophobic interactions during heating, but would dissociate upon cooling (Chuang et al., 2019; HadjSadok et al., 2008). Kehoe and Foegeding (2014) found that there was no evidence to prove that stable β-caseins/β-lg complex was formed after cooling. For this reason, in the HPPs/casein mixture, caseins are likely to dissociate from the HPPs during cooling.

Based on the particle size results and SDS-PAGE analysis, it could be inferred that both WPI and NaCN had the ability to decrease the extent of heat-induced aggregation of HPPs, but this effect may be achieved through different mechanisms. WPI would bind with the HPPs and form stable complexes, involving the formation of new disulphide bonds. However, the covalent interactions were absent in the HPPs/caseins interactions. It appears

that hydrophobic interactions occurred at high temperatures to prevent HPPs aggregation, but these interactions were diminished at low temperatures. Hence, no stable complexes were found when the mixture was cooled to room temperature.

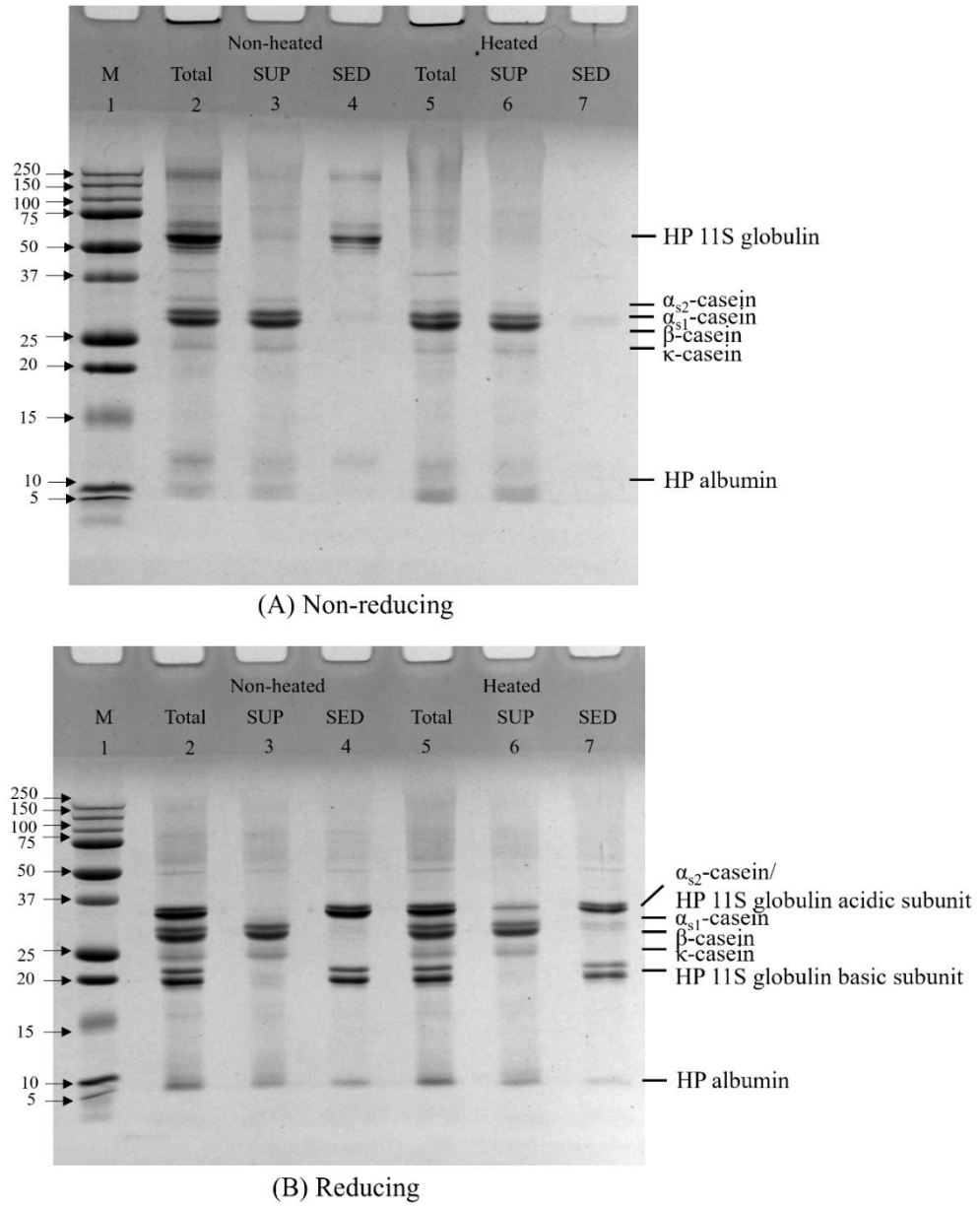


**Fig. 5.4.** SDS-PAGE under (A) non-reducing conditions and (B) reducing conditions of heated (95 °C for 20 min) and unheated hemp protein particles/sodium caseinate (HPPs/NaCN) dispersions, the total, supernatant and sediment fractions. Lanes are: 1, marker; 2, unheated HPPs/NaCN dispersion; 3, supernatant from unheated HPPs/NaCN dispersion; 4, sediment from unheated HPPs/NaCN dispersion; 5, heated HPPs/NaCN dispersion; 6, supernatant from heated HPPs/NaCN dispersion; 7, sediment from heated HPPs/NaCN dispersion.

### 5.3.4 Free sulphydryl groups and surface hydrophobicity

The changes in free sulphydryl (SH) groups of individual protein ingredients and their mixtures before and after heating are shown in **Fig. 5.5A**. Measuring the changes in free SH groups could provide us with useful information about the conversion of free SH to disulphide linkages during heating.

The HPPs dispersion contained 19 μmol/g free SH groups which after heating decreased to 7 μmol/g, suggesting either intra-particle or inter-particle disulphide bonds might have been formed. In the milk protein dispersions, the free SH content of unheated WPI was 41 μmol/g in agreement with the value previously reported for WPI (37 μmol/g) (Xu et al., 2022). A reduction in free SH groups after heating was observed; this could be attributed to the denaturation of whey proteins in which thiol groups were exposed and interacted to form new disulphide bonds (Boland, 2011). In contrast, unheated NaCN had 1 μmol/g free SH groups and there was no significant change after heating. This was expected because the main casein molecules in NaCN ($\alpha_{S1}$- and β-casein) do not contain free SH groups (Holt et al., 2013).

In HPPs/WPI dispersions, heat treatment led to a decrease in free SH groups (**Fig. 5.5A**). This is because of either thiol-disulphide exchange/sulphydryl oxidation between HPPs and unfolded whey proteins, or the intra- or inter-self-interactions in HPPs or whey proteins. A similar reduction in –SH groups was also reported in other protein mixtures of co-heated whey proteins and other plant proteins. For instance, Chihi et al. (2016) observed a decrease in the free SH group in a heated pea globulin/β-lg mixture indicating the disulphide bond formation.

The HPPs/NaCN dispersions also showed a decrease in free SH groups after heating (**Fig. 5.5A**). This would be mainly contributed by the intra- or inter-interaction of HPPs since no covalent link was formed between HPPs and caseins (**Fig. 5.4**). Both free SH

groups of HPPs/WPI and HPPs/NaCN after heat treatment were very close to their calculated theoretical values, which are the averages of individually heated proteins. This may suggest that the amount of available and reacted free SH groups in individual heated protein or heated protein mixtures were similar. It is possible that during the heat treatment of mixed protein, the exposed free SH groups of the individual proteins also participated in either self-interactions or interacted with other proteins.

The surface hydrophobicity values of HPPs, WPI, NaCN and their mixtures are shown in **Fig. 5.5B**. The determination of surface hydrophobicity could offer some additional information on the change of protein structure during heating and indicate possible hydrophobic interactions. The surface hydrophobicity of HPPs increased significantly after heating in accordance with the increased surface hydrophobicity in heated HP globulins. The surface hydrophobicity of whey proteins increased from 2800 to 4316 after heating while that of NaCN remained steady at 1600 to 1700 (**Fig. 5.5B**). This trend was consistent with other studies on the surface hydrophobicity of NaCN (Chuang et al., 2019) and whey proteins (Hussain et al., 2012; Ryan et al., 2012) before and after heating. It is expected that some of the buried hydrophobic groups would be exposed during the unfolding of the native globular structure of whey proteins under heat treatment and could contribute to the increase of surface hydrophobicity (Comfort & Howell, 2002; Ryan et al., 2013). As caseins have no well-defined tertiary structure there would be no change expected in surface hydrophobicity after heat treatment (Bryant & McClements, 1998).

The surface hydrophobicity of the heated HPPs/WPI mixture also increased, but the values were lower than the calculated theoretical value of the heated HPPs/WPI mixture possibly because of the lack of interactions. The lower actual surface hydrophobicity value suggests that HPPs and WPI interacted with each other via hydrophobic interactions rather than binding with fluorescence probes (ANS). Chihi et al. (2016) reported an increased

surface hydrophobicity value of the pea protein/β-lg mixture after heating and they proposed both covalent and non-covalent interactions helped the formation of protein aggregates. Gong et al. (2019) suggested that an increase in the surface hydrophobic groups may facilitate the formation of disulphide bonds during aggregation. Hence, hydrophobic interactions could be another driving force for creating the HPPs/WPI aggregates.

On the other hand, considering the low surface hydrophobicity of NaCN, the value of the HPPs/NaCN mixture had a greater extent of increase after heating compared with HPPs/WPI. In contrast to HPPs and WPI mixture, the increase of surface hydrophobicity was mainly contributed by HPPs. Compared with the calculated sum of HPPs/NaCN after heating, there was a slight decrease in actual surface hydrophobicity, and the extent of reduction was less than that of HPPs/WPI. The reduction of surface hydrophobicity may be attributed to some interaction between HPPs. This explanation could be supported by a finding from a study of the β-casein/β-lg system in which β-lg dominated the increase of surface hydrophobicity. The surface hydrophobicity of heated β-casein/β-lg was only slightly lower than the expected value (Kehoe & Foegeding, 2014). They suggested that β-casein bound with β-lg to improve the stability during heating and the complex might dissociate after cooling (Kehoe & Foegeding, 2011, 2014). A similar phenomenon would be expected to occur in HP and NaCN mixtures if we assume temperature-dependent reversible hydrophobic interactions between these proteins.

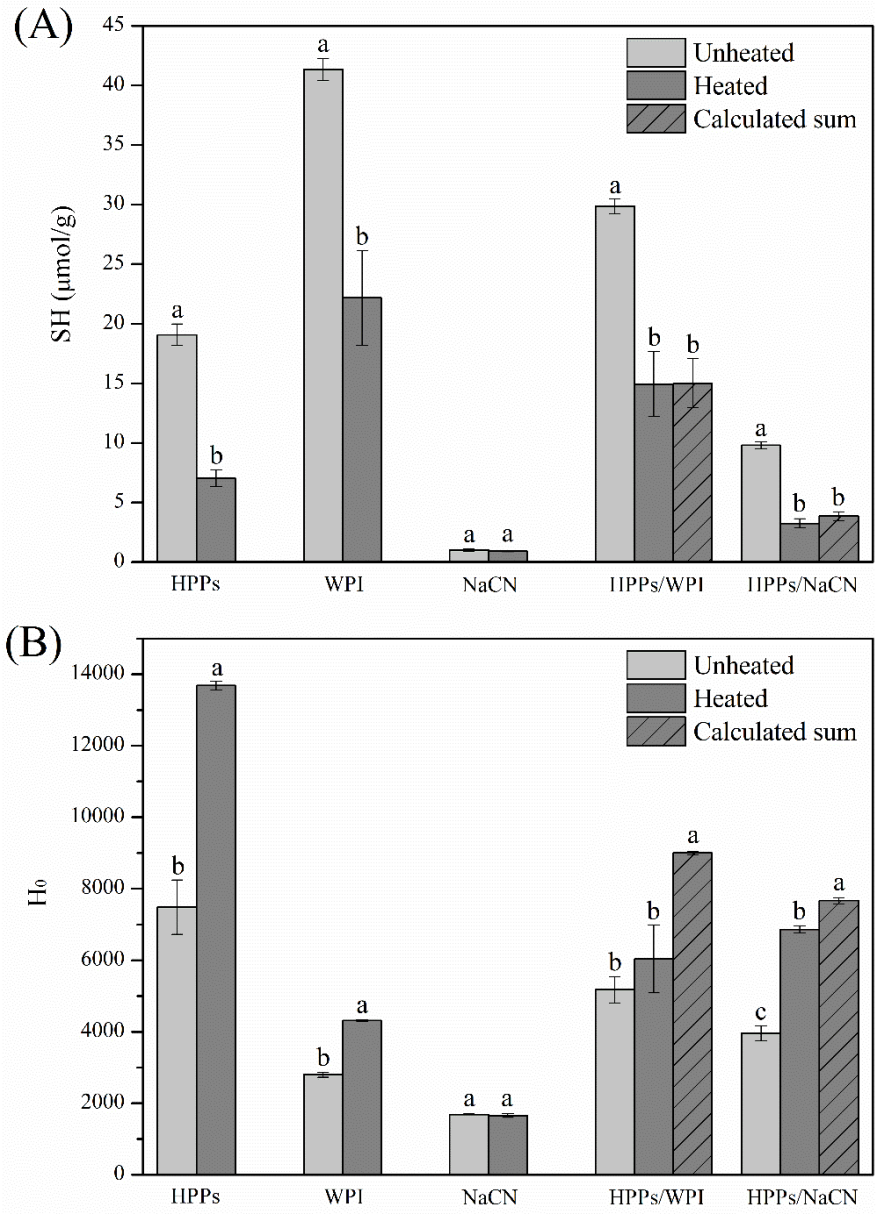


**Fig. 5.5.** Free sulphydryl (SH) groups (A) and surface hydrophobicity ($H_0$) (B) of unheated (light grey bar) and heated (dark grey bar) hemp protein particles (HPPs), whey protein isolate (WPI), sodium caseinate (NaCN), HPPs/WPI and HPPs/NaCN dispersions, and the calculated theoretical value (dark grey bar with stripes pattern) of heated HPPs/WPI and HPPs/NaCN mixtures, assuming no interactions. Different lowercase letters indicate significant differences of each sample before and after heating ($p < 0.05$).

### 5.3.5 Thermal stability of HPPs/milk protein hybrid particles

The heated HPPs/WPI and HPPs/NaCN mixtures resulting in hybrid particles were cooled to room temperature and then reheated (95 °C for 20 min) to assess their thermal stability. As can be seen in **Fig. 5.6A**, the particle size distributions of HPPs/WPI and HPPs/NaCN particles after heating were very similar to the original size distribution of the original protein mixtures, suggesting that these particle protein systems were heat-stable under the conditions tested.

The protein particles and soluble proteins of heated HPPs/WPI and HPPs/NaCN mixtures were separated by centrifugation. The dispersion of sediment was then re-heated to assess the heat stability of the hybrid particles themselves. The particle size distribution of re-dispersed sedimentable fractions from HPPs/WPI and HPPs/NaCN dispersions are shown in **Fig. 5.6B**. Firstly, results showed that re-dispersed particles from heated HPPs/WPI and HPPs/NaCN dispersions were slightly larger compared with the dispersions prior to centrifugation (**Fig. 5.6A**), which was expected because centrifugation can induce particle aggregation. Secondly, the particle size distribution of the re-dispersed HPPs/WPI did not change significantly after re-heating, which could be interpreted as if the proteins in the supernatant did not contribute to the thermal stability of the HPPs/WPI microparticles.

Microparticulated whey protein exhibits enhanced heat stability since the reduction of free thiol groups led to limited interactions among whey protein microparticles (Dissanayake & Vasiljevic, 2009). In this study, during the denaturation of whey proteins and the formation of irreversible HPPs/WPI microparticles, it was expected that most of the exposed reactive groups would have already interacted with each other, which resulted in fewer groups available during the subsequent heat treatment.

Interestingly, the particle size distribution of the re-dispersed sedimentable fraction obtained from HPPs/NaCN after re-heating showed significantly larger particle populations

from ~20 μm to ~60 μm. We could speculate that the HPPs/NaCN particles were reversible because the hydrophobic interactions were reduced at low temperatures (Chuang et al., 2021; Sun et al., 2022). The dissociated HPPs were susceptible to heating and self-aggregated without the chaperone-like action provided by caseins after removing soluble NaCN.

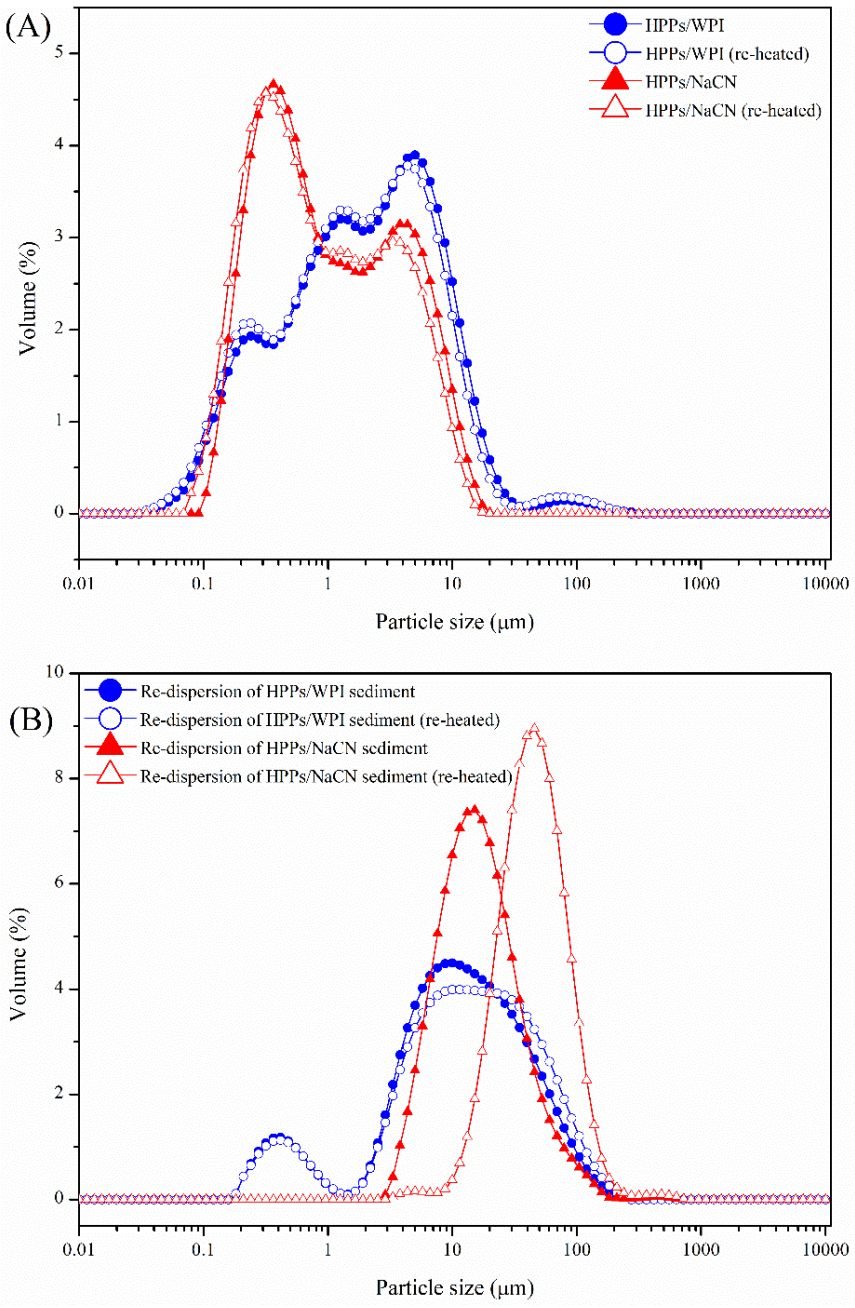


**Fig. 5.6.** Particle size distributions of (A) heated hemp protein particles/whey protein isolate (HPPs/WPI) and heated hemp protein particles/sodium caseinate (HPPs/NaCN) dispersions and their re-heated (95 °C for 20 min) dispersions; and of (B) the re-dispersion of the sediment collected from heated HPPs/WPI and HPPs/NaCN, and their re-heated (95 °C for 20 min) dispersions.

### 5.3.6 Hypothetical mechanism of heat-induced interactions of HPPs/WPI and HPPs/NaCN

According to all the results above, a possible mechanism of heat-induced interactions of each HP/milk protein mixture could be depicted (**Fig. 5.7**). Heat treatment exposes the free SH groups and hydrophobic groups on the surface of hemp protein particles. Meanwhile, heat treatment leads to the unfolding of β-lg in WPI to expose its free SH groups (Anema, 2020; Singh & Havea, 2003).

When the HPPs and WPI are co-heated (**Fig. 5.7A**), the denatured whey proteins may either self-aggregate or interact with the surface of the HPPs. This interaction may involve disulphide bond formation between hemp and whey protein involving sulphydryl-disulphide interchange reactions. The association of WPI on the surface of HPPs could restrict the further aggregation of HPPs since denatured WPI could occupy some of the reactive sites on the surface of HPPs. The resulting HPPs/WPI particles are stable after cooling because of the irreversible nature of the disulphide bonding between HHPs and WPI. After a second heating cycle, HPPs/WPI particles show heat stability as most of exposed reactive groups have already interacted when forming the HPPs/WPI particles and the fewer reactive sites remain for further aggregation.

In the case of HPPs/NaCN mixtures, when the HPPs are co-heated with NaCN (**Fig. 5.7B**), the exposed hydrophobic groups at the surface of HPPs preferentially interacted with caseins. The chaperone-like property of casein molecules may provide steric hindrance to prevent the further aggregation of HPPs during heating. However, the association of caseins onto the surface of HPP was reversible upon cooling. With the decrease in temperature, the hydrophobic interactions would decrease, which could lead to the dissociation of caseins from HHPs and the formation of large HPPs aggregates.

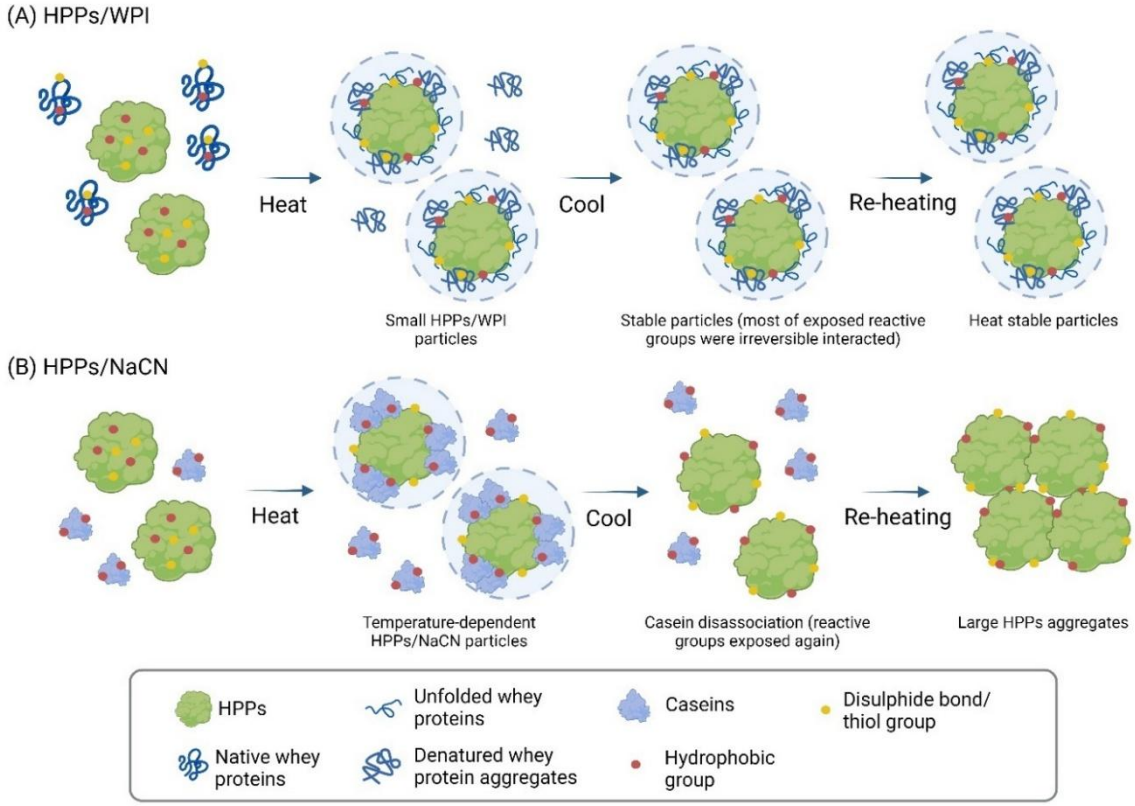


**Fig. 5.7.** Schematic representation of possible mechanisms by which (A) hemp protein particles/whey protein isolate (HPPs/WPI) and (B) hemp protein particles/sodium caseinate (HPPs/NaCN) interact during heat treatment (95 °C, 20 min) and cooling down.

## 5.4 Conclusions

This study revealed different possible mechanisms of heat-induced aggregation of HPPs in the presence of WPI or NaCN. It was found that the whey proteins associate irreversibly via disulphide bonds with HPPs upon heating. The modification of HPPs through this binding of whey proteins restricts further aggregation of HPPs upon continued heating. In addition, casein interacted with HPPs reversibly, possibly involving the chaperone-like property of casein molecules. This mechanism could be applied to enhance the heat stability of HPPs for various food applications. This study is pioneering in describing possible mechanisms of heat-induced interactions between hemp protein (HP) and milk proteins. However, future research should explore other factors affecting heat-induced aggregation, such as a range of protein concentrations and HP to milk protein ratios to gain a more comprehensive understanding of protein aggregation behaviour. In summary, this study explored a feasible strategy to develop more functional plant and dairy based food products by combining hemp proteins with milk proteins.

# Chapter 6: pH-dependent thermal aggregation of hemp protein in the presence of whey protein

## Chapter Overview:

This chapter investigates the influence of pH on the aggregation behaviour of hemp protein (HP) and whey protein isolate (WPI) mixtures. The objective was to identify whether pH affects the formation of HP/WPI aggregates under heat treatment, an important step for producing HP/WPI microparticles. This chapter serves as a foundation for the subsequent work described in Chapter 7, where the hybrid aggregates were processed into particles and assessed for their emulsifying properties.

## Abstract

This study investigates the heat-induced aggregation behaviour of hemp protein (HP) and whey protein isolate (WPI) mixtures across a range of pH conditions (pH 3–8). Static light scattering, transmission electron microscopy, and SDS electrophoresis were used to characterise aggregates' size, microstructure, and protein composition of soluble and insoluble aggregates. Results showed that heating HP/WPI mixtures at pH 8 produced small, spherical aggregates, attributed to the dissociation of HP globulin and enhanced thiol-disulphide exchange reactions under mildly alkaline conditions. In contrast, heating at pH 4–7 led to the formation of large, irregular aggregates, likely due to extensive disulphide bonding and reduced electrostatic repulsion. At pH 3, although relatively small aggregates formed, the acidic pH-induced suppression of thiol reactivity may have restricted protein complexation, and the interaction between a part of HP and WPI remained inconclusive. Overall, heating HP/WPI mixtures at pH 8 was identified as the most

favourable condition for generating hybrid protein aggregates, providing a foundational step for the future development of functional hybrid microparticulated protein systems in food applications.

## 6.1 Introduction

In the study of single protein systems, heat-induced aggregates can exhibit varied morphologies and new properties, which affect their functional performance in food products (Nicolai & Durand, 2013). The aggregated protein upon heating could be considered a promising additive-free procedure to block most reactive groups and reduce the susceptibility during secondary heat processing (Renard et al., 2002). For example, microparticulation is a strategy that usually combines thermal aggregation and high shear or pressure to produce both soluble and insoluble particulated proteins with controlled sizes (Çakır-Fuller, 2015; Renard et al., 2002; Shi et al., 2021). These particles typically contain fewer active sites and may offer good stability and functionality (Shi et al., 2021). As a prerequisite of microparticulation, it is important to investigate these heat-induced pre-aggregates to achieve the desired size and aggregation rate for the subsequent size reduction processing (Nicolai & Durand, 2013).

Extrinsic environmental conditions, such as pH, ionic strength and temperature, will affect the degree of protein aggregation. Among these, pH plays a critical role in modulating electrostatic repulsion, protein flexibility, intramolecular folding and intermolecular interactions. It has been reported that extreme pH (acidic and alkaline) conditions could increase the intra- and inter-molecular repulsive interaction to partially unfold proteins and modify their tertiary structure to be more flexible (Tang et al., 2024). The aggregation behaviour is largely dependent on the electrostatic repulsion and

hydrophobic attraction (Wang et al., 2010). In a single protein system such as whey protein, alkaline pH enhances the aggregation rates and forms small, uniform aggregates (de la Fuente et al., 2002). On the other hand, whey protein is more stable to heat-induced denaturation at pH 3. The hydrophobic interactions become the driving forces in aggregation, leading to relatively small aggregates (Dissanayake, Ramchandran, Piyadasa, et al., 2013; Lam & Nickerson, 2015). The largest aggregates are often observed near the isoelectric point (pH 5), where electrostatic repulsion is minimised (Lam & Nickerson, 2015). Similar trends are reported for plant proteins like pea protein, where limited aggregation occurs at extreme pH values, while extensive aggregation occurs near their pI (Klost et al., 2020; Tanger, Mertens, et al., 2022; Zhang et al., 2025). The alkaline pH (pH 12) with heat treatment has been shown to facilitate the unfolding of hemp protein and form soluble aggregates (Q. Wang, Y. Jin, et al., 2018).

Recently, research has shown increasing interest in partially replacing milk proteins with plant proteins. However, mixed protein systems introduce additional complexity due to the interactions between different types of protein. Most studies focused on the microstructure and rheological properties of heat-induced gel systems, such as rapeseed protein/whey protein (Ainis et al., 2018), soy protein/whey protein (McCann et al., 2018; Roesch & Corredig, 2005), soy protein/casein micelle (Roesch & Corredig, 2006), pea protein/whey protein (Kornet, Shek, et al., 2021; Wong et al., 2013b) and pea protein/casein micelle (Mession et al., 2017a, 2017b). Except for pea protein/β-lg (Chihi et al., 2016), pea/casein (Mession et al., 2017b) and soy protein/whey protein (Alu'datt et al., 2012; Jose et al., 2016; Roesch & Corredig, 2005), fewer have focused specifically on examining the heat-induced aggregation behaviour in such systems. Moreover, only a limited number of studies investigated the effect of pH on heat-induced aggregation in mixed protein systems. For example, Ainis et al. (2018) tested the structural and rheological properties of heat-

induced gelation of rapeseed protein/whey proteins at different mix ratios and pH. Allahdad et al. (2023) investigated the microparticles formed by egg white/whey protein mixture heated at pH 3-7, followed by sonication. These studies demonstrated that the various structures of aggregates or gels could be obtained by modulating the pH conditions.

Although several studies have examined heat-induced aggregation of HP (Chen et al., 2023; Dapčević-Hadnađev et al., 2018; Do et al., 2025; Fang et al., 2023; Malomo et al., 2014; Tang et al., 2006), the overall body of research remains limited, particularly regarding HP behaviour in mixed protein systems. Only a small number of studies have explored HP in combination with other proteins, such as egg white (Alavi et al., 2020) or casein (Chuang et al., 2019; X. Zhou et al., 2022). Our previous study was the first to explore heat-induced interaction between HP and WPI at neutral pH and low protein concentrations (0.25wt% each) (Ma, Ye, et al., 2024). However, the pH dependency of thermal aggregation of HP/WPI mixtures, at low protein concentration, is still unknown. Therefore, the objective of this work was to investigate the heat-induced aggregation behaviour of hemp protein (HP) and whey protein isolate (WPI) mixtures across a range of pH conditions (pH 3–8).

## 6.2 Materials and methods

### 6.2.1 Materials

Whey protein isolate (WPI) containing 92.0% protein, 0.9% fat, 1.6 % ash and 5.2% moisture was purchased from Fonterra Co-operative Group Limited, Auckland, New Zealand. The hempseed protein (HP) concentrate powder was purchased from Davis Food Ingredients (Davis Trading Company Ltd., Palmerston North, New Zealand). The HP powder contained 59.8% protein, 2.4% fat, 10.7% ash, 6.8% moisture and 20.2%

carbohydrate. The proximate composition of both protein ingredients was analysed as follows: protein content was determined using the Kjeldahl method (AOAC 991.20, nitrogen factor 5.21); fat, ash and moisture content were determined according to AOAC 922.06, AOAC 942.05 and AOAC 925.10, respectively; and carbohydrate content was calculated by subtracting the sum of the protein, ash and fat from the total solid. All chemicals were purchased from Sigma-Aldrich Ltd. (St. Louis, MO, USA), and the reagents were made up in Milli-Q water (Milli-Q apparatus; Millipore Corp., Bedford, MA, USA).

### 6.2.2 Preparation of heat-induced hemp/whey protein aggregates

HP dispersion was prepared by dissolving HP powder in Milli-Q water at a concentration of 2% (w/w), followed by magnetic stirring at 20 °C for 2 h. The pH was adjusted to 11, using 1 M NaOH, and the dispersion was stirred for an additional 2 h. The HP dispersion was centrifuged (3000 × *g*, 30 min) to remove insoluble material (such as insoluble fibre). The resulting supernatant (mostly containing HP) was collected and adjusted to pH 7 using 1 M HCl. The dispersion composed of the supernatant was processed by microfluidisation (M-110P, Microfluidics, Newton, MA, USA) at 200 MPa and 2 passes to produce HP particles that were used for subsequent mixing with whey protein.

Stock solutions of WPI were prepared by dissolving 3% (w/w) protein in Milli-Q water with magnetic stirring for 2 h. HP particle dispersion was mixed with WPI solution to achieve a final protein concentration of 0.5% (w/w) HP and 0.5% (w/w) WPI in the mixture. The individual 0.5% (w/w) HP dispersion, 0.5% (w/w) WPI solution and 0.5% (w/w) HP/0.5% (w/w) WPI mixture without heating were prepared as controls. The pH of both the mixed and individual protein dispersion/solution was adjusted to pH 3-8 using 1 M NaOH or HCl, followed by heating at 95 °C for 20 min in the water bath. The heating

condition was selected based on our previous study, which suggested that most interactions between HP and β-lg happened in the first 20 min of heating. After the heat treatment, the samples were cooled down in an ice bath to 20 °C immediately. Sodium azide (0.02%, w/w) was added to inhibit microbial growth.

### 6.2.3 Particle size analysis

Particle size distribution was measured as described in Section 5.2.5 (Chapter 5). The same instrument and settings were used unless otherwise stated.

### 6.2.4 Transmission electron microscopy

Transmission electron microscope was conducted following the procedure described in Section 5.2.6 (Chapter 5). Only sample preparation steps specific to the HP/WPI aggregates in this chapter are described in Section 6.2.2.

### 6.2.5 Light microscopy

The thermally aggregated particles at pH 4, 5, 6 and 7 had large particle sizes and could not be effectively visualised using TEM. Therefore, these samples were viewed under an Olympus BX53 light microscope (Olympus, Tokyo, Japan) equipped with an objective lens at 20× magnification. Aqueous dispersions of protein mixture samples were mounted onto microscope slides and covered with glass coverslips. Images were captured and analysed using XIMEA CamTool 4.24 software (XIMEA GmbH, Münster, Germany).

### 6.2.6 Sodium dodecyl sulphate polyacrylamide gel electrophoresis

To analyse the protein interactions in HP/WPI dispersions induced by heat treatment, sodium dodecyl sulphate polyacrylamide gel electrophoresis (SDS-PAGE) with a Tris-glycine gel under non-reducing and reducing conditions was carried out as per the method described in Section 5.2.7 in Chapter 5. SDS-PAGE was conducted on the dispersions and their corresponding supernatant and sediment fractions obtained by centrifugation (20,000g, 20 min). All other experimental conditions were identical to those previously described.

## 6.3 Results and discussion

### 6.3.1 Changes in particle size and microstructure of aggregates as a function of pH

The particle size distribution of unheated and heated HP/WPI dispersions at different pH are shown in **Fig. 6.1A**. At pH 7, the unheated HP/WPI dispersion exhibited a bimodal size distribution with two peaks located at 0.1–1 μm and 1–10 μm (**Fig. 6.1 A2**), consistent with our previous study (Ma, Ye, et al., 2024). Lowering the pH gradually shifted the size distribution toward larger particles (from pH 8 to 5) (**Fig. 6.1 A1-4**) and ultimately resulted in a monomodal distribution with predominantly large aggregates at pH 4 and 3 (**Fig. 6.1 A5-6**).

Upon heat treatment, strong heat-induced protein aggregation was observed at pH 4–7 (**Fig. 6.1 A2-5**). Among these, the aggregates formed at pH 4 were the smallest, and their size progressively increased with rising pH, suggesting that aggregation extent is pH-dependent. In contrast, minimal changes in particle size were detected after heating at pH 3 and pH 8 (**Fig. 6.1 A1 and A6**), indicating that aggregate growth was limited, possibly due to the very acidic or alkaline pH conditions (discussed in the later section). Interestingly, when HP alone was heated at pH 7, it formed notably large aggregates, whereas heating at

pH 8 did not result in significant changes in particle size (**Fig. 6.1 B)**, implying that alkaline pH may stabilise HP against extensive aggregation.

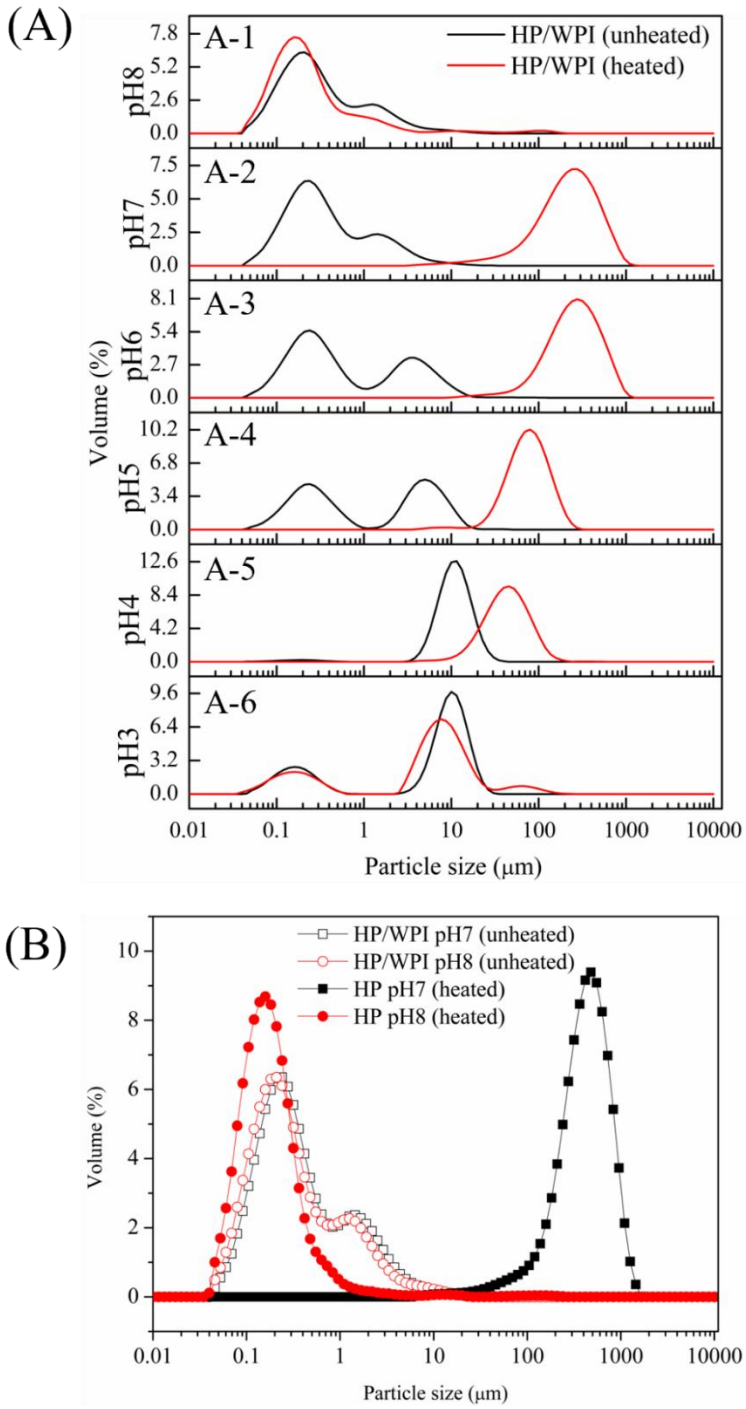


**Fig. 6.1.** Particle size distributions of (A) unheated and heated HP/WPI dispersion at various pH (3 – 8) conditions and (B) unheated HP/WPI and heated HP dispersion at pH 7 and 8.

Based on the particle size data, the morphological characteristics of the protein aggregates were examined using a light microscope (for pH 4 to 7) (**Fig. 6.2**) and transmission electron microscopy (TEM) (for pH 3 and 8) (**Fig. 6.3**). In unheated HP/WPI dispersions, decreasing the pH from pH 7 to 4 led to gradually increase in aggregation. At pH 7, the dispersion appeared very uniform with minimal visible aggregation (**Fig. 6.2D**), whereas at lower pH values (pH 6–4), larger, loosely packed, and irregular aggregates became evident (**Fig. 6.2A-C**).

After heating, the HP/WPI dispersions exhibited more extensive aggregation. The aggregate morphology also changed with pH. At pH 6 and 7, aggregates appeared highly compact with minimal porosity, resembling solidified masses (**Fig. 6.2G and H**), while at pH 4 and 5, the structures became more open and loosely clustered (**Fig. 6.2E and F**).

At pH 3 and 8, where light microscopy was not suitable due to smaller aggregate sizes, TEM images revealed only mild aggregation in unheated samples, with small protein particles (indicated by white arrows) (**Fig. 6.3A and B**). After heating, the aggregates formed at pH 3 and 8 remained small in size (**Fig. 6.3C and D**), in contrast to the pronounced aggregate development observed under other pH conditions (**Fig. 6.2**). Notably, spherical and relatively uniform aggregates were observed at pH 8 (indicated by white arrows) (**Fig. 6.3D**), while at pH 3, the fine particulate structures appeared alongside elongated, loosely connected aggregates (**Fig. 6.3C**).

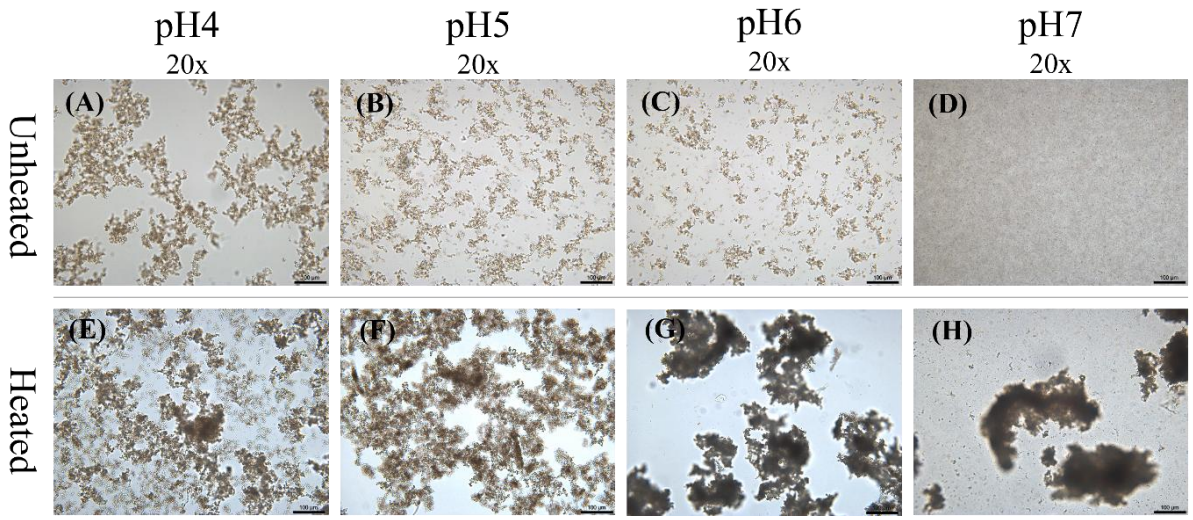


**Fig. 6.2.** Light microscopy of (A-D) unheated HP+WPI dispersion at pH 4 – 7 and (E-H) heated HP/WPI dispersion at pH 4 – 7 (Scale bar = 100 μm).

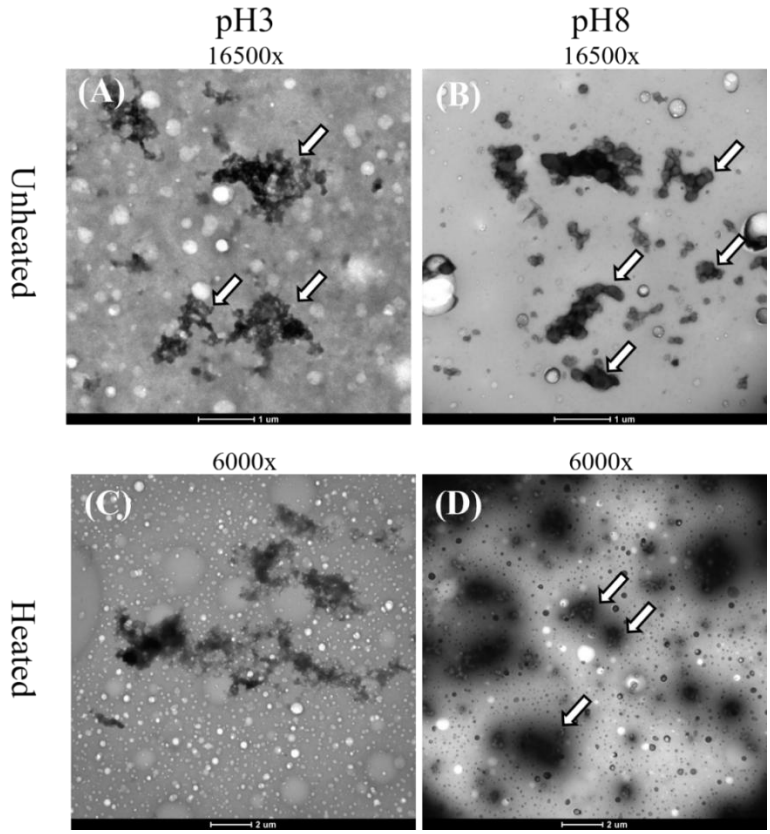


**Fig. 6.3.** Transmission electron microscopy of unheated HP+WPI dispersion at (A) pH 3 and (B) pH 8 (Scale bar = 1 μm) and heated HP/WPI dispersion at (C) pH 3 and (D) pH 8 (Scale bar = 2 μm).

The pH condition strongly influences the charge of proteins. Under acidic conditions (higher $H^+$ concentration), the protonation of acidic side chains of amino acids in proteins occurs, which results in an increase in positive charge. In contrast, under alkaline conditions (OH- is abundant), deprotonation of basic side chains occurs, which results in a more negative charge of the protein (Chanamai & McClements, 2002). The typical range of isoelectric point for HP is pH 4.5-5, and for β-lg is pH 5.2 (Do et al., 2024; Kim et al., 2020). When the pH was close to the protein's isoelectric point, the net charge was zero, and electrostatic repulsion was minimised due to the neutralisation of charge.

In this study, the unheated protein mixture tended to aggregate as the pH decreased from 7 to 4 due to reduced electrostatic repulsion. This trend is supported by the light microscope images of the unheated protein mixture (**Fig. 6.2A-D**), which show progressively larger aggregates at lower pH values. Similar pH-dependent behaviours have been described in HP (Tang et al., 2006). As the pH approaches 5, HP particles show increased aggregation due to diminished electrostatic repulsion. This phenomenon is consistent with observations in other plant proteins: for instance, soy protein formed larger, disordered clusters at pH 5 (Lin et al., 2024), and pea protein showed its lowest solubility at pH 4.5 and highest at pH 8.5 (Jiang et al., 2017; Zhang et al., 2025).

The pronounced heat-induced aggregation observed at pH 6 and 7 likely results from both covalent and non-covalent interactions between HP and whey protein, as demonstrated in our previous study (Ma, Ye, et al., 2024). Heat treatment applied to the pre-aggregated protein mixture (caused by pH reduction) at pH 4 and 5 may unfold the protein conformation to a more flexible structure (Lin et al., 2024). These aggregates were further connected upon heating, which resulted in a loose floc (**Fig. 6.2E and F**), in contrast to the compact, dense aggregates without open structures formed at pH 6 and 7(**Fig. 6.2G and H**). A similar network with voids connected by aggregated rapeseed protein and whey

protein was also observed at pH 5 (Ainis et al., 2018). The protein mixture heated at pH 4 had smaller aggregates than that at pH 5, as seen in both particle size and microscopy. This may be explained by that when heated at pH levels below its isoelectric point, the extent of aggregation decreases with further acidification, producing smaller, more open-structured aggregates (Cornacchia et al., 2014).

Under highly acidic conditions, like pH 2 and 3, the aggregation behaviour differs from that observed near neutral pH. The sulphydryl-disulphide interchange reactions are very unlikely to happen since the thiol groups are very stable at such low pH (de la Fuente et al., 2002). It was reported that a marked reduction in whey protein aggregation occurred upon heating at pH 3 and was mainly driven by disruption of hydrophobic interactions (Dissanayake, Ramchandran, Piyadasa, et al., 2013). Similarly, in plant protein, limited aggregation was noticed when heating pea protein at pH 3.5 (Zhang et al., 2025). In our study, the formation of disulphide bonds between HP and WPI is expected to be minimal at pH 3. Moreover, the strong electrostatic repulsion also further limited the protein interactions. As a result, only small aggregates with relatively loose structures were formed (**Fig. 6.3C**).

Interestingly, the HP particles heated at pH 8 did not form large aggregates as seen at pH 7. This observation aligns with previous findings in other plant proteins. For instance, Makinen et al. (2016) reported that heating quinoa globulins at alkaline pH (8.5–10.5) led to the disruption of disulphide bonds linking the acidic and basic subunits, resulting in the release of polypeptides and smaller aggregates. In contrast, such dissociation was not observed at pH 6.5, where strong aggregation occurred. Similarly, Renkema et al. (2000) found that varying pH can create different soy glycinin aggregates, where aggregation without dissociation of the subunits happened at pH 6.5, while the disulphide bonds between basic and acidic subunits were disrupted at pH 7.6. Zhang et al. (2025) also

reported limited aggregation in pea protein when heated at pH 8.5. These findings are consistent with our observation that individually heated HP remained in smaller aggregates at pH 8, whereas large aggregates were formed at pH 7.

Moreover, the presence of whey protein in the HP/WPI mixture could also restrict the large aggregation. The alkaline conditions facilitated the dissociation and unfolding of the protein and made the thiol group more active for reactions. For instance, β-lactoglobulin (β-lg) would undergo a conformational change and expose the buried responsible amino acid, Glu89, which makes β-lg more ready for reaction, increasing the thiol/disulphide exchange. Although these reactions are promoted at high pH, they may also facilitate faster termination of aggregation due to the rapid formation of disulphide bonds, thereby reducing the availability of free thiol groups and limiting further aggregate growth. This results in the formation of a higher number of smaller-sized protein aggregates. Previous studies have demonstrated that although the rate of β-lg aggregation increases with pH, the size of the aggregates tends to decrease compared to those formed at pH 6.4–6.8 (de la Fuente et al., 2002; Dissanayake, Ramchandran, Piyadasa, et al., 2013; Hoffmann & van Mil, 1999).

In our study, the disassociated acidic and basic units of HP could be re-aggregated through disulphide binding, forming small aggregates (Makinen et al., 2016). Additionally, the rapid interactions between HP and whey protein at pH 8 could promote early termination of the aggregation process, thereby limit particle connectivity and favouring the formation of uniformly distributed small spherical particles (**Fig. 6.3D**).

### 6.3.2 Composition of soluble and insoluble aggregates at different pH

To visualise the protein composition of soluble and insoluble aggregates of HP/WPI and their individual protein dispersions, SDS-PAGE under reducing conditions was

conducted on the heated protein dispersions (Total), as well as their respective supernatant (SUP) and sediment (SED) fractions obtained via centrifugation (**Fig. 6.4-6.9**). All samples were diluted to the same protein concentration before loading. It should be noted that protein solubility, band visibility and distribution in the supernatant or sediment fractions depend on the centrifugation conditions used; modifying these conditions may lead to different aggregate separations. In this study, centrifugation at 20,000 × *g* for 20 min was used, based on our previous work that effectively separated whey protein and HP particles (Ma, Ye, et al., 2024).

In agreement with our earlier work (Ma, Ye, et al., 2024), at pH 7, the major protein bands from both HP and WPI were observed in a heated protein mixture (Total) (**Fig. 6.4**, lane 5), which are HP 11S globulin acidic subunit (HP AS) ~ 34-36 kDa; HP 11S globulin basic subunit (HP BS) ~ 20 and 18 kDa and HP 2S albumin <20 kDa (Xu et al., 2022). β-lg and α-la remained in the supernatant fractions after heating (**Fig. 6.4**, lane 3), which is consistent with another study that reported 3% whey protein heated at pH 6.5–7.0 resulted in soluble protein aggregates (Iordache & Jelen, 2003). In contrast, no HP bands were detected in the supernatant of heated HP (**Fig. 6.4**, lane 8), confirming the existence of insoluble HP aggregates at pH 7 after heating, which is in agreement with another study (Do et al., 2025; Ma, Acevedo-Fani, et al., 2024), suggesting that heat-induced aggregation of HP was primarily driven by disulphide bonding. Notably, in the heated HP/WPI mixture, β-lg and α-la bands shifted from the supernatant to the sediment (**Fig. 6.4**, lane 7, indicated by arrow), suggesting the interactions between HP and whey protein to form hybrid aggregates, which could be driven by disulphide bonding and hydrophobic interactions (Ma, Acevedo-Fani, et al., 2024; Ma, Ye, et al., 2024).

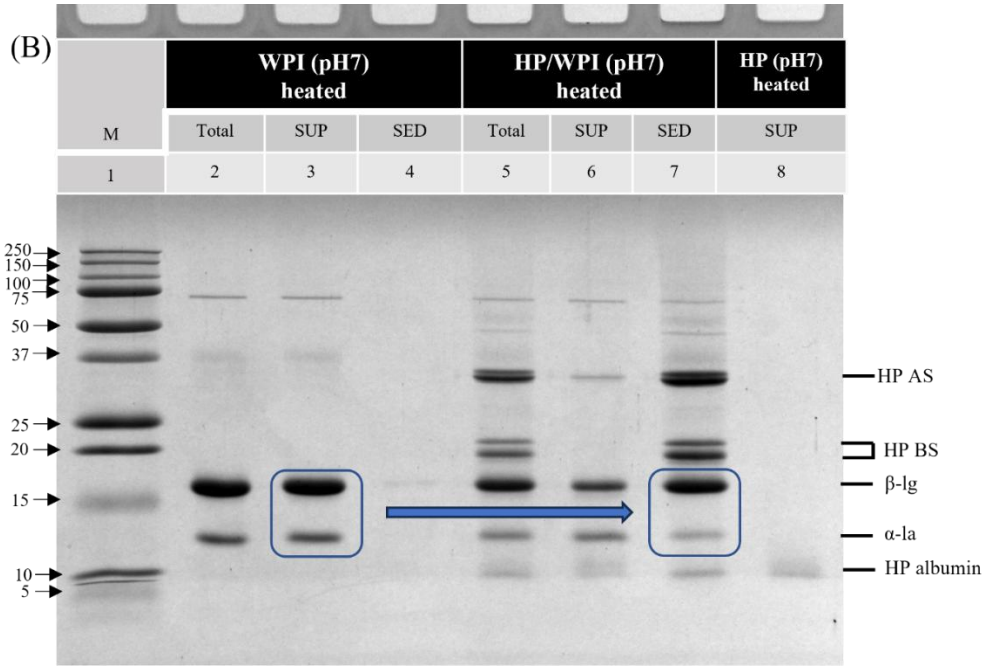


**Fig. 6.4.** SDS-PAGE under reducing conditions of heated WPI, HP and HP/WPI dispersion at pH 7. Lanes are: 1, marker; 2, heated WPI (total); 3, supernatant (SUP) from heated WPI; 4, sediment (SED) from heated WPI; 5, heated HP/WPI; 6, supernatant from heated HP/WPI; 7, sediment from heated HP/WPI; 8, supernatant from heated HP.

As discussed before, heated whey protein can form soluble aggregates at pH 8; therefore, the bands of whey protein were only present in the supernatant fraction (**Fig. 6.5,** lane 3). On the other hand, no clear HP bands were observed in the supernatant of heated HP dispersion at pH 4 to 8 (**Fig. 6.4-6.8**, lane 8), indicating that heated HP remained predominantly in aggregated form across this pH range. This is possibly due to the relatively higher free thiol groups in the HP, which led to a strong tendency for disulphide bonding (Xu et al., 2022).

Interestingly, the protein mixture heated under alkaline conditions (pH 8) showed different interaction behaviour compared to that which occurred at neutral pH. The soluble whey protein interacted with both the HP basic subunit (HP-BS) and a proportion of the

HP acidic subunit (HP-AS), leading to their co-sedimentation (**Fig. 6.5**, lane 7). However, the other portion of HP-AS became soluble when co-heated with whey protein, moving to the supernatant (**Fig. 6.5**, lane 6). SDS-PAGE analysis of the supernatant fraction under non-reducing conditions revealed the high molecular weight protein aggregates, exceeding 75 kDa and remaining in the stacking gel (data not shown), were dissociated into clear bands of HP and whey protein under reducing conditions (**Fig. 6.5**, lane 6). These findings may indicate the formation of soluble hybrid protein aggregates, stabilised by covalent and/or non-covalent interactions.

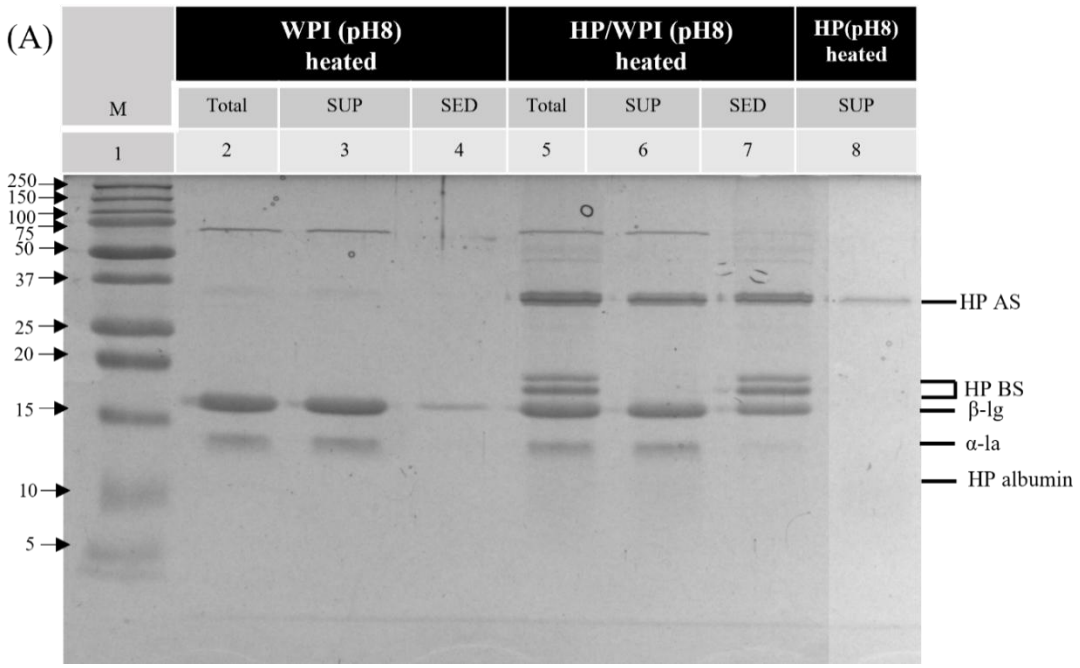


**Fig. 6.5.** SDS-PAGE under reducing conditions of heated WPI, HP and HP/WPI dispersion at pH 8. Lanes are: 1, marker; 2, heated WPI (total); 3, supernatant (SUP) from heated WPI; 4, sediment (SED) from heated WPI; 5, heated HP/WPI; 6, supernatant from heated HP/WPI; 7, sediment from heated HP/WPI; 8, supernatant from heated HP.

Do et al. (2025) proposed the dissociation of HP acidic subunit (HP-AS) and HP basic subunit (HP-BS) upon heating; subsequently, the dissociated HP-AS and HP-BS could re-aggregate to different extents. The dissociation and association of 11S globulin under heat treatment were also reported in soy proteins (Guo et al., 2012; Keerati-u-rai & Corredig, 2009; Renkema et al., 2002; Sorgentini et al., 1995; Yamagishi et al., 2014) and sunflower proteins (González-Pérez et al., 2004).

Although the insoluble aggregates were formed at pH 8, the particle size was much smaller than that formed at pH 4-7, as evidenced by the size distributions and microscope images. This behaviour may be attributed to the enhanced reactivity of free thiol (–SH) groups in both HP subunits and whey proteins under alkaline conditions. At high pH, the free-SH groups are more prone to deprotonation into reactive mercaptide ion species ($S^-$), promoting rapid thiol-disulphide exchange reactions (Mercade-Prieto & Gunasekaran, 2009). Consequently, the alkaline environment may facilitate fast intermolecular interactions among dissociated HP-AS, HP-BS, and whey protein, accelerating aggregate formation but also reducing the availability of free thiol groups, thereby promoting aggregation termination and limiting particle growth.

The trends of forming soluble aggregates may be related to the hydrophilicity and hydrophobicity properties of HP-AS and HP-BS. The HP-BS contains higher hydrophobic amino acids compared to HP-AS (Do et al., 2025; Kim & Lee, 2011), which makes HP-BS more hydrophobic. Similar features have been reported for soybean 11S globulin, in which the basic subunit (BS) contains higher hydrophobic amino acids than the acidic subunit (AS). The hydrophilicity of AS assists in the stabilisation of BS in the aqueous phase (Yamagishi et al., 2014). In our study, the dissociation of HP-AS likely exposed the more hydrophobic HP-BS, which made HP-BS more susceptible to forming large aggregates with whey protein through hydrophobic interactions and disulphide bonding. In contrast,

the relatively hydrophilic HP-AS likely had fewer hydrophobic interactions with whey protein, contributing to a lesser extent of aggregation and formation of soluble aggregates in the supernatant.

As mentioned above, heated HP dispersions still presented as insoluble HP aggregates in the sediment at pH 5 and 6 (**Fig. 6.6 and 6.7**, lane 8). As the pH of whey protein decreased to 6, the band of β-lg began to appear in both the supernatant and sediment fractions of heated whey protein (**Fig. 6.6**, lanes 3 and 4), indicating the onset of insoluble aggregate formation. This trend continued at pH 5, where β-lg and α-la were completely moved to the sediment fraction (**Fig. 6.7**, lane 4). This reflected stronger aggregation near the isoelectric point due to reduced electrostatic repulsion and enhanced protein-protein interactions through both covalent and non-covalent bonding (Verheul et al., 1998).

Different from partial co-precipitation of whey proteins observed in the heated HP/WPI mixture at pH 7 and 8, all soluble whey proteins migrated into the sediment when co-heated with HP at pH 6 (**Fig. 6.6**, lane 7), indicating extensive protein interactions at this pH. At pH 5, although whey proteins were no longer present in the supernatant (**Fig. 6.7**, lane 6), this sedimentation alone does not conclusively indicate hybrid aggregation with HP, since individually heated whey proteins also formed insoluble aggregates at this pH.

Nevertheless, the volume-weighted mean diameter ($d_{4,3}$) data provided supportive evidence that the aggregate size was significantly reduced from 310.5 ± 60.0 μm for heated HP alone to 78.3 ± 11.6 μm for the HP/WPI mixture. This size reduction suggests that whey protein may restrict larger HP aggregation through direct interaction. In other mixed systems, such as egg white protein and whey protein, the hybrid aggregation behaviour has

also been observed at pH 5 (Allahdad et al., 2023). The minimum intra- and inter-molecular repulsion, close to the isoelectric point, facilitates both covalent (disulphide) and non-covalent interactions (Verheul et al., 1998), which provides the possibility of hybrid protein interactions.

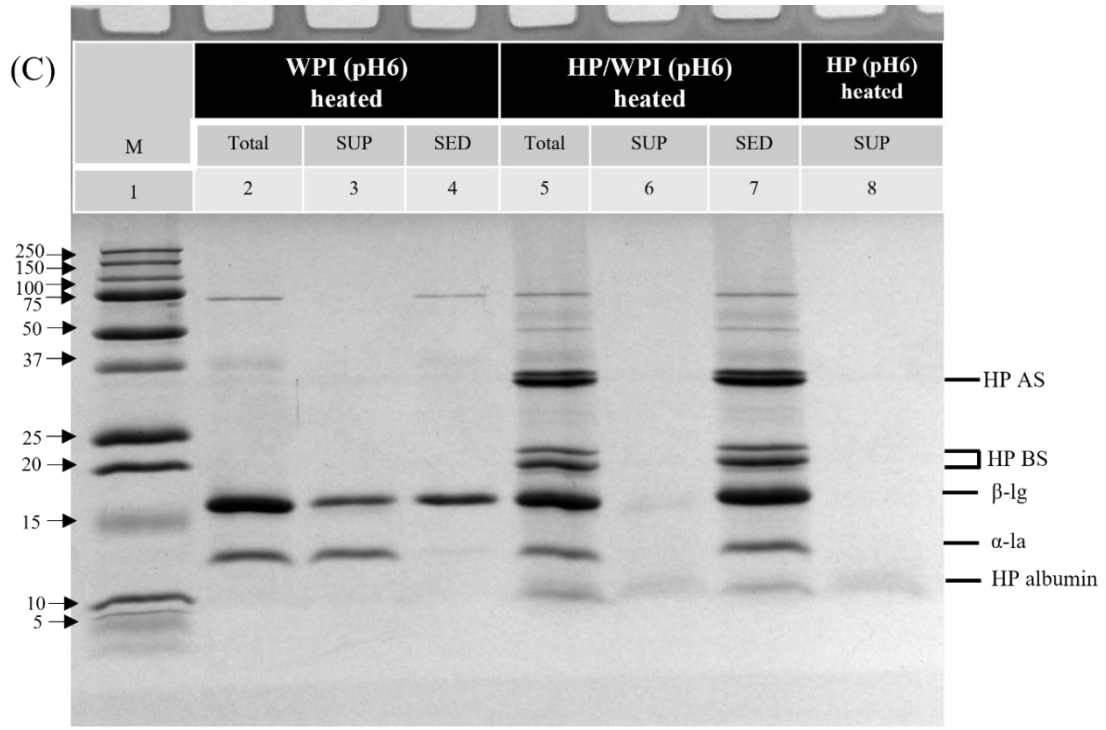


**Fig. 6.6.** SDS-PAGE under reducing conditions of heated WPI, HP and HP/WPI dispersion at pH 6. Lanes are: 1, marker; 2, heated WPI (total); 3, supernatant (SUP) from heated WPI; 4, sediment (SED) from heated WPI; 5, heated HP/WPI; 6, supernatant from heated HP/WPI; 7, sediment from heated HP/WPI; 8, supernatant from heated HP.

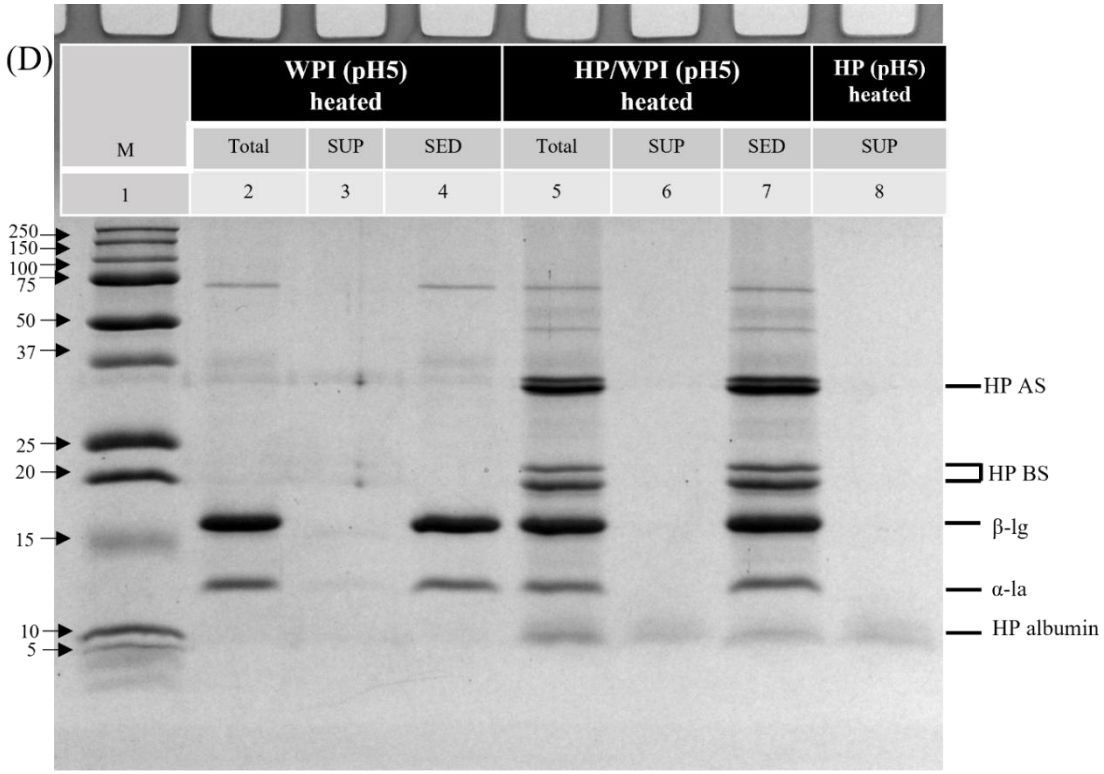


**Fig. 6.7.** SDS-PAGE under reducing conditions of heated WPI, HP and HP/WPI dispersion at pH 5. Lanes are: 1, marker; 2, heated WPI (total); 3, supernatant (SUP) from heated WPI; 4, sediment (SED) from heated WPI; 5, heated HP/WPI; 6, supernatant from heated HP/WPI; 7, sediment from heated HP/WPI; 8, supernatant from heated HP.

Interestingly, at more acidic conditions (pH 4 and 3), the bands of heated whey protein reappeared in the supernatant fractions (**Fig. 6.8 and 6.9**, lane 3), which indicates the heat stability of whey protein at these lower pH levels. This finding is consistent with other findings that whey protein exhibited increased resistance to thermal denaturation at pH 4 due to enhanced structural stability and reduced aggregation rate (Dissanayake, Ramchandran, Donkor, et al., 2013). When the protein mixture was heated at pH 4, the most soluble whey protein was found in the sediment alongside HP (**Fig. 6.8**, lane 7), indicating strong HP and whey protein interactions at this pH.

At pH 3, the bands of heated HP were observed in the supernatant (**Fig. 6.9**, lane 8), indicating that heating under very acidic conditions resulted in partial dissociation of HP aggregates. In other studies, Lakemond et al. (2000) reported the dissociation phenomenon in soy 11S globulin at pH 3.8. It is possible that the re-aggregation reaction of dissociated subunits at pH 3 was restricted, due to the stronger electrostatic repulsion and reduced activity of thiol groups under acidic conditions.

When heating the protein mixture at pH 3, a proportion of both HP and whey protein co-settled in the sediment (**Fig. 6.9**, lane 7). The thiol oxidation and thiol/disulphide exchange may be largely suppressed at such low pH (Dissanayake, Ramchandran, Piyadasa, et al., 2013), and the interactions between dissociated HP and WPI are presumed to be dominated by hydrophobic forces. Meanwhile, the other fractions of HP and WPI remained in the supernatant (**Fig. 6.9**, lane 6). However, given the partial dissociation of HP at pH 3, leading to soluble aggregates, it is difficult to identify the HP–WPI interactions solely based on SDS-PAGE data. Further analytical techniques will be required to confirm these interactions.

Overall, heating the HP/WPI mixture at pH 8 produced small aggregates, composed of both soluble HP-AS/whey protein aggregates and insoluble HP/whey protein aggregates. In contrast, heating at pH 4–7 resulted in larger, more irregular aggregates, comprising HP-AS, HP-BS and whey protein, which are less suitable for size reduction using high-shear homogenisation. Although heating at pH 3 produced relatively small aggregates, SDS-PAGE did not provide conclusive evidence of the interactions between HP and whey protein in the supernatant. Moreover, the unreacted free thiol groups may retain their reactivity post-heating, potentially compromising their stability during later processing.

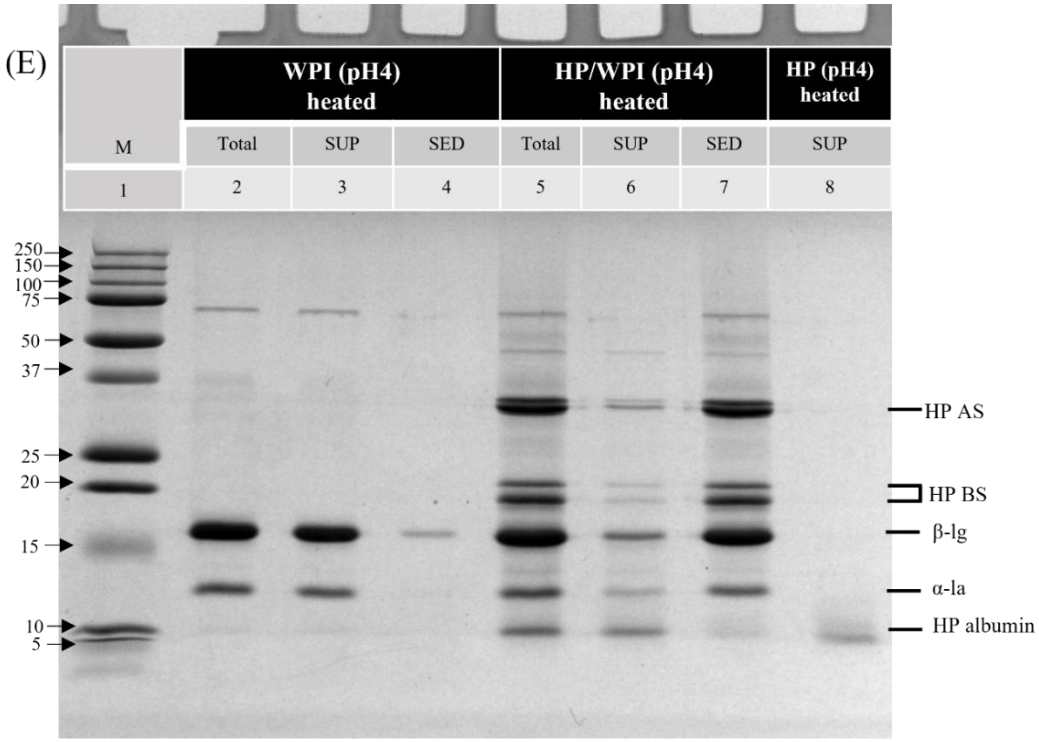


**Fig. 6.8.** SDS-PAGE under reducing conditions of heated WPI, HP and HP/WPI dispersion at pH 4. Lanes are: 1, marker; 2, heated WPI (total); 3, supernatant (SUP) from heated WPI; 4, sediment (SED) from heated WPI; 5, heated HP/WPI; 6, supernatant from heated HP/WPI; 7, sediment from heated HP/WPI; 8, supernatant from heated HP.

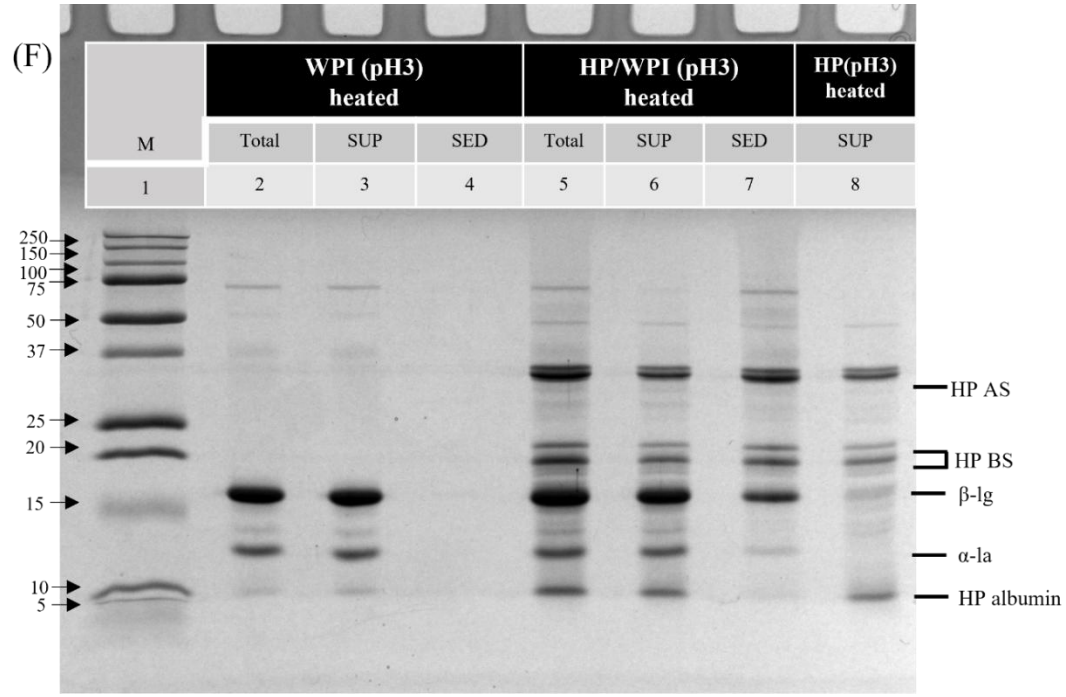


**Fig. 6.9.** SDS-PAGE under reducing conditions of heated WPI, HP and HP/WPI dispersion at pH 3. Lanes are: 1, marker; 2, heated WPI (total); 3, supernatant (SUP) from heated WPI; 4, sediment (SED) from heated WPI; 5, heated HP/WPI; 6, supernatant from heated HP/WPI; 7, sediment from heated HP/WPI; 8, supernatant from heated HP.

## 6.4 Conclusions

In summary, particle size distribution, microscopy and SDS-PAGE analysis demonstrated that pH strongly influences the interactions between HP and whey protein during heating. At pH 8, heating promoted the formation of small, spherical hybrid aggregates composed of both soluble (HP-AS/WPI) and insoluble HP–WPI aggregates, likely stabilised by disulphide bonding and hydrophobic interactions. Contrary, heating at pH 4–7 resulted in the formation of large, irregular aggregates. At pH 3, heating produced relatively small aggregates; however, evidence for HP–WPI interaction in the supernatant was limited, and the presence of residual reactive thiol groups may compromise the stability of aggregates during later processing. Overall, pH 8 was identified as the most favourable

condition for producing heat-induced HP/WPI aggregates and was therefore selected for the development of microparticulated WPI/HP mixtures in the subsequent chapters. These findings provide valuable insights for the design and optimization of HP/WPI aggregates in future microparticulation processes.

MASSEY UNIVERSITY
TE KUNENGA KI PŪREHUROA
UNIVERSITY OF NEW ZEALAND

GRADUATE RESEARCH SCHOOL

# STATEMENT OF CONTRIBUTION
# DOCTORATE WITH PUBLICATIONS/MANUSCRIPTS

We, the student and the student's main supervisor, certify that all co-authors have consented to their work being included in the thesis and they have accepted the student's contribution as indicated below in the Statement of Originality.

| | |
|---|---|
| Student name: | Sihan Ma |
| Name and title of main supervisor: | Dr Alejandra Acevedo-Fani |
| In which chapter is the manuscript/published work? | Chapter 7 |

Describe the contribution that the student and members of the supervisory team have made to the manuscript/published work:[1]

Sihan Ma: Investigation, Methodology, Formal analysis, Data curation, Writing - original draft, Visualisation.
Aiqian Ye: Methodology, Writing - review & editing, Supervision.
Harjinder Singh: Methodology, Writing - review & editing, Supervision, Funding acquisition.
Alejandra Acevedo-Fani: Conceptualisation, Supervision, Methodology, Validation, Resources, Writing - review & editing.

Please select one of the following three options:

- (●) **The manuscript/published work is published or in press**

  Please provide the full reference of the research output:

  Ma, S., Ye, A., Singh, H., & Acevedo-Fani, A. (2025). Emulsifying properties of hemp and whey protein complexes achieved by microparticulation. Food Hydrocolloids, 111833. https://doi.org/https://doi.org/10.1016/j.foodhyd.2025.111833

- ( ) **The manuscript is currently under review for publication**

  Please provide the name of the journal:

- ( ) **It is intended that the manuscript will be published, but it has not yet been submitted to a journal**

| | | | |
|---|---|---|---|
| Student's signature: | Sihan Ma — Digitally signed by Sihan Ma, DN: cn=Sihan Ma, c=NZ, email=s.ma@massey.ac.nz, Date: 2025.07.31 15:16:15 +12'00' | Main supervisor's signature: | Alejandra Acevedo Fani — Digitally signed by Alejandra Acevedo Fani, DN: cn=Alejandra Acevedo Fani, c=NZ, o=Massey University, ou=Riddet Institute, email=a.acevedo-fani@massey.ac.nz, Date: 2025.08.04 11:39:12 +12'00' |

*This form should be placed at the beginning of each relevant thesis chapter.*

[1] Refer to the Massey University Publishing and Authorship guidelines (OneMassey for staff, Stream for students) and/ or Contributor Roles Taxonomy (CRediT) guidelines for guidance.

# Chapter 7: Emulsifying properties of hemp and whey protein complexes achieved by microparticulation

This chapter has been published in a peer-reviewed journal:

Ma, S., Ye, A., Singh, H., & Acevedo-Fani, A. (2025). Emulsifying properties of hemp and whey protein complexes achieved by microparticulation. *Food Hydrocolloids*, 111833. https://doi.org/https://doi.org/10.1016/j.foodhyd.2025.111833

## Abstract

Hemp is a sustainable source of protein. However, the utilisation of commercial hemp protein (HP) is limited due to its poor functionality. This study provided a microparticulation method to produce hybrid microparticles by complexing HP and whey protein isolate (WPI), and investigated their emulsifying potential. The emulsions, composed of 10% oil and 0.25–1.8% protein (non-microparticulated or microparticulated HP/WPI), were produced and the impact of microparticulation on the emulsifying ability of HP/WPI was explored using static light scattering, CLSM, TEM and SDS electrophoresis analysis. The results showed that non-microparticulated HP/WPI stabilised emulsions exhibited preferential whey protein adsorption at the oil-water interface, leading to sufficient protein coverage at most protein concentrations (0.25–1.8%) with relatively small droplet size (~0.5 μm) and minimal flocculation. In contrast, in the 'emulsifier-poor' regime (0.25–1%), microparticulated HP/WPI stabilised emulsions displayed larger droplet size with clear signs of bridging flocculation. However, when the protein concentration was sufficient (≥ 1.5% protein), it reached a similar droplet size as that of non-microparticulated HP/WPI emulsion with minimal flocculation. Microparticulation increased HP loading at

the interface, while emulsions stabilised by non-microparticulated HP/WPI showed less HP adsorption. Transmission electron microscopy further confirmed the microparticle coverage. Moreover, the heat stability of microparticulated HP/WPI stabilised emulsions increased, compared with non-microparticulated HP/WPI. These findings highlight the potential of microparticulated HP/WPI systems in the application of emulsification and enhance HP applications in the food industry.

## 7.1 Introduction

An oil-in-water emulsion is a colloidal dispersion consisting of dispersed oil droplets within an aqueous phase (McClements & Jafari, 2018). Emulsifiers play an important role in stabilising oil droplets and improving mouthfeel and rheological properties (Aloo et al., 2024). Protein is widely used as an emulsifier in emulsion formulations and stabilisation due to its amphiphilic nature (Lam & Nickerson, 2013). Beyond isolated proteins, protein nanoparticles and microparticles are increasingly explored in food colloids to build novel emulsion structures (Amagliani & Schmitt, 2017; Dickinson, 2015; Nicolai, 2016).

Hemp (*Cannabis sativa* L.) protein has garnered increasing attention for its high nutritional value, excellent digestibility, and balanced amino acid profile (Wang & Xiong, 2019). However, its use in the food application, particularly as an emulsifier, is still limited (Ajibola & Aluko, 2022; Kahraman et al., 2022; Liu et al., 2024). One major limitation is its low water solubility, with only ~10% solubility at pH 7, which is significantly lower than that of other plant proteins such as soy protein (Hadnađev et al., 2018). Additionally, HP has a strong tendency to form large, dense aggregates at neutral pH, mainly due to its high free sulfhydryl content, inducing extensive disulphide bond formation (Dapčević-

Hadnađev et al., 2019; El-Sohaimy et al., 2022; Tang et al., 2006). These structural characteristics also hinder its functionality, such as emulsification. For instance, the presence of large protein aggregates and limited solubility also reduces its ability to rapidly and effectively adsorb to the oil–water interface, resulting in poor emulsifying properties. Studies have consistently shown that HP has inferior emulsifying activity compared to soy or canola proteins (Tang et al., 2006; Teh et al., 2014). Recent findings by Liu et al. (2023) also reported the low emulsifying activities and large standard deviations, with oil droplet sizes ranging from 40 to 90 μm in HP stabilised emulsions.

There have been only a limited number of studies done to improve the emulsifying properties of hemp protein. Yin et al. (2008) used enzymatic hydrolysis treatment to improve the protein solubility. However, the emulsifying activity index was remarkably decreased. Other strategies have focused on complexing hemp protein with polysaccharides at low pH. Y. Feng et al. (2021) complexed pectin with hemp protein at pH 3, and Gholivand et al. (2024) complexed hemp protein with carrageenan, alginate, gum arabic and pectin at pH 3 or pH 3.5 to improve the dispersibility of hemp protein. However, the complexation and emulsification were performed at a very acidic pH, which is not ideal for food applications. The neutralisation of pH after processing may cause re-aggregation of hemp protein (Chuang et al., 2021). High alkaline-thermal treatments have also been explored. Q. Wang, Y. Jin, et al. (2018) used alkaline conditions (pH 12) combined with thermal treatment to improve the solubility and emulsifying activity of hemp protein isolate. However, the toxic by-product, lysinoalanine, produced at high alkaline pH and high-temperature environment, needs to be carefully monitored. Therefore, a novel process that can reinforce the nutritional and functional properties of hemp protein is demanded.

One possible approach to improve plant protein emulsifying properties is by complexation with milk proteins (Alves & Tavares, 2019). The functional synergy effect

of the mix of some other plant proteins and milk proteins has been reported in recent years (Hinderink et al., 2019; Jose et al., 2016; Kim et al., 2020; Roesch & Corredig, 2006; Wong et al., 2013a; Yerramilli et al., 2017). Previous studies have shown that heat-induced interaction and complexation of soy protein with whey protein (Anuradha & Prakash, 2009; Roesch & Corredig, 2005) and pea protein with β-lactoglobulin (β-lg) (Chihi et al., 2016) lead to hybrid aggregates that are smaller than individual plant protein aggregates. These plant/milk protein complexes may offer great potential for improving functionality, especially emulsifying properties in this study.

Little work has been conducted on the complexation of hemp protein with milk proteins and their emulsifying properties. Only one published study reported that pH-cycling complexation turned insoluble hemp globulin into hemp globulin/sodium caseinate particles that have emulsifying functionality (Chuang et al., 2020). However, due to the relatively high free thiol content in hemp edestin, large hemp protein aggregates formed when heated above the denaturation temperature (92 °C) (Tang et al., 2006). Maintaining the thermal stability of hemp protein during food processing remains a challenge.

On the other hand, heat-induced protein interactions undertaken under control conditions can lead to the formation of protein microparticles that may have enhanced thermal stability (Ma, Ye, et al., 2024). This process, known as microparticulation, involves thermal treatment, shear, or pH shifts to form protein microparticles (Ipsen, 2017; Shi et al., 2021) and could offer a solution to overcome the limitations abovementioned of hemp protein. Our previous work was the first to report that whey protein can form complexes with hemp protein particles, effectively reducing aggregation and improving thermal stability (Ma, Acevedo-Fani, et al., 2024; Ma, Ye, et al., 2024). Nevertheless, the emulsifying properties of the hemp/whey protein microparticle have not yet been explored.

In oil-in-water emulsions, the particles could irreversibly adsorb at the oil–water interface and form a mechanical barrier due to their high desorption energy, thereby providing mechanical and steric stabilisation against coalescence and flocculation (Dickinson, 2012; Tcholakova et al., 2008). This is because microparticles often exhibit higher surface hydrophobicity, which could promote protein interaction at the interface to form thick and rigid films providing steric stabilisation (Sun et al., 2015). Previously, microparticulated protein stabilised emulsions show greater thermal stability compared to those stabilised by isolated proteins, likely because fewer reactive sites remain available for heat-induced aggregation (Çakır-Fuller, 2015).

In this study, we provided a microparticulation method for creating hemp/whey protein microparticles by heat treatment at a controlled pH environment, followed by size reduction. The emulsifying properties of hybrid protein microparticles, the surface structure of these resulting emulsions and their heat stability were examined.

## 7.2 Materials and methods

### 7.2.1 Materials

Whey protein isolate (WPI) containing 92.0% protein, 0.9% fat, 1.6% ash and 5.2% moisture was purchased from Fonterra Co-operative Group Limited, Auckland, New Zealand. The hempseed protein (HP) concentrate powder was purchased from Davis Food Ingredients (Davis Trading Company Ltd., Palmerston North, New Zealand). The HP powder contained 59.8% protein, 2.4% fat, 10.7% ash, 6.8% moisture and 20.2% carbohydrate. The proximate composition of both protein ingredients was analysed as follows: protein content was determined using the Kjeldahl method (AOAC 991.20, nitrogen factor 5.21; AOAC 2023a); fat, ash and moisture content were determined

according to AOAC 922.06, AOAC 942.05 and AOAC 925.10, respectively (AOAC 2023b,c,d, respectively); and carbohydrate content was calculated by subtracting the sum of the protein, ash and fat from the total solids. All chemicals were purchased from Sigma-Aldrich Ltd. (St. Louis, MO, USA), and the reagents were made up in Milli-Q water (Milli-Q apparatus; Millipore Corp., Bedford, MA, USA).

### 7.2.2 Preparation of HP/WPI microparticle

A hemp protein (HP) dispersion was prepared by mixing powdered HP in Milli-Q water at 2% (w/w) protein concentration. The mixture was stirred for 2 h at 20 °C. The pH was then adjusted to 11 with 1 M NaOH, followed by stirring for 2 h to increase protein solubility. The dispersion was centrifuged at 3000 × *g* for 30 min to remove insoluble materials (e.g., fibres). The resulting supernatant was adjusted to pH 8 using 1 M HCl, and homogenised using a two-stage valve homogeniser (APV 1000, SPX, Silkeborg, Denmark) set at 300 bar (first stage) and 50 bar (second stage). The protein dispersion was passed twice through the homogeniser with no holding time between passes. The resulting dispersion was used in subsequent steps. Separately, a whey protein isolate (WPI) stock solution was prepared by dissolving WPI powder in Milli-Q water at 3% (w/w) and stirring for 2 h. The pH of the protein dispersion was adjusted to 8 using 1 M NaOH.

To prepare the HP/WPI microparticles, HP and WPI dispersions were mixed to achieve a final protein concentration of 1% HP and 1% WPI (w/w) in the mixture. The pH was re-adjusted to 8. Then, the protein mixture was subjected to a heat treatment of 95 °C for 30 min in a water bath. After the treatment was completed, the protein dispersion was rapidly cooled down to 20 °C in an ice bath. Finally, the pH of the protein dispersion was adjusted to 7 (using 1 M HCl), and passed twice through a two-stage valve homogeniser using the same pressure conditions described to produce HP dispersions.

### 7.2.3 Preparation of HP/WPI emulsions

To prepare emulsions stabilised by either microparticulated or non-microparticulated HP/WPI, two types of coarse emulsions were first prepared. For microparticulated emulsions, preformed HP/WPI microparticles were dispersed in water containing 10% (w/w) soybean oil to achieve final protein concentrations of 0.25%, 0.5%, 1.0%, 1.5%, or 1.8% (w/w). For non-microparticulated emulsions, a dispersion of HP particles / WPI mixture (at the same protein ratios used in microparticle preparation) was directly dispersed at corresponding total protein concentrations and oil concentration. Coarse emulsions were prepared using a benchtop Ultra-Turrax mixer (IKA, Wilmington, NC, USA) for 30 s at room temperature. The resulting coarse emulsions were then passed 2 times through a two-stage homogeniser at 300 bar (first stage)/50 bar (second stage) to produce fine emulsions stabilised by either microparticulated or non-microparticulated HP/WPI. Sodium azide (0.02%, w/w) was added to inhibit microbial growth.

### 7.2.4 Droplet size analysis

The droplet size of the HP/WPI emulsion was measured by static light scattering using a Mastersizer 2000 and a Hydro MU unit (Malvern Instruments, Worcestershire, UK). The refractive index was 1.45. The data were reported in volume-weighted mean diameter $d_{(4, 3)}$, calculated as the average of triplicate measurements. The surface weighted mean diameter $d_{(3, 2)}$ was also collected to calculate surface protein coverage in the following section.

### 7.2.5 Transmission electron microscopy

Transmission electron microscopy (TEM) was employed to observe the microstructure of HP/WPI microparticles and their stabilised emulsions as described by (S. Li et al., 2021). Samples were sealed in agarose tubes (3% agarose) and placed into 3% glutaraldehyde in 0.1 M sodium cacodylate (pH 7.2) for 24 h, followed by washing 3 times with 0.1 M sodium cacodylate buffer. The samples were then post-fixed with 1% osmium tetroxide in 0.1 M sodium cacodylate for 1 h at room temperature, overnight at 4 °C and another 1 h at room temperature. The samples were washed 3 times again as described above and dehydrated with a graded acetone series (25, 50, 75, 95 and 100% acetone) for 45 min each concentration. The dehydrated samples were first embedded with resin and acetone (1:1, v/v) overnight on a rotator, then the resin and acetone (1:1, v/v) was replaced with fresh 100% resin for 8 h; this was repeated 4 times. After that, samples were embedded in moulds with 100% resin and incubated in a 60 °C oven for 48 h. Thin sections were cut from the resin blocks on an ultramicrotome and then mounted on copper grids using a Coat-Quick "G" pen (Daido Sangyo, Tokyo, Japan). The grids were stained with saturated uranyl acetate and lead citrate with 50% ethanol, respectively, followed by MilliQ water washing between each step. The stained sample was imaged by a transmission electron microscope (FEI Tecnai G2 Spirit BioTWIN, FEI Company, Prague, Czech Republic) paired with a Veleta TEM camera (Olympus SIS, Hamburg, Germany).

### 7.2.6 Sodium dodecyl sulphate polyacrylamide gel electrophoresis

The protein composition in the HP/WPI microparticle was analysed using sodium dodecyl sulphate polyacrylamide gel electrophoresis (SDS-PAGE) with a Tris-glycine gel under non-reducing and reducing conditions as per the protocol described by Dave et al. (2019) and Manderson et al. (1998). The protein sample was mixed with reducing sample

buffer to a final protein concentration of 1 mg/mL. Dithiothreitol was used as a reducing agent in the reducing sample buffer (200 mm), and the reducing samples were heated at 56 °C for 15 min. Ten microlitre samples were loaded onto Mini-Protean gels (Bio-Rad Laboratories, Richmond, CA, USA) and run at 150 V, followed by Coomassie brilliant blue staining and destaining (10% isopropanol and 10% glacial acetic acid in water, v/v). The destained gel was scanned by the molecular imager Gel Doc XR (Bio-Rad Laboratories, Richmond, CA, USA) and analysed by ImageLab software.

### 7.2.7 Confocal laser scanning microscopy

Confocal laser scanning microscopy (CLSM; Model Zeiss LSM900 with Airyscan 2, Carl Zeiss, Jena, Germany) was used to investigate the microstructure of HP/WPI emulsion using the staining protocols described by Gallier et al. (2012). Nile Red (1 mg/mL in acetone) and Fast Green FCF (1 mg/mL in Milli-Q water) were used to selectively stain neutral lipids and proteins, respectively. Each sample (100 μL) was mixed with Nile Red (2:100, v/v) and Fast Green FCF (6:100, v/v). The stained emulsion sample was placed on a concave microscope slide and covered by a coverslip (0.17 mm thick), avoiding an air bubble between the sample and the coverslip. The freshly prepared sample slide was immediately examined by CLSM with a 63x oil immersion objective lens.

### 7.2.8 Total protein coverage

The emulsions were centrifuged at 45,000 × *g* for 40 min at 20 °C. The subnatant layer and sediment layer were carefully collected. The cream layer was dispersed in deionised water and re-centrifuged at 45,000 × *g* for 40 min to obtain washed cream. The protein content in the subnatant and sediment was analysed separately using the Kjeldahl method.

Adsorbed protein (g) was calculated using equation (Eq. 7.1):

$$\text{Adsorbed protein (g)} = \text{Total protein (g) used in emulsion} - [\text{protein (g) in the subantant} + \text{protein (g) in the sediment}] \quad \text{(Eq. 7.1)}$$

Total surface protein ($mg/m^2$) was calculated using equation (Eq.7.2):

$$\text{Total surface protein } (mg/m^2) = \frac{[\text{Adsorbed protein (g)} \times d_{3,2}]}{[6 \times V \times \phi]} \times 10^{-2} \quad \text{(Eq. 7.2)}$$

where V (mL) is the volume of emulsions, and ϕ is the volume fraction of the oil in emulsions (Chang et al., 2016).

### 7.2.9 Protein composition on the emulsion surface

The washed emulsion cream was spread and dried on a filter paper, then was analysed using SDS-PAGE under reducing conditions as described in the previous section to determine the composition of the adsorbed protein at the surface of the emulsion. The resulting gels were scanned using a Gel Doc XR (Bio-Rad Laboratories) and analysed by ImageLab software for densitometric analysis. The percentage composition of each sample was expressed as the individual protein intensity as a fraction of the sum total.

### 7.2.10 Heat stability of emulsions

The heat stability of emulsions stabilised by microparticulated HP/WPI and non-microparticulated HP/WPI at protein concentrations ≥ 1% was evaluated. A 10 mL sample of emulsion was transferred into a glass tube and heated in a water bath at different temperatures (60, 70, 80 and 90 °C) for 20 min, followed by rapid cooling in ice to 20 °C. The droplet size of the heated emulsions was analysed to investigate their heat stability.

### 7.2.11 Data analysis

The results are reported as mean ± standard deviation. Statistical analysis was performed using SPSS software for Windows (version 29.0, SPSS Inc., Chicago, IL, USA). The data were analysed by independent t-tests between two groups with the level of significance set at $p < 0.05$.

## 7.3 Results and discussion

### 7.3.1 Particle size and morphology of HP/WPI microparticles

Microparticulated proteins, particularly microparticulated whey proteins, are commonly produced using heating and shearing treatment. This processing can create protein particles within the 0.1–10.0 μm size range that are desired for different protein functionalities (Shi et al., 2021). In this study, HP/WPI microparticles were produced through heat treatment under slightly alkaline conditions, followed by size reduction. To evaluate the functional effects of microparticulation, emulsions were also prepared using a non-microparticulated HP/WPI mixture as a control in the following sections. This control mixture contained the same HP particles and WPI blend (same protein ratio and concentration), but without undergoing any heat treatment. Thus, it represents the unstructured protein mixture before microparticle formation. Although both samples originate from the same components, the presence or absence of heat-induced interactions and particle formation may result in different functionality.

The heat treatment of protein particles at pH 8 was the initial step in creating the HP/WPI complexes. As shown by the appearance of heated HP/WPI dispersion (**Fig. 7.1 A-1**), this treatment produced a well-dispersed suspension of protein particles. In contrast, heating HP individually resulted in a strong coagulum (**Fig. 7.1 A-2**). This is attributed to the high free thiol content in HP, which leads to the formation of large protein aggregates

via disulphide bonds upon heating (Tang et al., 2006; Wang & Xiong, 2019). Consistent with our previous findings, WPI was observed to interact with HP particles, preventing excessive aggregation (Ma, Acevedo-Fani, et al., 2024). Because individual HP particles are not ideal for heat treatment, only HP/WPI microparticles were examined in this study.

The impact of microparticulation on the HP/WPI dispersion/complex was first assessed by particle size measurement (**Fig. 7.1B**). The size distribution of the non-microparticulated HP/WPI dispersion revealed a bimodal distribution, with two peaks at 0.1–1 μm and 1–10 μm. This indicates that the majority of particles before microparticulation present as large aggregates, which could potentially hinder their effectiveness as emulsifiers in stabilising emulsions (Li et al., 2022). In contrast, the distribution of the HP/WPI microparticles shifts significantly to the left, with a majority of particles concentrated around a main peak at approximately 0.1 μm. The size range (10–200 nm) is known to support the formation of stable Pickering emulsions (Gricius & Oye, 2023).

The inset bar graph further illustrates that the volume-weighted mean diameter ($d_{4,3}$) of HP/WPI decreased from 3 μm to 0.2 μm after microparticulation. This substantial reduction supports the hypothesis that the heat treatment introduced the complexation between HP and whey protein (Ma, Acevedo-Fani, et al., 2024), and the following homogenisation process effectively broke down the HP/WPI complex to a desired size for emulsification.

Transmission electron microscopy (TEM) illustrates the structural morphology of HP/WPI microparticles (**Fig. 7.1C**). In untreated HP/WPI dispersion (**Fig. 7.1C-1**), the particles appeared as large aggregates with irregular shapes in several micrometres in size, which were most likely HP particles. In contrast, the HP/WPI microparticles (**Fig. 7.1C-2**) were significantly smaller and more uniformly dispersed, which is consistent with the

particle size analysis shown in **Fig. 7.1B**. These findings suggest that microparticulation effectively breaks down aggregates and leads to more homogeneous size distribution..

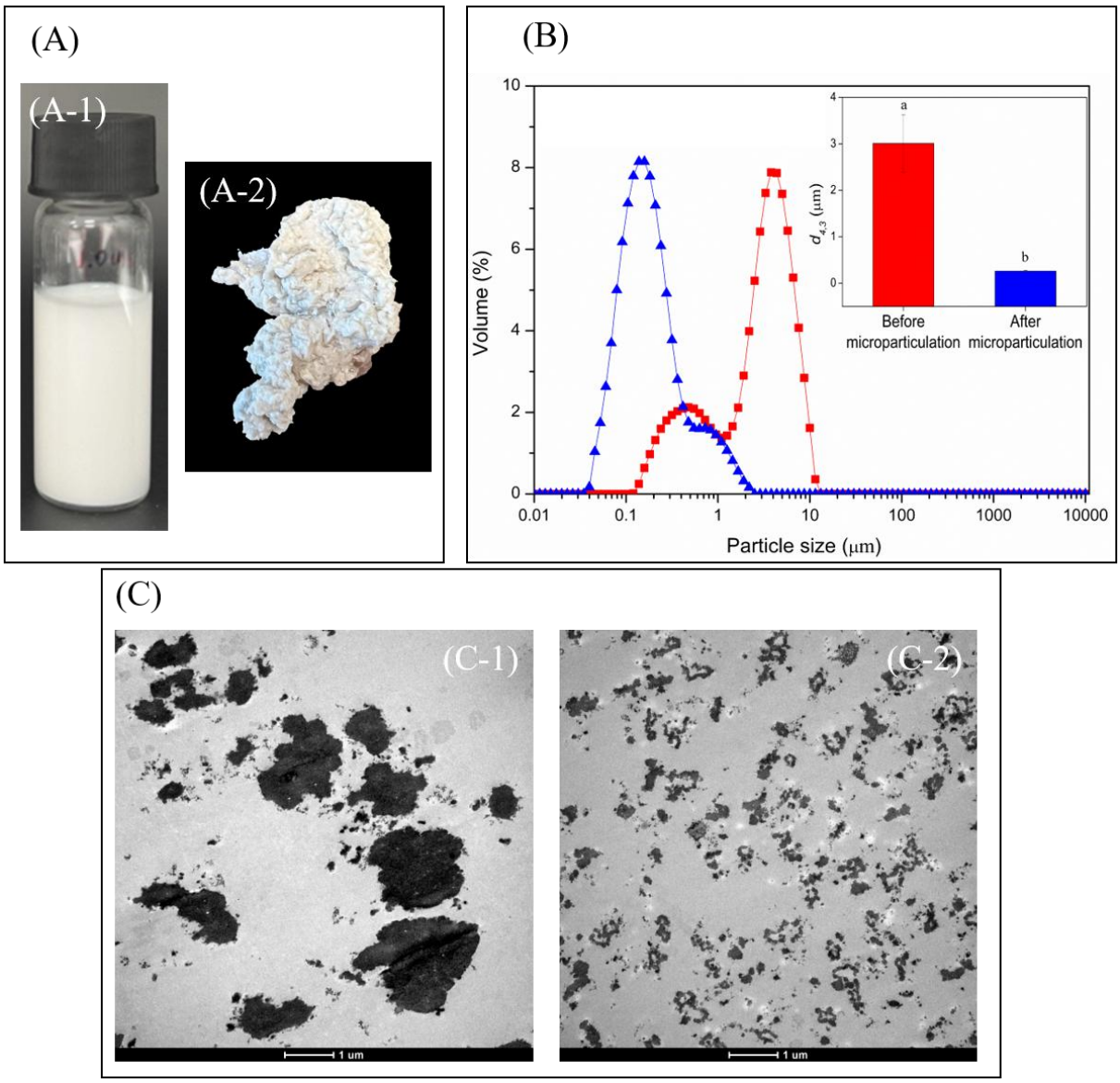


**Fig. 7.1.** Panel A: visual observations of heated HP with (A-1) the presence of WPI and (A-2) the absence of WPI at pH 8. Panel B: particle size distribution of HP/WPI before (■) and after (■) microparticulation; the inserted bar graph shows their corresponding volume-weighted mean diameters ($d_{4,3}$, μm), different lowercase letters indicate significant differences ($p < 0.05$). Panel C: transmission electron microscopy of HP/WPI particles before (C-1) and after (C-2) microparticulation.

### 7.3.2 Protein composition of HP/WPI microparticles

To analyse the protein interactions and compositions in HP/WPI microparticles, SDS-PAGE was conducted on the entire dispersion, as well as the corresponding supernatant and sediment fractions under both non-reducing and reducing conditions (**Fig. 7.2**).

Under reducing conditions, the disulphide bonds and hydrophobic interactions were disrupted with dithiothreitol (DTT) and SDS (Potin et al., 2022). Thus, the HP/WPI microparticles were disassociated into their monomeric forms. Therefore, the total fraction of HP/WPI showed 4 main predominant bands (lane 5, **Fig. 7.2**). The bands at 34 kDa, 21 kDa and 18 kDa correspond to the acidic subunit (AS) and two basic subunits (BS) of hemp globulin (Potin & Saurel, 2020; Wang & Xiong, 2019). On the other hand, the major whey protein, β-lg, was also observed and marked (Singh, 2009).

Notably, both individually unheated and heated WPI at pH 8 were still soluble and remained in the supernatant fraction. On the other hand, both individually unheated and heated HP globulin were still relatively insoluble at pH 8 and could be collected in the sediment pellet (data not shown). As reported in our previous study, at unheated conditions or with no protein-protein interactions, the WPI and HP can be separated upon centrifugation at 20,000 × *g* for 15 min (Ma, Ye, et al., 2024).

However, after co-heating with WPI and HP at pH 8, the band intensity of supernatant β-lg (lane 6, **Fig. 7.2**) was reduced, and part of β-lg was merged into the sediment fraction (lane 7, **Fig.7.2**). This suggests the heat-induced interactions between HP and WPI. A plausible explanation could be that heat treatment unfolded the globular structures of whey proteins and exposed the sulphydryl groups of both HP and whey proteins (Anema, 2020; Singh & Havea, 2003), leading to thiol/disulphide exchange to

form disulphide bridges between a proportion of WPI and HP and create HP/WPI hybrid particles. This observation aligns with the reported studies that WPI could bind with the HP via new disulphide bonds, thereby restricting the growth of HP aggregates (Ma, Acevedo-Fani, et al., 2024; Ma, Ye, et al., 2024).

Interestingly, a portion of the acidic subunit (AS) of HP was detected in the supernatant fraction after co-heating with WPI at pH 8 (lane 6, **Fig.7.2**). This band was absent in the supernatants of individually heated HP at pH 8 or co-heated HP/WPI at pH 7 (Ma, Acevedo-Fani, et al., 2024; Ma, Ye, et al., 2024), suggesting that the AS was present in the soluble phase only under specific co-heating conditions at pH 8. Moreover, under non-reducing conditions (lane 3, **Fig. 7.2**), high molecular weight protein bands exceeding 75 kDa and protein retained in the stacking gel were observed. These protein bands were absent in the co-heated HP/WPI at pH 7 (Ma, Ye, et al., 2024), indicating that disulphide cross-linking between the AS of HP and WPI proteins occurred only at pH 8. Upon subsequent reducing conditions, these high molecular weight aggregates dissociated into AS of HP and β-lg, supporting the involvement of thiol/disulphide exchange.

The stability of HP is closely related to the pH conditions. One study reported that the ζ-potential of the HP protein body was strongly negatively charged (~ –38 mV at pH 8), which led to strong internal electrostatic repulsion and the tendency of particle dissociation (Do et al., 2024). Q. Wang, Y. Jin, et al. (2018) also noted that combining alkaline pH and heating dissociated the complex of acidic and basic subunits of HP due to the strong electrostatic repulsion and weakening hydrogen bonding. Makinen et al. (2016) reported that the disulphide bonds linking acidic and basic subunits of quinoa globulin were disrupted by heating at pH 8.5. These findings in this study suggest that synergistic effects of combining heat treatment with mild alkaline conditions caused dissociation of HP globulin sub-units (aided by electrostatic repulsion and weakening of AS–BS interactions),

allowing the AS to become available for interactions with WPI, resulting in soluble HP AS–WPI aggregates. Although further experimental confirmation (e.g. LC-MS/MS identification or thiol-blocking assays) would strengthen this hypothesis, SDS-PAGE data provide compelling indirect evidence for such interactions at pH 8.

The combined data sets of SDS-PAGE, particle size analysis and TEM imaging (**Section 7.3.1**) support that the process described in this study successfully produced HP/WPI hybrid microparticles, with reduced mean size and improved dispersibility. Although additional characterisation could further reveal molecular-level interactions or surface properties, they were out of the scope of this investigation.

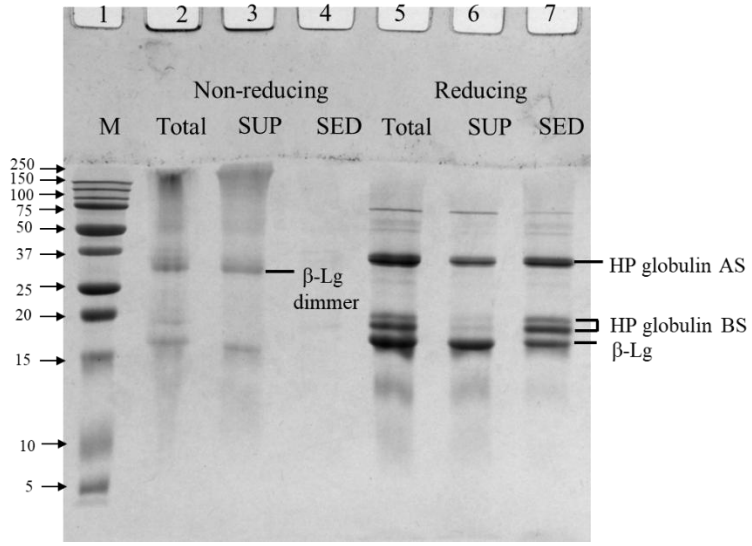


**Fig. 7.2.** SDS-PAGE under non-reducing (lanes 2–4) and reducing (lanes 5–7) conditions of HP/WPI microparticle dispersion (Total) and their supernatant (SUP) and sediment (SED). Lane 1, marker; lanes 2 and 5, HP/WPI dispersion; lanes 3 and 6, supernatant from HP/WPI; lanes 4 and 7, sediment from HP/WPI. AS, acidic subunit; BS, basic subunit; β-lg, β-lactoglobulin.

### 7.3.3 Emulsifying ability of microparticulated versus non-microparticulated HP/WPI

The emulsifying ability of non-microparticulated and microparticulated HP/WPI was evaluated by determining the average droplet diameter ($d_{4,3}$) as a function of the protein concentration (**Fig. 7.3A**). For non-microparticulated HP/WPI stabilised emulsions (**Fig. 7.3A**: blue line with solid triangles), the droplet size decreased from ~1.8 μm to ~0.7 μm as protein concentration increased from 0.25% to 0.5%, with minimal change at higher concentrations (0.5% to 1.8%). The "true" droplet size, measured after mixing the emulsions in SDS buffer (**Fig. 7.3A**: blue line with open triangles), only reduced from ~0.7 μm at 0.25% protein concentration to ~0.5 μm at 0.5% protein concentration and kept steady at higher protein concentrations. The small difference between the droplet sizes of SDS-treated and untreated emulsions indicates that the flocculation was not significant, particularly at 0.5% to 1.8% protein concentrations.

In contrast, the emulsions made with microparticulated HP/WPI exhibited larger $d_{4,3}$ values (**Fig. 7.3A**: red line with solid squares). Droplet size initially decreased rapidly from 33.4 μm to 4.1 μm with an increase in protein concentration from 0.25% to 1%, then kept steady at 0.6 μm between 1.5% to 1.8% protein. Interestingly, although the microparticulated HP/WPI emulsion exhibited larger average sizes at low protein concentrations (0.25–0.5%), the "true" droplet size (in SDS; **Fig. 7.3A**: red line with open squares) was much smaller, reducing from ~2.4 μm at 0.25% protein concentration to ~1.2 μm at 0.5% protein. Moreover, the gap in droplet size between microparticulated HP/WPI emulsion with SDS (0.7 μm) and without SDS (4.1 μm) was narrowed at 1% protein. With further increasing protein concentrations (1.5–1.8%), the droplet sizes of microparticulated and non-microparticulated HP/WPI emulsion (with or without SDS) were very close at ~0.5–0.6 μm.

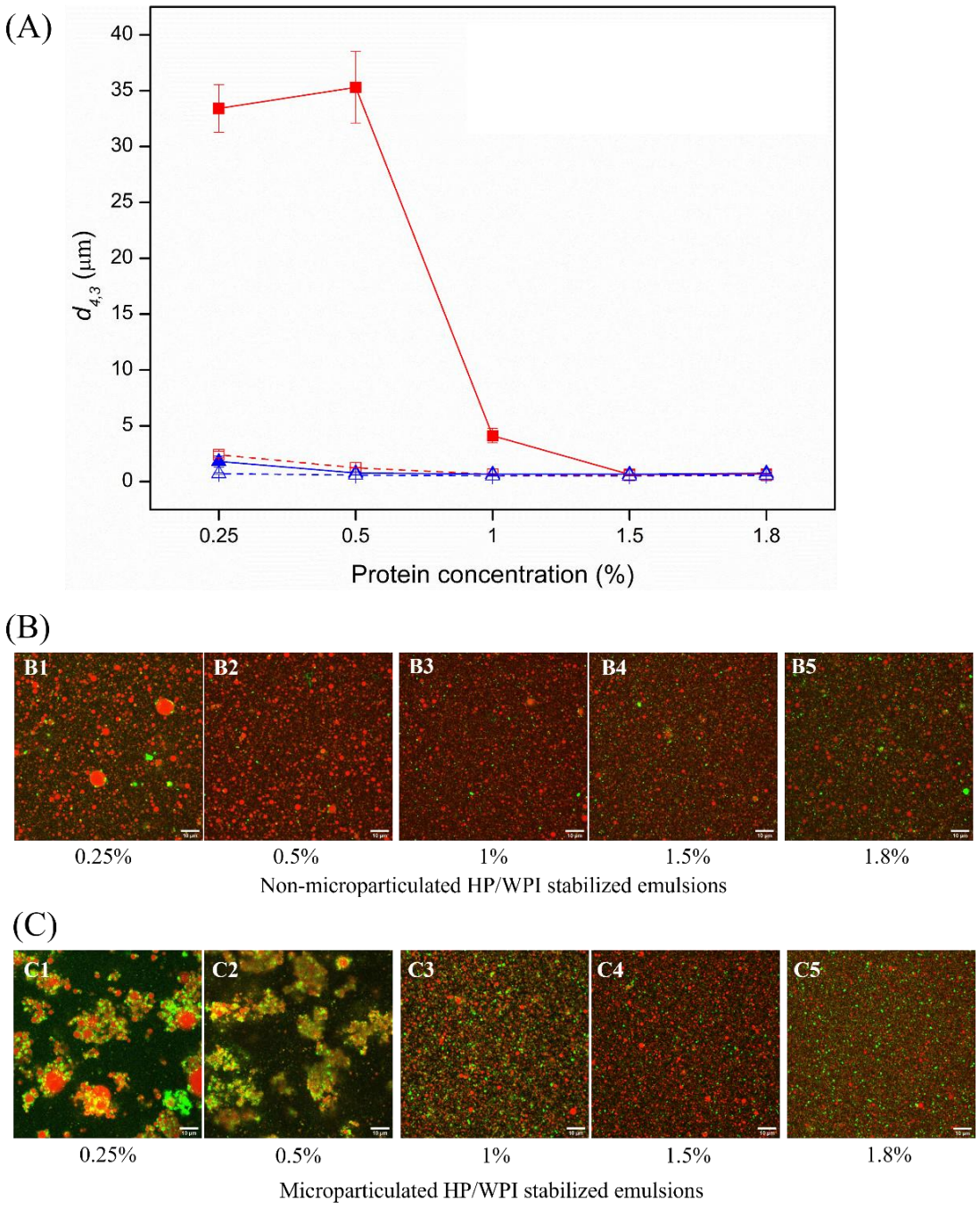


**Fig. 7.3.** Panel A, average droplet diameter ($d_{4,3}$) of non-microparticulated HP/WPI (▲,△) and microparticulated HP/WPI (■,□) stabilised emulsions as a function of the protein concentration, with (open symbols) and without (closed symbols) SDS. Panels B and C, CLSM images of non-microparticulated HP/WPI (B1–5) and microparticulated HP/WPI (C1–5) stabilised emulsions as a function of the protein concentration. The scale bar is 10 µm.

Although hemp protein generally has inferior emulsifying properties (Tang et al., 2006), typically 6–15 μm emulsion droplet size (Chen et al., 2023), the non-microparticulated HP/WPI mixture exhibited relatively good emulsifying properties with small droplet size, particularly at low protein concentrations. This could be attributed to the excellent emulsifying properties of whey proteins (Fan et al., 2021; Schröder et al., 2017), which may work as the main emulsifying ingredients in the protein mixture due to their preferential adsorption. In a mixed emulsifier system, the interfacial composition of droplets depends on the relative adsorption rates of the different types of emulsifiers (Dickinson, 1992). When multiple proteins are present, such as the mixed whey/other protein system, competition for adsorption sites can occur. For example, in pea/whey protein stabilised emulsions, a significant amount of pea protein was replaced by β-lactoglobulin (Hinderink et al., 2019; Hinderink, Sagis, et al., 2021). When both β-lg and egg ovalbumin participated in emulsification, β-lg dominated the interfacial composition, because of its higher interfacial activity (Dalgleish et al., 1991). In our study, whey proteins, due to their lower molecular mass compared with large HP particles, adsorbed more quickly than larger, more rigid hemp protein particles. This fast adsorption can lead to predomination in the interface, enhancing emulsion stability (McClements & Jafari, 2018).

The large differences between the emulsions with and without SDS suggest the existence of flocculation in microparticulated HP/WPI stabilised emulsions. The droplet size obtained is affected by two factors: droplet breakage during homogenisation and droplet coalescence after homogenisation (Schröder et al., 2017). In the 'emulsifier-poor' regime, where the microparticulated HP/WPI was insufficient to stabilise the newly created surface of emulsion droplets, and the final droplet size was strongly related to the droplet-droplet coalescence of initially formed small droplets (not completely covered by

emulsifiers). Thus, resulting in large droplet size and strong flocculation (Schwenzfeier et al., 2013; Tcholakova et al., 2008).

Generally, depletion and bridging flocculation are two types of droplet-droplet interactions in biopolymer-stabilised emulsions (Dickinson, 2003). The protein concentration is critical because high concentrations could induce osmotic pressure imbalance and depletion flocculation (Hinderink et al., 2019). However, insufficient protein concentration in the system leads to bridging flocculation because the droplets' surface cannot be completely covered by proteins, and the same macromolecule adsorbs on multiple droplets, creating flocs (McClements, 2015). In our study, the flocculation phenomenon is likely driven by bridging flocculation. The extent of flocculation also depends on the particle size and flexibility; larger or more rigid particles (such as microparticulated HP/WPI) are less able to deform and wrap tightly around droplets, increasing the likelihood of droplets bridging.

However, at 1.5% protein concentration and above, the droplet size became relatively independent of protein concentration, which indicates the 'emulsifier-rich' regime (Tcholakova et al., 2008). In this regime, microparticulated HP/WPI was sufficient to stabilise the small, broken-up droplets during homogenisation. At these higher concentrations, the surface of newly formed oil droplets becomes fully saturated with HP/WPI particles, minimising uncovered patches that would otherwise lead to coalescence or bridging flocculation. Additionally, increased surface coverage leads to greater steric hindrance, which contributes to enhanced droplet stability and reduced aggregation.

In comparison, due to the presence of unbound whey protein molecules in the non-microparticulated HP/WPI, better emulsifying ability was observed at low protein concentrations, with droplet size becoming independent of protein concentration at levels

≥ 0.5%. This 'emulsifier-rich' behaviour at low protein concentration is consistent with reports showing that as little as 0.4% WPI is sufficient to stabilise emulsions (Schwenzfeier et al., 2013). This can be attributed to the rapid interfacial adsorption of WPI molecules, which are small, flexible, and possess strong surface activity. These characteristics allow them to rapidly diffuse and rearrange at the oil-water interface, forming an interfacial layer even at relatively low concentrations.

However, although whey protein had excellent emulsifying ability, when the microparticulated HP/WPI was sufficient (≥ 1.5% protein concentration), the emulsifying ability of microparticulated HP/WPI matched that of non-microparticulated HP/WPI, as droplet size was predominantly determined by the efficiency of droplet breakup during homogenisation (Tcholakova et al., 2008).

The microstructures of the emulsions stabilised by microparticulated and non-microparticulated HP/WPI were analysed by CLSM (**Fig. 7.3B, C**). For non-microparticulated HP/WPI stabilised emulsions (**Fig. 7.3B1–5**), as protein concentration increased, the droplet size became more uniform, averaging ~0.5 μm, which aligned with the particle size data. Similarly, in a mixed plant/milk protein system, X. Zhang et al. (2021) also reported that the addition of whey protein in soy protein facilitated the formation of emulsion with smaller and more uniform emulsion droplets. These CLSM images confirmed that in non-microparticulated HP/WPI stabilised emulsions, whey protein, being the main emulsifier with its low molecular weight and fast adsorption rate, exhibited a superior emulsifying ability. This allowed it to stabilise oil droplets effectively with minimal size variation once the protein concentration exceeded 0.5%.

In contrast, the microparticulated HP/WPI stabilised emulsions at 'emulsifier-poor' regime (0.25% to 0.5% protein concentrations) (**Fig. 7.3C1, C2**) had larger droplet size and

were extensively flocculated and formed clusters. This microstructure reflects a system undergoing bridging flocculation, where HP/WPI microparticles act as physical connectors across droplets due to incomplete surface coverage. As the available emulsifiers were insufficient to saturate the newly formed oil–water interface, droplets became interconnected via shared particles. It has been reported that bridging flocculation was observed in low protein/oil ratio sodium caseinate stabilised emulsions by sharing of emulsifiers between droplets (Dickinson et al., 1997).

In contrast, at higher protein concentrations (≥ 1.5%), sufficient microparticulated HP/WPI was available to saturate the droplet surfaces. As a result, CLSM images showed well-dispersed, individual droplets below 1 μm in diameter, consistent with the particle size measurements. This transition from flocculated to uniform emulsions with increasing protein concentration highlights the critical role of protein concentration and surface coverage in determining emulsion microstructure and stability.

### 7.3.4 Adsorbed protein on emulsion surface

To help reveal the interfacial properties of non-microparticulated and microparticulated HP/WPI stabilised emulsions, the surface protein concentrations are measured (**Fig. 7.4**). For all emulsions, surface protein load increased with total protein concentration. However, the extent of increase was much greater for microparticulated HP/WPI stabilised emulsions than for non-microparticulated ones. It has been reported that 1.5 mg/m$^2$ whey protein was sufficient to provide monolayer coverage for 20% oil emulsion droplets (Hunt & Dalgleish, 1994). In this study, whey protein likely adsorbed preferentially onto the droplet surface, and the available whey protein was sufficient to

cover the surface. As a result, the further increase in protein concentration only marginally increased the surface protein adsorption.

In contrast, microparticulated HP/WPI emulsions exhibited much higher surface protein load, rapidly increased from ~1 mg/m$^2$ to ~5 mg/m$^2$ at the 'emulsifier-poor' regime (0.25–1% protein concentration), then slightly decreased to ~4.5 mg/m$^2$ at the 'emulsifier-rich' regime (**Fig. 7.4**). The large particles in microparticulated HP/WPI dispersion compared with protein molecules in non-microparticulated HP/WPI dispersion contributed to the higher surface protein load. In particle-stabilised interfaces, the surface load (mg/m$^2$) is generally much higher than in emulsions stabilised by conventional emulsifiers (Berton-Carabin & Schroen, 2015). The high surface load is likely to contribute to a protective shell that could help protect droplets from coalescence (Yan et al., 2020).

It should be noted that the surface protein concentration depends on both total adsorbed protein content and specific surface area (Zhao et al., 2015). In this study, the adsorbed protein kept increasing at 1.5% and 1.8% total protein concentration. Therefore, the slight decrease in the surface protein concentration may be attributed to a slight decrease in the droplet size, which means that more surface area was required to be covered.

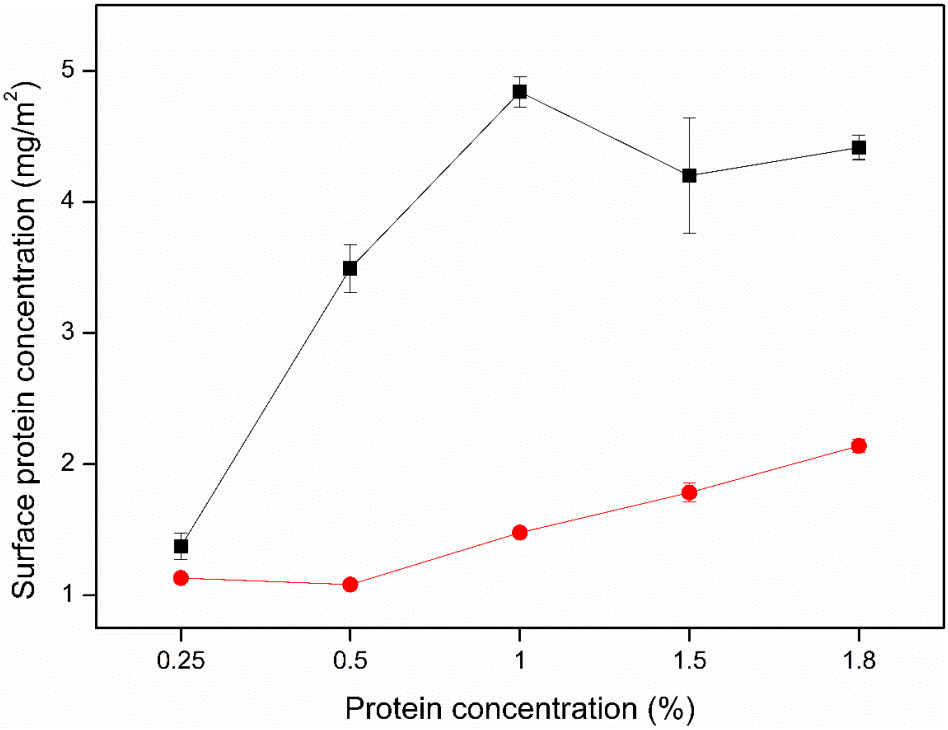


**Fig. 7.4.** Surface protein concentration of non-microparticulated (●) and microparticulated (■) HP/WPI stabilised emulsions as a function of the protein concentration.

### 7.3.5 Protein composition of the emulsion surface

To analyse the protein composition on the surface of emulsions, the SDS-PAGE (under reducing conditions) patterns of non-microparticulated HP/WPI and microparticulated HP/WPI dispersions and the adsorbed proteins in their corresponding emulsions were shown in **Fig. 7.5A and B.** As discussed in **Section 7.3.2**, the main predominant protein bands from HP and WPI, representing HP acidic subunit (AS), basic subunits (BS) and β-lg were marked in **Fig. 7.5**.

As can be seen, all major proteins (both HP and whey protein) participated in stabilising emulsions for all emulsions. However, compared with their dispersion, the non-microparticulated HP/WPI had a lower proportion of HP on the droplet surface (**Fig. 7.5A**), while the surface protein composition of microparticulated HP/WPI stabilised emulsion

was similar to its dispersion (**Fig. 7.5B**). This supports the hypothesis that in non-microparticulated HP/WPI, the whey protein molecules were preferentially adsorbed at the interface, compared with large HP particles. The preference adsorption of whey protein has also been reported by Ye (2008) that whey proteins adsorbed in preference to caseins at protein concentrations below 3%.

On the other hand, the proportion of interfacial HP in microparticulated HP/WPI was higher than that in non-microparticulated HP/WPI, suggesting that the adsorption of HP on emulsification was increased by the microparticulation process. These HP/WPI microparticles adsorbed at the interface as a hybrid protein complex, which eliminated the effect of preferential adsorption of whey proteins.

To obtain a better understanding of the adsorbed protein composition, the change of individual proteins was determined using densitometric analysis (**Fig. 7.5C and D**). The proportions of β-lg, HP AS and HP BS in both non-microparticulated HP/WPI and microparticulated HP/WPI dispersion were similar, at about 40%, 35% and 25%, respectively.

However, in non-microparticulated HP/WPI stabilised emulsions, the interface was dominated by β-lg (50–60%), which was higher than that in the original protein dispersion (**Fig. 7.5C**). Consequently, the proportions of HP AS and BS were lower than the original dispersion because of the preferential adsorption of whey protein. Interestingly, the effect of total protein concentration on the surface protein composition was minor. A possible explanation could be that there was sufficient protein to fully cover the droplets at low protein concentrations, hence the adsorbed protein composition did not significantly change when the protein concentration was increased. This is supported by the surface loading did not markedly change across different protein concentrations (**Fig. 7.4**).

On the contrary, the interface of microparticulated HP/WPI stabilised emulsion was dominated by both β-lg and HP (AS and BS) at all tested protein concentrations (**Fig. 7.5D**). The surface protein composition at the 'emulsifier-rich' regime (1.5–1.8%) was similar to the major constituents in the starting HP/WPI microparticle dispersion. It is possible that the complexation of two proteins results in co-adsorption as a group, leading to the same ratio of protein on the surface as in the aqueous phase.

Overall, non-microparticulated HP/WPI and microparticulated HP/WPI exhibited different adsorption behaviour. The latter can increase the HP loading on the emulsion, which improves total protein loading and the utilisation of HP.

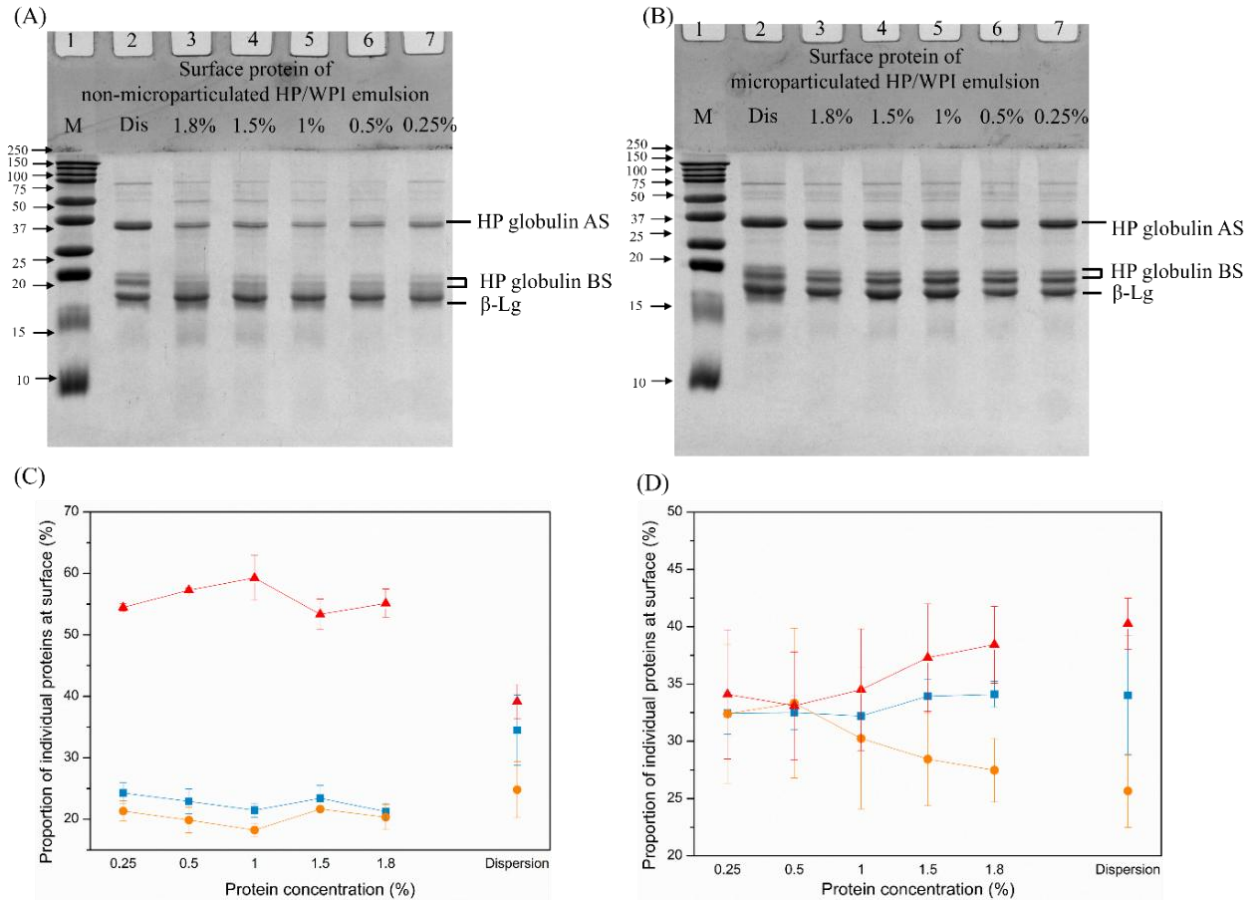


**Fig. 7.5.** SDS-PAGE under reducing conditions of surface proteins of (A) non-microparticulated HP/WPI and (B) microparticulated HP/WPI stabilised emulsions. Lane 1, marker; lane 2, HP/WPI dispersion (Dis); lanes 3–7, surface proteins of emulsions at 1.8–0.25% protein concentrations (AS, acidic subunit; BS, basic subunits; β-lg, β-lactoglobulin). Panels C and D show proportions (%) of HP acidic subunit (■), HP basic subunits (●) and β-lactoglobulin (▲) at the surface of non-microparticulated HP/WPI and microparticulated HP/WPI stabilised emulsions, respectively, as a function of the protein concentration.

### 7.3.6 Microstructure of emulsion surface

The morphology of microparticulated HP/WPI and non-microparticulated HP/WPI stabilised emulsions was analysed by transmission electron microscopy (TEM) (**Fig. 7.6**). As can be seen, most HP/WPI microparticles were well dispersed around the surface of the droplet at both 'emulsifier-rich' regime (1.5% protein) (**Fig. 7.6A**) and 'emulsifier-poor' regime (0.5% protein) (**Fig. 7.6B**). However, the surface coverage by the particles seems to be somewhat incomplete. Sarkar et al. (2016) also reported the incomplete coverage of whey protein microgel particle stabilised Pickering emulsions. It is well known that it is not necessary for coverage by particles to be complete to produce stable Pickering emulsions, as long as the adsorbed particle layer forms a rigid interface (Sarkar et al., 2016; Yusoff & Murray, 2011).

However, a significant proportion of particles remained in the continuous phase (highlighted in red boxes, **Fig. 7.6**) of non-microparticulated HP/WPI stabilised emulsions at 1.5% protein (**Fig. 7.6C**) and 0.5% protein (**Fig. 7.6D**). This observation is in agreement with earlier discussion, where the preference adsorption of whey protein led to less loading of HP particles at the surface.

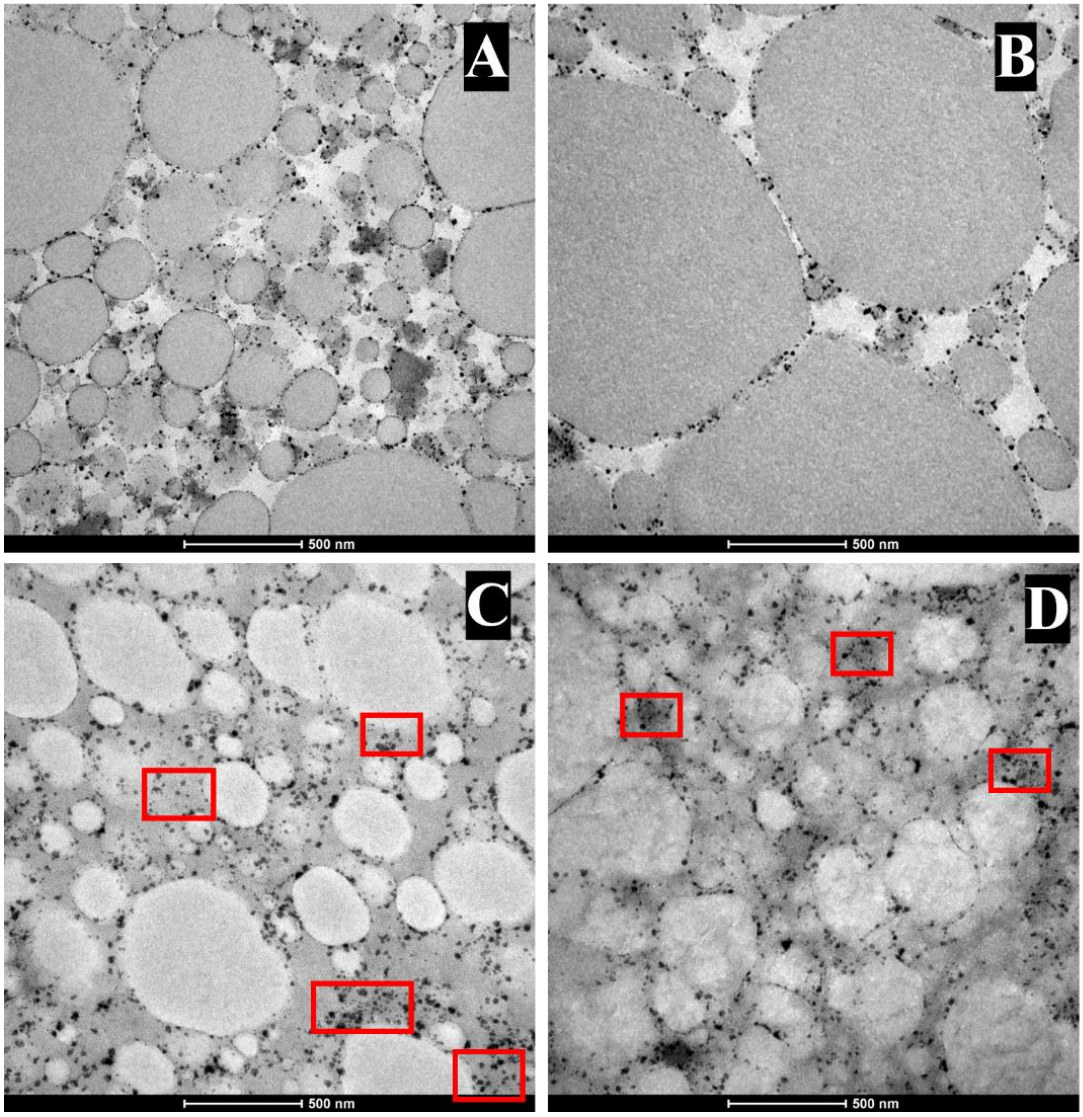


**Fig. 7.6.** Transmission electron microscopy of microparticulated HP/WPI stabilised emulsions at (A) 1.5% and (B) 0.5% protein concentrations and non-microparticulated HP/WPI stabilised emulsions at (C) 1.5% and (D) 0.5% protein concentrations. Red boxes highlight particles remaining in the continuous phase. The scale bar is 500 nm.

### 7.3.7 Heat stability of emulsions

The thermal stability of emulsions was evaluated by heating at different temperatures (60, 70, 80 and 90 °C) for 20 min. Only those emulsions with protein concentration ≥ 1% were tested because microparticulated HP/WPI at these concentrations produced emulsions with droplet sizes comparable with those of non-microparticulated HP/WPI that were considered physically stable (i.e., minimal aggregation).

As shown in **Fig. 7.7A**, there was a minor change in droplet size of non-microparticulated HP/WPI stabilised emulsions when heated at 60 °C. At 1% protein concentration, a negligible droplet size increase was observed when the temperature reached 90 °C. However, at higher protein concentrations (1.5% and 1.8%), droplet size slightly increased at 70 °C, followed by a substantial increase when the heating temperature reached 80 °C and 90 °C. The aggregation behaviour was visually confirmed in **Fig. 7.7C**, where a coagulation was observed for the 1.8% protein emulsion heated at 90 °C, as evidenced by settling at the bottom of the test tube when inverted.

In contrast, microparticulated HP/WPI emulsions showed significantly improved heat stability. As seen in **Fig. 7.7B**, the droplet size remained stable across all tested temperatures. Moreover, the influence of protein concentration on heat-induced aggregation was negligible. This improvement was visually supported by **Fig. 7.7D**, where the emulsion treated at the highest protein concentration and temperature (1.8% protein; 90 °C) retained fluid-like properties, still flowing when the test tube was inverted.

The droplet-droplet and protein-protein interactions would have an impact on the heat stability of emulsions (Liang et al., 2017). Without microparticulation, both HP and whey proteins remain heat sensitive. Therefore, it is expected that non-microparticulated HP/WPI stabilised emulsions exhibited thermal instability. It has been previously described

that irreversible β-lg aggregates start being formed above 70 °C (Boland, 2011). Sava et al. (2005) demonstrated that β-lg unfolds at 70 °C to 75 °C and consequently aggregates at 78 °C to 82.5 °C. In this study, a higher heating temperature (70 °C to 80 °C) facilitated that adsorbed protein interacted with other proteins, leading to the bridging of droplets.

Simultaneously, denaturation and structural rearrangement of non-adsorbed proteins resulted in exposure of the reactive groups, which could also induce their interactions with other non-adsorbed and adsorbed proteins in the aqueous phase (Allahdad et al., 2023). At 90 °C (close to the denaturation temperature of HP), HP also contributed to protein aggregation, which strengthened droplet and protein network formation. Similar temperature-dependent aggregation behaviour has been reported in soy protein stabilised emulsions, with more pronounced effects at 95 °C compared with 75 °C (Keerati-u-rai & Corredig, 2009).

Protein concentration also plays a crucial role in the heat-induced aggregation of emulsion. Heating hardly induced any aggregation when protein concentration was relatively low (1%) due to less non-adsorbed protein in the continuous phase. It was found that whey protein stabilised emulsions exhibited more extensive aggregation at 3% protein but showed no significant size change at 1.5% between 55 °C and 95 °C heat treatment, because of the reduced level of non-adsorbed protein (Sliwinski et al., 2003).

On the other hand, the thermal resilience of emulsions stabilised by microparticulated HP/WPI highlights the protective role of hybrid protein microparticles. As shown in our previous study (Ma, Ye, et al., 2024), the complexation between HP and whey proteins promoted the interactions among the reactive groups, such as hydrophobic and free thiol groups, leading to thermally stable HP/WPI microparticles. Results obtained in the current study suggest that heat-stable HP/WPI microparticles have the ability to form

emulsions that are heat resistant. In addition, our results are in agreement with previous studies on microparticulated whey protein stabilised emulsions, where those formed with up to 8% protein were found to be heat-stable (Çakır-Fuller, 2015). Preheating of proteins under controlled conditions can reduce the number of active sites available on protein particles to interact, inhibiting heat-induced aggregation (W. Ma et al., 2020).

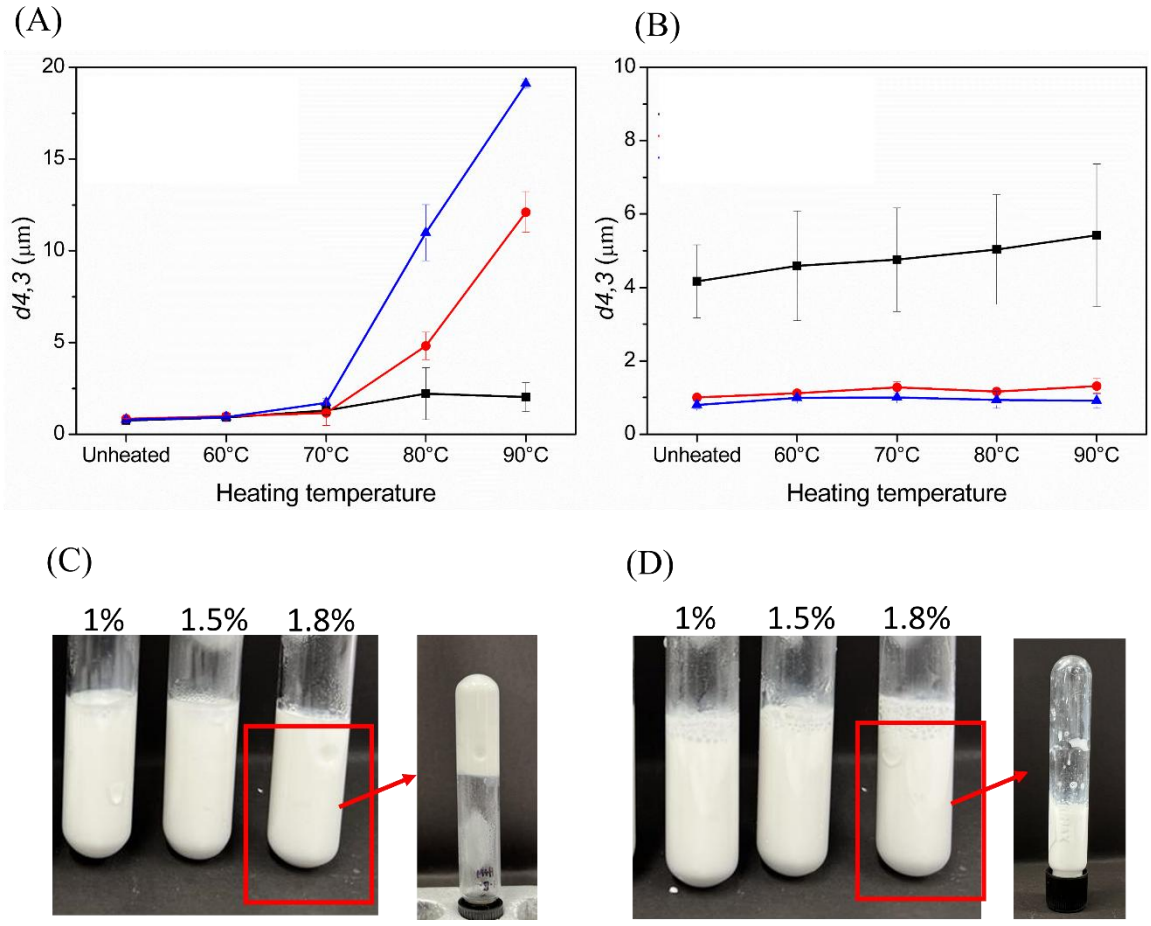


**Fig. 7.7.** Average droplet diameter ($d_{4,3}$) of (A) non-microparticulated HP/WPI and (B) microparticulated HP/WPI stabilised emulsions (■, 1%; ●, 1.5%; ▲, 1.8%) before and after heating at 60, 70, 80 and 90 °C for 20 min. Panels C and D show the visual appearance of emulsions stabilised by non-microparticulated HP/WPI and microparticulated HP/WPI, respectively, after heating at 90 °C and sitting for 20 min.

## 7.4 Conclusions

This study demonstrates the significant influence of microparticulation on the stabilisation of HP/WPI emulsions, particularly under varying protein concentrations. Non-microparticulated HP/WPI stabilised emulsions exhibited small droplet size with good stability at low protein concentrations, where whey protein dominated the interfacial layer. However, HP adsorption was limited in non-microparticulated systems due to whey protein's preferential adsorption at the droplet interface. On the other hand, the microparticulation process improved HP adsorption at the interface, allowing the formation of protective particle layers that contributed to the integrity of the droplets. When the microparticulated HP/WPI was sufficient (≥ 1.5% protein), a stable emulsion could be made with a similar droplet size as that of non-microparticulated HP/WPI. Moreover, microparticulation of HP/WPI markedly enhanced the heat stability of protein-stabilised emulsions compared with their non-microparticulated counterparts. This improved thermal resistance is attributed to the prior interaction and structural rearrangement during microparticle formation, which minimises further aggregation upon heating. The findings suggest that the microparticulation of HP/WPI systems offers a promising strategy for enhancing HP utilisation in emulsions and thermally processed food systems requiring enhanced stability. Future research should focus on optimising the microparticulation process and further exploring the potential applications of these hybrid protein systems in food formulations.

MASSEY UNIVERSITY
TE KUNENGA KI PŪREHUROA
UNIVERSITY OF NEW ZEALAND

GRADUATE RESEARCH SCHOOL

# STATEMENT OF CONTRIBUTION
# DOCTORATE WITH PUBLICATIONS/MANUSCRIPTS

We, the student and the student's main supervisor, certify that all co-authors have consented to their work being included in the thesis and they have accepted the student's contribution as indicated below in the Statement of Originality.

| | |
|---|---|
| Student name: | Sihan Ma |
| Name and title of main supervisor: | Dr Alejandra Acevedo-Fani |
| In which chapter is the manuscript/published work? | Chapter 8 |

Describe the contribution that the student and members of the supervisory team have made to the manuscript/published work:[1]

Sihan Ma: Conceptualisation, Investigation, Methodology, Formal analysis, Data curation, Writing - original draft, Visualization.
Aiqian Ye: Methodology, Writing - review & editing, Supervision.
Harjinder Singh: Methodology, Writing - review & editing, Supervision, Funding acquisition.
Alejandra Acevedo-Fani: Conceptualisation, Supervision, Methodology, Validation, Resources, Writing - review & editing.

Please select one of the following three options:

| | |
|---|---|
| ○ | The manuscript/published work is published or in press<br>Please provide the full reference of the research output: |
| ○ | The manuscript is currently under review for publication<br>Please provide the name of the journal: |
| ◉ | It is intended that the manuscript will be published, but it has not yet been submitted to a journal |

| | | | |
|---|---|---|---|
| Student's signature: | Sihan Ma<br>Digitally signed by Sihan Ma<br>DN: cn=Sihan Ma, c=NZ, email=s.ma@massey.ac.nz<br>Date: 2025.07.18 13:58:34 +12'00' | Main supervisor's signature: | Alejandra Acevedo Fani<br>Digitally signed by Alejandra Acevedo Fani<br>DN: cn=Alejandra Acevedo Fani, c=NZ, o=Massey University, ou=Riddet Institute, email=a.acevedo-fani@massey.ac.nz<br>Date: 2025.07.31 07:49:46 +12'00' |

*This form should be placed at the beginning of each relevant thesis chapter.*

[1] Refer to the Massey University Publishing and Authorship guidelines (OneMassey for staff, Stream for students) and/ or Contributor Roles Taxonomy (CRediT) guidelines for guidance.

# Chapter 8: High internal phase emulsion stabilised by hemp/whey protein particles: rheological properties and heat stability

## Abstract

Hemp (*Cannabis sativa* L.) protein has garnered increasing attention, but its applications are limited due to its poor functionality, including weak emulsifying properties and thermal stability. In this study, hybrid microparticles were developed by complexing HP and whey protein isolate (WPI) via the microparticulation method, enabling the successful formation of high internal phase emulsions (HIPEs). The rheological behaviour and thermal stability of HP/WPI HIPEs were investigated and compared to HIPEs stabilised by a HP and WPI mixture (HP+WPI) or their individual proteins (HP and WPI).

Viscosity and small amplitude oscillatory shear (SAOS) measurements demonstrated that all HIPEs exhibited solid-like behaviour at low strain amplitudes, with HP/WPI-stabilised HIPEs showing higher viscosity and storage modulus ($G'$), indicating a stronger internal network compared to HP and WPI-stabilised HIPEs. Large amplitude oscillatory shear (LAOS) analysis revealed that all HIPEs exhibited an initial linear viscoelastic response, followed by intracycle strain stiffening at higher strain amplitudes. HP/WPI and HP+WPI HIPEs demonstrated greater structural rigidity and resistance to deformation compared to WPI HIPEs. These findings were also confirmed by confocal laser scanning microscopy (CLSM) observations.

In the heat stability test, HP/WPI HIPEs maintained their viscosity and droplet size after thermal treatment at 95 °C for 20 min, while HP and HP+WPI HIPEs exhibited a significant increase, indicating heat-induced droplet aggregation. CLSM confirmed these

findings, showing extensive flocculation and coalescence in HP and HP+WPI HIPEs, whereas HP/WPI HIPEs remained structurally stable.

The enhanced rheological and thermal stability of HP/WPI HIPEs was attributed to microparticulation, which promoted interprotein interactions in protein microparticles and minimised heat-induced droplet flocculation and protein aggregation. These findings suggest that microparticulated HP/WPI can serve as an effective emulsifier for thermally stable food-grade HIPEs, offering the potential for plant-milk hybrid emulsions with improved functional properties.

## 8.1 Introduction

High internal phase emulsions (HIPEs) are highly concentrated emulsion systems, characterised by a high dispersed phase volume fraction ($\phi$ > 74%) (Kim et al., 2017). HIPEs offer superior stability against separation, aggregation and Ostwald ripening (McClements & Gumus, 2016). Recently, the growing demand for "clean-label" and "surfactant-free" foods has increased interest in biopolymer-based particles as alternatives to the traditional inorganic particles and synthetic surfactants (e.g., silica and Tweens) (Hu et al., 2016; Huang et al., 2019). Instead of surfactants, these emulsions are stabilised by solid particles, forming what is known as Pickering emulsions. The adsorption of particles at the interface requires high energy for removal, leading to strong resistance to coalescence (Binks, 2002).

Several studies have demonstrated that HIPEs can be prepared using low concentrations of particles. Wang et al. (2020) and Xu et al. (2019) successfully formulated highly concentrated emulsions (80% oil) using 1% starch particles and 0.2-1% soy protein particles, respectively. These studies also suggest that HIPEs have the potential for

applications in the area of encapsulation, controlled release and texture modification (Wang et al., 2020; Wei et al., 2019; Wijaya et al., 2017; Yang et al., 2020). One particularly interesting property of HIPEs is their tunable rheological properties, which depend on composition, including types of emulsifiers and volume of internal phase (Kim & Mason, 2017). The HIPEs were used as a novel route to transform liquid oils into solid-like emulsion gels (Hu et al., 2016). Therefore, exploring effective biopolymer-based particles for HIPE stabilisation is crucial for advancing their food applications.

Some protein-based particles have been shown to act as effective particle emulsifiers. Examples include whey protein (Zamani et al., 2018), soy protein (Xu et al., 2019), peanut protein particles (Jiao et al., 2018) and gliadin colloidal particles (Hu et al., 2016). To date, plant proteins are more commonly utilised in HIPEs than animal proteins (Abdullah et al., 2020). Various techniques have been used to prepare and strengthen the functionality of protein particles: e.g., centrifugation (Li et al., 2020), ultrasonification (Gao et al., 2014), pH adjustment (Xu et al., 2019), cross-linking (Dhayal et al., 2014; Wu et al., 2015), heat treatment (Liu & Tang, 2013; Su et al., 2018) and antisolvent precipitation (Hu et al., 2016). However, it is still a challenge to produce colloid particles which are effective in emulsifying performance (Dickinson, 2012). Some HIPEs may only exhibit stability under specific pH conditions (de Folter et al., 2012) or require excess protein particles in the continuous phase (Gao et al., 2014), which restricts their practical applications. Hence, selecting the appropriate methods to prepare protein particles for different types of proteins is essential.

The hemp protein (HP), derived from hemp seeds, has gained increasing attention due to its nutritional value, excellent digestibility, and balanced amino acid profile (Wang & Xiong, 2019). However, its poor water solubility limits its food functional performance (Dapčević-Hadnađev et al., 2019; Tang et al., 2006). Tang et al. (2006) reported that hemp

protein-stabilised emulsions had a lower emulsifying activity index and emulsifying stability index compared with those stabilised by soy protein. Limited studies have been done to improve the emulsifying properties of hemp protein. Q. Wang, Y. Jin, et al. (2018) studied high alkaline (pH 12)/thermal treatment to improve the solubility and emulsifying activity of hemp protein isolate. Other studies reported HP/ polysaccharides (pectin, carrageenan, alginate, and gum arabic) complexation at low pH (Y. Feng et al., 2021; Gholivand et al., 2024). However, the neutralisation of pH after processing may cause re-aggregation of hemp protein (Chuang et al., 2021).

One interesting approach for producing dispersible protein particles is the complexation of plant and milk proteins (Alves & Tavares, 2019). Previous studies have shown that heat-induced interaction and complexation of soy or pea protein with whey protein (Anuradha & Prakash, 2009; Chihi et al., 2016; Roesch & Corredig, 2005) lead to smaller hybrid aggregates than plant protein alone, which may offer the potential for emulsion stabilisation. Our previous study successfully developed hemp protein/whey protein isolate (HP/WPI) microparticles using the microparticulation method by heat-induced interaction at controlled pH and followed by size reduction (Ma et al., 2025). These hybrid particles effectively stabilised a 10% oil-in-water emulsion. The microparticulation of HP/WPI represents a new possible strategy for enhancing the functional properties of HP in food emulsions.

Limited studies have been carried out on the HIPEs stabilised by hybrid protein particles (Abdullah et al., 2020). The only reported study on this topic produced HP/sodium caseinate (HP/NaCas) particles via the pH-cycling method and used them to stabilise a high-oil-content (70%) emulsion (Chuang et al., 2020). However, considering the high level of free thiol content in HP, the protein aggregates formed above the denaturation temperature (92 °C) (Tang et al., 2006) may compromise emulsion stability. Thus, it

remains a challenge to improve the thermal stability of HIPEs for heat processing purposes. Microparticulation is a promising method that involves controlled thermal treatment during processing, which has the potential to enhance the heat stability of protein particles and the emulsions they stabilise (Ipsen, 2017; Shi et al., 2021). Previous studies have demonstrated that microparticulated whey protein emulsions (Çakır-Fuller, 2015) and heat-stable soy protein particle emulsions (W. Ma et al., 2020) exhibited enhanced heat stability compared to their native protein emulsions. These findings suggest that HP/WPI microparticles may improve the thermal stability of the emulsion.

To further investigate the effect of microparticulation on HP/WPI and the potential of the HP/WPI hybrid microparticles as an emulsifier for HIPEs, we developed the HP/WPI microparticle-stabilised HIPEs and analysed their structural, rheological properties and thermal stability in comparison to HP + WPI mixture or their individual proteins (HP particle and WPI) stabilised HIPEs.

## 8.2 Materials and methods

### 8.2.1 Materials

Whey protein isolate (WPI) containing 92.0% protein, 0.9% fat, 1.6 % ash and 5.2% moisture was purchased from Fonterra Co-operative Group Limited, Auckland, New Zealand. The hempseed protein (HP) concentrate powder was purchased from Davis Food Ingredients (Davis Trading Company Ltd., Palmerston North, New Zealand). The HP powder contained 59.8% protein, 2.4% fat, 10.7% ash, 6.8% moisture and 20.2% carbohydrate. The proximate composition of both protein ingredients was analysed as follows: protein content was determined using the Kjeldahl method (AOAC 991.20, nitrogen factor 5.21); fat, ash and moisture content were determined according to AOAC

922.06, AOAC 942.05 and AOAC 925.10, respectively; and carbohydrate content was calculated by subtracting the sum of the protein, ash and fat from the total solid. All chemicals were purchased from Sigma-Aldrich Ltd. (St. Louis, MO, USA), and the reagents were made up in Milli-Q water (Milli-Q apparatus; Millipore Corp., Bedford, MA, USA).

### 8.2.2 Preparation of HP/WPI microparticles

A dispersion of HP was prepared by mixing HP powder in Milli-Q water at 3% (w/w) protein concentration and stirring for 2 h at 20 °C. The pH was adjusted to 11, using 1 M NaOH, followed by 2 h stirring. The HP dispersion was centrifuged (3000 × *g*, 30 min) to remove insoluble material (such as insoluble fibre). The resulting supernatant (mostly containing HP) was collected and adjusted to pH 8 using 1 M HCl. The dispersion was then processed by passing 2 times through a two-stage valve homogeniser (APV 1000, SPX, Silkeborg, Denmark) at 300 bar (first stage)/50 bar (second stage) to produce HP particles, which served as the HP dispersion used in the subsequent steps.

Stock solutions of WPI were prepared by dissolving 5% (w/w) protein in Milli-Q water with magnetic stirring for 2 h. The pH of the WPI solution was adjusted to pH 8 using 1 M NaOH before being mixed with HP dispersion to achieve a final protein concentration in the mixture at 1% HP and 1% WPI (w/w). The pH of the protein mixtures was checked and adjusted to pH 8 as necessary, followed by heating at 95 °C for 30 min in the water bath. After the heat treatment, the samples were cooled down in ice to 20 °C, and the pH was adjusted to pH 7 using 1 M HCl. The dispersion was then processed by passing 2 times through a two-stage valve homogeniser at 300 bar (first stage)/50 bar (second stage) to produce the HP/WPI microparticles. The water was evaporated to achieve 4% protein

concentration at 40 °C and 500 rpm using rotary evaporation (Rotavapor R-124, Buchi, Switzerland).

### 8.2.3 Preparation of high internal phase emulsions

High internal phase emulsions (HIPEs) were prepared by using four different emulsifying materials: HP/WPI microparticles, dispersion of non-microparticulated HP+WPI mixture (HP+WPI) in a 1:1 ratio, HP dispersion and WPI solution. Soybean oil and aqueous protein dispersion (1%, 2% and 4% of protein) were mixed in containers at a volume ratio of 75:25. The HIPEs were then prepared using a benchtop Ultra-Turrax mixer (Wilmington, NC, USA) at 13,500 rev $min^{-1}$ for 2 min at room temperature. Sodium azide (0.02%, w/w) was added to inhibit microbial growth.

### 8.2.4 Droplet size analysis

The droplet size of the HP/WPI emulsion was measured by static light scattering using a Mastersizer 2000 and a Hydro MU unit (Malvern Instruments, Worcestershire, UK). The refractive index was 1.47 for oil and 1.33 for water. The data were reported in volume-weighted mean diameter $d_{(4,3)}$, calculated as the average of triplicate measurements.

### 8.2.5 Confocal laser scanning microscopy (CLSM)

Confocal laser scanning microscopy (Model Zeiss LSM900 with Airyscan 2, Carl Zeiss, Jena, Germany) was used to investigate the microstructure of HIPEs using the staining protocols described by Gallier et al. (2012). Nile Red (1 mg/mL in acetone) and Fast Green FCF (1 mg/mL in Milli-Q water) were used to selectively stain neutral lipids and proteins, respectively. 100 μL sample was mixed with Nile Red (2:100, v/v) and Fast Green FCF (6:100, v/v). The stained emulsion sample was placed on a concave microscope

slide and covered by a coverslip (0.17 mm thick), avoiding an air bubble between the sample and the coverslip. The freshly prepared sample slide was immediately examined by CLSM with an oil immersion objective lens.

### 8.2.6 Rheological properties

The rheological properties of the emulsions were measured using a rheometer (Discovery HR-20 rheometer, TA Instruments, USA) equipped with a 2° cone-and-plate geometry (diameter 40 mm). The temperature was maintained at 20 °C. Emulsion samples were loaded, and the cone was lowered into position. The excess sample was carefully removed using a spatula.

#### 8.2.6.1 The shear viscosity experiment

The sample was first equilibrated for 1 min to allow the temperature to be stabilised. The shear viscosity of emulsions was characterised at the shear rate range of 0.1 – 300 $s^{-1}$. The apparent viscosity was recorded as a function of shear rate.

#### 8.2.6.2 The small amplitude oscillation shear (SAOS) measurements

SAOS behaviour was characterised through the frequency sweeps (0.1 – 100 Hz, 0.5% strain). Storage modulus ($G'$) and loss modulus ($G''$) as a function of frequency were calculated by Trios software (TA Instruments).

#### 8.2.6.3 The large amplitude oscillation shear (LAOS) measurements

The LAOS behaviour of HIPEs was examined through strain sweeps performed over a strain range of 0.1 – 1000% at a frequency of 1 Hz. The raw waveform data of stress

and strain signals were collected directly by Trios software in transient mode and analysed by the MITlaos program (MITlaos v2.2 Beta) based on MATLAB R2020b (MathWorks, USA) (Ewoldt et al., 2007). The Lisssajous-Bowditch plots were constructed based on the instantaneous stress signal.

Using the LAOs moduli, the strain-stiffening index (S) was calculated according to Equations 1 – 3. A positive S value indicates intracycle strain stiffening, a S value equal to 0 represents a linear elastic/viscous response, and a negative S value indicates intracycle strain softening.

$$G'_M = \sum_{n\ odd} nG'_n \quad \text{(Eq.8.1)}$$

$$G'_L = \sum_{n\ odd} G'_n\,(-1)^{(n-1)/2} \quad \text{(Eq.8.2)}$$

$$S = \frac{G'_L - G'_M}{G'_L} \quad \text{(Eq.8.3)}$$

where $G'_M$ and $G'_L$ represent the tangent modulus and secant modulus at the minimum strain and the maximum strain. $G'_n$ and $G''_n$ are the elastic and viscous Fourier coefficients calculated from the Fourier spectrum of the stress responses by the MITlaos program.

### 8.2.7 Heat stability test of emulsion

10 mL of emulsion was transferred into a glass tube and heated in a water bath at 95 °C for 20 min, followed by rapid cooling in ice to 20 °C. The droplet size, microstructure (using CLSM) and viscosity of the heated emulsions were analysed.

### 8.2.8 Data analysis

The results are reported as mean ± standard deviation. Statistical analysis was performed using SPSS software for Windows (version 29.0, SPSS Inc., Chicago, IL, USA). The data were analysed by independent t-tests between two groups, and one-way analysis

of variance (ANOVA) for multiple comparisons, using Duncan's test with the level of significance set at $P < 0.05$.

## 8.3 Results and discussion

### 8.3.1 Characterisation of HIPEs: influence of protein concentration

#### 8.3.1.1 Droplet size

To investigate the effect of protein emulsifier type and concentration, HIPEs were prepared using 4 different protein preparations (HP/WPI microparticles, HP particles, a mixture of HP particles and WPI (HP+WPI) and WPI solution), each at protein concentrations of 1%, 2% and 4%. The mixture of HP particles and WPI (HP+WPI) refers to the same HP particles and WPI blend (same protein ratio and concentration), but without undergoing any heat treatment. Thus, it represents the unstructured protein mixture before microparticle formation. The droplet size of all HIPEs was evaluated by determining the average droplet diameter ($d_{4,3}$) and their corresponding size distributions as a function of the protein concentrations (**Fig. 8.1**).

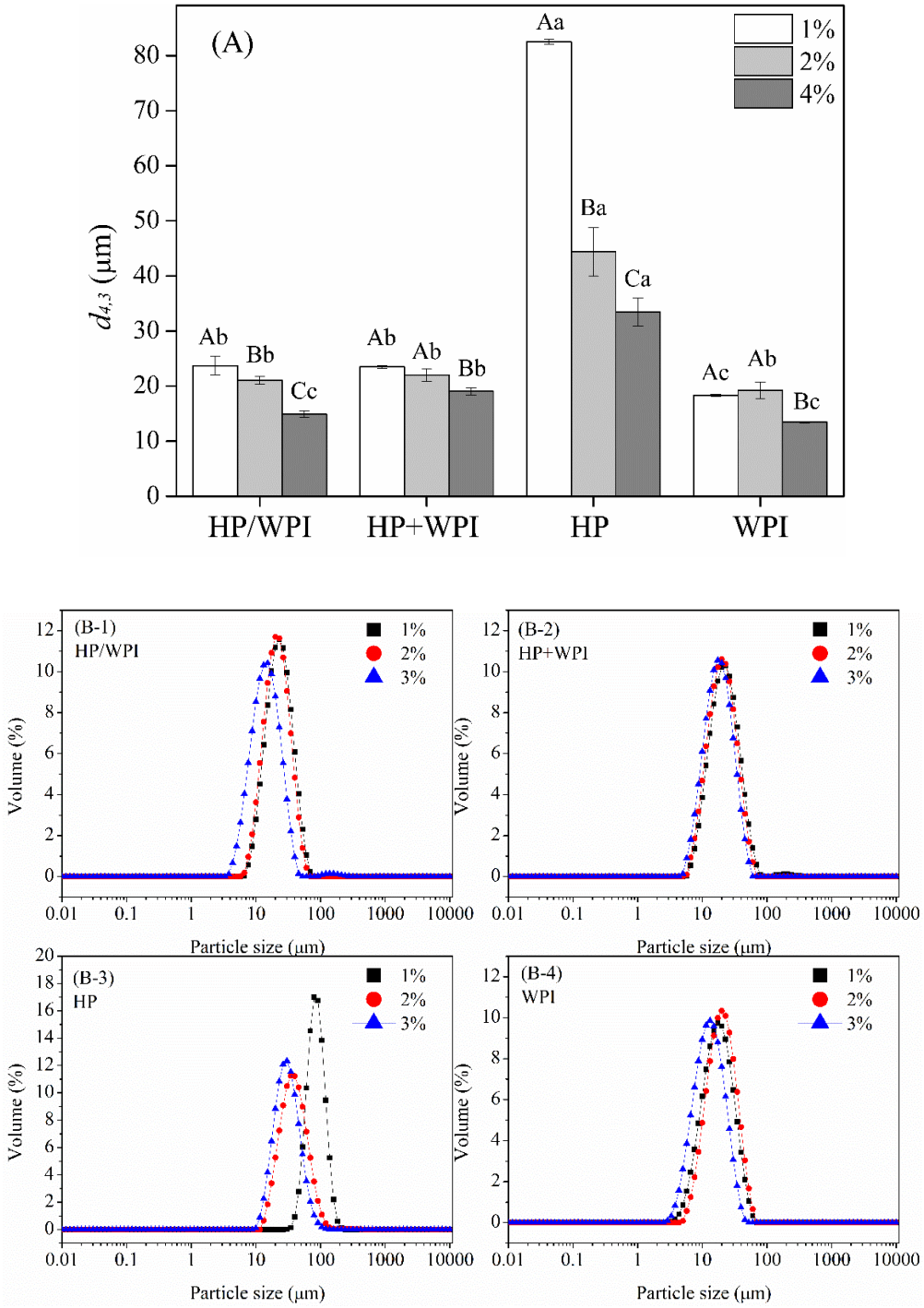


**Fig. 8.1.** Average droplet diameter (*d4,3*) (A) of HIPEs stabilised by HP/WPI, HP+WPI, HP and WPI at 1%, 2% and 4% aqueous phase protein concentrations, and their corresponding droplet size distributions (B 1 – 4). Different uppercase letters mean significant differences among HIPEs stabilised by the same protein emulsifier at different protein concentrations ($p < 0.05$). Different lowercase letters indicate significant differences among HIPEs stabilised by different protein emulsifiers at the same protein concentration ($p < 0.05$).

Generally, all HIPEs were successfully formed, regardless of the emulsifier type, and the average droplet size decreased with increasing protein concentration, though to varying extents (**Fig. 8.1A**). Specifically, the droplet size of HP/WPI HIPEs decreased from 23.76 μm to 14.9 μm. HIPEs stabilised by HP alone had the largest initial droplet size (82.5 μm), which dropped rapidly to 33.5 μm as protein concentration increased. In contrast, the droplet size of HIPEs made with HP+WPI and WPI decreased more gradually from 23.5 μm and 18.6 μm to 19.1 μm and 13.5 μm, respectively. Additionally, the monomodal size distributions were observed for all the HIPEs at all protein concentrations. As the concentration of protein increased, the shift of the size distribution of HIPEs aligned with the average droplet size trends (**Fig. 8.1B**).

The reduction in droplet size at higher protein concentrations can be attributed to the greater availability of proteins to cover newly formed oil surfaces during homogenisation, leading to smaller droplets (Hunter et al., 2008; Sun & Gunasekaran, 2009; Ye, 2008). The dependence on protein concentration has been observed in other studies, where droplet size of HIPEs decreased with increasing wheat gluten concentrations (X. Liu et al., 2018) and gliadin particles (Hu et al., 2016).

HP particles exhibited relatively inferior emulsifying properties, as evidenced by the consistently larger droplet size of HP-stabilised HIPEs at all protein concentrations, consistent with the findings of Tang et al. (2006). However, HP/WPI, HP+WPI and WPI demonstrated better emulsifying properties, which is consistent with our previous study (Ma et al., 2025).

WPI HIPEs had the smallest droplet size at all protein concentrations, likely attributed to the superior emulsifying properties of whey proteins (Schröder et al., 2017). Interestingly, despite the presence of HP, HP+WPI HIPEs exhibited similar droplet sizes

to those of HP/WPI HIPEs. This could be possible because the preferential adsorption of whey protein at the oil-water interface had a dominant effect on the droplet size. In mixed protein systems, such as whey/pea protein and β-lg/egg ovalbumin, competition for interfacial adsorption sites has been reported (Dalgleish et al., 1991; Hinderink et al., 2019; Hinderink, Sagis, et al., 2021). Our previous study also confirmed a higher amount of whey protein adsorption compared to HP in 10% oil HP+WPI emulsions (Ma et al., 2025).

#### 8.3.1.2 Visual appearance

The HIPEs showed an opaque and whitish appearance (**Fig. 8.2**). HP/WPI-stabilised HIPEs were stable and viscous at all protein concentrations. Notably, they displayed self-supporting, gel-like properties, as indicated by their retention at the bottom when the vials were inverted. As protein concentration increased, the HP/WPI HIPEs demonstrated greater structural integrity, spreading less and maintaining a more upright shape when placed on a Petri dish. The HIPEs stabilised by HP+WPI and HP had a similar appearance to those stabilised by HP/WPI.

Generally, as the internal phase volume fraction increases (typically > 74%), the closely packed and jammed droplets contribute to the viscoelastic, semi-solid characteristics of HIPEs (Li et al., 2019). Similar gel-like behaviour has been reported in other HIPEs stabilised by different particles, e.g., zein/casein (C. Sun et al., 2018), HP/casein (Chuang et al., 2020), gliadin (Hu et al., 2016) and soy protein (W. Ma et al., 2020).

In contrast to HP/WPI stabilised HIPEs, the WPI stabilised HIPEs had fluid-like behaviour. The viscoelastic properties of HIPEs can vary depending on the nature of the emulsifying particles (Gao et al., 2021). Different from particulate stabilisers, the molecular

form of whey protein has usually been used to prepare fluid HIPEs (Gao et al., 2021; Liu et al., 2019). The effect is likely due to their inability to form a rigid interfacial layer and interconnected protein network in the continuous phase at protein concentrations applied in this study.

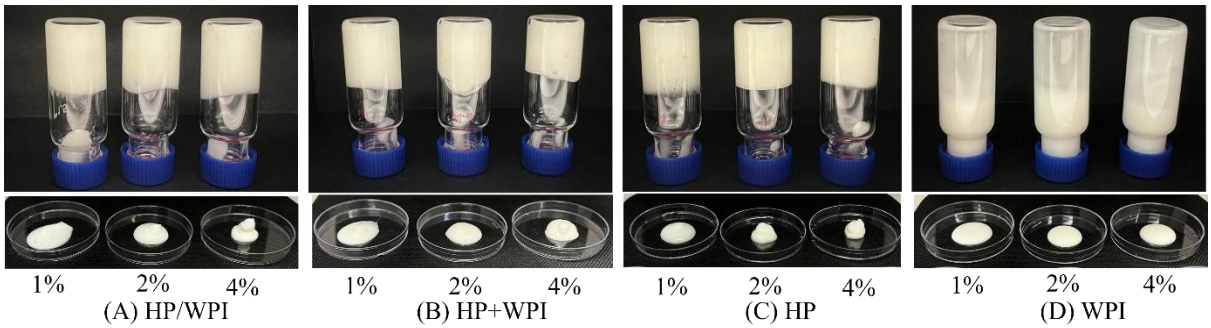


**Fig. 8.2.** Visual appearance of HIPEs stabilised by (A)HP/WPI, (B) HP+WPI, (C) HP and (D) WPI as a function of the protein concentration.

### 8.3.1.3 Microstructure (CLSM)

To gain deeper insight into the internal microstructure of the HIPEs, confocal laser scanning microscopy (CLSM) was used to visualise the emulsions, with proteins labelled in green and oil in red (**Fig. 8.3**). The CLSM images confirmed the droplet size trends observed in **Fig. 8.1**, showing a significant reduction in droplet size for HP/WPI and HP stabilised HIPEs with increasing protein concentration, while only a slight decrease was observed in HP+WPI and WPI HIPEs.

Distinct microstructural differences were evident among the HIPEs. In HP-stabilised HIPEs, HP particles were clearly visible on the droplet surfaces (**Fig. 8.3C**), forming a rigid interfacial layer. At higher protein concentrations, droplet connectivity became more pronounced. In contrast, no visible protein particles were observed in WPI

HIPEs (**Fig. 8.3D**), likely due to the molecular size of whey protein, which does not form distinct particulate structures.

In HP+WPI HIPEs, the presence of WPI resulted in smaller droplet sizes compared to individual HP stabilised HIPEs (**Fig. 8.3B**). HP particles were observed both on the interface and in the continuous phase, contributing to droplet connectivity. In HP/WPI HIPEs (**Fig. 8.3A**), microparticulation processing appeared to enhance protein particle participation. Similar to HP+WPI HIPEs, HP/WPI microparticles were observed in CLSM images, while there were more particles in the continuous phase, which led to an interconnected protein network.

These observations align with previous studies on hybrid protein-stabilised emulsions. For instance, in the HP/sodium caseinate (HP/NaCas) system (Chuang et al., 2020), the protein particles were visible on the surface of hybrid protein-stabilised emulsions, while individual caseinate was not observed in single caseinate emulsions. They also suggested that in a highly concentrated emulsion, structural features such as connected droplets and protein networks in the continuous phase contribute to gel-like properties. Similarly, X. Liu et al. (2018) reported a protein network in wheat gluten-stabilised HIPEs, where jammed droplets strongly interacted, enhancing gel strength.

To further understand the effect of the internal structure on the bulk structural properties of HIPEs, 2% HIPEs were selected for subsequent studies. This selection minimises the influence of droplet size variations, as no significant difference was observed among these HIPEs, except for HP HIPEs (**Fig. 8.1**).

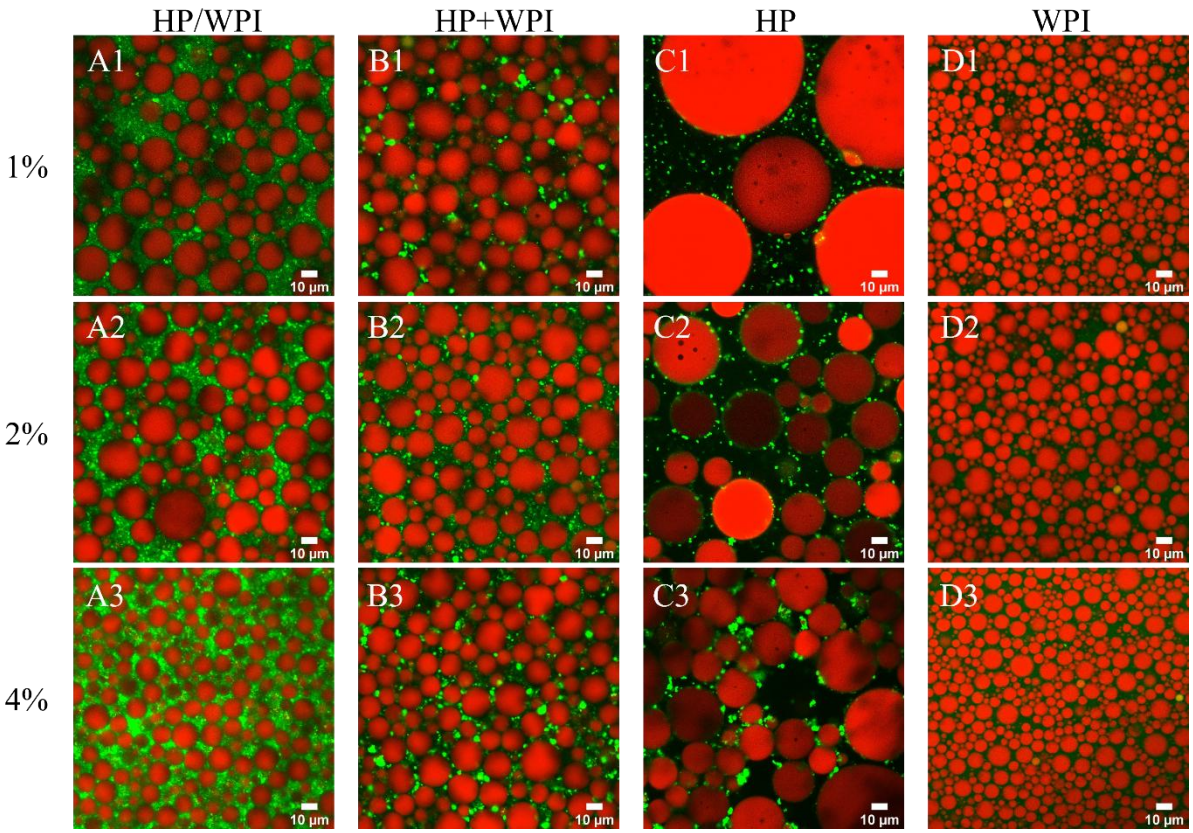


**Fig. 8.3.** CLSM images of HIPEs stabilised by (A)HP/WPI, (B) HP+WPI, (C) HP and (D) WPI as a function of the protein concentration. The scale bar is 10 µm.

### 8.3.2 Rheological properties of HIPEs

The rheological properties of HIPEs were determined using rheometry to explore the internal structure and interaction between droplets in the emulsions (Li et al., 2023).

#### 8.3.2.1 Viscosity

All HIPEs exhibited non-Newtonian shear-thinning behaviour over the shear rate range of 0.1-300 $s^{-1}$ (**Fig. 8.4**). This behaviour is in agreement with other studies on highly concentrated emulsions, e.g., HP/NaCas (Chuang et al., 2020), WPI (Li et al., 2023) and zein/CNC (Cui et al., 2025).

In concentrated emulsions, the shear-thinning behaviour is typically attributed to the transition from aggregated to dissociated droplet structures under shear stress (Manoi & Rizvi, 2009). At low shear rates, the close proximity of droplets facilitates strong interactions, leading to the formation of interconnected droplet aggregates. In addition, the protein particles on the droplet surface or in the continuous phase could also enhance network formation (Keerati-u-rai & Corredig, 2009). This internal structure could still be held when the shear rate was low, resulting in high viscosity. However, as the shear rate increases, the network of aggregated droplets could be deformed and dissociated into individual droplets, leading to lower viscosity.

Among the HIPEs, HP/WPI stabilised HIPEs had the highest viscosity than the other emulsions at a given shear rate, while WPI stabilised HIPEs had the lowest viscosity, which may be attributed to the stronger network structures and densely packed interfacial layer provided by HP/WPI microparticles, as a greater proportion of protein was presented in the particulate form with a suitable size (Ma et al., 2025). The more structured and interconnected protein networks could also be observed by the CLSM image (**Fig. 8.3**), further supporting this finding. Similar trends have been reported in previous studies, where higher viscosity was observed when using whey protein microgel (WPM) to replace WPI or Tween 20 (Zamani et al., 2018) and using WPI/pectin complexes to replace WPI (Wijaya et al., 2017). Likewise, Cui et al. (2025) demonstrated that higher concentrations of Zein/CNC particles led to increased viscosity, which may be because the enhanced interaction between particles created a stronger network structure.

A previous study showed that there were more HP/WPI particles adsorbed on the interface compared to non-microparticulated HP+WPI (Ma et al., 2025). The denser particles packed interface may restrict the free-flowing behaviour of droplets, which contributes to the high viscosity (J. Zhang et al., 2023). This is in agreement with the study

that showed HIPEs containing a thick interfacial layer formed by pea protein isolate-high pectin-epigallocatechin gallate complexes had a high viscosity (T. Feng et al., 2021).

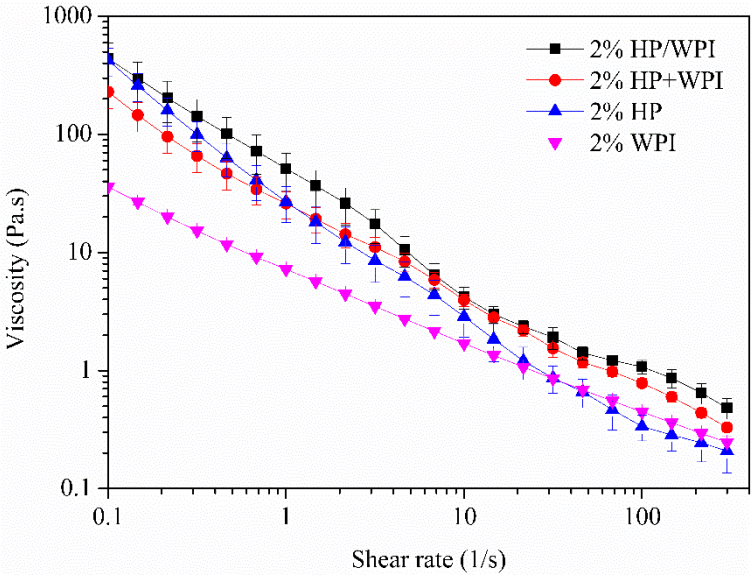


**Fig. 8.4.** Apparent viscosity of HIPEs stabilised by HP/WPI, HP+WPI, HP and WPI as a function of shear rate (0.1-300 1/s).

### 8.3.2.2 SAOS measurements – Frequency sweep

The gel-like properties of HIPEs were further characterised by small-amplitude oscillatory shear (SAOS) rheometry. The frequency sweep can reflects their viscoelastic behaviour and provide insights into their internal structures (Liu et al., 2019). All HIPEs exhibited gel-like behaviour, as indicated by the storage modulus ($G'$) being consistently higher than the loss modulus ($G''$) across the entire frequency range (0.1-100 Hz) (**Fig. 8.5**) (Hu et al., 2016; Pal, 2006). Both $G'$ and $G''$ were weakly frequency dependent, which may indicate the HIPEs were not markedly affected by the deformation even at high frequency (X. Liu et al., 2018). This behaviour is characteristic of highly flocculated elastic structures that primarily exhibit solid-like properties (Pal, 2006; Xiao et al., 2016).

The $G'$ of HP/WPI HIPEs was greater than other HIPEs, which could be attributed to the formation of a strong internal structure reinforced by HP/WPI microparticles. In other studies, HP/NaCas particles stabilised highly concentrated emulsions, also demonstrated gel-like properties (Chuang et al., 2020). It has been suggested that the possible reason for increasing elasticity in such systems could be the droplet-droplet interactions as evidenced by connected droplets observed in CLSM images (**Fig. 8.3**). Another contributing factor could be the interactions between excess particles in the continuous phase, which may aggregate into gel-like structures, leading to solid-like properties (Chevalier & Bolzinger, 2013; Chuang et al., 2020; Dickinson, 2017).

It has been suggested that the hydrophobic interactions play an important role in the formation of protein aggregates in the continuous phase. The studies on kafirin (Xiao et al., 2016), zein (Zou et al., 2017) and soy protein (Tang & Liu, 2013) nanoparticles stabilised emulsions have shown that adjusting ionic strength can suppress electrostatic repulsion and strengthen hydrophobic interactions. They all proposed that the enhanced gel-like properties primarily result from the particle interactions at the droplet interface (connected droplets) and within the continuous phase (gel-like network) via hydrophobic interactions.

Heat treatment could expose the hydrophobic groups of globular protein, e.g., whey protein (Ryan et al., 2013). The increased hydrophobicity in a heated β-lg/pea protein mixture was reported by Chihi et al. (2016). It is reasonable to speculate that HP/WPI microparticles, having undergone microparticulation (including heat treatment), would exhibit higher hydrophobicity than the other emulsifiers used in this study. This enhanced hydrophobicity may promote stronger hydrophobic interactions between droplets and particles, further contributing to the formation of an elastic, gel-like network.

On the other hand, the $G'$ of HP stabilised HIPEs was the lowest, which may be attributed to its larger droplet size compared to the other HIPEs. Smaller droplets could

provide a larger contact area, which results in more droplet-droplet interactions and reinforces the network structure. Additionally, the reduction of droplet size could increase the Laplace pressure, which requires more energy to deform the structure (Gao et al., 2021; Ling et al., 2024; Xu et al., 2019).

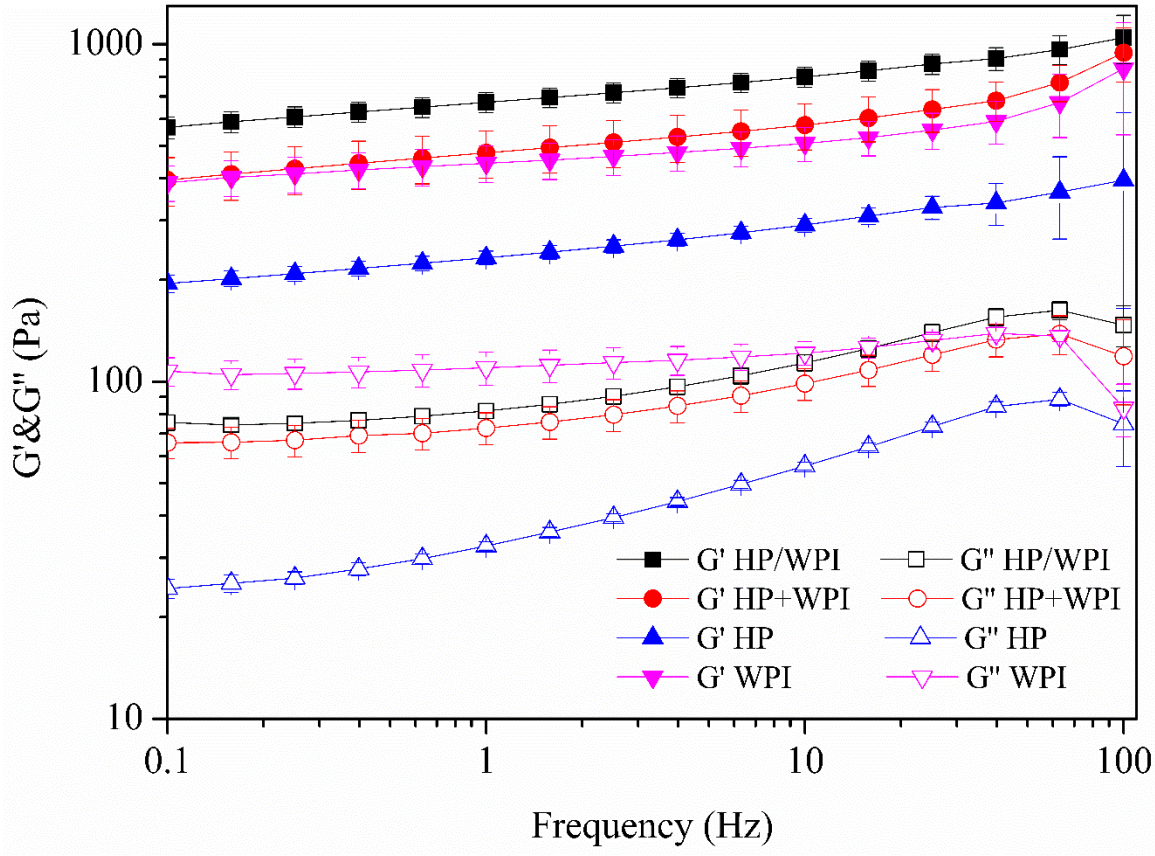


**Fig. 8.5.** Storage moduli *G′* and loss moduli *G″* of HIPEs stabilised by HP/WPI, HP+WPI, HP and WPI as a function of frequency (0.1-100 Hz).

### 8.3.2.3 LAOS measurements

Small amplitude oscillatory shear (SAOS) measurement can provide useful information in the linear viscoelastic region (LVR) at small strains without disturbing the structure of the materials (Duvarci et al., 2017). However, most food would experience large and rapid deformations during processing, transportation, storage, and consumption

(Joyner, 2019). To fully understand their rheological behaviour under such conditions, it is essential to investigate the nonlinear rheological response.

Conventional strain sweep analysis is calculated by the first harmonic coefficients in a Fourier series (Ewoldt et al., 2009). However, the first-harmonic moduli are insufficient to describe the nonlinear response because large deformation distorts the sinusoidal waveform of the oscillation stress to non-sinusoidal forms involving higher harmonic components, which are not considered during the calculation of conventional first-harmonic moduli (Hyun et al., 2002; Schreuders et al., 2021). To address this limitation, a new fundamental theory to interpret nonlinear rheological behaviours was developed by Ewoldt et al. (2007), who incorporated Fourier transforms with Chebyshev polynomials, which considered higher harmonic contributions (Joyner, 2019). The resulting rheology response is represented by Lissajous-Bowditch curves, which are intracycle stress versus strain plots.

In Lissajous plots, the instantaneous stress is decomposed as a function of strain, indicating the viscoelastic response of the material. The shape and area of these curves provide insights into structural changes during deformation (Schreuders et al., 2021). The enclosed area in the Lissajous curve indicates the dissipated energy during intracycle deformation of the oscillatory. A purely viscous material forms a circle curve, while a purely elastic solid results in a straight line. A viscoelastic material combines both viscous and elastic behaviour; therefore, it shows elliptical shapes (Ewoldt et al., 2008; Ewoldt et al., 2009).

The overview of LAOS behaviour of HIPEs is exhibited as Pipkin diagrams of Lissajous plots (**Fig. 8.6A**). At a strain amplitude of 0.1%, the narrow ellipses with little area in the curves were observed in all test emulsions, indicating the very elastic gel-like structures of HIPEs, remained undeformed at low strain (Farias & Khan, 2021). At slightly

higher strain amplitude (1% - 12%), the ellipses (excluding WPI stabilised HIPEs) widened slightly, but the enclosed area in the ellipses remained relatively small and narrow. This indicates a slight increase in viscous dissipation while maintaining an elastic-dominated response. With further increase in the strain amplitude (44% - 135%), the ellipses became significantly distorted into parallelograms with larger enclosed areas, indicating greater viscous dissipation and structure breakdown happened under applied strain stress, which resulted in the change from elastic-dominated to more viscous-dominated behaviour (Q. Li et al., 2021). Eventually, at maximum strain amplitude (435% - 1000%), the Lissajous curve transformed into an almost rectangular shape, suggesting plastic behaviour (Schreuders et al., 2021).

The onset of shape distortion in WPI-stabilised HIPEs occurred at lower strain amplitudes than in other HIPEs containing protein particles, suggesting that WPI-stabilised HIPEs were more susceptible to deformation. This aligns with the weaker network structure observed in whey protein-stabilised HIPEs as discussed earlier. A similar trend was reported by Sridharan et al. (2021), who found that concentrated emulsion stabilised by pea protein exhibited a nonlinear viscoelastic response at relatively low strain (10%) and had relatively weaker droplet-droplet interactions compared to those stabilised by pea protein particles.

Although the shape distortion patterns from the Lissajous plot for HP/WPI, HP+WPI and HP stabilised HIPEs were generally similar, some differences emerged when comparing them together at each strain amplitude (**Fig. 8.6B**). At low strains, maximum stress values and slope of the ellipse of both mixed protein HIPEs (HP/WPI and HP+WPI) were greater than those of single protein stabilised HIPEs (HP or WPI), indicating a stiffer network in HP/WPI and HP+WPI HIPEs (B. Zhou et al., 2022). Additionally, HP/WPI and HP+WPI HIPEs showed a distinct distortion at a strain amplitude of 44%, while HP HIPEs

showed a more gradual distortion (**Fig. 8.6B**). This may suggest that their transition from linear to nonlinear range occurred at a relatively lower strain amplitude than HP HIPEs. This is likely due to less flexible and less deformable droplets (more elastic interfaces) (B. Zhou et al., 2022). The greater droplet-droplet interactions contributed to the formation of a rigid internal network with reduced flexibility. As a result, while this structure enhanced elasticity under small strains, it became susceptible to greater structural damage when the structure could no longer accommodate high strains and leading to higher viscous dissipation (Anvari & Joyner, 2017, 2018).

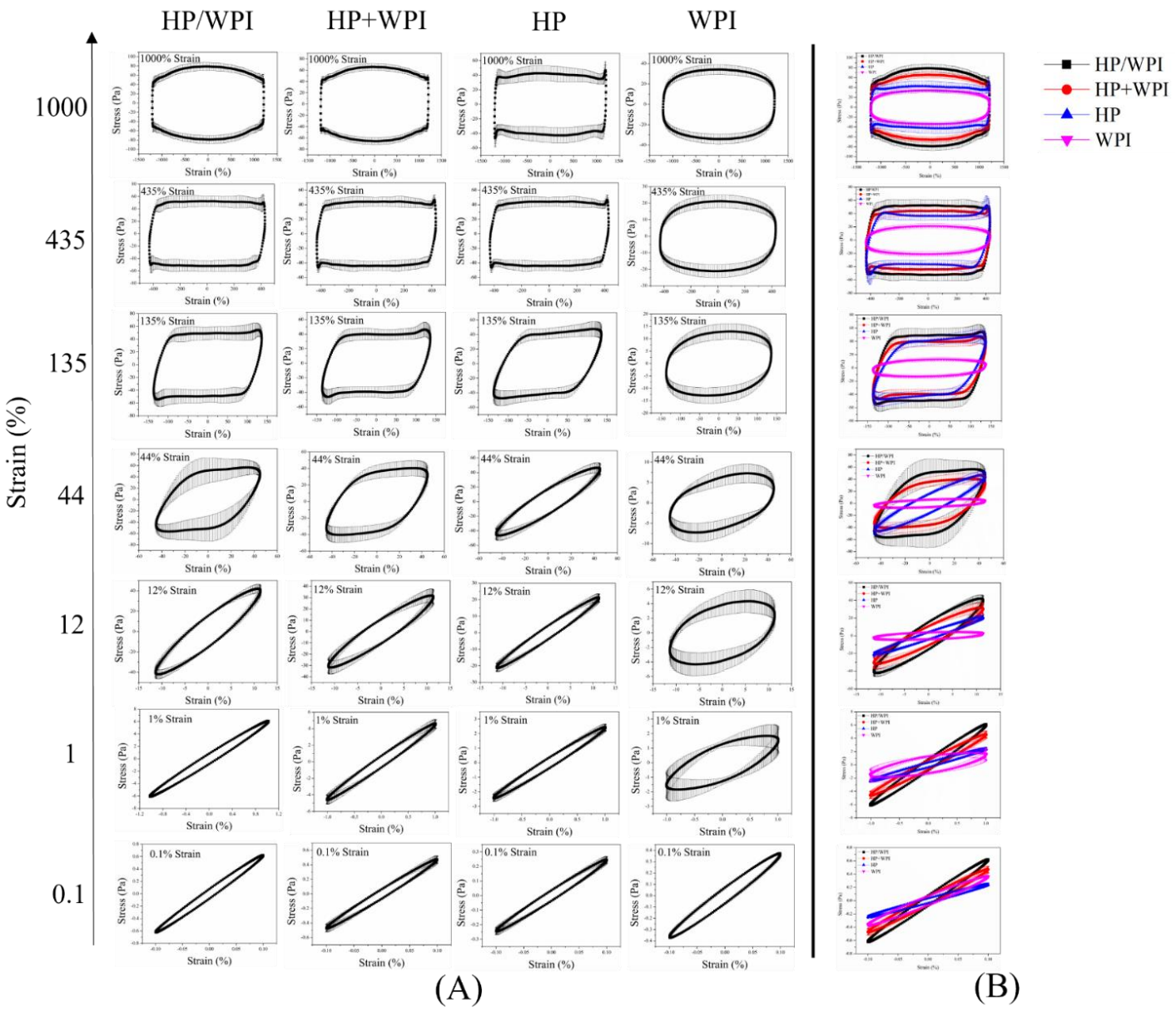


**Fig. 8.6.** (A) Lissajous-Bowditch curves of HIPEs stabilised by HP/WPI, HP+WPI, HP and WPI as a function of strain amplitude. (B) Their comparison as each strain amplitude.

The dimensionless shear-stiffening index (S) was calculated according to Eqs. 1-3 to better understand nonlinear rheological behaviour. An S value equal to 0 represents a linear elastic/viscous response, a positive S value indicates intracycle strain stiffening, and a negative S value indicates intracycle strain softening.

As shown in **Fig. 8.7**, all HIPEs had negligibly small absolute S values (< 0.05) at 0.1% strain amplitude, suggesting the linear elastic response. As strain increased, S values increased, indicating intracycle strain stiffening behaviour. Eventually, at the highest strain amplitudes, S values reached about 1, which is commonly associated with plastic response (Ewoldt et al., 2009). Similar shear stiffening behaviour has been frequently observed in many concentrated emulsions (Q. Li et al., 2021; B. Zhou et al., 2022; Zhou et al., 2023). The transition from a linear elastic to a strain-stiffening regime occurred more rapidly in WPI-stabilised HIPEs, followed by HP/WPI and HP+WPI HIPEs. This trend is consistent with the results obtained from the Lissajous plot.

The strain stiffening effect indicates resistance against large deformation, likely due to the alignment and stretching of internal structure, e.g., droplet clusters, particle networks and deformation of the interfacial structure. Notably, HP/WPI and HP+WPI HIPEs exhibited higher S values in the strain range of 10%–100%, which suggests a greater strain stiffening effect. This behaviour indicates a more elastic interfacial and internal structure in these systems (Zhou et al., 2023).

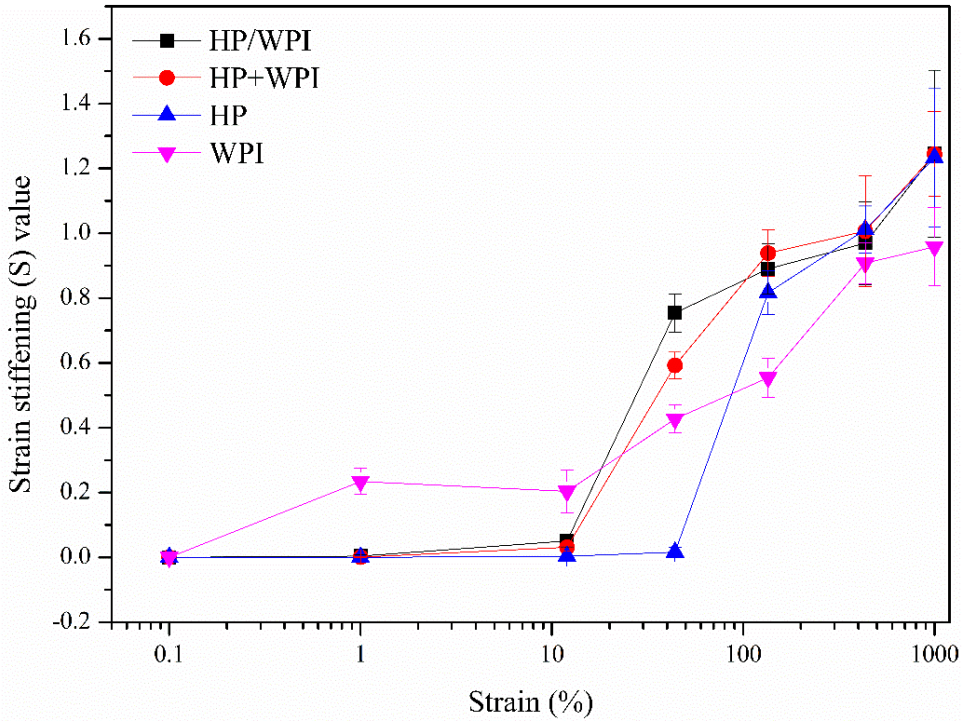


**Fig. 8.7.** Shear-stiffening index (S) of HIPEs stabilised by HP/WPI, HP+WPI, HP and WPI as a function of strain amplitude.

### 8.3.3 Heat stability of HIPEs

#### 8.3.3.1 Droplet size

When the HIPEs were heated at 95 °C for 20 min, only minor changes in the droplet size were observed in HP/WPI and WPI HIPEs, whereas HP+WPI and HP HIPEs exhibited a substantial increase in droplet size (**Fig. 8.8**).

The use of microparticulated HP/WPI as an emulsifier significantly improved the heat stability of emulsions compared to HP+WPI or individual HP. This advantage aligns with findings on microparticulated WPI, which has been shown to have enhanced thermal stability in emulsions due to the pre-heating process (Shi et al., 2021). Similarly, previous studies have reported excellent heat stability in emulsions stabilised by microparticulated

whey protein concentrate (WPC) (Çakır-Fuller, 2015), whey protein microgels (Zamani et al., 2018) and preheated soy protein particles (W. Ma et al., 2020).

Interestingly, WPI-stabilised HIPEs exhibited no significant change in droplet size after heating. Protein concentration might be the key factor in the heat stability of whey protein-stabilised emulsions. Çakır-Fuller (2015) found that emulsions stabilised with 2% whey protein concentrate remained unchanged in size after heating, whereas emulsions with 3% protein concentration experienced an increase in droplet size.

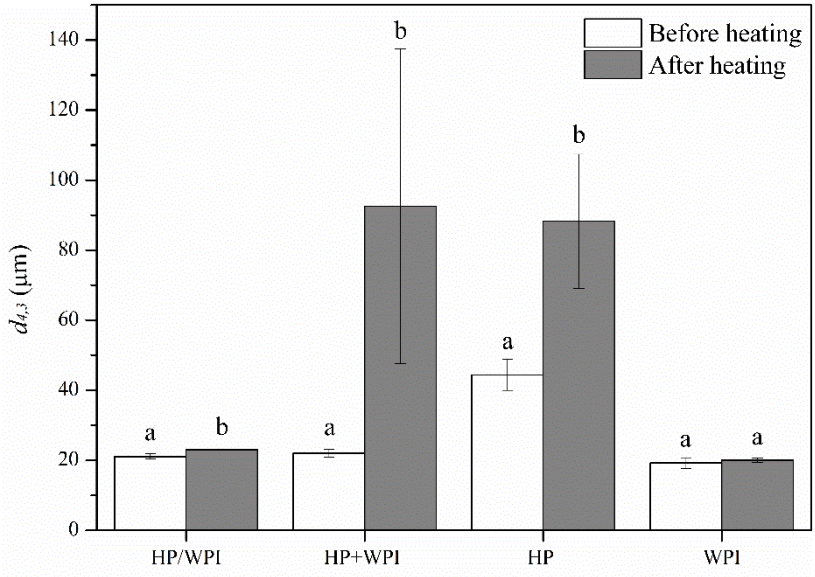


**Fig. 8.8.** Average droplet diameter (*d4,3*) of HIPEs stabilised by HP/WPI, HP+WPI, HP and WPI before and after heating. Different lowercase letters indicate significant differences in HIPEs after heat treatment ($p < 0.05$).

### 8.3.3.2 Microstructure

Confocal laser scanning microscopy (CLSM) images correlated well with the droplet size data. After heating at 95 °C for 20 minutes, no obvious changes in the

microstructure of HP/WPI and WPI HIPEs were observed (**Fig. 8.9A and D**). However, HP and WPI HIPEs showed noticeable droplet flocculation and coalescence (**Fig. 8.9B and C**).

The observed emulsion instability may be attributed to multiple aggregation mechanisms: protein-protein, droplet-droplet and droplet-protein interactions (Euston et al., 2000). The non-adsorbed protein particles in the continuous phase likely interacted with each other and formed large aggregates. Meanwhile, the interfacial proteins may have undergone structural disruption and interacted with each other or with protein aggregates, ultimately resulting in droplet aggregation and droplet coalescence.

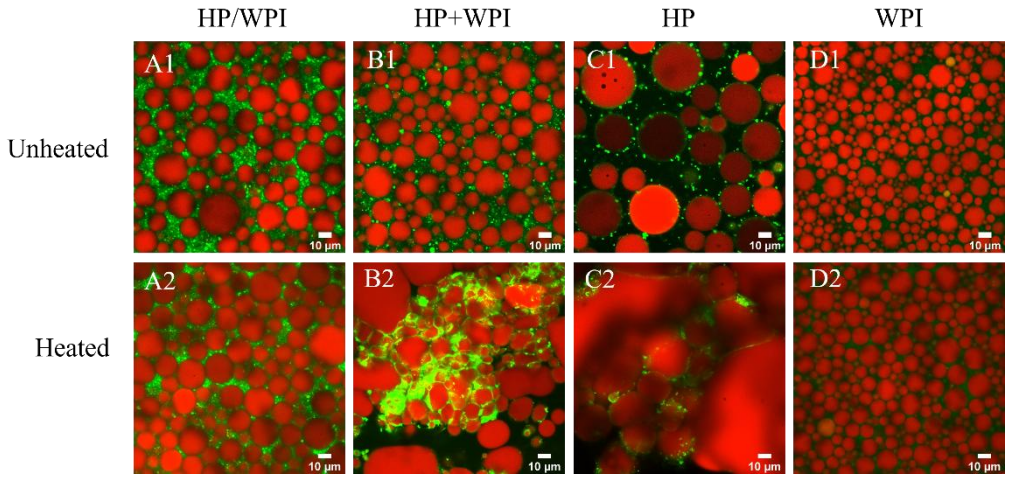


**Fig. 8.9.** CLSM images of HIPEs stabilised by (A)HP/WPI, (B) HP+WPI, (C) HP and (D) WPI, (1) before and (2) after heating. The scale bar is 10 µm.

### 8.3.3.3 Viscosity

The effect of thermal processing on the HIPEs was assessed through viscosity measurement. The viscosity of heated HP/WPI and WPI HIPEs remained similar to their unheated counterparts, indicating that the heat treatment may not induce significant internal

structural changes (**Fig. 8.10A and D**). The enhanced heat stability of HP/WPI HIPEs was expected due to the presence of microparticulated proteins (Ipsen, 2017). In the case of whey protein, the result was in agreement with Çakır-Fuller (2015), who reported that there was no significant change in the viscosity of WPC stabilised emulsions at relatively low protein concentrations (below 2%).

In contrast, the viscosity of HP+WPI and HP HIPEs increased after heating (**Fig. 8.10B and C**), which suggests structural instability under thermal treatment. This is consistent with the results of droplet size and microstructure observations, where droplet aggregation was observed, leading to increased viscosity (Keerati-u-rai & Corredig, 2009). Similarly, viscosity increases have been reported in pea protein (Keerati-u-rai & Corredig, 2009; Peng et al., 2016) and soy protein (W. Ma et al., 2020) because of the formation of droplet flocculation and protein aggregates upon heating. The flocs and aggregates would lead to higher resistance to flow compared to the initial emulsions (McClements, 2015).

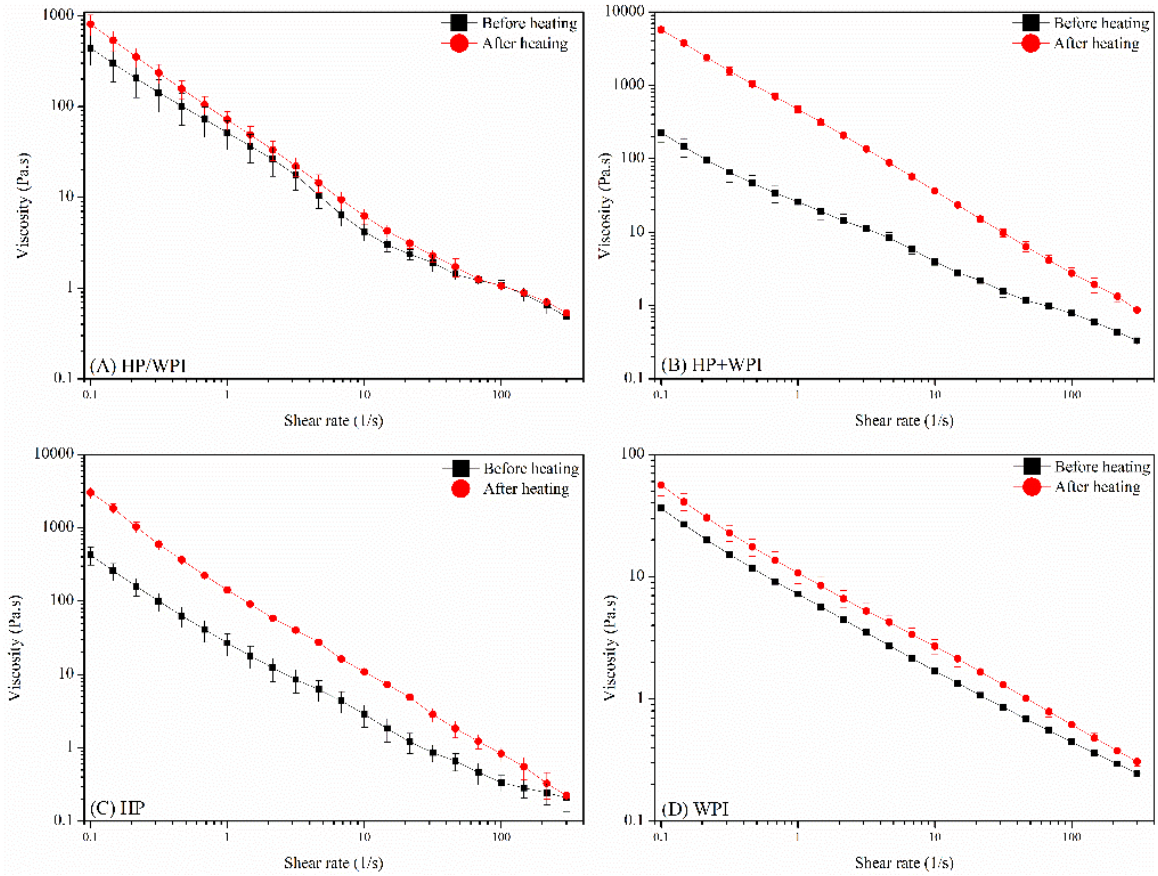


**Fig. 8.10.** Apparent viscosity of HIPEs stabilised by (A)HP/WPI, (B) HP+WPI, (C) HP and (D) WPI before and after heating as a function of shear rate (0.1-300 1/s).

Heat stability of emulsions is influenced by droplet-droplet interactions and protein-protein interactions in the continuous phase during heating (Liang et al., 2017). Our previous study demonstrated that HP/WPI microparticles had excellent heat stability because most of the reactive groups in HP and WPI, e.g., free thiol groups and hydrophobic groups, were exposed and interacted with each other during the microparticulation processing (Ma, Ye, et al., 2024). The consistency between droplet size, microstructure, and viscosity measurements suggests that thermal treatment had minimal effects on HP/WPI microparticles.

It is important to note that the improved heat stability of HP/WPI HIPEs is attributed to the pre-heating and pre-interactions that occurred during microparticulation, rather than complexation of WPI with HP alone. The complexation was specifically designed to control HP aggregation. Attempting to heat HP alone or to mix separately heated HP and WPI without microparticulation would be impractical, as HP at this high protein concentration severely aggregated during heating, making it unsuitable for subsequent processing. This is why WPI was incorporated to restrict HP aggregation and enable the formation of stable HP/WPI microparticles.

However, the HP+WPI or individual HP without microparticulation treatment remained heat-sensitive. Previous studies have shown that HP has poor heat stability and tends to aggregate, mainly due to its relatively high free thiol content (Ma, Ye, et al., 2024; Tang et al., 2006). On the other hand, whey proteins are also well known to undergo denaturation upon heating, leading to the unfolding of buried hydrophobic and sulfhydryl groups, which then participate in aggregate formation via sulfhydryl–disulphide interchange and hydrophobic interactions (Anema, 2020). Therefore, based on these results, we speculated that unfolding and subsequent interactions of individual HP, individual WPI or both HP and WPI contribute to droplet-droplet, protein-protein and droplet-protein aggregations (Dissanayake & Vasiljevic, 2009), which lead to internal structural modifications in the HIPEs.

Although whey proteins are generally heat-sensitive, the heat stability of WPI HIPEs in this study may be attributed to their relatively low protein concentration. It has been suggested that the extent of heat-induced destabilisation, e.g., droplet-droplet and droplet-protein aggregations, is strongly influenced and strengthened by the non-adsorbed proteins in the continuous phase (Sliwinski et al., 2003). When the non-adsorbed protein was removed and replaced with fresh buffer, the aggregation reactions decreased. Moreover,

3% non-adsorbed native whey protein was proposed as a threshold of significant aggregation (Euston et al., 2000; Liang et al., 2013; Sliwinski et al., 2003). In WPI HIPEs, only 2% WPI solution was used to stabilise the 75% oil phase, meaning most of the whey protein was adsorbed at the oil-water interface to stabilise the emulsion, leaving limited aqueous-phase protein, which restricted droplet interactions. In addition, the jammed droplet structure may also reduce the flexibility of droplets and particles, preventing aggregation.

## 8.4 Conclusions

This study demonstrated that HP/WPI microparticles can effectively stabilise HIPEs, exhibiting superior rheological properties and thermal stability compared to HIPEs stabilised by HP, WPI, or their simple mixtures (HP+WPI).

Rheological analyses revealed that all HIPEs displayed solid-like behaviour at low strain amplitudes, with HP/WPI HIPEs showing the highest viscosity and storage modulus ($G'$), indicating a robust internal structure. Large amplitude oscillatory shear (LAOS) measurements further confirmed that HP/WPI HIPEs exhibited enhanced intracycle strain stiffening behaviour, suggesting stronger resistance to deformation due to reinforced droplet-droplet and protein particle interactions. Heat stability assessments demonstrated that HP/WPI HIPEs maintained their viscosity and droplet size after thermal treatment at 95 °C for 20 min, while HP and HP+WPI HIPEs experienced significant droplet aggregation, flocculation, and coalescence.

Beyond their rheological and thermal stability, HIPEs have inherent advantages in storage stability due to their densely packed oil droplet network, which can help prevent phase separation and coalescence over time. Future research could focus on the long-term

stability of HP/WPI HIPEs under different storage conditions, including variations in temperature, pH, ionic strength and mechanical stress.

Overall, this study highlights the potential of microparticulated HP/WPI as an effective emulsifier for thermally stable food-grade HIPEs. The combination of HP and WPI through microparticulation enhances both emulsification and structural integrity, making it a promising strategy for developing plant–milk protein hybrid emulsions with improved functional properties.

# Chapter 9: Overall discussion and future recommendations

## 9.1 Overall discussion and conclusion

In recent years, growing environmental and sustainability concerns, coupled with the need for cost-effective and nutritionally rich food ingredients, have led to increasing interest in substituting animal proteins with plant-based alternatives. However, the relatively poor functional properties of most plant proteins limit their direct applications in food systems. As a result, hybrid systems, combining plant and milk proteins, have gained attention for their potential to enhance technological functionality. This project systematically investigated the heat-induced interactions between hemp protein (HP) and milk proteins, with the aim of developing hybrid protein microparticles suitable for food emulsification applications.

### 9.1.1 Microfluidisation enhanced HP dispersibility

In **Chapter 4**, microfluidisation was used as a pre-treatment to disintegrate large HP aggregates and improve the dispersibility. This process significantly increased the dispersible protein fraction (protein retained in the supernatant after centrifugation) from 10% (non-microfluidised) to a maximum of 58% (200 MPa, 6 passes) (**Fig. 4.1**). The "insoluble" HP globulin increased from ~35% to ~80% in the supernatant (**Fig. 4.2**). The intense shear and turbulence during microfluidisation could likely expose the buried free thiol groups and hydrophobic groups, leading to structural changes and reaggregation. This effect was more pronounced at high protein concentrations (2-3%). It aligns with previous findings demonstrating that microfluidisation increases the surface reactivity of plant proteins (Gong et al., 2019). If this approach is to be extended to other types of protein, the processing conditions (e.g., pressure, number of passes, and protein concentration) would

need to be carefully optimised according to the specific structure of the proteins. In this study, 1% HP (200 MPa, 4 passes) was carefully selected as the optimal condition to produce globulin-dominated, uniformly dispersed particles (~0.4 μm, $d_{4,3}$).

### 9.1.2 Interaction between HP and β-lg

SDS-PAGE analysis under reducing conditions (**Fig. 4.7**) showed that β-lg remained fully soluble after heating, and HP formed large insoluble aggregates. However, the presence of β-lg in both the sediment phases after co-heating with HP confirmed the formation of disulphide-linked hybrid aggregates. Heat treatment above the denaturation temperatures of β-lg (~75 °C) triggered unfolding and exposure of reactive thiol and hydrophobic groups, and above the denaturation point of HP (~91 °C), creating conditions favourable for sulphydryl-disulphide exchange reactions with HP particles.

Other factors, such as heating time and mixing ratios, are also important in protein interactions. To further characterise the interactions, the association between β-lg and HP was monitored under varying heating durations (0–60 min) and protein ratios (HP:β-lg from 0.25:0.25 to 0.25:0.05). The rapid protein-protein interactions took place in the initial period of heating (10-20 min), in which β-lg either preferentially interacted with HP or rapidly form dimers/higher polymers at low temperatures (74–76 °C), then associate with HP (**Fig. 4.8**). Increasing the HP:β-lg ratio resulted in greater incorporation of β-lg into the sediment fraction, indicating that β-lg and HP interaction was limited by the availability of reactive sites on HP particles (**Fig. 4.9**).

Unlike previous studies that primarily evaluated plant proteins using their soluble fractions (Beghdadi et al., 2022; Chihi et al., 2016; Roesch & Corredig, 2005), this research uniquely demonstrated that the heat-induced interaction of microfluidised HP with β-lg

significantly restricted HP self-aggregation, resulting in the formation of smaller, more spherical aggregates. A possible mechanism (**Fig. 4.11**) was proposed that the β-lg would first unfold at around 75 °C, and its monomers either bound to HP particles via disulphide bonds or self-associated into higher-order structures. As the temperature increased to the denaturation temperature of HP (~91 °C), more reactive groups of HP became exposed, allowing further association of β-lg with HP particles. Since the β-lg occupied the reactive groups of HP particles, the aggregation of HP would be restricted, resulting in smaller aggregates compared with the individually heated HP particles.

These findings provided the first evidence that HP could interact with β-lg under thermal conditions, which can prevent the formation of large, functionally undesirable aggregates. This chapter established core principles and methods, including particle preparation, thermal treatment and determination of interactions using SDS-PAGE, which were adopted in the following chapters.

### 9.1.3 Distinct interaction mechanisms between HP and milk proteins (WPI vs. NaCN)

Building on Chapter 4, **Chapter 5** extended the investigation to heat-induced interactions between HP particles and two commercially available milk protein products, whey protein isolate (WPI) and sodium caseinate (NaCN). The key finding of this work was the distinct interaction mechanisms exhibited by WPI and NaCN during heat treatment with HP, despite both WPI and NaCN having the ability to decrease the extent of heat-induced aggregation of HP.

**HP-WPI interactions: formation of a stable complex**

Similar to HP/β-lg mixtures, co-heating HP with WPI or NaCN produced well-dispersed small particles with spherical shape under TEM observation (**Fig. 5.2**). The heat treatment exposed the reactive group of both HP particles and whey protein. When the HP and WPI were co-heated, the denatured whey protein may either self-aggregate or interact with the HP particles. SDS-PAGE under reducing conditions (**Fig. 5.3**) revealed that the disulphide-linked complexes between HP and whey proteins (mainly β-lg) were formed.

Notably, the band of α-la was also observed in the HP/WPI aggregates, although to a lesser extent than β-lg (**Fig. 5.3**). This supports the hypothesis that HP preferentially interacts with β-lg, likely due to β-lg's exposed free thiol groups after denaturation, whereas α-la, lacking free thiols, may require co-aggregation with β-lg to participate in the complex formation, which is similar to the heat-induced aggregation of α-la in the milk proteins (Anema & Li, 2003a). The formation of HP/WPI complexes likely shielded HP reactive sites, thereby preventing further HP-HP aggregation. Due to the irreversible nature of disulphide bonding, these hybrid aggregates were thermally stable and did not dissociate upon cooling (**Fig. 5.7**). Moreover, as most of the exposed reactive groups already interacted when forming the HP/WPI particles, the HP/WPI particles show excellent heat stability during the second heat treatment (**Fig. 5.6**).

**HP–NaCN interactions: reversible, chaperone-like protection**

In contrast, in the HP/NaCN systems, caseins remained largely in the supernatant after heating, suggesting no stable complexes with HP particles were formed (**Fig. 5.4**). This difference arises from NaCN's major components (αS1- and β-caseins), which lack free thiol groups and therefore cannot participate in disulphide bonding. In contrast to

HP/WPI complexation, the mechanism of restricting the aggregation of HP could be the reversible association between HP and caseins, likely due to hydrophobic interactions. As proposed in **Fig. 5.7**, caseins may act as molecular chaperones, shielding HP particles from aggregation through steric hindrance and transient hydrophobic interactions.

However, these chaperone-like interactions were not thermally stable. Upon cooling, hydrophobic interactions weakened, leading to the dissociation of caseins from the HP. This was confirmed by the surface hydrophobicity measurement (**Fig. 5.5**), indicating re-exposure of buried hydrophobic groups. Therefore, no thermally stable complexes were formed in the HP/NaCN system. Once caseins dissociated, the protective effect was lost, and HP particles were prone to aggregation upon subsequent heating. This chaperone-like action of NaCN aligns well with earlier studies (Guyomarc'h et al., 2009; Kehoe & Foegeding, 2014; Yong & Foegeding, 2010), but importantly, this study provided the novel insight that NaCN dissociated upon cooling, leaving HP vulnerable to subsequent aggregation.

This comparative study uniquely highlighted how the intrinsic differences between WPI and NaCN influence plant-milk protein interaction mechanisms (**Fig. 5.7**), which is a concept rarely addressed previously. These findings highlight that the selection of milk protein has a significant impact on the plant-milk protein interactions, and consequently, on the design of heat-stable hybrid protein particles. Due to the formation of an irreversible and heat-stable hybrid protein complex, WPI was selected as the preferred milk protein partner for developing HP-based hybrid particles in the following studies.

### 9.1.4 pH-dependent control of hybrid aggregate formation

In **Chapter 6**, the influence of pH (3-8) on the heat-induced aggregation of the HP and WPI mixture was investigated. The objective was to identify the most favourable pH conditions for generating hybrid protein aggregates suitable for microparticulation. This chapter served as an important foundational step for the subsequent development of microparticulated HP/WPI particles in Chapter 7.

#### Heat-induced HP-WPI interactions at pH 8

Among the tested conditions, heating HP/WPI mixtures at pH 8 produced small, spherical aggregates (**Fig. 6.3**), ideal for further size reduction (**Fig. 6.1**) via high-pressure homogenisation. The different heat-induced interaction behaviour at pH 8 compared to that at neutral pH was attributed to the dissociation of HP globulin into HP acidic subunit (HP-AS) and HP basic subunit (HP-BS), and subsequently interacted with whey proteins to form soluble HP-AS/whey protein aggregates and insoluble HP-AS/HP-BS/whey protein aggregates via enhanced thiol-disulphide exchange reactions (**Fig. 6.5**).

Heating at alkaline pH led to the disruption of disulphide bonds linking the acidic subunits (AS) and basic subunits (BS), resulting in the release of polypeptides and smaller aggregates, which aligns well with earlier studies on plant proteins (Do et al., 2025; Makinen et al., 2016; Renkema et al., 2000). The alkaline conditions promoted the unfolding of the protein and enhanced the reactivity of free thiol groups (Mercade-Prieto & Gunasekaran, 2009). Consequently, it may facilitate rapid interactions among dissociated HP subunits and whey protein, accelerating aggregate formation, thereby reducing the availability of free thiol groups, promoting aggregation termination and

limiting particle growth, which aligns well with earlier studies on whey protein (de la Fuente et al., 2002).

**Heat-induced HP-WPI interactions at pH 3-7**

In contrast, heating at pH 4-7 led to the formation of large, irregular aggregates, likely due to extensive disulphide bonding, non-covalent interactions and reduced electrostatic repulsion when close to the isoelectric point (**Fig. 6.1 and 6.2)**. These large aggregates were less suitable for size reduction using high-pressure homogenisation. On the other hand, heating at pH 3 resulted in partial dissociation of HP aggregates (**Fig. 6.9**). The sulphydryl-disulphide interchange reactions are largely suppressed since the thiol groups of HP and whey protein remained stable and less reactive at such low pH. The interactions between a proportion of dissociated HP and WPI were presumed to be dominated by hydrophobic forces and led to insoluble aggregates (Dissanayake, Ramchandran, Piyadasa, et al., 2013; Zhang et al., 2025). Meanwhile, the other fractions of HP and WPI remained in the supernatant (**Fig. 6.9**). However, given the partial solubilisation of HP at pH 3, it is difficult to identify the HP-WPI interactions in this study. Moreover, the presence of residual reactive thiol groups may compromise the stability of aggregates during later processing.

Although the effect of pH on heat-induced aggregation has been studied in whey protein (de la Fuente et al., 2002; Dissanayake, Ramchandran, Donkor, et al., 2013; Dissanayake, Ramchandran, Piyadasa, et al., 2013), applying these insights to hybrid plant-milk protein systems is novel. This study uniquely provided evidence on how adjusting pH modulates the heat-induced interactions between HP and WPI, and identified pH 8 as the

optimal condition for producing heat-induced HP/WPI aggregates, which were then used for microparticle production in the following studies.

### 9.1.5 Emulsifying performance of HP/WPI microparticles with improved heat stability

In **Chapter 7**, microparticulated HP/WPI particles through the combination of thermal aggregation (at pH 8) and high-pressure homogenisation were developed. The objective of this chapter was to evaluate how microparticulation influences the HP/WPI systems in emulsification and their thermal stability, particularly under different protein concentrations (0.25–1.8%).

#### Formation of stable HP/WPI microparticles

During the microparticulation process, the HP dispersion underwent severe heat-induced aggregation, forming a large coagulum (**Fig. 7.1A**), which is not suitable for the following homogenisation. In contrast, the strategy of combining WPI and HP successfully prevented excessive aggregation of HP and produced a well-dispersed HP/WPI microparticle suspension, with a majority of particles at ~0.1 μm (**Fig. 7.1**). Previous studies mostly explored single proteins or non-aggregated blends; the novelty of this study lies in demonstrating controlled conditions to generate microparticles from plant-milk protein combinations.

#### Emulsifying performance: non-microparticulated vs. microparticulated HP/WPI

The emulsifying ability of these microparticles was then tested in 10% oil-in-water emulsions, with protein concentrations ranging from 0.25% to 1.8%. Their performance

was directly compared to non-microparticulated HP/WPI mixtures, blends of the same composition but without heat or shear treatment. This comparison allowed the direct assessment of the functional impact of microparticulation.

The non-microparticulated HP/WPI stabilised emulsions exhibited small droplet sizes (~0.5 μm) with minimal flocculation across a protein concentration range (0.25-1.8%) (**Fig. 7.3**). This could be attributed to the preferential adsorption of whey protein as evidenced by the SDS-PAGE analysis of the interfacial layer showing higher whey protein content at the interface compared to the bulk phase (**Fig. 7.5**). It is consistent with the earlier studies that competition for adsorption can occur when multiple proteins are present (Hinderink et al., 2019; Hinderink, Sagis, et al., 2021). The small and flexible whey protein molecules could rapidly adsorb and rearrange at the droplet surface, which can stabilise emulsions at relatively low concentrations (Schwenzfeier et al., 2013). However, HP was largely excluded from the interface when competing with the more surface-active whey proteins, likely due to its poor solubility, large aggregates and slow adsorption. This highlighted a key limitation in mixed plant-milk protein systems: without processing, the plant protein, with a larger size and rigid structure, may not significantly contribute to interfacial functionality.

In contrast, the microparticulated HP/WPI stabilised emulsions at low concentrations (0.25–1.0%) exhibited larger droplet sizes and extensive bridging flocculation (**Fig. 7.3**), characteristic of a system in the "emulsifier-poor" regime. The microparticles were insufficient to fully cover the interface and likely bridged multiple droplets. In comparison, because of the unbound whey protein molecules in the non-microparticulated HP/WPI, better emulsifying ability was observed at low protein concentrations. However, at higher concentrations (≥1.5%) ("emulsifier-rich" regime), the droplet size of microparticulated HP/WPI stabilised emulsions was significantly reduced

to ~0.5-0.6 μm, which was close to those of whey protein-dominated emulsions, and flocculation was minimised. It indicates that microparticulated HP/WPI was sufficient to stabilise the small, broken-up droplets during homogenisation at the given protein concentrations.

Importantly, the interfacial protein measurement (**Fig. 7.4**) revealed that microparticulated HP/WPI stabilised emulsions had higher surface protein loading (~4.5 mg/m$^2$ at 1% protein concentration), compared to those of non-microparticulated HP/WPI stabilised emulsions (~1.5 mg/m$^2$). Higher surface protein loading, typical of particle-stabilised (Pickering-type) emulsions, likely contributed to a stronger protective shell at the interface, reducing droplet coalescence (Yan et al., 2020). SDS-PAGE analysis of the interfacial protein (**Fig. 7.5**) confirmed greater incorporation of HP into the interface in microparticulated systems than in non-microparticulated blends (Fig. 7.5). This is a novel outcome, clearly demonstrating that hybrid protein microparticulation enabled weakly emulsifying HP (Tang et al., 2006), typically 6–15 μm emulsion droplet size (Chen et al., 2023), to become an active emulsifying agent, participating at the oil-water interface.

**Enhanced heat stability of microparticulated HP/WPI stabilised emulsions**

One of the key advantages observed in this study was the improved thermal stability of emulsions stabilised by microparticulated HP/WPI. Upon heating, these emulsions showed limited aggregation or coalescence (**Fig. 7.7**). In contrast, non-microparticulated HP/WPI emulsions experienced greater destabilisation, likely due to heat-induced unfolding and aggregation of non-adsorbed or loosely bound proteins. The enhanced heat stability of microparticulated systems was attributed to the prior interaction and structural rearrangement within the particles (illustrated previously in Chapter 4 and Chapter 5). Such

structured microparticles resist further denaturation or aggregation upon subsequent thermal exposure.

Previous studies often used microparticulated proteins alone as an inert filler or emulsifier (Nourmohammadi et al., 2023; Shi et al., 2021). In contrast, this study demonstrated the novelty of applying microparticulation to a hybrid system, showing that HP-WPI microparticles can not only enhance the dispersibility of HP but also provide a practical approach, incorporating inferior functional HP with milk proteins, to achieve active emulsification capacity and thermal resilience.

### 9.1.6 HP/WPI microparticles effectively stabilised high internal phase emulsions (HIPEs)

**Formation of HIPEs using microparticulated HP/WPI**

**Chapter 8** investigated the performance of microparticulated HP/WPI particles as stabilisers in high internal phase emulsions (HIPEs), compared to those stabilised by non-microparticulated HP/WPI blends or by their individual proteins.

Microparticulated HP/WPI, non-microparticulated HP/WPI and individual WPI successfully stabilised HIPEs in a droplet size range (~15-25 μm), with good visual stability. However, HP particles exhibited the poorest emulsifying performance, as evidenced by significantly larger droplet size (**Fig. 8.1**). This further demonstrated the effectiveness of microparticulation in overcoming HP's inherent emulsifying limitations, possibly through enhanced particle size reduction and increased surface activity (supported by Chapter 7).

**Rheological properties of HIPEs**

In HIPEs, the closely packed droplets result in the viscoelastic and semi-solid characteristics (Li et al., 2019). Consistent with prior reports on particle-stabilised HIPEs (Chuang et al., 2020; W. Ma et al., 2020; C. Sun et al., 2018), HIPEs stabilised by microparticulated HP/WPI exhibited shear-thinning and gel-like behaviour (storage modulus, $G'$, being consistently higher than the loss modulus, $G''$), shown by the viscosity analysis (**Fig. 8.4**) and small amplitude oscillation shear measurements (**Fig. 8.5**). However, microparticulated HP/WPI HIPEs exhibited higher visocity and storage modulus ($G'$) compared to other HIPEs, indicating a robust internal structure, attributed to enhanced droplets connection and stronger protein networks in the continuous phase. The more structured and interconnected protein networks of microparticulated HP/WPI HIPEs, revealed by the CLSM image (**Fig. 8.3**), further support this finding. Conversely, the $G'$ of HP stabilised HIPEs was the lowest, which may be attributed to their larger droplet size, which is not able to provide a larger contact area for droplet-droplet interactions.

In contrast, WPI stabilised HIPEs had fluid-like behaviour (**Fig. 8.2**) and slightly weaker rheological behaviour (**Fig. 8.5**). This finding aligns with previous research indicating that molecular stabilisers like whey proteins typically form fewer rigid interfaces and weaker networks in HIPEs (Gao et al., 2021; Liu et al., 2019). Thus, it clearly demonstrated that microparticulated particles significantly enhance gel strength and internal structural rigidity compared to conventional molecular stabilisers.

Large amplitude oscillation shear (LAOS) measurements monitored the non-linear behaviour of the HIPEs, distinguishing between solid-like and liquid-like responses under large deformations (**Fig. 8.6**). The Lissajous plots revealed that HIPEs stabilised by microparticulated HP/WPI behaved as elastic-dominated responses at low strain

amplitudes (1%-12%), followed by gradual yielding at higher strain (≥44%), suggesting the transition from linear to nonlinear range. The greater maximum stress values and slope of the ellipse of HP/WPI HIPEs than those of single protein (HP or WPI) HIPEs indicate the presence of greater droplet-droplet interactions and a less flexible network, which provided structural rigidity and resistance to deformation.

**Improved heat stability of HIPEs**

Another major contribution of this chapter was the demonstration of enhanced heat stability in HIPEs stabilised by microparticulated HP/WPI. When heated at 90 °C, the HIPEs retained intact droplet structures, viscosity and interconnected protein networks (**Fig. 8.8-8.10**), demonstrating outstanding thermal stability, whereas HIPEs formed from non-microparticulated blends or HP-alone showed destabilisation. This observed thermal stability of microparticulated protein-stabilised HIPEs agrees with findings from previous microparticulated emulsion studies (Çakır-Fuller, 2015; W. Ma et al., 2020). This thermal resilience is attributed to the pre-formed interactions (e.g., disulphide bonds) within the microparticles, which are less prone to denaturation or aggregation during heating.

To the best of our knowledge, this is one of the first studies to demonstrate the use of hemp-milk protein hybrid microparticles for stabilising HIPEs. These findings expand existing research on hybrid proteins on HIPEs (Chuang et al., 2020) and show clear evidence of their unique potential in food applications.

### 9.1.7 Conclusions and future food applications

Overall, this thesis explored a novel approach to improving the functionality of HP by forming hybrid protein systems with WPI. The graphical summary of the thesis is

presented in **Fig. 9.1**, which illustrates a stepwise investigation, from molecule-particle interactions, milk protein selection (WPI vs. NaCN) and optimisation of interaction conditions to microparticle formation and functional application. This systematic workflow was designed to address the limitations of HP in food systems, particularly its low dispersibility, poor heat stability, and limited emulsifying ability.

This work addresses crucial knowledge gaps in plant-dairy hybridisation, specifically by:

- Providing mechanisms for distinct heat-induced interactions between HP and WPI, and between HP and NaCN (**Fig. 9.1**, Panel A).
- Establishing microparticulation as an effective strategy to transform unstable, aggregation-prone HP into colloidally stable and functionally microparticles via pH and thermal treatments in the presence of WPI (**Fig. 9.1**, Panel B).
- Demonstrating microparticulation of HP and WPI as an effective method to convert inferior functional HP into effective emulsifiers, capable of stabilising both conventional oil-in-water (O/W) emulsions and high internal phase emulsions (HIPEs) with improved heat stability (**Fig. 9.1**, Panel C).

These findings significantly advance fundamental understanding of hybrid protein complexation, particle design, and demonstrate how plant-milk protein hybrids can be strategically utilised as effective emulsifiers with exceptional thermal stability. The incorporation of HP into the oil–water interface demonstrated that the strategies, such as microparticulation combined with hybridisation, can improve the emulsifying potential of plant proteins. These insights lay the groundwork for developing more functional protein ingredients from underutilised plant sources.

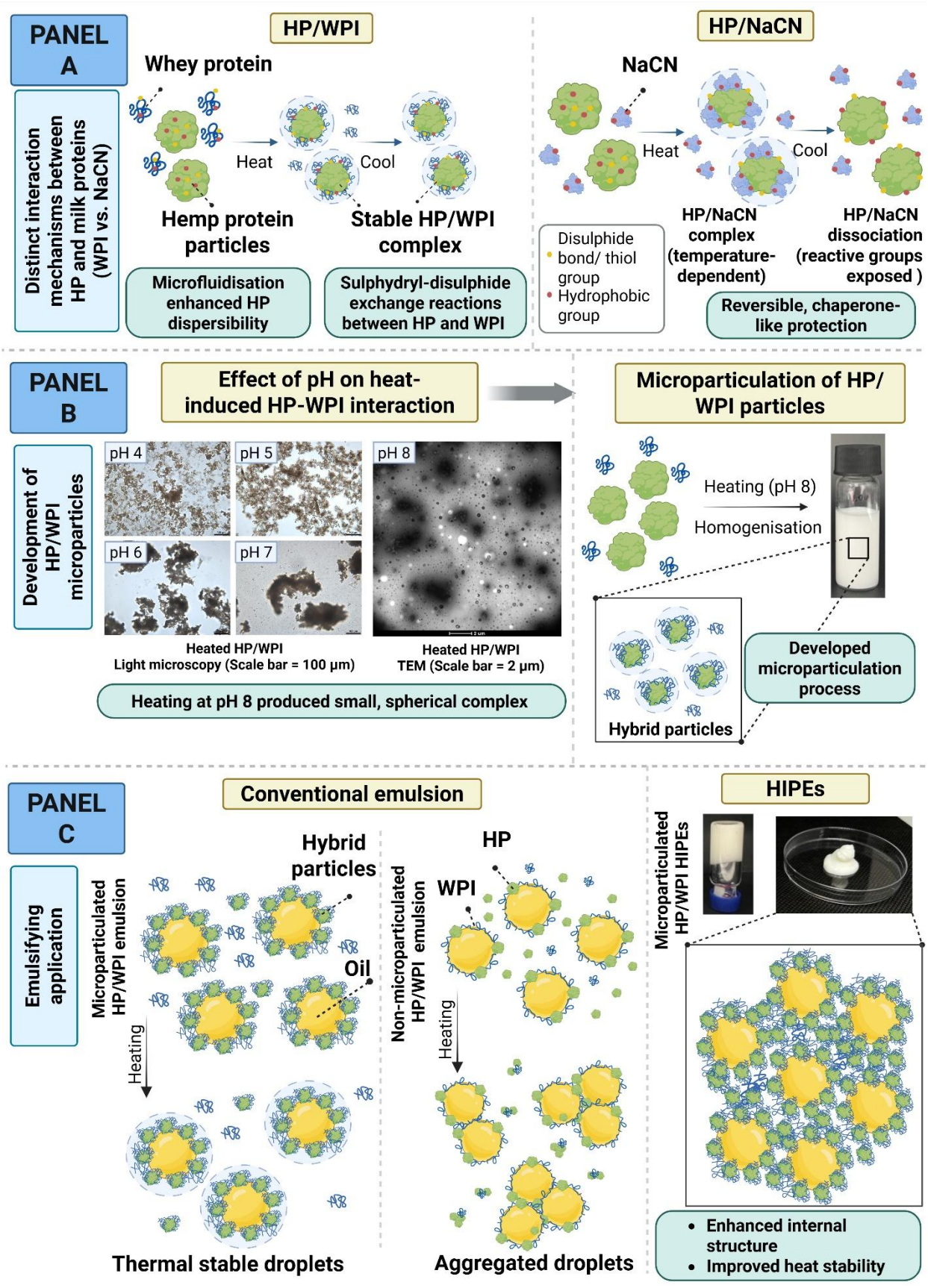


**Fig. 9.1.** Graphical summary of the key findings presented in this thesis.

## 9.2 Recommendation for future work

This thesis has provided valuable insights into the development of functional hybrid protein ingredients through the microparticulation of hemp protein and milk proteins, particularly whey protein isolate. However, several aspects remain to be explored in future studies to further advance this research and facilitate practical applications.

### 9.2.1 Structural changes in hybrid protein particles

Although this study demonstrated the interaction mechanism between HP and milk protein, the specific protein structural changes during heat-induced complexation remain unclear. Future studies could be conducted to investigate how the heat treatment and binary protein environment influence the secondary and tertiary protein structures. Techniques such as circular dichroism (CD), Fourier transform infrared spectroscopy (FTIR) and Raman spectroscopy could be used to provide insights into protein unfolding, conformational rearrangements and binding location between hemp and milk proteins. At the same time, examining the spatial distribution and localisation of hemp and whey proteins within the hybrid microparticles would further clarify how internal particle structure relates to functionality.

### 9.2.2 Heat-induced interactions between other plant proteins and milk proteins

Given the diversity in plant protein composition, structure, and functional properties, different plant proteins are likely to interact differently with milk proteins. To gain in-depth knowledge of plant-milk protein hybridisation, it is recommended to expand this approach to other plant-animal protein systems, such as soy, pea, faba bean, or oat proteins in combination with whey protein or caseins. Such studies could help identify protein-specific

or universal models for protein interactions and microparticulation strategies across various protein sources.

### 9.2.3 Production of HP/WPI microparticles at a pilot scale

To assess the industrial feasibility of using HP/WPI microparticles, future research should focus on scaling up the microparticulation process to a pilot scale. It is worth noting that the protein concentration used in this study might be relatively low (2%) when it comes to industrial scale. Therefore, future work could investigate whether the microparticulation process can be adapted to higher protein concentrations, which requires finding suitable processing equipment and conditions (e.g., thermal processing and shear conditions) to handle more concentrated protein dispersions.

### 9.2.4 Effect of drying on hybrid protein particles and their techno-functionality

The transformation of HP/WPI particle dispersions into a dry powder via spray-drying or freeze-drying would enhance their shelf-life and transportability and extend their applications in different food formulations. However, the drying process may alter the structural integrity and interfacial properties of the hybrid particles, which in turn could influence their functional performance. Future studies could investigate how different drying methods and conditions affect the re-dispersibility, rheological behaviour, and emulsifying capacity.

### 9.2.5 Other techno-functional properties of hybrid particles

While this thesis focused on the emulsion properties of hybrid protein microparticles, their unique structure may offer a broader range of techno-functional

properties in food systems. They may have potential as structural agents in protein-based gel systems, where they could influence gelation, network microstructure, and rheological behaviour. Hybrid particles may also contribute to other techno-functional properties such as foaming capacity and stability, water-holding ability, or even acting as fat replacers or texture modifiers in complex food matrices. Future studies could explore how these hybrid particles perform across different applications. The hybrid particles may be particularly useful in products such as salad dressings, sauces, beverages, fat-reduced spreads and cream or yoghurt style products, where stable emulsions and controlled texture are essential.

### 9.2.6 Effect of the degree of plant protein denaturation on microparticulation

In this thesis, the hemp protein used for microparticulation was subjected to extensive processing, which likely had a high level of denaturation before its interaction with milk proteins. However, the extent of plant protein denaturation is expected to have a significant structural and functional influence on the resulting hybrid particles. Future research could prepare hemp protein in-house through different extraction methods, such as acid precipitation or salt extraction, to obtain hemp protein with varying degrees of native structure. Investigating how different levels of denaturation affect particle formation, protein-protein interactions, and the final techno-functional properties (e.g., emulsification efficiency, gelation behaviour, and rheology).

### 9.2.7 Long-term storage and oxidative stability of emulsions

One of the advantages of Pickering emulsions is that they generally have long-term storage stability due to the irreversible adsorption and physical barrier against coalescence. A thicker interfacial layer formed by particles may improve the oxidative stability of

emulsions. Future research could examine the long-term storage and oxidative stability under different temperature and light storage conditions.

### 9.2.8 Digestion behaviour of emulsions

Understanding the digestive fate of emulsions stabilised by HP/WPI microparticles is recommended for assessing their nutritional performance and bioavailability of encapsulated compounds, as mentioned above. Simulated *in vitro* gastrointestinal digestion models can be used to monitor droplet breakdown, protein hydrolysis and lipid release. Such studies could also investigate the influence of protein microparticulation on particle structures and the digestion behaviour of emulsions.

## Bibliography

Abdullah, Weiss, J., Ahmad, T., Zhang, C., & Zhang, H. (2020). A review of recent progress on high internal-phase Pickering emulsions in food science. *Trends in Food Science & Technology*, *106*, 91-103. https://doi.org/10.1016/j.tifs.2020.10.016

Ainis, W. N., Boire, A., Sole-Jamault, V., Nicolas, A., Bouhallab, S., & Ipsen, R. (2019). Contrasting Assemblies of Oppositely Charged Proteins. *Langmuir*, *35*(30), 9923-9933. https://doi.org/10.1021/acs.langmuir.9b01046

Ainis, W. N., Ersch, C., Farinet, C., Yang, Q., Glover, Z. J., & Ipsen, R. (2019). Rheological and water holding alterations in mixed gels prepared from whey proteins and rapeseed proteins. *Food Hydrocolloids*, *87*, 723-733. https://doi.org/https://doi.org/10.1016/j.foodhyd.2018.08.023

Ainis, W. N., Ersch, C., & Ipsen, R. (2018). Partial replacement of whey proteins by rapeseed proteins in heat-induced gelled systems: Effect of pH. *Food Hydrocolloids*, *77*, 397-406. https://doi.org/10.1016/j.foodhyd.2017.10.016

Ajibola, C. F., & Aluko, R. E. (2022). Physicochemical and Functional Properties of 2S, 7S, and 11S Enriched Hemp Seed Protein Fractions. *Molecules*, *27*(3), 1059. https://doi.org/10.3390/molecules27031059

Akbari, A., Bamdad, F., & Wu, J. (2018). Chaperone-like food components: from basic concepts to food applications. *Food & function*, *9*(7), 3597-3609. https://doi.org/10.1039/C7FO01902E

Akharume, F. U., Aluko, R. E., & Adedeji, A. A. (2021). Modification of plant proteins for improved functionality: A review. *Comprehensive Reviews in Food Science and Food Safety*, *20*(1), 198-224. https://doi.org/10.1111/1541-4337.12688

Alavi, F., Emam-Djomeh, Z., & Chen, L. (2020). Acid-induced gelation of thermal co-aggregates from egg white and hempseed protein: Impact of microbial transglutaminase on mechanical and microstructural properties of gels. *Food Hydrocolloids*, *107*, 105960. https://doi.org/10.1016/j.foodhyd.2020.105960

Allahdad, Z., Salmieri, S., & Lacroix, M. (2023). Fabrication of heat-stable composite microparticles from egg and whey proteins and their application in emulsion stabilization. *Food Hydrocolloids*, *144*. https://doi.org/10.1016/j.foodhyd.2023.108943

Aloo, S. O., Mwiti, G., Ngugi, L. W., & Oh, D. H. (2024). Uncovering the secrets of industrial hemp in food and nutrition: The trends, challenges, and new-age perspectives. *Crit Rev Food Sci Nutr*, *64*(15), 5093-5112. https://doi.org/10.1080/10408398.2022.2149468

Alrosan, M., Tan, T.-C., Easa, A. M., Gammoh, S., & Alu'datt, M. H. (2021). Molecular forces governing protein-protein interaction: Structure-function relationship of complexes protein in the food industry. *Critical Reviews in Food Science and Nutrition*, 1-17. https://doi.org/10.1080/10408398.2021.1871589

**Bibliography**


Alu'datt, M. H., Alli, I., & Nagadi, M. (2012). Preparation, characterization and properties of whey-soy proteins co-precipitates. *Food Chemistry*, *134*(1), 294-300. https://doi.org/10.1016/j.foodchem.2012.02.142

Aluko, R. E. (2017). Chapter 7 - Hemp Seed (Cannabis sativa L.) Proteins: Composition, Structure, Enzymatic Modification, and Functional or Bioactive Properties. In S. R. Nadathur, J. P. D. Wanasundara, & L. Scanlin (Eds.), *Sustainable Protein Sources* (pp. 121-132). Academic Press. https://doi.org/https://doi.org/10.1016/B978-0-12-802778-3.00007-X

Alves, A. C., & Tavares, G. M. (2019). Mixing animal and plant proteins: Is this a way to improve protein techno-functionalities? *Food Hydrocolloids*, *97*, 105171. https://doi.org/https://doi.org/10.1016/j.foodhyd.2019.06.016

Amagliani, L., & Schmitt, C. (2017). Globular plant protein aggregates for stabilization of food foams and emulsions. *Trends in Food Science & Technology*, *67*, 248-259. https://doi.org/10.1016/j.tifs.2017.07.013

Anema, S. G. (2007). Role of κ-Casein in the Association of Denatured Whey Proteins with Casein Micelles in Heated Reconstituted Skim Milk. *Journal of Agricultural and Food Chemistry*, *55*(9), 3635-3642. https://doi.org/10.1021/jf062734m

Anema, S. G. (2020). Chapter 9 - The whey proteins in milk: Thermal denaturation, physical interactions, and effects on the functional properties of milk. In M. Boland & H. Singh (Eds.), *Milk Proteins (Third Edition)* (pp. 325-384). Academic Press. https://doi.org/https://doi.org/10.1016/B978-0-12-815251-5.00009-8

Anema, S. G. (2021). Heat-induced changes in caseins and casein micelles, including interactions with denatured whey proteins. *International Dairy Journal*, *122*, 105136. https://doi.org/https://doi.org/10.1016/j.idairyj.2021.105136

Anema, S. G., & Li, Y. (2003a). Association of denatured whey proteins with casein micelles in heated reconstituted skim milk and its effect on casein micelle size. *Journal of Dairy Research*, *70*(1), 73-83. https://doi.org/10.1017/S0022029902005903

Anema, S. G., & Li, Y. (2003b). Effect of pH on the Association of Denatured Whey Proteins with Casein Micelles in Heated Reconstituted Skim Milk. *Journal of Agricultural and Food Chemistry*, *51*(6), 1640-1646. https://doi.org/10.1021/jf025673a

Anuradha, S., & Prakash, V. (2009). Complexation of bovine β-lactoglobulin with 11S protein fractions of soybean (Glycine max) and sesame (Sesamum indicum). *International journal of food sciences and nutrition*, *60*(sup1), 27-42. https://doi.org/10.1080/09637480701877736

Anvari, M., & Joyner, H. S. (2017). Effect of formulation on structure-function relationships of concentrated emulsions: Rheological, tribological, and microstructural characterization. *Food Hydrocolloids*, *72*, 11-26. https://doi.org/10.1016/j.foodhyd.2017.04.034

**Bibliography**


Anvari, M., & Joyner, H. S. (2018). Effect of fish gelatin and gum arabic interactions on concentrated emulsion large amplitude oscillatory shear behavior and tribological properties. *Food Hydrocolloids*, *79*, 518-525. https://doi.org/10.1016/j.foodhyd.2017.12.016

AOAC Official Method 922.06Fat in Flour: Acid Hydrolysis Method. (2023). In G. W. Latimer, Jr. (Ed.), *Official Methods of Analysis of AOAC INTERNATIONAL* (pp. 0). Oxford University Press. https://doi.org/10.1093/9780197610145.003.2938

AOAC Official Method 925.10Solids (Total) and Loss on Drying (Moisture) in Flour: Air Oven Method. (2023). In G. W. Latimer, Jr. (Ed.), *Official Methods of Analysis of AOAC INTERNATIONAL* (pp. 0). Oxford University Press. https://doi.org/10.1093/9780197610145.003.2927

AOAC Official Method 942.05Ash of Animal Feed. (2023). In *Official Methods of Analysis of AOAC INTERNATIONAL* (pp. 0). Oxford University Press. https://doi.org/10.1093/9780197610145.003.1389

AOAC Official Method 991.20Nitrogen (Total) in Milk: Kjeldahl Methods. (2023). In G. W. Latimer, Jr. (Ed.), *Official Methods of Analysis of AOAC INTERNATIONAL* (pp. 0). Oxford University Press. https://doi.org/10.1093/9780197610145.003.3045

Arntfield, S. D., & Maskus, H. D. (2011). Peas and other legume proteins. In G. O. Phillips & P. A. Williams (Eds.), *Handbook of Food Proteins* (pp. 233-266). Woodhead Publishing. https://doi.org/https://doi.org/10.1533/9780857093639.233

Augustin, M. A., Oliver, C. M., & Hemar, Y. (2011). Casein, caseinates, and milk protein concentrates. *Dairy ingredients for food processing*, *1*, 161-178. https://doi.org/10.1002/9780470959169.ch7

Bárta, J., Roudnický, P., Jarošová, M., Zdráhal, Z., Stupková, A., Bártová, V., Krejčová, Z., Kyselka, J., Filip, V., & Říha, V. (2023). Proteomic profiles of whole seeds, hulls, and dehulled seeds of two industrial hemp (Cannabis sativa L.) cultivars. *Plants*, *13*(1), 111.

Beghdadi, A., Picart-Palmade, L., Cunault, C., Marchesseau, S., & Chevalier-Lucia, D. (2022). Impact of two thermal processing routes on protein interactions and acid gelation properties of casein micelle-pea protein mixture compared to casein micelle-whey protein one. *Food Research International*, *155*, 111060. https://doi.org/https://doi.org/10.1016/j.foodres.2022.111060

Beliciu, C. M., & Moraru, C. I. (2011). The effect of protein concentration and heat treatment temperature on micellar casein–soy protein mixtures. *Food Hydrocolloids*, *25*(6), 1448-1460. https://doi.org/https://doi.org/10.1016/j.foodhyd.2011.01.011

Beliciu, C. M., & Moraru, C. I. (2013). Physico-chemical changes in heat treated micellar casein - Soy protein mixtures [Article]. *LWT - Food Science and Technology*, *54*(2), 469-476. https://doi.org/10.1016/j.lwt.2013.06.013

**Bibliography**


Beran, M., Drahorad, J., Vltavsky, O., Urban, M., Laknerova, I., Fronek, M., Sova, J., Ondracek, J., Ondrackova, L., & Kralova, M. (2018). Pilot-scale production and application of microparticulated plant proteins. *J Nutr Food Sci*, *8*(1), 655-662. https://doi.org/10.4172/2155-9600.1000655

Berton-Carabin, C. C., & Schroen, K. (2015). Pickering emulsions for food applications: background, trends, and challenges. *Annu Rev Food Sci Technol*, *6*, 263-297. https://doi.org/10.1146/annurev-food-081114-110822

Bhattacharyya, J., & Das, K. P. (1999). Molecular chaperone-like properties of an unfolded protein, alpha(s)-casein. *J Biol Chem*, *274*(22), 15505-15509. https://doi.org/10.1074/jbc.274.22.15505

Binks, B. P. (2002). Particles as surfactants—similarities and differences. *Current Opinion in Colloid & Interface Science*, *7*(1), 21-41. https://doi.org/https://doi.org/10.1016/S1359-0294(02)00008-0

Boland, M. (2011). Whey proteins. In G. O. Phillips & P. A. Williams (Eds.), *Handbook of Food Proteins* (pp. 30-55). Woodhead Publishing. https://doi.org/https://doi.org/10.1533/9780857093639.30

Boland, M., & Singh, H. (2019). *Milk proteins: from expression to food*. Academic Press.

Boland, M. J., Rae, A. N., Vereijken, J. M., Meuwissen, M. P. M., Fischer, A. R. H., van Boekel, M. A. J. S., Rutherfurd, S. M., Gruppen, H., Moughan, P. J., & Hendriks, W. H. (2013). The future supply of animal-derived protein for human consumption. *Trends in Food Science & Technology*, *29*(1), 62-73. https://doi.org/10.1016/j.tifs.2012.07.002

Brodkorb, A., Croguennec, T., Bouhallab, S., & Kehoe, J. J. (2016). Heat-Induced Denaturation, Aggregation and Gelation of Whey Proteins. In P. L. H. McSweeney & J. A. O'Mahony (Eds.), *Advanced Dairy Chemistry: Volume 1B: Proteins: Applied Aspects* (pp. 155-178). Springer New York. https://doi.org/10.1007/978-1-4939-2800-2_6

Broyard, C., & Gaucheron, F. (2015). Modifications of structures and functions of caseins: a scientific and technological challenge. *Dairy Science & Technology*, *95*(6), 831-862. https://doi.org/10.1007/s13594-015-0220-y

Bryant, C. M., & McClements, D. J. (1998). Molecular basis of protein functionality with special consideration of cold-set gels derived from heat-denatured whey. *Trends in Food Science & Technology*, *9*(4), 143-151. https://doi.org/https://doi.org/10.1016/S0924-2244(98)00031-4

Çakır-Fuller, E. (2015). Enhanced heat stability of high protein emulsion systems provided by microparticulated whey proteins. *Food Hydrocolloids*, *47*, 41-50. https://doi.org/10.1016/j.foodhyd.2015.01.003

Callaway, J. C. (2004). Hempseed as a nutritional resource: An overview. *Euphytica*, *140*(1), 65-72. https://doi.org/10.1007/s10681-004-4811-6

**Bibliography**


Cattaneo, C., Givonetti, A., Leoni, V., Guerrieri, N., Manfredi, M., Giorgi, A., & Cavaletto, M. (2021). Biochemical aspects of seeds from Cannabis sativa L. plants grown in a mountain environment. *Sci Rep*, *11*(1), 3927. https://doi.org/10.1038/s41598-021-83290-1

Chanamai, R., & McClements, D. J. (2002). Comparison of Gum Arabic, Modified Starch, and Whey Protein Isolate as Emulsifiers: Influence of pH, CaCl2 and Temperature. *Journal of Food Science*, *67*(1), 120-125. https://doi.org/10.1111/j.1365-2621.2002.tb11370.x

Chang, C., Niu, F., Gu, L., Li, X., Yang, H., Zhou, B., Wang, J., Su, Y., & Yang, Y. (2016). Formation of fibrous or granular egg white protein microparticles and properties of the integrated emulsions. *Food Hydrocolloids*, *61*, 477-486. https://doi.org/https://doi.org/10.1016/j.foodhyd.2016.06.002

Cheison, S. C., & Kulozik, U. (2017). Impact of the environmental conditions and substrate pre-treatment on whey protein hydrolysis: A review. *Critical Reviews in Food Science and Nutrition*, *57*(2), 418-453. https://doi.org/10.1080/10408398.2014.959115

Chen, H., Xu, B., Wang, Y., Li, W., He, D., Zhang, Y., Zhang, X., & Xing, X. (2023). Emerging natural hemp seed proteins and their functions for nutraceutical applications. *Food Science and Human Wellness*, *12*(4), 929-941. https://doi.org/10.1016/j.fshw.2022.10.016

Chen, J., Liang, R.-H., Liu, W., Liu, C.-M., Li, T., Tu, Z.-C., & Wan, J. (2012). Degradation of high-methoxyl pectin by dynamic high pressure microfluidization and its mechanism. *Food Hydrocolloids*, *28*(1), 121-129. https://doi.org/https://doi.org/10.1016/j.foodhyd.2011.12.018

Chen, L., Remondetto, G. E., & Subirade, M. (2006). Food protein-based materials as nutraceutical delivery systems. *Trends in Food Science & Technology*, *17*(5), 272-283. https://doi.org/10.1016/j.tifs.2005.12.011

Chen, N., Lin, L., Sun, W., & Zhao, M. (2014). Stable and pH-sensitive protein nanogels made by self-assembly of heat denatured soy protein. *J Agric Food Chem*, *62*(39), 9553-9561. https://doi.org/10.1021/jf502572d

Chevalier, Y., & Bolzinger, M.-A. (2013). Emulsions stabilized with solid nanoparticles: Pickering emulsions. *Colloids and Surfaces A: Physicochemical and Engineering Aspects*, *439*, 23-34. https://doi.org/https://doi.org/10.1016/j.colsurfa.2013.02.054

Chihi, M.-L., Mession, J.-l., Sok, N., & Saurel, R. (2016). Heat-Induced Soluble Protein Aggregates from Mixed Pea Globulins and β-Lactoglobulin. *Journal of Agricultural and Food Chemistry*, *64*(13), 2780-2791. https://doi.org/10.1021/acs.jafc.6b00087

Chihi, M.-L., Sok, N., & Saurel, R. (2018). Acid gelation of mixed thermal aggregates of pea globulins and β-lactoglobulin. *Food Hydrocolloids*, *85*, 120-128. https://doi.org/https://doi.org/10.1016/j.foodhyd.2018.07.006

**Bibliography**


Chuang, C.-C., Wegrzyn, T. F., Anema, S. G., & Loveday, S. M. (2019). Hemp globulin heat aggregation is inhibited by the chaperone-like action of caseins. *Food Hydrocolloids*, *93*, 46-55. https://doi.org/10.1016/j.foodhyd.2019.01.061

Chuang, C.-C., Ye, A., Anema, S. G., & Loveday, S. M. (2020). Concentrated Pickering emulsions stabilised by hemp globulin–caseinate nanoparticles: tuning the rheological properties by adjusting the hemp globulin: caseinate ratio. *Food & function*, *11*(11), 10193-10204. https://doi.org/10.1039/D0FO01745K

Chuang, C.-C., Ye, A., Anema, S. G., & Loveday, S. M. (2021). Hemp globulin forms colloidal nanocomplexes with sodium caseinate during pH-cycling. *Food Research International*, *150*, 110810. https://doi.org/https://doi.org/10.1016/j.foodres.2021.110810

Chung, C., Degner, B., & McClements, D. J. (2014a). Development of Reduced-calorie foods: Microparticulated whey proteins as fat mimetics in semi-solid food emulsions. *Food Research International*, *56*, 136-145. https://doi.org/https://doi.org/10.1016/j.foodres.2013.11.034

Chung, C., Degner, B., & McClements, D. J. (2014b). Reduced calorie emulsion-based foods: Protein microparticles and dietary fiber as fat replacers. *Food Research International*, *64*, 664-676. https://doi.org/https://doi.org/10.1016/j.foodres.2014.07.034

Clark, A. H., Kavanagh, G. M., & Ross-Murphy, S. B. (2001). Globular protein gelation—theory and experiment. *Food Hydrocolloids*, *15*(4), 383-400. https://doi.org/https://doi.org/10.1016/S0268-005X(01)00042-X

Comfort, S., & Howell, N. K. (2002). Gelation properties of soya and whey protein isolate mixtures. *Food Hydrocolloids*, *16*(6), 661-672. https://doi.org/https://doi.org/10.1016/S0268-005X(02)00033-4

Cornacchia, L., Forquenot de la Fortelle, C., & Venema, P. (2014). Heat-induced aggregation of whey proteins in aqueous solutions below their isoelectric point. *J Agric Food Chem*, *62*(3), 733-741. https://doi.org/10.1021/jf404456q

Corredig, M., & Dalgleish, D. G. (1996). Effect of temperature and pH on the interactions of whey proteins with casein micelles in skim milk. *Food Research International*, *29*(1), 49-55. https://doi.org/https://doi.org/10.1016/0963-9969(95)00058-5

Corredig, M., & Dalgleish, D. G. (1999). The mechanisms of the heat-induced interaction of whey proteins with casein micelles in milk. *International Dairy Journal*, *9*(3), 233-236. https://doi.org/https://doi.org/10.1016/S0958-6946(99)00066-7

Cui, L., Bandillo, N., Wang, Y., Ohm, J.-B., Chen, B., & Rao, J. (2020). Functionality and structure of yellow pea protein isolate as affected by cultivars and extraction pH. *Food Hydrocolloids*, *108*, 106008. https://doi.org/https://doi.org/10.1016/j.foodhyd.2020.106008

Cui, S., Yu, Y., McClements, D. J., Liu, C., Xu, X., Sun, Q., Wang, P., & Dai, L. (2025). High internal phase Pickering emulsions co-stabilized by zein nanoparticles and

cellulose nanocrystals: Fabrication, characterization, and application. *Food Hydrocolloids*, *159*. https://doi.org/10.1016/j.foodhyd.2024.110650

Cui, Z., Chen, Y., Kong, X., Zhang, C., & Hua, Y. (2014). Emulsifying Properties and Oil/Water (O/W) Interface Adsorption Behavior of Heated Soy Proteins: Effects of Heating Concentration, Homogenizer Rotating Speed, and Salt Addition Level. *Journal of Agricultural and Food Chemistry*, *62*(7), 1634-1642. https://doi.org/10.1021/jf404464z

da Silva, R. R., Odelli, D., Descamps, A., Scudeller, L. A., Doumert, B., Perez, J., Delaplace, G., de Carvalho, A. F., & de Sa Peixoto Junior, P. P. (2025). Multi-scale organization and rheology of casein and pea protein mixed hydrogels formed by acidification: Effects of ratio and temperature. *Food Res Int*, *209*, 116242. https://doi.org/10.1016/j.foodres.2025.116242

Dai, L., Yang, S., Wei, Y., Sun, C., McClements, D. J., Mao, L., & Gao, Y. (2019). Development of stable high internal phase emulsions by pickering stabilization: Utilization of zein-propylene glycol alginate-rhamnolipid complex particles as colloidal emulsifiers. *Food Chem*, *275*, 246-254. https://doi.org/10.1016/j.foodchem.2018.09.122

Dalgleish, D. G. (2011). On the structural models of bovine casein micelles—review and possible improvements. *Soft matter*, *7*(6), 2265-2272. https://doi.org/10.1039/c0sm00806k

Dalgleish, D. G., Euston, S. E., Hunt, J. A., & Dickinson, E. (1991). Competitive adsorption of β-lactoglobulin in mixed protein emulsions. In *Food polymers, gels and colloids* (pp. 485-489). Elsevier. https://doi.org/10.1533/9781845698331.1.485

Dalgleish, D. G., van Mourik, L., & Corredig, M. (1997). Heat-Induced Interactions of Whey Proteins and Casein Micelles with Different Concentrations of α-Lactalbumin and β-Lactoglobulin. *Journal of Agricultural and Food Chemistry*, *45*(12), 4806-4813. https://doi.org/10.1021/jf970524r

Damodaran, S. (2005). Protein Stabilization of Emulsions and Foams. *Journal of Food Science*, *70*(3), R54-R66. https://doi.org/https://doi.org/10.1111/j.1365-2621.2005.tb07150.x

Dapčević-Hadnađev, T., Dizdar, M., Pojić, M., Krstonošić, V., Zychowski, L. M., & Hadnađev, M. (2019). Emulsifying properties of hemp proteins: Effect of isolation technique. *Food Hydrocolloids*, *89*, 912-920. https://doi.org/https://doi.org/10.1016/j.foodhyd.2018.12.002

Dapčević-Hadnađev, T., Hadnađev, M., Dizdar, M., & Lješković, N. J. (2020). Functional and bioactive properties of hemp proteins. In *Sustainable Agriculture Reviews 42* (pp. 239-263). Springer. https://doi.org/10.1007/978-3-030-41384-2_8

Dapčević-Hadnađev, T., Hadnađev, M., Lazaridou, A., Moschakis, T., & Biliaderis, C. G. (2018). Hempseed meal protein isolates prepared by different isolation techniques.

Part II. gelation properties at different ionic strengths. *Food Hydrocolloids*, *81*, 481-489. https://doi.org/10.1016/j.foodhyd.2018.03.022

Dave, A. C., Ye, A., & Singh, H. (2019). Structural and interfacial characteristics of oil bodies in coconuts (Cocos nucifera L.). *Food Chemistry*, *276*, 129-139. https://doi.org/https://doi.org/10.1016/j.foodchem.2018.09.125

Day, L. (2013). Proteins from land plants – Potential resources for human nutrition and food security. *Trends in Food Science & Technology*, *32*(1), 25-42. https://doi.org/https://doi.org/10.1016/j.tifs.2013.05.005

de Folter, J. W. J., van Ruijven, M. W. M., & Velikov, K. P. (2012). Oil-in-water Pickering emulsions stabilized by colloidal particles from the water-insoluble protein zein. *Soft matter*, *8*(25). https://doi.org/10.1039/c2sm07417f

de la Fuente, M. A., Singh, H., & Hemar, Y. (2002). Recent advances in the characterisation of heat-induced aggregates and intermediates of whey proteins. *Trends in Food Science & Technology*, *13*(8), 262-274. https://doi.org/10.1016/S0924-2244(02)00133-4

Dewettinck, K., Rombaut, R., Thienpont, N., Le, T. T., Messens, K., & Van Camp, J. (2008). Nutritional and technological aspects of milk fat globule membrane material. *International Dairy Journal*, *18*(5), 436-457. https://doi.org/https://doi.org/10.1016/j.idairyj.2007.10.014

Dhayal, S. K., Gruppen, H., de Vries, R., & Wierenga, P. A. (2014). Controlled formation of protein nanoparticles by enzymatic cross-linking of α-lactalbumin with horseradish peroxidase. *Food Hydrocolloids*, *36*, 53-59. https://doi.org/10.1016/j.foodhyd.2013.09.003

Dias, C. L., Ala-Nissila, T., Wong-ekkabut, J., Vattulainen, I., Grant, M., & Karttunen, M. (2010). The hydrophobic effect and its role in cold denaturation. *Cryobiology*, *60*(1), 91-99. https://doi.org/10.1016/j.cryobiol.2009.07.005

Dickinson, E. (1992). Faraday research article. Structure and composition of adsorbed protein layers and the relationship to emulsion stability. *Journal of the Chemical Society, Faraday Transactions*, *88*(20), 2973-2983. https://doi.org/10.1039/FT9928802973

Dickinson, E. (2003). Hydrocolloids at interfaces and the influence on the properties of dispersed systems. *Food Hydrocolloids*, *17*(1), 25-39. https://doi.org/10.1016/S0268-005X(01)00120-5

Dickinson, E. (2012). Use of nanoparticles and microparticles in the formation and stabilization of food emulsions. *Trends in Food Science & Technology*, *24*(1), 4-12. https://doi.org/10.1016/j.tifs.2011.09.006

Dickinson, E. (2013). Stabilising emulsion-based colloidal structures with mixed food ingredients. *J Sci Food Agric*, *93*(4), 710-721. https://doi.org/10.1002/jsfa.6013

**Bibliography**


Dickinson, E. (2015). Colloids in food: ingredients, structure, and stability. *Annu Rev Food Sci Technol*, *6*, 211-233. https://doi.org/10.1146/annurev-food-022814-015651

Dickinson, E. (2017). Biopolymer-based particles as stabilizing agents for emulsions and foams. *Food Hydrocolloids*, *68*, 219-231. https://doi.org/10.1016/j.foodhyd.2016.06.024

Dickinson, E., Golding, M., & Povey, M. J. W. (1997). Creaming and Flocculation of Oil-in-Water Emulsions Containing Sodium Caseinate. *Journal of Colloid and Interface Science*, *185*(2), 515-529. https://doi.org/https://doi.org/10.1006/jcis.1996.4605

Dissanayake, M., Liyanaarachchi, S., & Vasiljevic, T. (2012). Functional properties of whey proteins microparticulated at low pH. *Journal of Dairy Science*, *95*(4), 1667-1679. https://doi.org/https://doi.org/10.3168/jds.2011-4823

Dissanayake, M., Ramchandran, L., Donkor, O. N., & Vasiljevic, T. (2013). Denaturation of whey proteins as a function of heat, pH and protein concentration. *International Dairy Journal*, *31*(2), 93-99. https://doi.org/10.1016/j.idairyj.2013.02.002

Dissanayake, M., Ramchandran, L., Piyadasa, C., & Vasiljevic, T. (2013). Influence of heat and pH on structure and conformation of whey proteins. *International Dairy Journal*, *28*(2), 56-61. https://doi.org/10.1016/j.idairyj.2012.08.014

Dissanayake, M., & Vasiljevic, T. (2009). Functional properties of whey proteins affected by heat treatment and hydrodynamic high-pressure shearing. *Journal of Dairy Science*, *92*(4), 1387-1397. https://doi.org/https://doi.org/10.3168/jds.2008-1791

Do, D. T., Ye, A., Singh, H., & Acevedo-Fani, A. (2024). Protein bodies from hemp seeds: Isolation, microstructure and physicochemical characterisation. *Food Hydrocolloids*, *149*. https://doi.org/10.1016/j.foodhyd.2023.109597

Do, D. T., Ye, A., Singh, H., & Acevedo-Fani, A. (2025). Heat-induced dissociation and association of proteins in hempseed protein bodies. *Food Hydrocolloids*, *166*. https://doi.org/10.1016/j.foodhyd.2025.111372

Docimo, T., Caruso, I., Ponzoni, E., Mattana, M., & Galasso, I. (2014). Molecular characterization of edestin gene family in Cannabis sativa L. *Plant Physiology and Biochemistry*, *84*, 142-148. https://doi.org/https://doi.org/10.1016/j.plaphy.2014.09.011

Duvarci, O. C., Yazar, G., & Kokini, J. L. (2017). The SAOS, MAOS and LAOS behavior of a concentrated suspension of tomato paste and its prediction using the Bird-Carreau (SAOS) and Giesekus models (MAOS-LAOS). *Journal of Food Engineering*, *208*, 77-88. https://doi.org/10.1016/j.jfoodeng.2017.02.027

Edwards, P. J., & Jameson, G. B. (2020). Structure and stability of whey proteins. In *Milk proteins* (pp. 251-291). Elsevier. https://doi.org/10.1016/B978-0-12-815251-5.00007-4

**Bibliography**


El-Sohaimy, S. A., Androsova, N. V., Toshev, A. D., & El Enshasy, H. A. (2022). Nutritional Quality, Chemical, and Functional Characteristics of Hemp (Cannabis sativa ssp. sativa) Protein Isolate. *Plants (Basel)*, *11*(21). https://doi.org/10.3390/plants11212825

Euston, S. R., Finnigan, S. R., & Hirst, R. L. (2000). Aggregation kinetics of heated whey protein-stabilized emulsions. *Food Hydrocolloids*, *14*(2), 155-161. https://doi.org/https://doi.org/10.1016/S0268-005X(99)00061-2

Evans, M., Ratcliffe, I., & Williams, P. A. (2013). Emulsion stabilisation using polysaccharide–protein complexes. *Current Opinion in Colloid & Interface Science*, *18*(4), 272-282. https://doi.org/10.1016/j.cocis.2013.04.004

Ewoldt, R., Hosoi, A. E., & McKinley, G. H. (2007). Rheological fingerprinting of complex fluids using large amplitude oscillatory shear (LAOS) flow. *Annual Transactions-Nordic Rheology Society*, *15*, 3.

Ewoldt, R. H., Hosoi, A., & McKinley, G. H. (2008). New measures for characterizing nonlinear viscoelasticity in large amplitude oscillatory shear. *Journal of Rheology*, *52*(6), 1427-1458. https://doi.org/10.1122/1.2970095

Ewoldt, R. H., Winter, P., Maxey, J., & McKinley, G. H. (2009). Large amplitude oscillatory shear of pseudoplastic and elastoviscoplastic materials. *Rheologica Acta*, *49*(2), 191-212. https://doi.org/10.1007/s00397-009-0403-7

Fan, Y., Peng, G., Pang, X., Wen, Z., & Yi, J. (2021). Physicochemical, emulsifying, and interfacial properties of different whey protein aggregates obtained by thermal treatment. *LWT*, *149*. https://doi.org/10.1016/j.lwt.2021.111904

Fang, B., Chang, L., Ohm, J.-B., Chen, B., & Rao, J. (2023). Structural, functional properties, and volatile profile of hemp protein isolate as affected by extraction method: Alkaline extraction–isoelectric precipitation vs salt extraction. *Food Chemistry*, *405*, 135001. https://doi.org/10.1016/j.foodchem.2022.135001

Farias, B. V., & Khan, S. A. (2021). Probing gels and emulsions using large-amplitude oscillatory shear and frictional studies with soft substrate skin surrogates. *Colloids Surf B Biointerfaces*, *201*, 111595. https://doi.org/10.1016/j.colsurfb.2021.111595

Farrell, H. M., Malin, E. L., Brown, E. M., & Mora-Gutierrez, A. (2009). Review of the chemistry of αS2-casein and the generation of a homologous molecular model to explain its properties1. *Journal of Dairy Science*, *92*(4), 1338-1353. https://doi.org/https://doi.org/10.3168/jds.2008-1711

Farrell, H. M., Malin, E. L., Brown, E. M., & Qi, P. X. (2006). Casein micelle structure: What can be learned from milk synthesis and structural biology? *Current Opinion in Colloid & Interface Science*, *11*(2), 135-147. https://doi.org/https://doi.org/10.1016/j.cocis.2005.11.005

Feng, T., Wang, X., Wang, X., Zhang, X., Gu, Y., Xia, S., & Huang, Q. (2021). High internal phase pickering emulsions stabilized by pea protein isolate-high methoxyl

pectin-EGCG complex: Interfacial properties and microstructure. *Food Chem*, *350*, 129251. https://doi.org/10.1016/j.foodchem.2021.129251

Feng, Y., & Lee, Y. (2016). Surface modification of zein colloidal particles with sodium caseinate to stabilize oil-in-water pickering emulsion. *Food Hydrocolloids*, *56*, 292-302. https://doi.org/https://doi.org/10.1016/j.foodhyd.2015.12.030

Feng, Y., Yu, D., Lin, T., Jin, Q., Wu, J., Chen, C., & Huang, H. (2021). Complexing hemp seed protein with pectin for improved emulsion stability. *J Food Sci*, *86*(7), 3137-3147. https://doi.org/10.1111/1750-3841.15810

Foegeding, E. A., & Davis, J. P. (2011). Food protein functionality: A comprehensive approach. *Food Hydrocolloids*, *25*(8), 1853-1864. https://doi.org/https://doi.org/10.1016/j.foodhyd.2011.05.008

Forte, A., D'amico, F., Charalambides, M., Dini, D., & Williams, J. (2015). Modelling and experimental characterisation of the rate dependent fracture properties of gelatine gels. *Food Hydrocolloids*, *46*, 180-190. https://doi.org/10.1016/j.foodhyd.2014.12.028

Galazka, V. B., Dickinson, E., & Ledward, D. A. (2000). Influence of high pressure processing on protein solutions and emulsions. *Current Opinion in Colloid & Interface Science*, *5*(3), 182-187. https://doi.org/https://doi.org/10.1016/S1359-0294(00)00055-8

Gallier, S., Gordon, K. C., & Singh, H. (2012). Chemical and structural characterisation of almond oil bodies and bovine milk fat globules. *Food Chemistry*, *132*(4), 1996-2006. https://doi.org/https://doi.org/10.1016/j.foodchem.2011.12.038

Gao, H., Ma, L., Cheng, C., Liu, J., Liang, R., Zou, L., Liu, W., & McClements, D. J. (2021). Review of recent advances in the preparation, properties, and applications of high internal phase emulsions. *Trends in Food Science & Technology*, *112*, 36-49. https://doi.org/10.1016/j.tifs.2021.03.041

Gao, Z. M., Wang, J. M., Wu, N. N., Wan, Z. L., Guo, J., Yang, X. Q., & Yin, S. W. (2013). Formation of complex interface and stability of oil-in-water (O/W) emulsion prepared by soy lipophilic protein nanoparticles. *J Agric Food Chem*, *61*(32), 7838-7847. https://doi.org/10.1021/jf4018349

Gao, Z. M., Yang, X. Q., Wu, N. N., Wang, L. J., Wang, J. M., Guo, J., & Yin, S. W. (2014). Protein-based pickering emulsion and oil gel prepared by complexes of zein colloidal particles and stearate. *J Agric Food Chem*, *62*(12), 2672-2678. https://doi.org/10.1021/jf500005y

Gholivand, S., Tan, T. B., Mat Yusoff, M., Choy, H. W., Teow, S. J., Wang, Y., Liu, Y., & Tan, C. P. (2024). Elucidation of synergistic interactions between anionic polysaccharides and hemp seed protein isolate and their functionalities in stabilizing the hemp seed oil-based nanoemulsion. *Food Hydrocolloids*, *146*. https://doi.org/10.1016/j.foodhyd.2023.109181

**Bibliography**


Gong, K., Chen, L., Xia, H., Dai, H., Li, X., Sun, L., Kong, W., & Liu, K. (2019). Driving forces of disaggregation and reaggregation of peanut protein isolates in aqueous dispersion induced by high-pressure microfluidization. *International Journal of Biological Macromolecules*, *130*, 915-921. https://doi.org/https://doi.org/10.1016/j.ijbiomac.2019.02.123

González-Pérez, S., Vereijken, J. M., Merck, K. B., van Koningsveld, G. A., Gruppen, H., & Voragen, A. G. (2004). Conformational states of sunflower (Helianthus annuus) helianthinin: effect of heat and pH. *Journal of Agricultural and Food Chemistry*, *52*(22), 6770-6778. https://doi.org/10.1021/jf049612j

Goulding, D. A., Fox, P. F., & O'Mahony, J. A. (2020). Chapter 2 - Milk proteins: An overview. In M. Boland & H. Singh (Eds.), *Milk Proteins (Third Edition)* (pp. 21-98). Academic Press. https://doi.org/https://doi.org/10.1016/B978-0-12-815251-5.00002-5

Gricius, Z., & Oye, G. (2023). Recent advances in the design and use of Pickering emulsions for wastewater treatment applications. *Soft matter*, *19*(5), 818-840. https://doi.org/10.1039/d2sm01437h

Grossmann, L., & Weiss, J. (2021). Alternative Protein Sources as Technofunctional Food Ingredients. *Annual Review of Food Science and Technology*, *12*(1), 93-117. https://doi.org/10.1146/annurev-food-062520-093642

Grygorczyk, A., Alexander, M., & Corredig, M. (2013). Combined acid‐and rennet‐induced gelation of a mixed soya milk–cow's milk system. *International Journal of Food Science & Technology*, *48*(11), 2306-2314. https://doi.org/10.1111/ijfs.12218

Gu, J., Xin, Z., Meng, X., Sun, S., Qiao, Q., & Deng, H. (2016). A "reduced-pressure distillation" method to prepare zein-based fat analogue for application in mayonnaise formulation. *Journal of Food Engineering*, *182*, 1-8. https://doi.org/https://doi.org/10.1016/j.jfoodeng.2016.01.026

Guo, J., Yang, X.-Q., He, X.-T., Wu, N.-N., Wang, J.-M., Gu, W., & Zhang, Y.-Y. (2012). Limited Aggregation Behavior of β-Conglycinin and Its Terminating Effect on Glycinin Aggregation during Heating at pH 7.0. *Journal of Agricultural and Food Chemistry*, *60*(14), 3782-3791. https://doi.org/10.1021/jf300409y

Guyomarc'h, F., Arvisenet, G., Bouhallab, S., Canon, F., Deutsch, S.-M., Drigon, V., Dupont, D., Famelart, M.-H., Garric, G., Guédon, E., Guyot, T., Hiolle, M., Jan, G., Le Loir, Y., Lechevalier, V., Nau, F., Pezennec, S., Thierry, A., Valence, F., & Gagnaire, V. (2021). Mixing milk, egg and plant resources to obtain safe and tasty foods with environmental and health benefits. *Trends in Food Science & Technology*, *108*, 119-132. https://doi.org/10.1016/j.tifs.2020.12.010

Guyomarc'h, F., Nono, M., Nicolai, T., & Durand, D. (2009). Heat-induced aggregation of whey proteins in the presence of κ-casein or sodium caseinate. *Food Hydrocolloids*, *23*(4), 1103-1110. https://doi.org/https://doi.org/10.1016/j.foodhyd.2008.07.001

**Bibliography**


HadjSadok, A., Pitkowski, A., Nicolai, T., Benyahia, L., & Moulai-Mostefa, N. (2008). Characterisation of sodium caseinate as a function of ionic strength, pH and temperature using static and dynamic light scattering. *Food Hydrocolloids*, *22*(8), 1460-1466. https://doi.org/https://doi.org/10.1016/j.foodhyd.2007.09.002

Hadnađev, M., Dapčević-Hadnađev, T., Lazaridou, A., Moschakis, T., Michaelidou, A. M., Popović, S., & Biliaderis, C. G. (2018). Hempseed meal protein isolates prepared by different isolation techniques. Part I. physicochemical properties. *Food Hydrocolloids*, *79*, 526-533. https://doi.org/https://doi.org/10.1016/j.foodhyd.2017.12.015

Hao, Z.-Z., Peng, X.-Q., & Tang, C.-H. (2020). Edible pickering high internal phase emulsions stabilized by soy glycinin: Improvement of emulsification performance and pickering stabilization by glycation with soy polysaccharide. *Food Hydrocolloids*, *103*. https://doi.org/10.1016/j.foodhyd.2020.105672

He, C., Hu, Y., Liu, Z., Woo, M. W., Xiong, H., & Zhao, Q. (2020). Interaction between casein and rice glutelin: Binding mechanisms and molecular assembly behaviours. *Food Hydrocolloids*, *107*, 105967. https://doi.org/https://doi.org/10.1016/j.foodhyd.2020.105967

He, X., Chen, J., He, X., Feng, Z., Li, C., Liu, W., Dai, T., & Liu, C. (2021). Industry-scale microfluidization as a potential technique to improve solubility and modify structure of pea protein. *Innovative Food Science & Emerging Technologies*, *67*, 102582. https://doi.org/https://doi.org/10.1016/j.ifset.2020.102582

Hinderink, E. B. A., Boire, A., Renard, D., Riaublanc, A., Sagis, L. M. C., Schroën, K., Bouhallab, S., Famelart, M.-H., Gagnaire, V., Guyomarc'h, F., & Berton-Carabin, C. C. (2021). Combining plant and dairy proteins in food colloid design. *Current Opinion in Colloid & Interface Science*, *56*, 101507. https://doi.org/https://doi.org/10.1016/j.cocis.2021.101507

Hinderink, E. B. A., Münch, K., Sagis, L., Schroën, K., & Berton-Carabin, C. C. (2019). Synergistic stabilisation of emulsions by blends of dairy and soluble pea proteins: Contribution of the interfacial composition. *Food Hydrocolloids*, *97*, 105206. https://doi.org/https://doi.org/10.1016/j.foodhyd.2019.105206

Hinderink, E. B. A., Sagis, L., Schroen, K., & Berton-Carabin, C. C. (2021). Sequential adsorption and interfacial displacement in emulsions stabilized with plant-dairy protein blends. *J Colloid Interface Sci*, *583*, 704-713. https://doi.org/10.1016/j.jcis.2020.09.066

Hinderink, E. B. A., Sagis, L., Schroën, K., & Berton-Carabin, C. C. (2020). Behavior of plant-dairy protein blends at air-water and oil-water interfaces. *Colloids and Surfaces B: Biointerfaces*, *192*, 111015. https://doi.org/https://doi.org/10.1016/j.colsurfb.2020.111015

Hinderink, E. B. A., Schröder, A., Sagis, L., Schroën, K., & Berton-Carabin, C. C. (2021). Physical and oxidative stability of food emulsions prepared with pea protein fractions. *LWT*, *146*, 111424. https://doi.org/https://doi.org/10.1016/j.lwt.2021.111424

**Bibliography**


Ho, K. K. H. Y., Schroën, K., San Martín-González, M. F., & Berton-Carabin, C. C. (2018). Synergistic and antagonistic effects of plant and dairy protein blends on the physicochemical stability of lycopene-loaded emulsions. *Food Hydrocolloids*, *81*, 180-190. https://doi.org/10.1016/j.foodhyd.2018.02.033

Hoagland, P. D., Unruh, J. J., Wickham, E. D., & Farrell, H. M. (2001). Secondary Structure of Bovine αS2-Casein: Theoretical and Experimental Approaches1. *Journal of Dairy Science*, *84*(9), 1944-1949. https://doi.org/https://doi.org/10.3168/jds.S0022-0302(01)74636-X

Hoffmann, M. A., & van Mil, P. J. (1997). Heat-induced aggregation of β-lactoglobulin: role of the free thiol group and disulfide bonds. *Journal of Agricultural and Food Chemistry*, *45*(8), 2942-2948. https://doi.org/10.1021/jf960789q

Hoffmann, M. A., & van Mil, P. J. (1999). Heat-induced aggregation of β-lactoglobulin as a function of pH. *Journal of Agricultural and Food Chemistry*, *47*(5), 1898-1905. https://doi.org/10.1021/jf980886e

Holt, C., Carver, J. A., Ecroyd, H., & Thorn, D. C. (2013). Invited review: Caseins and the casein micelle: Their biological functions, structures, and behavior in foods1. *Journal of Dairy Science*, *96*(10), 6127-6146. https://doi.org/https://doi.org/10.3168/jds.2013-6831

Howell, N. K. (1992). Protein-protein interactions. In *Biochemistry of food proteins* (pp. 35-74). Springer. https://doi.org/10.1007/978-1-4684-9895-0_2

Hu, M., McClements, D. J., & Decker, E. A. (2003). Lipid oxidation in corn oil-in-water emulsions stabilized by casein, whey protein isolate, and soy protein isolate. *Journal of Agricultural and Food Chemistry*, *51*(6), 1696-1700. https://doi.org/10.1021/jf020952j

Hu, X., Zhao, M., Sun, W., Zhao, G., & Ren, J. (2011). Effects of Microfluidization Treatment and Transglutaminase Cross-Linking on Physicochemical, Functional, and Conformational Properties of Peanut Protein Isolate. *Journal of Agricultural and Food Chemistry*, *59*(16), 8886-8894. https://doi.org/10.1021/jf201781z

Hu, Y.-Q., Yin, S.-W., Zhu, J.-H., Qi, J.-R., Guo, J., Wu, L.-Y., Tang, C.-H., & Yang, X.-Q. (2016). Fabrication and characterization of novel Pickering emulsions and Pickering high internal emulsions stabilized by gliadin colloidal particles. *Food Hydrocolloids*, *61*, 300-310. https://doi.org/10.1016/j.foodhyd.2016.05.028

Huang, X.-N., Zhou, F.-Z., Yang, T., Yin, S.-W., Tang, C.-H., & Yang, X.-Q. (2019). Fabrication and characterization of Pickering High Internal Phase Emulsions (HIPEs) stabilized by chitosan-caseinophosphopeptides nanocomplexes as oral delivery vehicles. *Food Hydrocolloids*, *93*, 34-45. https://doi.org/10.1016/j.foodhyd.2019.02.005

Hunt, J. A., & Dalgleish, D. G. (1994). Adsorption behaviour of whey protein isolate and caseinate in soya oil-in-water emulsions. *Food Hydrocolloids*, *8*(2), 175-187. https://doi.org/10.1016/S0268-005X(09)80042-8

Hunter, T. N., Pugh, R. J., Franks, G. V., & Jameson, G. J. (2008). The role of particles in stabilising foams and emulsions. *Adv Colloid Interface Sci*, *137*(2), 57-81. https://doi.org/10.1016/j.cis.2007.07.007

Huppertz, T., Fox, P., & Kelly, A. (2018). The caseins: Structure, stability, and functionality. In *Proteins in food processing* (pp. 49-92). Elsevier. https://doi.org/10.1016/B978-0-08-100722-8.00004-8

Hussain, R., Gaiani, C., Jeandel, C., Ghanbaja, J., & Scher, J. (2012). Combined effect of heat treatment and ionic strength on the functionality of whey proteins. *Journal of Dairy Science*, *95*(11), 6260-6273. https://doi.org/https://doi.org/10.3168/jds.2012-5416

Hyun, K., Kim, S. H., Ahn, K. H., & Lee, S. J. (2002). Large amplitude oscillatory shear as a way to classify the complex fluids. *Journal of Non-Newtonian Fluid Mechanics*, *107*(1), 51-65. https://doi.org/https://doi.org/10.1016/S0377-0257(02)00141-6

Iordache, M., & Jelen, P. (2003). High pressure microfluidization treatment of heat denatured whey proteins for improved functionality. *Innovative Food Science & Emerging Technologies*, *4*(4), 367-376. https://doi.org/10.1016/S1466-8564(03)00061-4

Ipsen, R. (2017). Microparticulated whey proteins for improving dairy product texture. *International Dairy Journal*, *67*, 73-79. https://doi.org/https://doi.org/10.1016/j.idairyj.2016.08.009

Ismail, B. P., Senaratne-Lenagala, L., Stube, A., & Brackenridge, A. (2020). Protein demand: review of plant and animal proteins used in alternative protein product development and production. *Animal Frontiers*, *10*(4), 53-63. https://doi.org/10.1093/af/vfaa040

Ji, J., Zhang, J., Chen, J., Wang, Y., Dong, N., Hu, C., Chen, H., Li, G., Pan, X., & Wu, C. (2015). Preparation and stabilization of emulsions stabilized by mixed sodium caseinate and soy protein isolate. *Food Hydrocolloids*, *51*, 156-165. https://doi.org/https://doi.org/10.1016/j.foodhyd.2015.05.013

Jiang, J., Chen, J., & Xiong, Y. L. (2009). Structural and Emulsifying Properties of Soy Protein Isolate Subjected to Acid and Alkaline pH-Shifting Processes. *Journal of Agricultural and Food Chemistry*, *57*(16), 7576-7583. https://doi.org/10.1021/jf901585n

Jiang, J., Xiong, Y. L., & Chen, J. (2010). pH Shifting Alters Solubility Characteristics and Thermal Stability of Soy Protein Isolate and Its Globulin Fractions in Different pH, Salt Concentration, and Temperature Conditions. *Journal of Agricultural and Food Chemistry*, *58*(13), 8035-8042. https://doi.org/10.1021/jf101045b

Jiang, S., Ding, J., Andrade, J., Rababah, T. M., Almajwal, A., Abulmeaty, M. M., & Feng, H. (2017). Modifying the physicochemical properties of pea protein by pH-

shifting and ultrasound combined treatments. *Ultrasonics Sonochemistry*, *38*, 835-842. https://doi.org/10.1016/j.ultsonch.2017.03.046

Jiao, B., Shi, A., Wang, Q., & Binks, B. P. (2018). High-Internal-Phase Pickering Emulsions Stabilized Solely by Peanut-Protein-Isolate Microgel Particles with Multiple Potential Applications. *Angew Chem Int Ed Engl*, *57*(30), 9274-9278. https://doi.org/10.1002/anie.201801350

Jose, J., Pouvreau, L., & Martin, A. H. (2016). Mixing whey and soy proteins: Consequences for the gel mechanical response and water holding. *Food Hydrocolloids*, *60*, 216-224. https://doi.org/10.1016/j.foodhyd.2016.03.031

Joyner, H. S. (2019). *Rheology of semisolid foods*. Springer. https://doi.org/10.1007/978-3-030-27134-3

Kahraman, O., Petersen, G. E., & Fields, C. (2022). Physicochemical and Functional Modifications of Hemp Protein Concentrate by the Application of Ultrasonication and pH Shifting Treatments. *Foods*, *11*(4), 587. https://doi.org/10.3390/foods11040587

Keerati-u-rai, M., & Corredig, M. (2009). Heat-induced changes in oil-in-water emulsions stabilized with soy protein isolate. *Food Hydrocolloids*, *23*(8), 2141-2148. https://doi.org/10.1016/j.foodhyd.2009.05.010

Kehoe, J. J., & Foegeding, E. A. (2011). Interaction between β-Casein and Whey Proteins As a Function of pH and Salt Concentration. *Journal of Agricultural and Food Chemistry*, *59*(1), 349-355. https://doi.org/10.1021/jf103371g

Kehoe, J. J., & Foegeding, E. A. (2014). The characteristics of heat-induced aggregates formed by mixtures of β-lactoglobulin and β-casein. *Food Hydrocolloids*, *39*, 264-271. https://doi.org/https://doi.org/10.1016/j.foodhyd.2014.01.019

Kesari, P., Neetu, Sharma, A., Katiki, M., Kumar, P., R. Gurjar, B., Tomar, S., K. Sharma, A., & Kumar, P. (2017). Structural, functional and evolutionary aspects of seed globulins. *Protein and peptide letters*, *24*(3), 267-277.

Kethireddipalli, P., Hill, A. R., & Dalgleish, D. G. (2011). Interaction between Casein Micelles and Whey Protein/κ-Casein Complexes during Renneting of Heat-Treated Reconstituted Skim Milk Powder and Casein Micelle/Serum Mixtures. *Journal of Agricultural and Food Chemistry*, *59*(4), 1442-1448. https://doi.org/10.1021/jf103943e

Khalesi, M., Dowling, S., Comerford, J., Sweeney, C., Esteghlal, S., & FitzGerald, R. J. (2025). Emulsification Properties of Plant and Milk Protein Concentrate Blends. *Foods*, *14*(19). https://doi.org/10.3390/foods14193406

Kilara, A., & Vaghela, M. N. (2018). 4 - Whey proteins. In R. Y. Yada (Ed.), *Proteins in Food Processing (Second Edition)* (pp. 93-126). Woodhead Publishing. https://doi.org/https://doi.org/10.1016/B978-0-08-100722-8.00005-X

**Bibliography**


Kim, H. S., & Mason, T. G. (2017). Advances and challenges in the rheology of concentrated emulsions and nanoemulsions. *Adv Colloid Interface Sci*, *247*, 397-412. https://doi.org/10.1016/j.cis.2017.07.002

Kim, J.-J., & Lee, M.-Y. (2011). Isolation and characterization of edestin from Cheungsam hempseed. *Journal of Applied Biological Chemistry*, *54*(2), 84-88. https://doi.org/10.3839/jabc.2011.015

Kim, K., Kim, S., Ryu, J., Jeon, J., Jang, S. G., Kim, H., Gweon, D. G., Im, W. B., Han, Y., Kim, H., & Choi, S. Q. (2017). Processable high internal phase Pickering emulsions using depletion attraction. *Nat Commun*, *8*, 14305. https://doi.org/10.1038/ncomms14305

Kim, W., Wang, Y., & Selomulya, C. (2020). Dairy and plant proteins as natural food emulsifiers. *Trends in Food Science & Technology*, *105*, 261-272. https://doi.org/10.1016/j.tifs.2020.09.012

Kim, W., Wang, Y., & Selomulya, C. (2025). Exploring the relationship between physicochemical stability and interfacial properties in pea/whey protein blend-Stabilised emulsions. *Food Hydrocolloids*, *169*. https://doi.org/10.1016/j.foodhyd.2025.111622

Kim, W., Yiu, C. C., Wang, Y., Zhou, W., & Selomulya, C. (2024). Toward Diverse Plant Proteins for Food Innovation. *Adv Sci (Weinh)*, *11*(38), e2408150. https://doi.org/10.1002/advs.202408150

Klost, M., Brzeski, C., & Drusch, S. (2020). Effect of protein aggregation on rheological properties of pea protein gels. *Food Hydrocolloids*, *108*, 106036. https://doi.org/10.1016/j.foodhyd.2020.106036

Kornet, R., Penris, S., Venema, P., van der Goot, A. J., Meinders, M. B. J., & van der Linden, E. (2021). How pea fractions with different protein composition and purity can substitute WPI in heat-set gels. *Food Hydrocolloids*, *120*, Article 106891. https://doi.org/10.1016/j.foodhyd.2021.106891

Kornet, R., Shek, C., Venema, P., Jan van der Goot, A., Meinders, M., & van der Linden, E. (2021). Substitution of whey protein by pea protein is facilitated by specific fractionation routes. *Food Hydrocolloids*, *117*, 106691. https://doi.org/10.1016/j.foodhyd.2021.106691

Koudelka, T., Hoffmann, P., & Carver, J. A. (2009). Dephosphorylation of αs- and β-Caseins and Its Effect on Chaperone Activity: A Structural and Functional Investigation. *Journal of Agricultural and Food Chemistry*, *57*(13), 5956-5964. https://doi.org/10.1021/jf9008372

Kristensen, H. T., Christensen, M., Hansen, M. S., Hammershøj, M., & Dalsgaard, T. K. (2021a). Mechanisms behind protein-protein interactions in a β-lg-legumin co-precipitate. *Food Chemistry*, 131509. https://doi.org/https://doi.org/10.1016/j.foodchem.2021.131509

**Bibliography**


Kristensen, H. T., Christensen, M., Hansen, M. S., Hammershøj, M., & Dalsgaard, T. K. (2021b). Protein–protein interactions of a whey–pea protein co-precipitate. *International Journal of Food Science & Technology*, *56*(11), 5777-5790. https://doi.org/https://doi.org/10.1111/ijfs.15165

Kristensen, H. T., Denon, Q., Tavernier, I., Gregersen, S. B., Hammershøj, M., Van der Meeren, P., Dewettinck, K., & Dalsgaard, T. K. (2021). Improved food functional properties of pea protein isolate in blends and co-precipitates with whey protein isolate. *Food Hydrocolloids*, *113*, 106556. https://doi.org/https://doi.org/10.1016/j.foodhyd.2020.106556

Kristensen, H. T., Møller, A. H., Christensen, M., Hansen, M. S., Hammershøj, M., & Dalsgaard, T. K. (2020). Co-precipitation of whey and pea protein – indication of interactions. *International Journal of Food Science & Technology*, *55*(8), 2920-2930. https://doi.org/https://doi.org/10.1111/ijfs.14553

Lakemond, C. M. M., de Jongh, H. H. J., Hessing, M., Gruppen, H., & Voragen, A. G. J. (2000). Soy Glycinin: Influence of pH and Ionic Strength on Solubility and Molecular Structure at Ambient Temperatures. *Journal of Agricultural and Food Chemistry*, *48*(6), 1985-1990. https://doi.org/10.1021/jf9908695

Lam, R. S., & Nickerson, M. T. (2013). Food proteins: a review on their emulsifying properties using a structure-function approach. *Food Chem*, *141*(2), 975-984. https://doi.org/10.1016/j.foodchem.2013.04.038

Lam, R. S. H., & Nickerson, M. T. (2015). The effect of pH and temperature pre-treatments on the physicochemical and emulsifying properties of whey protein isolate. *LWT - Food Science and Technology*, *60*(1), 427-434. https://doi.org/10.1016/j.lwt.2014.07.031

Lawrence, M. C. (1999). Structural Relationships of 7S and 11S Globulins. In P. R. Shewry & R. Casey (Eds.), *Seed Proteins* (pp. 517-541). Springer Netherlands. https://doi.org/10.1007/978-94-011-4431-5_22

Lefevre, T., & Subirade, M. (2000). Molecular differences in the formation and structure of fine-stranded and particulate β-lactoglobulin gels. *Biopolymers: Original Research on Biomolecules*, *54*(7), 578-586. https://doi.org/10.1002/1097-0282(200012)54:7<578::AID-BIP100>3.0.CO;2-2

Li-Chan, E. C. Y., & Lacroix, I. M. E. (2018). Properties of proteins in food systems: An introduction. In R. Y. Yada (Ed.), *Proteins in Food Processing (Second Edition)* (pp. 1-25). Woodhead Publishing. https://doi.org/https://doi.org/10.1016/B978-0-08-100722-8.00002-4

Li, M., Li, H., Jiang, Q., Gantumur, M.-A., Liu, Y., Jiang, Z., & Qian, S. (2023). Insight into oil-water interfacial behaviors of whey protein isolate and sterol towards stabilizing high internal phase Pickering emulsion gels. *Food Hydrocolloids*, *144*. https://doi.org/10.1016/j.foodhyd.2023.108968

Li, Q., Xu, M., Xie, J., Su, E., Wan, Z., Sagis, L. M. C., & Yang, X. (2021). Large amplitude oscillatory shear (LAOS) for nonlinear rheological behavior of

heterogeneous emulsion gels made from natural supramolecular gelators. *Food Res Int*, *140*, 110076. https://doi.org/10.1016/j.foodres.2020.110076

Li, R., He, Q., Guo, M., Yuan, J., Wu, Y., Wang, S., Rong, L., & Li, J. (2020). Universal and simple method for facile fabrication of sustainable high internal phase emulsions solely using meat protein particles with various pH values. *Food Hydrocolloids*, *100*. https://doi.org/10.1016/j.foodhyd.2019.105444

Li, S., Ye, A., & Singh, H. (2021). Physicochemical changes and age gelation in stored UHT milk: Seasonal variations. *International Dairy Journal*, *118*, 105028. https://doi.org/10.1016/j.idairyj.2021.105028

Li, W., Jiao, B., Li, S., Faisal, S., Shi, A., Fu, W., Chen, Y., & Wang, Q. (2022). Recent Advances on Pickering Emulsions Stabilized by Diverse Edible Particles: Stability Mechanism and Applications. *Front Nutr*, *9*, 864943. https://doi.org/10.3389/fnut.2022.864943

Li, W., Nian, Y., Huang, Y., Zeng, X., Chen, Q., & Hu, B. (2019). High loading contents, distribution and stability of β-carotene encapsulated in high internal phase emulsions. *Food Hydrocolloids*, *96*, 300-309. https://doi.org/10.1016/j.foodhyd.2019.05.038

Liang, H.-N., & Tang, C.-h. (2014). Pea protein exhibits a novel Pickering stabilization for oil-in-water emulsions at pH 3.0. *LWT - Food Science and Technology*, *58*(2), 463-469. https://doi.org/https://doi.org/10.1016/j.lwt.2014.03.023

Liang, Y., Matia-Merino, L., Gillies, G., Patel, H., Ye, A., & Golding, M. (2017). The heat stability of milk protein-stabilized oil-in-water emulsions: A review. *Current Opinion in Colloid & Interface Science*, *28*, 63-73. https://doi.org/10.1016/j.cocis.2017.03.007

Liang, Y., Patel, H., Matia-Merino, L., Ye, A., & Golding, M. (2013). Structure and stability of heat-treated concentrated dairy-protein-stabilised oil-in-water emulsions: A stability map characterisation approach. *Food Hydrocolloids*, *33*(2), 297-308. https://doi.org/10.1016/j.foodhyd.2013.03.012

Liang, Y., Wong, S.-S., Pham, S. Q., & Tan, J. J. (2016). Effects of globular protein type and concentration on the physical properties and flow behaviors of oil-in-water emulsions stabilized by micellar casein–globular protein mixtures. *Food Hydrocolloids*, *54*, 89-98. https://doi.org/https://doi.org/10.1016/j.foodhyd.2015.09.024

Lima Nascimento, L. G., Odelli, D., Fernandes de Carvalho, A., Martins, E., Delaplace, G., Peres de Sa Peixoto Junior, P., Nogueira Silva, N. F., & Casanova, F. (2023). Combination of Milk and Plant Proteins to Develop Novel Food Systems: What Are the Limits? *Foods*, *12*(12). https://doi.org/10.3390/foods12122385

Lima, R. R., Stephani, R., Perrone, Í. T., & de Carvalho, A. F. (2023). Plant-based proteins: A review of factors modifying the protein structure and affecting emulsifying properties. *Food Chemistry Advances*, *3*. https://doi.org/10.1016/j.focha.2023.100397

**Bibliography**


Lin, D., Lu, W., Kelly, A. L., Zhang, L., Zheng, B., & Miao, S. (2017). Interactions of vegetable proteins with other polymers: Structure-function relationships and applications in the food industry. *Trends in Food Science & Technology*, *68*, 130-144. https://doi.org/https://doi.org/10.1016/j.tifs.2017.08.006

Lin, Y., Luo, W., Xiong, B., Guo, J., Wang, J., Tan, W., & Yang, X. (2024). Microstructure change and functional characteristic promotion: the structural manipulation of soy protein microparticles through pH. *International Journal of Food Science & Technology*, *59*(6), 3823-3833. https://doi.org/10.1111/ijfs.17125

Ling, M., Huang, X., He, C., & Zhou, Z. (2024). Tunable rheological properties of high internal phase emulsions stabilized by phosphorylated walnut protein/pectin complexes: The effects of pH conditions, mass ratios, and concentrations. *Food Res Int*, *175*, 113670. https://doi.org/10.1016/j.foodres.2023.113670

Linke, C., & Drusch, S. (2017). Pickering emulsions in foods - opportunities and limitations. *Critical Reviews in Food Science and Nutrition*, *58*(12), 1971-1985. https://doi.org/10.1080/10408398.2017.1290578

Liu, C.-M., Zhong, J.-Z., Liu, W., Tu, Z.-C., Wan, J., Cai, X.-F., & Song, X.-Y. (2011). Relationship between Functional Properties and Aggregation Changes of Whey Protein Induced by High Pressure Microfluidization. *Journal of Food Science*, *76*(4), E341-E347. https://doi.org/https://doi.org/10.1111/j.1750-3841.2011.02134.x

Liu, F., Huang, Y., Han, C., Wang, G., Wan, Z., Guo, J., & Yang, X. (2025). Enhancing protein content and lubrication behavior of plant-based milk with microparticulated wheat gluten protein via SS-SH interchange. *Food Hydrocolloids*, *159*. https://doi.org/10.1016/j.foodhyd.2024.110640

Liu, F., Ou, S.-Y., & Tang, C.-H. (2017). Ca 2+ -induced soy protein nanoparticles as pickering stabilizers: Fabrication and characterization. *Food Hydrocolloids*, *65*, 175-186. https://doi.org/10.1016/j.foodhyd.2016.11.011

Liu, F., & Tang, C.-H. (2013). Soy Protein Nanoparticle Aggregates as Pickering Stabilizers for Oil-in-Water Emulsions. *Journal of Agricultural and Food Chemistry*, *61*(37), 8888-8898. https://doi.org/10.1021/jf401859y

Liu, F., & Tang, C.-H. (2016a). Soy glycinin as food-grade Pickering stabilizers: Part. I. Structural characteristics, emulsifying properties and adsorption/arrangement at interface. *Food Hydrocolloids*, *60*, 606-619. https://doi.org/10.1016/j.foodhyd.2015.04.025

Liu, F., & Tang, C.-H. (2016b). Soy glycinin as food-grade Pickering stabilizers: Part. II. Improvement of emulsification and interfacial adsorption by electrostatic screening. *Food Hydrocolloids*, *60*, 620-630. https://doi.org/10.1016/j.foodhyd.2015.10.024

Liu, F., & Tang, C. H. (2014). Emulsifying properties of soy protein nanoparticles: influence of the protein concentration and/or emulsification process. *J Agric Food Chem*, *62*(12), 2644-2654. https://doi.org/10.1021/jf405348k

**Bibliography**


Liu, G., Jæger, T. C., Lund, M. N., Nielsen, S. B., Ray, C. A., & Ipsen, R. (2016). Effects of disulphide bonds between added whey protein aggregates and other milk components on the rheological properties of acidified milk model systems. *International Dairy Journal*, *59*, 1-9. https://doi.org/10.1016/j.idairyj.2016.03.002

Liu, K., Stieger, M., van der Linden, E., & van de Velde, F. (2016). Effect of microparticulated whey protein on sensory properties of liquid and semi-solid model foods. *Food Hydrocolloids*, *60*, 186-198. https://doi.org/https://doi.org/10.1016/j.foodhyd.2016.03.036

Liu, M., Toth, J. A., Childs, M., Smart, L. B., & Abbaspourrad, A. (2023). Composition and functional properties of hemp seed protein isolates from various hemp cultivars. *J Food Sci*, *88*(3), 942-951. https://doi.org/10.1111/1750-3841.16467

Liu, R., Tian, Z., Song, Y., Wu, T., Sui, W., & Zhang, M. (2018). Optimization of the Production of Microparticulated Egg White Proteins as Fat Mimetic in Salad Dressings Using Uniform Design. *Food Science and Technology Research*, *24*(5), 817-827. https://doi.org/10.3136/fstr.24.817

Liu, R., Wang, L., Liu, Y., Wu, T., & Zhang, M. (2018). Fabricating soy protein hydrolysate/xanthan gum as fat replacer in ice cream by combined enzymatic and heat-shearing treatment. *Food Hydrocolloids*, *81*, 39-47. https://doi.org/https://doi.org/10.1016/j.foodhyd.2018.01.031

Liu, W., Gao, H., McClements, D. J., Zhou, L., Wu, J., & Zou, L. (2019). Stability, rheology, and β-carotene bioaccessibility of high internal phase emulsion gels. *Food Hydrocolloids*, *88*, 210-217. https://doi.org/10.1016/j.foodhyd.2018.10.012

Liu, X., Guo, J., Wan, Z.-L., Liu, Y.-Y., Ruan, Q.-J., & Yang, X.-Q. (2018). Wheat gluten-stabilized high internal phase emulsions as mayonnaise replacers. *Food Hydrocolloids*, *77*, 168-175. https://doi.org/10.1016/j.foodhyd.2017.09.032

Liu, X., Xue, F., & Adhikari, B. (2024). Recent advances in plant protein modification: spotlight on hemp protein. *Sustainable Food Technology*, *2*(4), 893-907. https://doi.org/10.1039/d3fb00215b

Liyanaarachchi, W. S., Ramchandran, L., & Vasiljevic, T. (2015). Controlling heat induced aggregation of whey proteins by casein inclusion in concentrated protein dispersions. *International Dairy Journal*, *44*, 21-30. https://doi.org/https://doi.org/10.1016/j.idairyj.2014.12.010

Loveday, S. M. (2019). Food Proteins: Technological, Nutritional, and Sustainability Attributes of Traditional and Emerging Proteins. *Annual Review of Food Science and Technology*, *10*(1), 311-339. https://doi.org/10.1146/annurev-food-032818-121128

Loveday, S. M. (2020). Plant protein ingredients with food functionality potential. *Nutrition Bulletin*, *45*(3), 321-327. https://doi.org/https://doi.org/10.1111/nbu.12450

**Bibliography**


Lucey. (2017). Formation, structural properties, and rheology of acid-coagulated milk gels. In *Cheese* (pp. 179-197). Elsevier. https://doi.org/10.1016/B978-0-443-15956-5.00012-9

Lucey. (2020). Chapter 16 - Milk protein gels. In M. Boland & H. Singh (Eds.), *Milk Proteins (Third Edition)* (pp. 599-632). Academic Press. https://doi.org/https://doi.org/10.1016/B978-0-12-815251-5.00016-5

Ma, L., Zou, L., McClements, D. J., & Liu, W. (2020). One-step preparation of high internal phase emulsions using natural edible Pickering stabilizers: Gliadin nanoparticles/gum Arabic. *Food Hydrocolloids*, *100*. https://doi.org/10.1016/j.foodhyd.2019.105381

Ma, S., Acevedo-Fani, A., Ye, A., & Singh, H. (2024). Heat-induced interactions of hemp protein particles formed by microfluidisation with β-lactoglobulin. *LWT*, *203*. https://doi.org/10.1016/j.lwt.2024.116370

Ma, S., Ye, A., Singh, H., & Acevedo-Fani, A. (2024). Heat-induced interactions between microfluidized hemp protein particles and caseins or whey proteins. *Food Chemistry*, 141290. https://doi.org/10.1016/j.foodchem.2024.141290

Ma, S., Ye, A., Singh, H., & Acevedo-Fani, A. (2025). Emulsifying properties of hemp and whey protein complexes achieved by microparticulation. *Food Hydrocolloids*, 111833. https://doi.org/https://doi.org/10.1016/j.foodhyd.2025.111833

Ma, W., Wang, J., Wu, D., Chen, H., Wu, C., & Du, M. (2020). The mechanism of improved thermal stability of protein-enriched O/W emulsions by soy protein particles. *Food Funct*, *11*(2), 1385-1396. https://doi.org/10.1039/c9fo02270h

Mahmoudi, N., Mehalebi, S., Nicolai, T., Durand, D., & Riaublanc, A. (2007). Light-Scattering Study of the Structure of Aggregates and Gels Formed by Heat-Denatured Whey Protein Isolate and β-Lactoglobulin at Neutral pH. *Journal of Agricultural and Food Chemistry*, *55*(8), 3104-3111. https://doi.org/10.1021/jf063029g

Makinen, O. E., Zannini, E., Koehler, P., & Arendt, E. K. (2016). Heat-denaturation and aggregation of quinoa (Chenopodium quinoa) globulins as affected by the pH value. *Food Chem*, *196*, 17-24. https://doi.org/10.1016/j.foodchem.2015.08.069

Malin, E. L., Brown, E. M., Wickham, E. D., & Farrell, H. M. (2005). Contributions of Terminal Peptides to the Associative Behavior of αs1-Casein*. *Journal of Dairy Science*, *88*(7), 2318-2328. https://doi.org/https://doi.org/10.3168/jds.S0022-0302(05)72910-6

Malomo, S. A., & Aluko, R. E. (2015a). A comparative study of the structural and functional properties of isolated hemp seed (Cannabis sativa L.) albumin and globulin fractions. *Food Hydrocolloids*, *43*, 743-752. https://doi.org/https://doi.org/10.1016/j.foodhyd.2014.08.001

Malomo, S. A., & Aluko, R. E. (2015b). Conversion of a low protein hemp seed meal into a functional protein concentrate through enzymatic digestion of fibre coupled with

membrane ultrafiltration. *Innovative Food Science & Emerging Technologies*, *31*, 151-159. https://doi.org/https://doi.org/10.1016/j.ifset.2015.08.004

Malomo, S. A., He, R., & Aluko, R. E. (2014). Structural and Functional Properties of Hemp Seed Protein Products. *Journal of Food Science*, *79*(8), C1512-C1521. https://doi.org/10.1111/1750-3841.12537

Maltais, A., Remondetto, G. E., & Subirade, M. (2009). Soy protein cold-set hydrogels as controlled delivery devices for nutraceutical compounds. *Food Hydrocolloids*, *23*(7), 1647-1653. https://doi.org/10.1016/j.foodhyd.2008.12.006

Manderson, G., Hardman, M., & Creamer, L. (1998). Effect of heat treatment on the conformation and aggregation of β-lactoglobulin A, B, and C. *Journal of Agricultural and Food Chemistry*, *46*(12), 5052-5061. https://doi.org/10.1021/jf980515y

Manoi, K., & Rizvi, S. S. H. (2009). Emulsification mechanisms and characterizations of cold, gel-like emulsions produced from texturized whey protein concentrate. *Food Hydrocolloids*, *23*(7), 1837-1847. https://doi.org/10.1016/j.foodhyd.2009.02.011

Mao, Y., Dubot, M., Xiao, H., & McClements, D. J. (2013). Interfacial engineering using mixed protein systems: emulsion-based delivery systems for encapsulation and stabilization of beta-carotene. *J Agric Food Chem*, *61*(21), 5163-5169. https://doi.org/10.1021/jf401350t

Marcone, M. F., Kakuda, Y., & Yada, R. Y. (1998a). Salt-soluble seed globulins of dicotyledonous and monocotyledonous plants II. Structural characterization. *Food Chemistry*, *63*(2), 265-274. https://doi.org/https://doi.org/10.1016/S0308-8146(97)00159-3

Marcone, M. F., Kakuda, Y., & Yada, R. Y. (1998b). Salt-soluble seed globulins of various dicotyledonous and monocotyledonous plants—I. Isolation/purification and characterization. *Food Chemistry*, *62*(1), 27-47. https://doi.org/https://doi.org/10.1016/S0308-8146(97)00158-1

Martin, A. H., de los Reyes Jiménez, M. L., & Pouvreau, L. (2016). Modulating the aggregation behaviour to restore the mechanical response of acid induced mixed gels of sodium caseinate and soy proteins. *Food Hydrocolloids*, *58*, 215-223. https://doi.org/https://doi.org/10.1016/j.foodhyd.2016.02.029

McCann, T. H., Guyon, L., Fischer, P., & Day, L. (2018). Rheological properties and microstructure of soy-whey protein. *Food Hydrocolloids*, *82*, 434-441. https://doi.org/10.1016/j.foodhyd.2018.04.023

McClements, D. J. (2007). Critical review of techniques and methodologies for characterization of emulsion stability. *Critical Reviews in Food Science and Nutrition*, *47*(7), 611-649. https://doi.org/10.1080/10408390701289292

McClements, D. J. (2015). *Food emulsions: principles, practices, and techniques*. CRC press. https://doi.org/10.1201/9781420039436

**Bibliography**


McClements, D. J., & Grossmann, L. (2021). The science of plant-based foods: Constructing next-generation meat, fish, milk, and egg analogs. *Comprehensive Reviews in Food Science and Food Safety*, *20*(4), 4049-4100. https://doi.org/https://doi.org/10.1111/1541-4337.12771

McClements, D. J., & Gumus, C. E. (2016). Natural emulsifiers—Biosurfactants, phospholipids, biopolymers, and colloidal particles: Molecular and physicochemical basis of functional performance. *Advances in Colloid and Interface Science*, *234*, 3-26. https://doi.org/10.1016/j.cis.2016.03.002

McClements, D. J., & Jafari, S. M. (2018). Improving emulsion formation, stability and performance using mixed emulsifiers: A review. *Advances in Colloid and Interface Science*, *251*, 55-79. https://doi.org/https://doi.org/10.1016/j.cis.2017.12.001

McClements, D. J., & Keogh, M. K. (1995). Physical properties of cold-setting gels formed from heat-denatured whey protein isolate. *Journal of the Science of Food and Agriculture*, *69*(1), 7-14. https://doi.org/10.1002/jsfa.2740690103

McSweeney, P. L., & Fox, P. F. (2003). *Advanced dairy chemistry Volume 1B: Proteins: Applied Aspects*. Springer. https://doi.org/10.1007/978-3-030-48686-0

Mercade-Prieto, R., & Gunasekaran, S. (2009). Alkali cold gelation of whey proteins. Part I: sol-gel-sol(-gel) transitions. *Langmuir*, *25*(10), 5785-5792. https://doi.org/10.1021/la804093d

Mert, I. D. (2020). The applications of microfluidization in cereals and cereal-based products: An overview. *Critical Reviews in Food Science and Nutrition*, *60*(6), 1007-1024. https://doi.org/10.1080/10408398.2018.1555134

Mession, J.-L., Roustel, S., & Saurel, R. (2017a). Interactions in casein micelle - Pea protein system (Part II): Mixture acid gelation with glucono-δ-lactone. *Food Hydrocolloids*, *73*, 344-357. https://doi.org/10.1016/j.foodhyd.2017.06.029

Mession, J.-L., Roustel, S., & Saurel, R. (2017b). Interactions in casein micelle – Pea protein system (part I): Heat-induced denaturation and aggregation. *Food Hydrocolloids*, *67*, 229-242. https://doi.org/10.1016/j.foodhyd.2015.12.015

Molina, M. I., Petruccelli, S., & Añón, M. C. (2004). Effect of pH and Ionic Strength Modifications on Thermal Denaturation of the 11S Globulin of Sunflower (Helianthus annuus). *Journal of Agricultural and Food Chemistry*, *52*(19), 6023-6029. https://doi.org/10.1021/jf0494175

Moll, P., Salminen, H., Schmitt, C., & Weiss, J. (2021). Impact of microfluidization on colloidal properties of insoluble pea protein fractions. *European Food Research and Technology*, *247*(3), 545-554. https://doi.org/10.1007/s00217-020-03629-2

Momen, S., Rodrigue, D., & Aider, M. (2023). Fabrication and characterization of heat-set composite gels obtained from complexation of electro-activated whey/canola proteins mixture. *Food Hydrocolloids*, 108751. https://doi.org/https://doi.org/10.1016/j.foodhyd.2023.108751

**Bibliography**


Monroy-Rodríguez, I., Gutiérrez-López, G., Hernández-Sánchez, H., López-Hernández, R., Mazón, M. C., Dorántes-Álvarez, L., & Alamilla-Beltrán, L. (2021). Surface roughness and textural image analysis, particle size and stability of microparticles obtained by microfluidization of soy protein isolate aggregates suspensions. *Revista Mexicana de Ingeniería Química*, *20*(2), 787-805. https://doi.org/10.24275/rmiq/Alim2311

Morand, M., Dekkari, A., Guyomarc'h, F., & Famelart, M.-H. (2012). Increasing the hydrophobicity of the heat-induced whey protein complexes improves the acid gelation of skim milk. *International Dairy Journal*, *25*(2), 103-111. https://doi.org/10.1016/j.idairyj.2012.03.002

Morgan, P. E., Treweek, T. M., Lindner, R. A., Price, W. E., & Carver, J. A. (2005). Casein Proteins as Molecular Chaperones. *Journal of Agricultural and Food Chemistry*, *53*(7), 2670-2683. https://doi.org/10.1021/jf048329h

Morris, E. R. (2009). CHAPTER 5 - Functional Interactions in Gelling Biopolymer Mixtures. In S. Kasapis, I. T. Norton, & J. B. Ubbink (Eds.), *Modern Biopolymer Science* (pp. 167-198). Academic Press. https://doi.org/https://doi.org/10.1016/B978-0-12-374195-0.00005-7

Nicolai, T. (2016). Formation and functionality of self-assembled whey protein microgels. *Colloids and Surfaces B: Biointerfaces*, *137*, 32-38. https://doi.org/https://doi.org/10.1016/j.colsurfb.2015.05.055

Nicolai, T., & Chassenieux, C. (2019). Heat-induced gelation of plant globulins. *Current Opinion in Food Science*, *27*, 18-22. https://doi.org/https://doi.org/10.1016/j.cofs.2019.04.005

Nicolai, T., & Durand, D. (2013). Controlled food protein aggregation for new functionality. *Current Opinion in Colloid & Interface Science*, *18*(4), 249-256. https://doi.org/10.1016/j.cocis.2013.03.001

Ning, F., Ge, Z., Qiu, L., Wang, X., Luo, L., Xiong, H., & Huang, Q. (2020). Double-induced se-enriched peanut protein nanoparticles preparation, characterization and stabilized food-grade pickering emulsions. *Food Hydrocolloids*, *99*. https://doi.org/10.1016/j.foodhyd.2019.105308

Nourmohammadi, N., Austin, L., & Chen, D. (2023). Protein-Based Fat Replacers: A Focus on Fabrication Methods and Fat-Mimic Mechanisms. *Foods*, *12*(5). https://doi.org/10.3390/foods12050957

Odani, S., & Odani, S. (1998). Isolation and primary structure of a methionine-and cystine-rich seed protein of Cannabis sativa. *Bioscience, biotechnology, and biochemistry*, *62*(4), 650-654. https://doi.org/10.1271/bbb.62.650

Oldfield, Singh, H., & Taylor, M. W. (2005). Kinetics of heat-induced whey protein denaturation and aggregation in skim milks with adjusted whey protein concentration. *Journal of Dairy Research*, *72*(3), 369-378. https://doi.org/10.1017/S002202990500107X

**Bibliography**


Oldfield, Taylor, M. W., & Singh, H. (2005). Effect of preheating and other process parameters on whey protein reactions during skim milk powder manufacture. *International Dairy Journal*, *15*(5), 501-511. https://doi.org/https://doi.org/10.1016/j.idairyj.2004.09.004

Oldfield, D. J., Singh, H., & Taylor, M. W. (1998). Association of β-Lactoglobulin and β-Lactalbumin with the Casein Micelles in Skim Milk Heated in an Ultra-high Temperature Plant. *International Dairy Journal*, *8*(9), 765-770. https://doi.org/https://doi.org/10.1016/S0958-6946(98)00127-7

Oliete, B., Potin, F., Cases, E., & Saurel, R. (2018). Modulation of the emulsifying properties of pea globulin soluble aggregates by dynamic high-pressure fluidization. *Innovative Food Science & Emerging Technologies*, *47*, 292-300. https://doi.org/https://doi.org/10.1016/j.ifset.2018.03.015

Osborne, T. B. (1924). *The vegetable proteins*. Longmans, Green and Company.

Öztürk, O. K. (2014). *The Production and characterization of microparticulated corn zein, and its applications on emulsions and bread-making* Middle East Technical University].

Pace, C. N., & Tanford, C. (1968). Thermodynamics of the unfolding of β-lactoglobulin A in aqueous urea solutions between 5 and 55. *Biochemistry*, *7*(1), 198-208.

Pal, R. (2006). Rheology of high internal phase ratio emulsions. *Food Hydrocolloids*, *20*(7), 997-1005. https://doi.org/10.1016/j.foodhyd.2005.12.001

Pan, K., & Zhong, Q. (2013). Improving clarity and stability of skim milk powder dispersions by dissociation of casein micelles at pH 11.0 and acidification with citric acid. *J Agric Food Chem*, *61*(38), 9260-9268. https://doi.org/10.1021/jf402870y

Pan, K., & Zhong, Q. (2016). Low energy, organic solvent-free co-assembly of zein and caseinate to prepare stable dispersions. *Food Hydrocolloids*, *52*, 600-606. https://doi.org/https://doi.org/10.1016/j.foodhyd.2015.08.014

Patel, H. A., & Huppertz, T. (2014). Effects of High-pressure Processing on Structure and Interactions of Milk Proteins. In H. Singh, M. Boland, & A. Thompson (Eds.), *Milk Proteins (Second Edition)* (pp. 243-267). Academic Press. https://doi.org/https://doi.org/10.1016/B978-0-12-405171-3.00008-8

Patel, S., Cudney, R., & McPherson, A. (1994). Crystallographic characterization and molecular symmetry of edestin, a legumin from hemp. *Journal of Molecular Biology*, *235*(1), 361-363. https://doi.org/https://doi.org/10.1016/S0022-2836(05)80040-3

Pelegrine, D. H. G., & Gasparetto, C. A. (2005). Whey proteins solubility as function of temperature and pH. *LWT - Food Science and Technology*, *38*(1), 77-80. https://doi.org/https://doi.org/10.1016/j.lwt.2004.03.013

Peng, W., Kong, X., Chen, Y., Zhang, C., Yang, Y., & Hua, Y. (2016). Effects of heat treatment on the emulsifying properties of pea proteins. *Food Hydrocolloids*, *52*, 301-310. https://doi.org/https://doi.org/10.1016/j.foodhyd.2015.06.025

Pickering, S. U. (1907). Cxcvi.—emulsions. *Journal of the Chemical Society, Transactions*, *91*, 2001-2021.

Pizones Ruiz-Henestrosa, V. M., Martinez, M. J., Carrera Sánchez, C., Rodríguez Patino, J. M., & Pilosof, A. M. R. (2014). Mixed soy globulins and β-lactoglobulin systems behaviour in aqueous solutions and at the air–water interface. *Food Hydrocolloids*, *35*, 106-114. https://doi.org/10.1016/j.foodhyd.2013.04.021

Potin, F., Goure, E., Lubbers, S., Husson, F., & Saurel, R. (2022). Functional properties of hemp protein concentrate obtained by alkaline extraction and successive ultrafiltration and spray-drying. *International Journal of Food Science & Technology*, *57*(1), 436-446. https://doi.org/https://doi.org/10.1111/ijfs.15425

Potin, F., & Saurel, R. (2020). Hemp Seed as a Source of Food Proteins. In G. Crini & E. Lichtfouse (Eds.), *Sustainable Agriculture Reviews 42: Hemp Production and Applications* (pp. 265-294). Springer International Publishing. https://doi.org/10.1007/978-3-030-41384-2_9

Qin, X. S., Luo, Z. G., Peng, X. C., Lu, X. X., & Zou, Y. X. (2018). Fabrication and Characterization of Quinoa Protein Nanoparticle-Stabilized Food-Grade Pickering Emulsions with Ultrasound Treatment: Effect of Ionic Strength on the Freeze-Thaw Stability. *J Agric Food Chem*, *66*(31), 8363-8370. https://doi.org/10.1021/acs.jafc.8b02407

Raikos, V., Duthie, G., & Ranawana, V. (2015). Denaturation and oxidative stability of hemp seed (Cannabis sativa L.) protein isolate as affected by heat treatment. *Plant foods for human nutrition*, *70*(3), 304-309. https://doi.org/10.1007/s11130-015-0494-5

Rayner, M., Marku, D., Eriksson, M., Sjöö, M., Dejmek, P., & Wahlgren, M. (2014). Biomass-based particles for the formulation of Pickering type emulsions in food and topical applications. *Colloids and Surfaces A: Physicochemical and Engineering Aspects*, *458*, 48-62. https://doi.org/10.1016/j.colsurfa.2014.03.053

Rehman, I., Farooq, M., & Botelho, S. (2021). Biochemistry, secondary protein structure. In *StatPearls [Internet]*. StatPearls Publishing.

Renard, D., Lavenant, L., Sanchez, C., Hemar, Y., & Horne, D. (2002). Heat-induced flocculation of microparticulated whey proteins (MWP); consequences for mixed gels made of MWP and β-lactoglobulin. *Colloids and Surfaces B: Biointerfaces*, *24*(1), 73-85. https://doi.org/10.1016/S0927-7765(01)00246-6

Renkema, J. M. S., Gruppen, H., & van Vliet, T. (2002). Influence of pH and Ionic Strength on Heat-Induced Formation and Rheological Properties of Soy Protein Gels in Relation to Denaturation and Their Protein Compositions. *Journal of Agricultural and Food Chemistry*, *50*(21), 6064-6071. https://doi.org/10.1021/jf020061b

**Bibliography**


Renkema, J. M. S., Lakemond, C. M. M., de Jongh, H. H. J., Gruppen, H., & van Vliet, T. (2000). The effect of pH on heat denaturation and gel forming properties of soy proteins. *Journal of Biotechnology*, *79*(3), 223-230. https://doi.org/10.1016/S0168-1656(00)00239-X

Ritchie, H., & Rodés-Guirao, L. (2024, July 11, 2024). *Peak global population and other key findings from the 2024 UN World Population Prospects*. Retrieved February 20 from https://ourworldindata.org/un-population-2024-revision

Roesch, R. R., & Corredig, M. (2005). Heat-induced soy− whey proteins interactions: Formation of soluble and insoluble protein complexes. *Journal of Agricultural and Food Chemistry*, *53*(9), 3476-3482. https://doi.org/10.1021/jf048870d

Roesch, R. R., & Corredig, M. (2006). Study of the Effect of Soy Proteins on the Acid-Induced Gelation of Casein Micelles. *Journal of Agricultural and Food Chemistry*, *54*(21), 8236-8243. https://doi.org/10.1021/jf060875i

Roesch, R. R., Juneja, M., Monagle, C., & Corredig, M. (2004). Aggregation of soy/milk mixes during acidification. *Food Research International*, *37*(3), 209-215. https://doi.org/https://doi.org/10.1016/j.foodres.2003.11.003

Rout, S., Dash, P., Panda, P. K., Yang, P. C., & Srivastav, P. P. (2024). Interaction of dairy and plant proteins for improving the emulsifying and gelation properties in food matrices: a review. *Food Sci Biotechnol*, *33*(14), 3199-3212. https://doi.org/10.1007/s10068-024-01671-4

Ryan, K. N., Vardhanabhuti, B., Jaramillo, D. P., van Zanten, J. H., Coupland, J. N., & Foegeding, E. A. (2012). Stability and mechanism of whey protein soluble aggregates thermally treated with salts. *Food Hydrocolloids*, *27*(2), 411-420. https://doi.org/10.1016/j.foodhyd.2011.11.006

Ryan, K. N., Zhong, Q., & Foegeding, E. A. (2013). Use of whey protein soluble aggregates for thermal stability-a hypothesis paper. *J Food Sci*, *78*(8), R1105-1115. https://doi.org/10.1111/1750-3841.12207

Sarkar, A., & Dickinson, E. (2020). Sustainable food-grade Pickering emulsions stabilized by plant-based particles. *Current Opinion in Colloid & Interface Science*, *49*, 69-81. https://doi.org/10.1016/j.cocis.2020.04.004

Sarkar, A., Murray, B., Holmes, M., Ettelaie, R., Abdalla, A., & Yang, X. (2016). In vitro digestion of Pickering emulsions stabilized by soft whey protein microgel particles: influence of thermal treatment [10.1039/C5SM02998H]. *Soft matter*, *12*(15), 3558-3569. https://doi.org/10.1039/C5SM02998H

Sathe, S. K. (2012). Protein solubility and functionality. *Food proteins and peptides: chemistry, functionality, interactions, and commercialization*, 95-124. https://doi.org/10.1201/b11768

Sava, N., Van der Plancken, I., Claeys, W., & Hendrickx, M. (2005). The Kinetics of Heat-Induced Structural Changes of β-Lactoglobulin. *Journal of Dairy Science*,

*88*(5), 1646-1653. https://doi.org/https://doi.org/10.3168/jds.S0022-0302(05)72836-8

Scheraga, H. A., Némethy, G., & Steinberg, I. Z. (1962). The contribution of hydrophobic bonds to the thermal stability of protein conformations. *Journal of Biological Chemistry*, *237*(8), 2506-2508. https://doi.org/10.1016/S0021-9258(19)73780-6

Schmitt, C., Silva, J. V. C., Amagliani, L., Chassenieux, C., & Nicolai, T. (2019). Heat-induced and acid-induced gelation of dairy/plant protein dispersions and emulsions. *Current Opinion in Food Science*, *27*, 43-48. https://doi.org/https://doi.org/10.1016/j.cofs.2019.05.002

Schokker, E., Singh, H., Pinder, D., Norris, G., & Creamer, L. (1999). Characterization of intermediates formed during heat-induced aggregation of β-lactoglobulin AB at neutral pH. *International Dairy Journal*, *9*(11), 791-800. https://doi.org/10.1016/S0958-6946(99)00148-X

Schreuders, F. K. G., Sagis, L. M. C., Bodnár, I., Erni, P., Boom, R. M., & van der Goot, A. J. (2021). Small and large oscillatory shear properties of concentrated proteins. *Food Hydrocolloids*, *110*. https://doi.org/10.1016/j.foodhyd.2020.106172

Schröder, A., Berton-Carabin, C., Venema, P., & Cornacchia, L. (2017). Interfacial properties of whey protein and whey protein hydrolysates and their influence on O/W emulsion stability. *Food Hydrocolloids*, *73*, 129-140. https://doi.org/10.1016/j.foodhyd.2017.06.001

Schwartz, J.-M., Solé, V., Guéguen, J., Ropers, M.-H., Riaublanc, A., & Anton, M. (2015). Partial replacement of β-casein by napin, a rapeseed protein, as ingredient for processed foods: Thermoreversible aggregation. *LWT - Food Science and Technology*, *63*(1), 562-568. https://doi.org/10.1016/j.lwt.2015.03.084

Schwenzfeier, A., Helbig, A., Wierenga, P. A., & Gruppen, H. (2013). Emulsion properties of algae soluble protein isolate from Tetraselmis sp. *Food Hydrocolloids*, *30*(1), 258-263. https://doi.org/10.1016/j.foodhyd.2012.06.002

Semenova, M. G., & Dickinson, E. (2010). *Biopolymers in food colloids: Thermodynamics and molecular interactions*. CRC Press. https://doi.org/10.1201/b12817

Serrano León, G., Gravel, A., Perreault, V., Pouliot, Y., & Doyen, A. (2024). Impact of high hydrostatic pressure on casein micelle‐pea protein systems and comparison with heat treatment. *Sustainable Food Proteins*, *2*(4), 268-281.

Shao, Y., & Tang, C.-H. (2016). Gel-like pea protein Pickering emulsions at pH3.0 as a potential intestine-targeted and sustained-release delivery system for β-carotene. *Food Research International*, *79*, 64-72. https://doi.org/10.1016/j.foodres.2015.11.025

Shen, L., & Tang, C.-H. (2012). Microfluidization as a potential technique to modify surface properties of soy protein isolate. *Food Research International*, *48*(1), 108-118. https://doi.org/https://doi.org/10.1016/j.foodres.2012.03.006

**Bibliography**


Shen, P., Gao, Z., Fang, B., Rao, J., & Chen, B. (2021). Ferreting out the secrets of industrial hemp protein as emerging functional food ingredients. *Trends in Food Science & Technology*, *112*, 1-15. https://doi.org/https://doi.org/10.1016/j.tifs.2021.03.022

Shen, P., Gao, Z., Xu, M., Ohm, J.-B., Rao, J., & Chen, B. (2020). The impact of hempseed dehulling on chemical composition, structure properties and aromatic profile of hemp protein isolate. *Food Hydrocolloids*, *106*, 105889. https://doi.org/https://doi.org/10.1016/j.foodhyd.2020.105889

Shewry, P. R., & Casey, R. (1999). Seed Proteins. In P. R. Shewry & R. Casey (Eds.), *Seed Proteins* (pp. 1-10). Springer Netherlands. https://doi.org/10.1007/978-94-011-4431-5_1

Shewry, P. R., Napier, J. A., & Tatham, A. S. (1995). Seed storage proteins: structures and biosynthesis. *The plant cell*, *7*(7), 945. https://doi.org/10.1105/tpc.7.7.945

Shi, D., Li, C., Stone, A. K., Guldiken, B., & Nickerson, M. T. (2021). Recent Developments in Processing, Functionality, and Food Applications of Microparticulated Proteins. *Food Reviews International*, 1-24. https://doi.org/10.1080/87559129.2021.1933515

Silva, J. V. C., Balakrishnan, G., Schmitt, C., Chassenieux, C., & Nicolai, T. (2018). Heat-induced gelation of aqueous micellar casein suspensions as affected by globular protein addition. *Food Hydrocolloids*, *82*, 258-267. https://doi.org/https://doi.org/10.1016/j.foodhyd.2018.04.002

Silva, J. V. C., Cochereau, R., Schmitt, C., Chassenieux, C., & Nicolai, T. (2019). Heat-induced gelation of mixtures of micellar caseins and plant proteins in aqueous solution. *Food Research International*, *116*, 1135-1143. https://doi.org/https://doi.org/10.1016/j.foodres.2018.09.058

Silva, J. V. C., Jacquette, B., Amagliani, L., Schmitt, C., Nicolai, T., & Chassenieux, C. (2019). Heat-induced gelation of micellar casein/plant protein oil-in-water emulsions. *Colloids and Surfaces A: Physicochemical and Engineering Aspects*, *569*, 85-92. https://doi.org/https://doi.org/10.1016/j.colsurfa.2019.01.065

Silva, J. V. C., & O'Mahony, J. A. (2018). Microparticulated whey protein addition modulates rheological and microstructural properties of high-protein acid milk gels. *International Dairy Journal*, *78*, 145-151. https://doi.org/10.1016/j.idairyj.2017.11.013

Silva, R. R. D., Souza, L. H. P., Sousa, L. S., Rodrigues, L. D., Nogueira, G. S., Nascimento, L. G. L., & Carvalho, A. F. (2025). Effect of pH-shifting on the Physicochemical Properties of Pea Proteins and Its Effect on the Texture of Hybrid Gels Formed with Casein Micelles. *Foods*, *14*(16). https://doi.org/10.3390/foods14162887

Sim, S. Y. J., Srv, A., Chiang, J. H., & Henry, C. J. (2021). Plant Proteins for Future Foods: A Roadmap. *Foods*, *10*(8), 1967. https://doi.org/10.3390/foods10081967

**Bibliography**


Singer, N. S., Yamamoto, S., & Latella, J. (1988). Protein product base. In: Google Patents.

Singh, H. (2009). Protein interactions and functionality of milk protein products. In *Dairy-Derived Ingredients* (pp. 644-674). Elsevier. https://doi.org/10.1533/9781845697198.3.644

Singh, H., & Havea, P. (2003). ADVANCED DAIRY CHEMISTRY-l PROTEINS. In P. F. Fox & P. L. H. McSweeney (Eds.), *Advanced Dairy Chemistry—1 Proteins: Part A / Part B* (pp. 1261-1287). Springer US. https://doi.org/10.1007/978-1-4419-8602-3_34

Sirikulchayanont, P., Jayanta, S., Pradipasena, P., & Miyawaki, O. (2007). Characteristics of Microparticulated Particles from Mung Bean Protein. *International Journal of Food Properties*, *10*(3), 621-630. https://doi.org/10.1080/10942910601051212

Sliwinski, E. L., Roubos, P. J., Zoet, F. D., van Boekel, M. A. J. S., & Wouters, J. T. M. (2003). Effects of heat on physicochemical properties of whey protein-stabilised emulsions. *Colloids and Surfaces B: Biointerfaces*, *31*(1-4), 231-242. https://doi.org/10.1016/s0927-7765(03)00143-7

Sorgentini, D. A., Wagner, J. R., & Anon, M. C. (1995). Effects of thermal treatment of soy protein isolate on the characteristics and structure-function relationship of soluble and insoluble fractions. *Journal of Agricultural and Food Chemistry*, *43*(9), 2471-2479. https://doi.org/10.1021/jf00057a029

Sridharan, S., Meinders, M. B. J., Sagis, L. M., Bitter, J. H., & Nikiforidis, C. V. (2021). Jammed Emulsions with Adhesive Pea Protein Particles for Elastoplastic Edible 3D Printed Materials. *Advanced Functional Materials*, *31*(45). https://doi.org/10.1002/adfm.202101749

Sturaro, A., De Marchi, M., Zorzi, E., & Cassandro, M. (2015). Effect of microparticulated whey protein concentration and protein-to-fat ratio on Caciotta cheese yield and composition. *International Dairy Journal*, *48*, 46-52. https://doi.org/https://doi.org/10.1016/j.idairyj.2015.02.003

Su, J., Wang, X., Li, W., Chen, L., Zeng, X., Huang, Q., & Hu, B. (2018). Enhancing the Viability of Lactobacillus plantarum as Probiotics through Encapsulation with High Internal Phase Emulsions Stabilized with Whey Protein Isolate Microgels. *J Agric Food Chem*, *66*(46), 12335-12343. https://doi.org/10.1021/acs.jafc.8b03807

Sun, C., Gao, Y., & Zhong, Q. (2018). Effects of acidification by glucono-delta-lactone or hydrochloric acid on structures of zein-caseinate nanocomplexes self-assembled during a pH cycle. *Food Hydrocolloids*, *82*, 173-185. https://doi.org/https://doi.org/10.1016/j.foodhyd.2018.04.007

Sun, C., Gao, Y., & Zhong, Q. (2018). Properties of Ternary Biopolymer Nanocomplexes of Zein, Sodium Caseinate, and Propylene Glycol Alginate and Their Functions of Stabilizing High Internal Phase Pickering Emulsions. *Langmuir*, *34*(31), 9215-9227. https://doi.org/10.1021/acs.langmuir.8b01887

**Bibliography**


Sun, C., & Gunasekaran, S. (2009). Effects of protein concentration and oil-phase volume fraction on the stability and rheology of menhaden oil-in-water emulsions stabilized by whey protein isolate with xanthan gum. *Food Hydrocolloids*, *23*(1), 165-174. https://doi.org/https://doi.org/10.1016/j.foodhyd.2007.12.006

Sun, C., Liu, R., Wu, T., Liang, B., Shi, C., Cong, X., Hou, T., & Zhang, M. (2016). Combined Superfine Grinding and Heat-Shearing Treatment for the Microparticulation of Whey Proteins. *Food and Bioprocess Technology*, *9*(2), 378-386. https://doi.org/10.1007/s11947-015-1629-2

Sun, C., Liu, R., Wu, T., Liang, B., Shi, C., & Zhang, M. (2015). Effect of superfine grinding on the structural and physicochemical properties of whey protein and applications for microparticulated proteins. *Food Science and Biotechnology*, *24*(5), 1637-1643. https://doi.org/10.1007/s10068-015-0212-y

Sun, Q., Fu, Y., & Wang, W. (2022). Temperature effects on hydrophobic interactions: Implications for protein unfolding. *Chemical Physics*, *559*. https://doi.org/10.1016/j.chemphys.2022.111550

Sun, X., Sun, Y., Li, Y., Wu, Q., & Wang, L. (2021). Identification and Characterization of the Seed Storage Proteins and Related Genes of Cannabis sativa L. *Front Nutr*, *8*, 678421. https://doi.org/10.3389/fnut.2021.678421

Sun, Y., Chai, X., Han, W., Farah, Z., Tian, T., Xu, Y.-J., & Liu, Y. (2023). Pickering emulsions stabilized by hemp protein nanoparticles: Tuning the emulsion characteristics by adjusting anti-solvent precipitation. *Food Hydrocolloids*, *138*. https://doi.org/10.1016/j.foodhyd.2022.108434

Tamayo Tenorio, A., Kyriakopoulou, K. E., Suarez-Garcia, E., van den Berg, C., & van der Goot, A. J. (2018). Understanding differences in protein fractionation from conventional crops, and herbaceous and aquatic biomass - Consequences for industrial use. *Trends in Food Science & Technology*, *71*, 235-245. https://doi.org/https://doi.org/10.1016/j.tifs.2017.11.010

Tan, M., Xu, J., Gao, H., Yu, Z., Liang, J., Mu, D., Li, X., Zhong, X., Luo, S., Zhao, Y., Jiang, S., & Zheng, Z. (2021). Effects of combined high hydrostatic pressure and pH-shifting pretreatment on the structure and emulsifying properties of soy protein isolates. *Journal of Food Engineering*, *306*. https://doi.org/10.1016/j.jfoodeng.2021.110622

Tang, C.-H., & Liu, F. (2013). Cold, gel-like soy protein emulsions by microfluidization: Emulsion characteristics, rheological and microstructural properties, and gelling mechanism. *Food Hydrocolloids*, *30*(1), 61-72. https://doi.org/10.1016/j.foodhyd.2012.05.008

Tang, C.-H., Ten, Z., Wang, X.-S., & Yang, X.-Q. (2006). Physicochemical and Functional Properties of Hemp (Cannabis sativa L.) Protein Isolate. *Journal of Agricultural and Food Chemistry*, *54*(23), 8945-8950. https://doi.org/10.1021/jf0619176

Tang, C. H. (2017). Emulsifying properties of soy proteins: A critical review with emphasis on the role of conformational flexibility. *Crit Rev Food Sci Nutr*, *57*(12), 2636-2679. https://doi.org/10.1080/10408398.2015.1067594

Tang, Q., Roos, Y. H., & Miao, S. (2024). Structure, gelation mechanism of plant proteins versus dairy proteins and evolving modification strategies. *Trends in Food Science & Technology*, *147*. https://doi.org/10.1016/j.tifs.2024.104464

Tanger, C., Mertens, J., & Kulozik, U. (2022). Influence of extraction method on the aggregation of pea protein during thermo-mechanical treatment. *Food Hydrocolloids*, *127*, 107514. https://doi.org/10.1016/j.foodhyd.2022.107514

Tanger, C., Quintana Ramos, P., & Kulozik, U. (2021). Comparative Assessment of Thermal Aggregation of Whey, Potato, and Pea Protein under Shear Stress for Microparticulation. *ACS Food Science & Technology*, *1*(5), 975-985. https://doi.org/10.1021/acsfoodscitech.1c00104

Tanger, C., Schmidt, F., Utz, F., Kreissl, J., Dawid, C., & Kulozik, U. (2021). Pea protein microparticulation using extrusion cooking: Influence of extrusion parameters and drying on microparticle characteristics and sensory by application in a model milk dessert. *Innovative Food Science & Emerging Technologies*, *74*, 102851. https://doi.org/https://doi.org/10.1016/j.ifset.2021.102851

Tanger, C., Utz, F., Spaccasassi, A., Kreissl, J., Dombrowski, J., Dawid, C., & Kulozik, U. (2022). Influence of Pea and Potato Protein Microparticles on Texture and Sensory Properties in a Fat-Reduced Model Milk Dessert. *ACS Food Science & Technology*, *2*(1), 169-179. https://doi.org/10.1021/acsfoodscitech.1c00394

Tcholakova, S., Denkov, N., & Lips, A. (2008). Comparison of solid particles, globular proteins and surfactants as emulsifiers. *Physical Chemistry Chemical Physics*, *10*(12), 1608-1627.

Teh, S.-S., Bekhit, A. E.-D., Carne, A., & Birch, J. (2014). Effect of the defatting process, acid and alkali extraction on the physicochemical and functional properties of hemp, flax and canola seed cake protein isolates. *Journal of Food Measurement and Characterization*, *8*(2), 92-104. https://doi.org/10.1007/s11694-013-9168-x

Toro-Sierra, J., Schumann, J., & Kulozik, U. (2013). Impact of spray-drying conditions on the particle size of microparticulated whey protein fractions. *Dairy Science & Technology*, *93*(4), 487-503. https://doi.org/10.1007/s13594-013-0124-7

Torres, I. C., Amigo, J. M., Knudsen, J. C., Tolkach, A., Mikkelsen, B. Ø., & Ipsen, R. (2018). Rheology and microstructure of low-fat yoghurt produced with whey protein microparticles as fat replacer. *International Dairy Journal*, *81*, 62-71. https://doi.org/10.1016/j.idairyj.2018.01.004

Torres, I. C., Janhøj, T., Mikkelsen, B. Ø., & Ipsen, R. (2011). Effect of microparticulated whey protein with varying content of denatured protein on the rheological and sensory characteristics of low-fat yoghurt. *International Dairy Journal*, *21*(9), 645-655. https://doi.org/https://doi.org/10.1016/j.idairyj.2010.12.013

**Bibliography**


Torres, I. C., Mutaf, G., Larsen, F. H., & Ipsen, R. (2016). Effect of hydration of microparticulated whey protein ingredients on their gelling behaviour in a non-fat milk system. *Journal of Food Engineering*, *184*, 31-37. https://doi.org/https://doi.org/10.1016/j.jfoodeng.2016.03.018

Treweek, T. M., Thorn, D. C., Price, W. E., & Carver, J. A. (2011). The chaperone action of bovine milk alphaS1- and alphaS2-caseins and their associated form alphaS-casein. *Arch Biochem Biophys*, *510*(1), 42-52. https://doi.org/10.1016/j.abb.2011.03.012

United Nations, D. o. E. a. S. A., Population Division. (2024). *World Population Prospects 2024*. https://population.gov.au/sites/population.gov.au/files/2025-02/2024-un-world-pop-prospects.pdf

Verheul, M., Roefs, S. P., & de Kruif, K. G. (1998). Kinetics of heat-induced aggregation of β-lactoglobulin. *Journal of Agricultural and Food Chemistry*, *46*(3), 896-903. https://doi.org/10.1021/jf970751t

Vincekovic, M., Curlin, M., & Jurasin, D. (2014). Impact of cationic surfactant on the self-assembly of sodium caseinate. *Journal of Agricultural and Food Chemistry*, *62*(34), 8543-8554. https://doi.org/10.1021/jf5016472

Visschers, R. W., & de Jongh, H. H. J. (2005). Disulphide bond formation in food protein aggregation and gelation. *Biotechnology Advances*, *23*(1), 75-80. https://doi.org/https://doi.org/10.1016/j.biotechadv.2004.09.005

Wang, C., Pei, X., Tan, J., Zhang, T., Zhai, K., Zhang, F., Bai, Y., Deng, Y., Zhang, B., Wang, Y., Tan, Y., Xu, K., & Wang, P. (2020). Thermoresponsive starch-based particle-stabilized Pickering high internal phase emulsions as nutraceutical containers for controlled release. *Int J Biol Macromol*, *146*, 171-178. https://doi.org/10.1016/j.ijbiomac.2019.12.269

Wang, L., & Zhang, Y. (2017). Eugenol Nanoemulsion Stabilized with Zein and Sodium Caseinate by Self-Assembly. *Journal of Agricultural and Food Chemistry*, *65*(14), 2990-2998. https://doi.org/10.1021/acs.jafc.7b00194

Wang, Q., Jiang, J., & Xiong, Y. L. (2018). High pressure homogenization combined with pH shift treatment: A process to produce physically and oxidatively stable hemp milk. *Food Research International*, *106*, 487-494. https://doi.org/https://doi.org/10.1016/j.foodres.2018.01.021

Wang, Q., Jin, Y., & Xiong, Y. L. (2018). Heating-Aided pH Shifting Modifies Hemp Seed Protein Structure, Cross-Linking, and Emulsifying Properties. *Journal of Agricultural and Food Chemistry*, *66*(41), 10827-10834. https://doi.org/10.1021/acs.jafc.8b03901

Wang, Q., & Xiong, Y. L. (2019). Processing, Nutrition, and Functionality of Hempseed Protein: A Review. *Comprehensive Reviews in Food Science and Food Safety*, *18*(4), 936-952. https://doi.org/https://doi.org/10.1111/1541-4337.12450

Wang, R., Xu, P., Chen, Z., Zhou, X., & Wang, T. (2019). Complexation of rice proteins and whey protein isolates by structural interactions to prepare soluble protein composites. *LWT*, *101*, 207-213. https://doi.org/https://doi.org/10.1016/j.lwt.2018.11.006

Wang, T., Chen, X., Zhong, Q., Chen, Z., Wang, R., & Patel, A. R. (2019). Facile and Efficient Construction of Water-Soluble Biomaterials with Tunable Mesoscopic Structures Using All-Natural Edible Proteins. *Advanced Functional Materials*, *29*(31). https://doi.org/10.1002/adfm.201901830

Wang, T., Yue, M., Xu, P., Wang, R., & Chen, Z. (2018). Toward water-solvation of rice proteins via backbone hybridization by casein. *Food Chemistry*, *258*, 278-283. https://doi.org/https://doi.org/10.1016/j.foodchem.2018.03.084

Wang, W., Nema, S., & Teagarden, D. (2010). Protein aggregation--pathways and influencing factors. *Int J Pharm*, *390*(2), 89-99. https://doi.org/10.1016/j.ijpharm.2010.02.025

Wang, X.-S., Tang, C.-H., Yang, X.-Q., & Gao, W.-R. (2008). Characterization, amino acid composition and in vitro digestibility of hemp (Cannabis sativa L.) proteins. *Food Chemistry*, *107*(1), 11-18. https://doi.org/https://doi.org/10.1016/j.foodchem.2007.06.064

Wang, Y., Bamdad, F., Song, Y., & Chen, L. (2012). Hydrogel particles and other novel protein-based methods for food ingredient and nutraceutical delivery systems. In N. Garti & D. J. McClements (Eds.), *Encapsulation Technologies and Delivery Systems for Food Ingredients and Nutraceuticals* (pp. 412-450). Woodhead Publishing. https://doi.org/https://doi.org/10.1533/9780857095909.3.412

Wei, Y., Zhan, X., Dai, L., Zhang, L., Mao, L., Yuan, F., Liu, J., & Gao, Y. (2021). Formation mechanism and environmental stability of whey protein isolate-zein core-shell complex nanoparticles using the pH-shifting method. *LWT*, *139*, 110605. https://doi.org/https://doi.org/10.1016/j.lwt.2020.110605

Wei, Z., Cheng, Y., & Huang, Q. (2019). Heteroprotein complex formation of ovotransferrin and lysozyme: Fabrication of food-grade particles to stabilize Pickering emulsions. *Food Hydrocolloids*, *96*, 190-200. https://doi.org/10.1016/j.foodhyd.2019.05.024

Wijaya, W., Van der Meeren, P., Wijaya, C. H., & Patel, A. R. (2017). High internal phase emulsions stabilized solely by whey protein isolate-low methoxyl pectin complexes: effect of pH and polymer concentration. *Food Funct*, *8*(2), 584-594. https://doi.org/10.1039/c6fo01027j

Wijayanti, H. B., Bansal, N., & Deeth, H. C. (2014). Stability of whey proteins during thermal processing: A review. *Comprehensive Reviews in Food Science and Food Safety*, *13*(6), 1235-1251. https://doi.org/10.1111/1541-4337.12105

Wong, D., Vasanthan, T., & Ozimek, L. (2013a). Synergistic enhancement in the co-gelation of salt-soluble pea proteins and whey proteins. *Food Chem*, *141*(4), 3913-3919. https://doi.org/10.1016/j.foodchem.2013.05.082

Wong, D., Vasanthan, T., & Ozimek, L. (2013b). Synergistic enhancement in the co-gelation of salt-soluble pea proteins and whey proteins. *Food Chemistry*, *141*(4), 3913-3919. https://doi.org/10.1016/j.foodchem.2013.05.082

Wu, C., Wang, T., Ren, C., Ma, W., Wu, D., Xu, X., Wang, L.-S., & Du, M. (2021). Advancement of food-derived mixed protein systems: Interactions, aggregations, and functional properties. *Comprehensive Reviews in Food Science and Food Safety*, *20*(1), 627-651. https://doi.org/https://doi.org/10.1111/1541-4337.12682

Wu, J., Shi, M., Li, W., Zhao, L., Wang, Z., Yan, X., Norde, W., & Li, Y. (2015). Pickering emulsions stabilized by whey protein nanoparticles prepared by thermal cross-linking. *Colloids Surf B Biointerfaces*, *127*, 96-104. https://doi.org/10.1016/j.colsurfb.2015.01.029

Wusigale, Liang, L., & Luo, Y. (2020). Casein and pectin: Structures, interactions, and applications. *Trends in Food Science & Technology*, *97*, 391-403. https://doi.org/https://doi.org/10.1016/j.tifs.2020.01.027

Xia, W., Czaja, T. P., Via, M., Zhang, H., Clausen, M. P., & Ahrné, L. (2024). Acid-induced gels from mixtures of micellar casein and pea protein: Effect of protein ratio and preheating route. *Food Hydrocolloids*, *153*. https://doi.org/10.1016/j.foodhyd.2024.110045

Xiao, J., Wang, X. a., Perez Gonzalez, A. J., & Huang, Q. (2016). Kafirin nanoparticles-stabilized Pickering emulsions: Microstructure and rheological behavior. *Food Hydrocolloids*, *54*, 30-39. https://doi.org/https://doi.org/10.1016/j.foodhyd.2015.09.008

Xu, Y.-T., Liu, T.-X., & Tang, C.-H. (2019). Novel pickering high internal phase emulsion gels stabilized solely by soy β-conglycinin. *Food Hydrocolloids*, *88*, 21-30. https://doi.org/10.1016/j.foodhyd.2018.09.031

Xu, Y., Sismour, E., Britland, J. W., Sellers, A., Abraha-Eyob, Z., Yousuf, A., Rao, Q., Kim, J., & Zhao, W. (2022). Physicochemical, Structural, and Functional Properties of Hemp Protein vs Several Commercially Available Plant and Animal Proteins: A Comparative Study. *ACS Food Science & Technology*, *2*(10), 1672-1680. https://doi.org/10.1021/acsfoodscitech.2c00250

Yamagishi, T., Yamauchi, F., & Shibasaki, K. (2014). Isolation and Partial Characterization of Heat-denatured Products of Soybean 11S Globulin and Their Analysis by Electrophoresis. *Agricultural and Biological Chemistry*, *44*(7), 1575-1582. https://doi.org/10.1080/00021369.1980.10864172

Yan, X., Ma, C., Cui, F., McClements, D. J., Liu, X., & Liu, F. (2020). Protein-stabilized Pickering emulsions: Formation, stability, properties, and applications in foods. *Trends in Food Science & Technology*, *103*, 293-303. https://doi.org/10.1016/j.tifs.2020.07.005

Yang, T., Li, X.-T., & Tang, C.-H. (2020). Novel edible pickering high-internal-phase-emulsion gels efficiently stabilized by unique polysaccharide-protein hybrid

nanoparticles from Okara. *Food Hydrocolloids*, *98*. https://doi.org/10.1016/j.foodhyd.2019.105285

Yang, Y., Fang, Z., Chen, X., Zhang, W., Xie, Y., Chen, Y., Liu, Z., & Yuan, W. (2017). An overview of Pickering emulsions: solid-particle materials, classification, morphology, and applications. *Frontiers in pharmacology*, *8*, 235054. https://doi.org/10.3389/fphar.2017.00287

Ye, A. (2008). Interfacial composition and stability of emulsions made with mixtures of commercial sodium caseinate and whey protein concentrate. *Food Chem*, *110*(4), 946-952. https://doi.org/10.1016/j.foodchem.2008.02.091

Yerramilli, M., Longmore, N., & Ghosh, S. (2017). Improved stabilization of nanoemulsions by partial replacement of sodium caseinate with pea protein isolate. *Food Hydrocolloids*, *64*, 99-111. https://doi.org/https://doi.org/10.1016/j.foodhyd.2016.10.027

Yin, S.-W., Tang, C.-H., Cao, J.-S., Hu, E.-K., Wen, Q.-B., & Yang, X.-Q. (2008). Effects of limited enzymatic hydrolysis with trypsin on the functional properties of hemp (Cannabis sativa L.) protein isolate. *Food Chemistry*, *106*(3), 1004-1013. https://doi.org/https://doi.org/10.1016/j.foodchem.2007.07.030

Yong, Y. H., & Foegeding, E. A. (2010). Caseins: Utilizing Molecular Chaperone Properties to Control Protein Aggregation in Foods. *Journal of Agricultural and Food Chemistry*, *58*(2), 685-693. https://doi.org/10.1021/jf903072g

Yusoff, A., & Murray, B. S. (2011). Modified starch granules as particle-stabilizers of oil-in-water emulsions. *Food Hydrocolloids*, *25*(1), 42-55. https://doi.org/10.1016/j.foodhyd.2010.05.004

Zamani, S., Malchione, N., Selig, M. J., & Abbaspourrad, A. (2018). Formation of shelf stable Pickering high internal phase emulsions (HIPE) through the inclusion of whey protein microgels. *Food Funct*, *9*(2), 982-990. https://doi.org/10.1039/c7fo01800b

Zhan, X., Dai, L., Zhang, L., & Gao, Y. (2020). Entrapment of curcumin in whey protein isolate and zein composite nanoparticles using pH-driven method. *Food Hydrocolloids*, *106*, 105839. https://doi.org/https://doi.org/10.1016/j.foodhyd.2020.105839

Zhang, J., Zhao, S., Li, L., Kong, B., & Liu, H. (2023). High Internal Phase Emulsions Stabilized by Pea Protein Isolate Modified by Ultrasound Combined with pH-Shifting: Micromorphology, Rheology, and Physical Stability. *Foods*, *12*(7). https://doi.org/10.3390/foods12071433

Zhang, R., Cheng, L., Luo, L., Hemar, Y., & Yang, Z. (2021). Formation and characterisation of high-internal-phase emulsions stabilised by high-pressure homogenised quinoa protein isolate. *Colloids and Surfaces A: Physicochemical and Engineering Aspects*, *631*, 127688. https://doi.org/https://doi.org/10.1016/j.colsurfa.2021.127688

**Bibliography**


Zhang, S., Holmes, M., Ettelaie, R., & Sarkar, A. (2020). Pea protein microgel particles as Pickering stabilisers of oil-in-water emulsions: Responsiveness to pH and ionic strength. *Food Hydrocolloids*, *102*. https://doi.org/10.1016/j.foodhyd.2019.105583

Zhang, T., Guo, J., Chen, J.-F., Wang, J.-M., Wan, Z.-L., & Yang, X.-Q. (2020). Heat stability and rheological properties of concentrated soy protein/egg white protein composite microparticle dispersions. *Food Hydrocolloids*, *100*, 105449. https://doi.org/https://doi.org/10.1016/j.foodhyd.2019.105449

Zhang, X., Wang, Q., Liu, Z., Zhi, L., Jiao, B., Hu, H., Ma, X., Agyei, D., & Shi, A. (2023). Plant protein-based emulsifiers: Mechanisms, techniques for emulsification enhancement and applications. *Food Hydrocolloids*, *144*. https://doi.org/10.1016/j.foodhyd.2023.109008

Zhang, X., Zhang, S., Xie, F., Han, L., Li, L., Jiang, L., Qi, B., & Li, Y. (2021). Soy/whey protein isolates: interfacial properties and effects on the stability of oil-in-water emulsions. *Journal of the Science of Food and Agriculture*, *101*(1), 262-271. https://doi.org/https://doi.org/10.1002/jsfa.10638

Zhang, Y., Herneke, A., Langton, M., Johansson, M., & Corredig, M. (2025). Effect of pH and ionic strength on heat-induced pea protein isolate aggregation and gel formation. *Food Hydrocolloids*, *167*. https://doi.org/10.1016/j.foodhyd.2025.111393

Zhao, Q., Long, Z., Kong, J., Liu, T., Sun-Waterhouse, D., & Zhao, M. (2015). Sodium caseinate/flaxseed gum interactions at oil–water interface: Effect on protein adsorption and functions in oil-in-water emulsion. *Food Hydrocolloids*, *43*, 137-145. https://doi.org/10.1016/j.foodhyd.2014.05.009

Zheng, J., Gao, Q., Tang, C.-h., Ge, G., Zhao, M., & Sun, W. (2020). Heteroprotein complex formation of soy protein isolate and lactoferrin: Thermodynamic formation mechanism and morphologic structure. *Food Hydrocolloids*, *100*. https://doi.org/10.1016/j.foodhyd.2019.105415

Zheng, L., Regenstein, J. M., Zhou, L., & Wang, Z. (2022). Soy protein isolates: A review of their composition, aggregation, and gelation. *Comprehensive Reviews in Food Science and Food Safety*, *21*(2), 1940-1957. https://doi.org/https://doi.org/10.1111/1541-4337.12925

Zhou, B., Drusch, S., & Hogan, S. A. (2022). Rheological fingerprinting and tribological assessment of high internal phase emulsions stabilized by whey protein isolate: Effects of protein concentration and pH. *Food Hydrocolloids*, *131*. https://doi.org/10.1016/j.foodhyd.2022.107816

Zhou, B., Drusch, S., & Hogan, S. A. (2023). Effects of temperature and pH on interfacial viscoelasticity, bulk rheology and tribological properties of whey protein isolate-stabilized high internal phase emulsions. *Food Hydrocolloids*, *142*. https://doi.org/10.1016/j.foodhyd.2023.108756

**Bibliography**

Zhou, F. Z., Huang, X. N., Wu, Z. L., Yin, S. W., Zhu, J. H., Tang, C. H., & Yang, X. Q. (2018). Fabrication of Zein/Pectin Hybrid Particle-Stabilized Pickering High Internal Phase Emulsions with Robust and Ordered Interface Architecture. *J Agric Food Chem*, *66*(42), 11113-11123. https://doi.org/10.1021/acs.jafc.8b03714

Zhou, X., Zheng, Y., Zhong, Y., Wang, D., & Deng, Y. (2022). Casein-hempseed protein complex via cross-link catalyzed by transglutaminase for improving structural, rheological, emulsifying and gelation properties. *Food Chemistry*, *383*, 132366. https://doi.org/10.1016/j.foodchem.2022.132366

Zou, Y., Pan, R., Wan, Z., Guo, J., Wang, J., & Yang, X. (2017). Gel-like emulsions prepared with zein nanoparticles produced through phase separation from acetic acid solutions. *International Journal of Food Science & Technology*, *52*(12), 2670-2676. https://doi.org/10.1111/ijfs.13558